# Characterisation of DJ-1 (*PARK7*) in human brain: possible involvement in idiopathic Parkinson's disease and other neurodegenerative disorders

By

Ravindran Kumaran

A thesis submitted for the degree of Doctor of Philosophy in Neuroscience from University College London

June 2009

Reta Lila Weston Institute of Neurological Studies

University College London

London

# Declaration

I, Ravindran Kumaran confirm that the work presented in this thesis is my own. Where information has been derived from other sources, I confirm that this has been indicated in the thesis.

# Abstract

Mutations in the DJ-1 gene can induce the development of early-onset Parkinson's disease (PD) through a loss of protein function. Currently any possible role for DJ-1 in sporadic PD remains undetermined. To address this, we have studied the characteristics and activities of DJ-1 in post-mortem human brain tissue in order to gain insights into its contribution to the development of PD and other neurodegenerative disorders.

Western blotting revealed DJ-1 protein expression to be reduced in several brain regions associated with PD pathology including nigra, striatum and frontal cortex. Similarly levels of DJ-1 mRNA were also shown to also be lower in PD striatum and frontal cortex suggesting a transcriptional regulation of protein expression in human brain. Further analysis of DJ-1 gene expression showed PD related changes to be variable throughout the brain, with regions like the amygdala and entorhinal cortex displaying an up-regulation. DJ-1 protein was also shown to undergo increased oxidation in PD cases, highlighting the elevated oxidative stress conditions in PD

By using immunoprecipitation to investigate a possible role for DJ-1 as an *in vivo* regulator of translation, we found DJ-1 protein associates with RNA transcripts for selenoproteins, PTEN/Akt pathway components and mitochondrial subunits of complex 1. Protein levels for a number of these transcripts were altered in PD tissue without any parallel change in mRNA levels. DJ-1 is reportedly involved in a diverse range of cellular activities and its proclivity to associate with multiple RNA species provides a simple biochemical mechanism for this. Moreover it demonstrates that under conditions of elevated oxidative stress, DJ-1 can instigate a rapid and compartmentalised up-regulation of pro-survival proteins in a transcriptionally independent manner.

Analysis of DJ-1 in tauopathies showed co-localisation with 3R and 4R tau, implicating a possible chaperone function for DJ-1. Unlike in PD, no altered expression of DJ-1 mRNA and protein was observed.

Together, these findings suggest the neuroprotective activity of DJ-1 is compromised in PD and delineates a role for DJ-1 as a rapid response protein that is crucial to maintaining mitochondrial functioning and combating oxidative stress, two instrumental factors in the development of neurodegenerative disorders.

# Acknowledgements

Firstly I would like to thank my principle supervisor, Dr Rina Bandopadhyay for providing an exciting research project. She has been a great mentor and I am deeply grateful for all the encouragement, guidance and support she has provided over the last few years. I am also indebted to Prof. Andrew Lees, my secondary supervisor and Director of the Reta Lila Weston Institute of Neurological Studies, for providing me with a stimulating and enjoyable environment to work in. Thanks are also given to the Reta Lila Weston Trust, Parkinson's Disease Society and Spring for financial support.

I am also grateful to all the staff and lab colleagues at the Reta Lila Weston Institue and Queen Square Brain Bank. I would especially like to thank Dr Tammaryn Lashley for all the help with tissue sectioning and immunohistochemistry. Special thanks also to Dr Connie Luk, Dr Jana Vandrovcova and Dr Alan Pittman for not only their technical support, but also for the welcomed distractions they provided. Thanks are also given to Linda Kilford, Simone Sharma and Alan Renton for help with tissue collection and RNA extractions. I am also grateful to all other colleagues and friends at Wakefield Street for the fond memories they have left me with.

Thanks are also due to collaborators and staff at the Cell Biology and Gene Expression Unit for taking me under their wing during my visit, which was generously funded by a Bogue Fellowship. In particular, Dr Mark Cookson, Dr Marcel van der Brug and Dr Jeff Blackinton for helping me get to grips with novel and exciting techniques in the lab and local beverages at Rockbottom.

I am also especially grateful to all the patient donors and their families, without whom none of this would have been possible.

Lastly, I express my warmest gratitude and love to my family and friends especially to Tejal Patel to whom I am deeply indebted to for her constant words of encouragement and selfless act of proofreading this thesis.

# Publications arising from this thesis

DJ-1 (PARK7) is associated with 3R and 4R tau neuronal and glial inclusions in neurodegenerative disorders.

Kumaran R, Kingsbury A, Coulter I, Lashley T, Williams D, de Silva R, Mann D, Revesz T, Lees A, Bandopadhyay R.

Neurobiol Dis. 2007 Oct;28(1):122-32.

Post-transcriptional regulation of mRNA associated with DJ-1 in sporadic Parkinson disease.

Blackinton J, Kumaran R, van der Brug MP, Ahmad R, Olson L, Galter D, Lees A, Bandopadhyay R, Cookson MR.

Neurosci Lett. 2009 Mar 6;452(1):8-11.

Differential DJ-1 gene expression in Parkinson's disease

Kumaran R, Vandrovcova J, Luk C, Sharma S, Renton R, Wood N, Hardy J, Lees A, Bandopadhyay R.

Neurobiol Dis. 2009 (In press).

# Contents table

# List of figures

# List of tables

# List of abbreviations

2DGE = 2-dimensional gel electrophoresis

3R = 3 repeat

4R = 4 repeat

6-OHDA = 6-hydroxydopamine

ABC = Avidin-biotin complex

AD = Alzheimer's disease

ADP = adenosine diphosphate

ALS = Amyotrophic lateral sclerosis

AR = Androgen receptor

aRNA = antisense RNA

ASK1 = Apoptosis signal-regulating kinase 1

ATP = adenosine triphosphate

B2M = β-2-microglobulin

BAD = Bcl-2-associated death promoter

BAX = Bcl-2-associated X protein

BBB = Blood-brain barrier

BCA = Bincinchoninic acid

BSA = Bovine serum albumin

CAP1 = Contraceptive associated protein 1

CBD = Corticobasal degeneration

CL = Cleared lysate

Con = Control

CNS = Central nervous system

D2R = D2 dopamine autoreceptors

DAB = Diaminobenzidine

DAT = Dopamine transporter

DFCM = Double fluorescent confocal microscopy

DJBP = DJ-1 binding protein

DNP = 2,4-dinitropheylhydrazine

DTT = Dithiothreitol

ECL = Enhanced chemilluminescent substrate

ELISA = Enzyme-linked immunosorbent assay

ETC = Electron transport chain

F. cortex = Frontal cortex

FPLC = Fast protein liquid chromatograpy

FR = Free radical

FTLD = Frontotemporal lobe dementia

GPx = Glutathione peroxidase

HD = Huntington's disease

HSP = Heat shock protein

IP = Immunoprecipitation

IPD = Idiopathic PD

IR = Immunoreactivity

JNK = Jun N-terminal kinase

KO = Knockout

LB = Lewy body

LRRK2 = Leucine-rich repeat kinase 2

Maneb = Ethylenebisdithiocarbamate

MAP = microtubule-associated protein

MAPK8IP1 = Mitogen-activated protein kinase 8 interacting protein 1

MAPT = microtubule-associated protein tau

MPP+ = 1-methyl-4-phenylpyridine

MPTP = 1-methyl-4-phenyl-1,2,3,6-tetrahydropyridine

MS = Multiple sclerosis

ND1 = NADH dehydrogenase subunit 1

ND2 = NADH dehydrogenase subunit 2

ND4 = NADH dehydrogenase subunit 4

ND5 = NADH dehydrogenase subunit 5

NFL = Neurofibrillary lesion

NFT = Neurofibrillary tangle

Nrf2 = NF-E2-related factor 2

NT = Neuropil thread

OCB = Oligodendroglial coiled bodies

p53 = Protein 53

PB = Pick body

PBS = Phosphate buffered saline

PBS-Tw = PBS tween

PD = Parkinson's disease

PHL = Paired-helical filament

pI = Isoelectric point

PI3'K = Phosphatidylinositol 3' kinase

PIAS = protein inhibitor of activated STAT

PIC = Protease inhibitor cocktail

PiD = Pick's disease

PINK1 = PTEN-induced kinase 1

PPP2R2C = Protein phosphatase 2, regulatory subunit B, gamma isoform

PSF = Protein-associated splicing factor

PSP = Progressive supranuclear palsy

PTEN = Phosphatise and tensin homologue on chromosome 10

QSBB = Queen Square Brain Bank

RBP = RNA-binding protein

RNAi = RNA interference

ROS = Reactive oxygen species

RS = Regulatory subunit

RT = room temperature

SDS = Sodium dodecyl sulphate

SDS-PAGE = SDS polyacrylamide gel electrophoresis

SEPHS2 = Selenophosphate synthetase 2

SEPW1 = Selenoprotein W1

SF = Straight filaments

TA = Tufted astrocytes

TAE = Tris-acetate EDTA

TBS = Tris buffered saline

UCLH1 = Ubiquitin C-terminal hydroxylase L1

UPS = Ubiquitin protease system

WT = Wild-type

# 1. Introduction

# 1.1. Parkinson's disease

In 1817 James Parkinson, an English physician, published a monograph "An essay on the Shaking Palsy" which eloquently described the clinical features of a disease he called "paralysis agitans" based on his observations of 6 patients (see Parkinson, 2002 for latest reprint). This medical classic contains chapters describing observed clinical symptoms, his differential diagnosis and educated guesses as to its aetiology and possible treatments. He wrote this in order to draw the attention of the scientific and medical community to what he thought was a poorly characterised and often unrecognised disease in the hope that they would investigate it further. Unfortunately it was only after the work of the famous French neurologist Jean-Martin Charcot who named the disease after James Parkinson that significant progress was made, enabling better diagnosis and treatment of patients. Today Parkinson's disease (PD) is acknowledged as the second most common human neurodegenerative disorder after Alzheimer's disease (AD). It affects 0.5-1% of the population aged over 65, rising to 1-3% of those aged over 80 (de Lau and Breteler, 2006; de Rijk et al., 2000). With the ever increasing aged population, particularly in the western world, the incidence rate is steadily rising and thus furthering our knowledge of the disease becomes ever-more important. With this in mind millions of pounds are currently being poured into research to better our overall management of this phenomenon. It is nearly 200 years since James Parkinson started the journey towards understanding this disorder and though initially others were slow to pick up the torch, our knowledge has progressed a great deal particularly over the last 10-15 years and with the emergence of new technologies this is sure to continue in leaps and bounds with the ultimate goal of creating novel treatments becoming more plausible.

## 1.1.1. Clinical symptoms

Though only based on his observation of 6 individuals, 3 of whom were observed at a distance, James Parkinson summed up the major symptoms of paralysis agitans as follows:

> "Involuntary tremulous motion, with lessened muscular power, in parts not in action and even when supported; with a propensity to bend the trunk forward, and to pass from a walking to a running pace: the senses and intellects being uninjured." (Parkinson, 1817)

Thus he recognised that the pathognomonic symptoms of this disease were the gait disorder and tremor and that the resting tremor could differentiate paralysis agitans from other tremors (Finger, 1994). He describes the long duration and the progressive nature of the ailment; starting with minor inconveniences before developing into major disabilities. So detailed were his notes that sleep disorder, problems with speech and constipation were also mentioned (Parkinson, 2002).

In the 1860's, Jean-Martin Charcot, the famous French neurologist and professor of anatomy, with the aid of his colleague Alfred Vulpian expanded and refined Parkinson's clinical description. Together they worked at the famous Salpêtrière hospital in Paris, France and sought to put an end to the clinical confusion between multiple sclerosis (MS) and paralysis agitans, both of which featured prominent tremors. Using novel and ingenious techniques Charcot was able to discern that tremors instigated by movement where characteristic of MS whilst resting tremor alongside rigidity, slowness of movement and balance difficulties described paralysis agitans. Through further work on tremors, Charcot was able to show that resting tremors were often, though not always; a symptom of paralysis agitans and that akinesia was not due to rigidity, tremor or muscle weakness. Thus he felt the term 'paralysis agitans' was a misnomer and relabelled it 'la maladie de Parkinson's' (Parkinson's disease) and detailed its cardinal features as tremor at rest, rigidity, bradykinesia and stance, posture and gait abnormalities (Fig. 1.1) (reviewed in Factor and Weiner, 2008)

Almost 150 years later these same motor symptoms are crucial to the diagnosis of PD, however they are the foundation and by no means make up the whole picture. With the complexity of PD better understood a wide range of secondary symptoms are today taken into consideration. These include autonomic symptoms: sexual dysfunction, constipation and various sleep disorders as well as neuropsychiatric symptoms like dementia and depression (discussed in Chaudhuri KR and Y., 2008). A number of these non-motor symptoms such as depression, anxiety, anosmia and sleep disturbances have been shown to precede the onset of motor symptoms. It is thought that alterations in the sense of smell are one of the earliest indicators of PD and occur years before any clinical diagnosis (Berendse et al., 2001; Tissingh et al., 2001). The importance of non-motor symptoms is

reflected in their inclusion in the Movement Disorder Society's unified Parkinson's disease rating scale (Goetz et al., 2007). With PD now encompassing a broader and more diverse range of symptoms greater emphasis is being placed on studying its pathogenesis in order to decipher the underlying mechanisms.

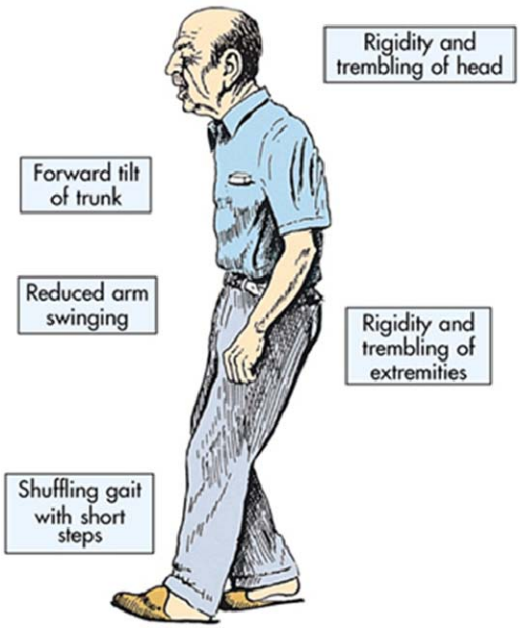


**Figure 1.1: Cartoon illustrating a selection of Parkinson's disease motor symptoms** (reproduced from http://www.enza-kr.com/nzaierbb/system/img_files/parkinsonsdisease.jpg)

## 1.1.2. Understanding PD: a history

In James Parkinson's original paper he hypothesized that PD was a disease of the central nervous system (CNS), particularly of the brainstem and upper cervical spine. As he saw no changes to his patients senses or intellect, he reasoned that any damage did not extend to the cerebral cortex (Parkinson, 2002). Even Charcot found no basis for the disorder and considered it a neurosis i.e. a disorder that possesses no proper lesions, brought about from exposure to excessive damp, cold and emotions. A link to the basal ganglia was suggested by Theodor Meynert who showed in 1871 a case where shrinkage of the corpus striatum and lenticular nucleus on one side of the brain accounted for severe tremors on the other side of the body. This was narrowed down in 1894 when Edward Brissaud, a former student of Charcots, stated that the "the locus Niger might well be its anatomical substratum". He

reached this conclusion after carrying out a post-mortem on a PD patient who had a tuberculoma in the substantia nigra (reviewed in Finger, 1994).

The next major breakthrough arrived in 1912 when Frederic Lewy initially described spherical intracytoplasmic eosinophilic inclusion bodies in the dorsal motor nucleus of vagus and substantia innominata of Meynert in the basal forebrain (reviewed in Holdorff, 2002). He later found these pathological inclusion bodies throughout the CNS, but predominantly in basal ganglia and brain stem. His original description of these inclusion bodies was as a 'dense core' enveloped in a 'glassy transparent and lighter stained cytoplasmic sheath' now commonly referred to as the body and halo structure (Gibb et al., 1991).

Frederic Lewy was unable to initially find lesions in the substantia nigra of his cases and it was left to Konstantin Trétiakoff in 1919 to report the presence of inclusion bodies he called 'Corps de Lewy' (Lewy bodies) in this region (Holdorff, 2002). For a while the importance of the substantia nigra in PD was debated. However the majority of evidence produced post 1925 supported the strong association between lesions of the substantia nigra and PD. This included work demonstrating shrinkage of the pigmented cells, chromatolysis and the almost exclusive termination of nigral processes in the lenticular nucleus of corpus striatum meaning any nigral damage would diminish the influence the striatum had on corticospinal pathways resulting in the clinical signs of rigidity and tremor (Finger, 1994). Lesions in the nigra and the presence of Lewy bodies (LBs) were soon listed as the definitive criteria for the definition of PD (Factor and Weiner, 2008; Greenfield and Bosanquet, 1953).

Since its discovery the LB remains a focal point in understanding PD and it was hypothesised that they form from altered neurofilaments when ultrastructural studies revealed it was composed of a dense granular centre and a radially arranged fibrillary periphery (Roy and Wolman, 1969). Interestingly, staining of cortical LBs reveal that they lack the characteristic halo of their brainstem counterparts (Fig. 1.2). Immunohistochemistry has shown neurofilaments and ubiquitin to be consistently present within LBs (Goldman et al., 1983; Kuzuhara et al., 1988). However it was not until 1997 that the main component of LBs was found to be α-synuclein (Spillantini et al., 1998; Spillantini et al., 1997). To date over 70 proteins have been identified to reside within LBs (Wakabayashi et al., 2007). LBs are

generally restricted to the somata of nerve cells, but thread like inclusions termed Lewy neurites (LN) can be found within the cellular processes.

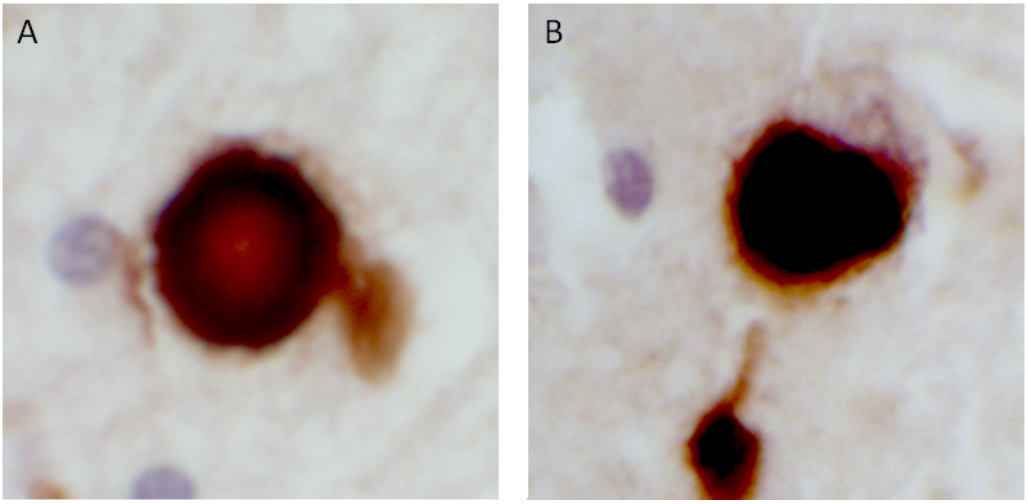


**Figure 1.2: Lewy bodies stained with α-synuclein.** A) Classic lewy body with core and halo from PD midbrain. B) Cortical lewy body from frontal cortex of PD patient.

The link between the nigral pathology and PD symptomology was cemented in the 1950s and 60s with the identification of dopamine (Carlsson et al., 1958; Raab and Gigee, 1951). It was demonstration to be highly concentrated in the striatum (Bertler and Rosengren, 1959; Carlsson et al., 1958; Sano et al., 1959) and that its levels are decreased in the caudate striatum of PD patients positively correlating with nigral cell loss (Ehringer and Hornykiewicz, 1960). From these findings the nigrostriatal dopaminergic pathway was established and became the primary focus for PD research.

## 1.1.3. Modern day neuropathology of PD

### 1.1.3.1. Neuropathology of nigrostriatal dopaminergic pathway

Dopaminergic neurons of the substantia nigra have a characteristically black appearance macroscopically (Fig. 1.3), due to the intracellular presence of melanin which in Greek means black. It is this substance which gives the substantia nigra its name: meaning black substance in Latin. By the time the clinical symptoms of PD manifest, approximately 50% of these neurons in the nigra are lost, with the pattern of cell death specific to PD pathology

(Fearnley and Lees, 1991). Neuronal loss is more concentrated within the ventro-lateral regions of the nigra compared to the dorsal-medial areas and this pattern is mirrored in the appearance of LBs (Gibb et al., 1991). Processes from the ventrolateral regions of the nigra extend into the dorsal putamen and in line with the increased degeneration, a greater degree of dopamine depletion is observed here when compared to the caudate, which receives projections from the medial nigra. Reasons for the increased susceptibility of ventrolateral nigral dopaminergic neurons to cell death have been suggested to include higher cell density (Gibb, 1992) and levels of dopamine transporters (Gonzalez-Hernandez et al., 2004). One interesting difference between the two is that the neurons in the ventrolateral areas contain smaller amounts of neuromelanin though it remains to be seen whether neuromelanin is protective or toxic (Gerlach et al., 2003; Zecca et al., 2008a).

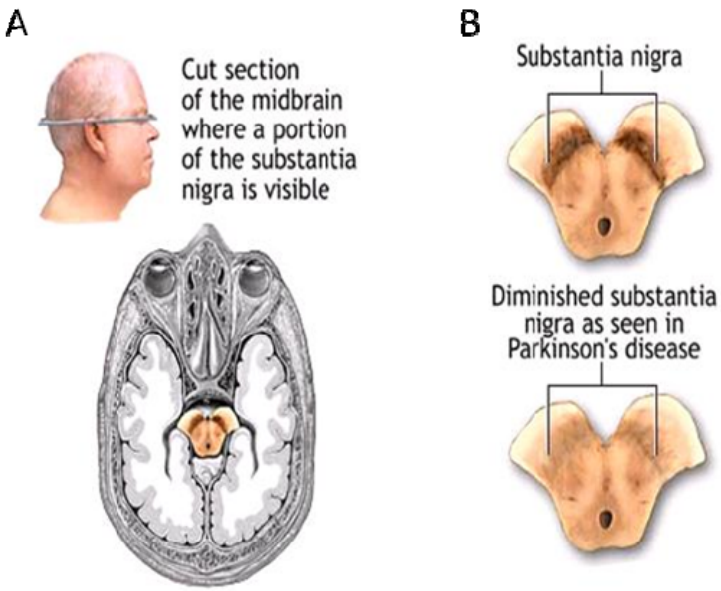


**Figure 1.3: Loss of pigmented neurons in PD substantia nigra.** A) Cross section of midbrain showing substantia nigra. B) substantia nigra from control and PD individual showing severe loss of pigmented dopaminergic neurons.
(Image kindly provided by Dr Mark Cookson, NIH)

## 1.1.3.2. Neuropathology of other brain areas

Though the nigra seems to have stolen the spotlight with regards to PD pathology, lesions are seen in multiple brain areas. The discovery of α-synuclein within PD inclusions has

enabled neuropathologists to map out a route for PD pathology progression. Based on the presence of LBs and LNs, Braak and colleagues have proposed that PD neuropathology exhibits a caudorostral spread with the earliest pathological changes occurring in the anterior olfactory, locus ceruleus and dorsal motor nuclei (seen as preclinical symptoms). It then progresses up the brainstem into the medulla and pons (associated with rapid eye movement disorder) before revealing itself as classical motor symptoms via damage to the nigra/striatum (Braak et al., 2003). These encompass the first three phases of Braaks stages of PD-related pathology (Fig. 1.4). The remaining three deal with the spread of the degenerative process into the higher order centres of the mesocortex and neocortex (Braak et al., 2004)

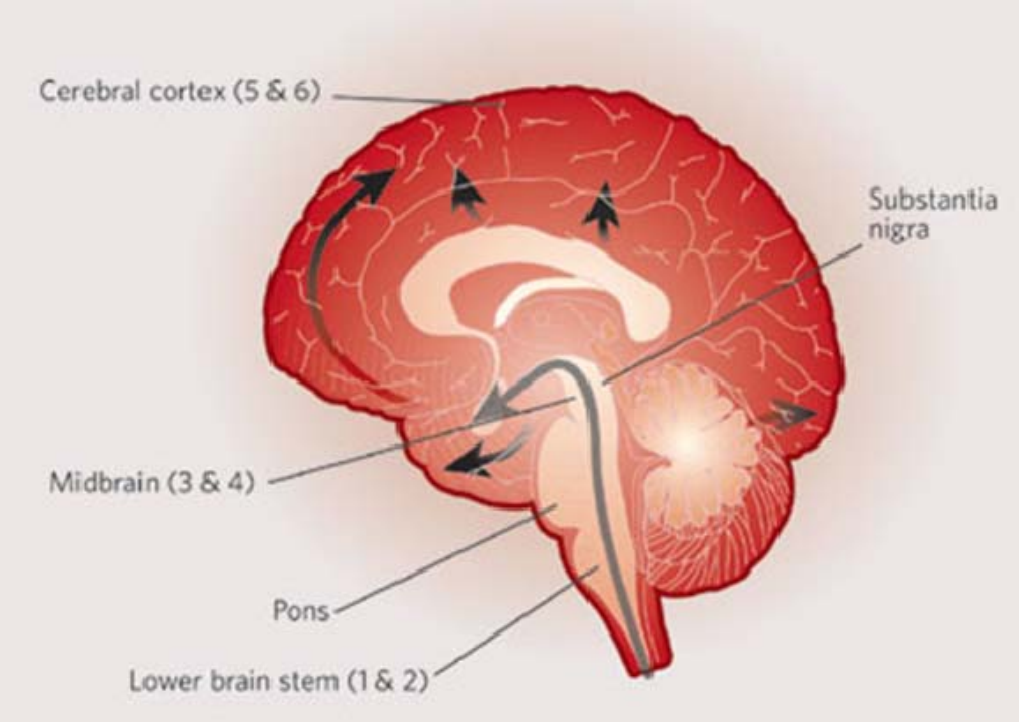


**Figure 1.4: Braak staging of PD based on appearance of Lewy body pathology.** Stages 1 and 2 describe early pathology in lower brainstem regions including dorsal motor nucleus, locus ceruleus and anterior olfactory nucleus. Pathology then ascends into the midbrain with the substantia nigra affected in stage 3 before spreading into the amygdala and basal forebrain (stage 4). The limbic cortices and frontal cortex become afflicted in stage 5 and stage 6 sees the pathology affect the parietal cortex (primary motor and sensory cortex).
(Reproduced from Abbott, 2005)

#### 1.1.3.2.1. Braak stages 1-3: subcortical neuropathology

Within the CNS, the first inclusion bodies occur in the dorsal motor nucleus of the vagus nerve, the olfactory bulb and the anterior olfactory nucleus (Braak et al., 2004). Degeneration of the olfactory bulb is likely to be behind the impairment of smell that afflicts PD patients (Shah et al., 2008). The dorsal motor nucleus is connected to autonomic function and pathology in this area probably gives rise to the clinical manifestations of drooling and swallowing difficulties. Stage 2, sees the degenerative process spread to the areas that work together to form the "gain/level setting" system including the locus ceruleus, the lower raphe nucleus and the magnocellular portions of the reticular formation (Braak et al., 2004). The level setting system receives inputs from limbic and motor systems and is able to limit the sensation of pain during times of stress and places the motor neurons in a heighten state of preparedness for action (Braak and Del Tredici, 2009). Damage to these areas may therefore disconnect the patients actions from their emotional state. Stage 3 sees the pathology enter the substantia nigra giving rise to the typical features of PD. Other areas affected include the tegmental peduculopontine nucleus and the magnocellar nuclei of the basal forebrain, both of which contain cholinergic neurons (Braak et al., 2004). Together with the serotonergic neurons of the raphe nuclei, they may account for the sleep disturbances associated with PD (Braak and Del Tredici, 2009).

#### 1.1.3.2.2. Braak stages 4-6: limbic and cortical neuropathology

Following on from stage 3, Lewy pathology ascends into the amygdala and other regions of the limbic system like the entorhinal cortex and hippocampus (Braak et al., 2004). These mesocortical regions also experience a decrease in cholinergic innervation due to the severe cellular loss in the basal nucleus of Meynert (part of magnocellular nuclei). Collectively, these regions are associated with cognitive function and memory and the emergence of pathology her provides a rationale for the cognitive decline, dementia, hallucinations and autonomic dysfunction experienced by patients (Braak et al., 2003; Chaudhuri KR and Y., 2008; Factor and Weiner, 2008). It is not uncommon for AD pathology to be found in these regions which would further contribute to the development of these clinical features (Braak and Del Tredici, 2009; Jellinger, 2006).

In stages 5 and 6, PD pathology extends into the cingulate gyrus and frontal cortex before spreading into the primary motor and sensory cortex (Braak et al., 2003; Braak et al., 2004). Given time pathology spreads throughout the neocortex in an anterior to posterior direction, with the least pathology in the occipital cortex. By this stage, the full scope of clinical symptoms is expressed by the patient.

#### 1.1.3.2.3. Limitations of Braak's staging system

Though a number of independent groups have verified the caudo-rosteral progression of LB pathology in PD (Halliday et al., 2008; Jellinger, 2004), a number of other studies have reported that not all cases follow this pattern (Attems and Jellinger, 2008; Kalaitzakis et al., 2008b). According to Braak and colleagues, LB pathology begins to appear in the dorsal motor nucleus of the vagus nerve (Braak et al., 2003), however between 7-10% of cases show no evidence of staining in this region (Kalaitzakis et al., 2008a). Furthermore some cases such as homoxygous Parkin mutations do not display LB pathology in the substantia nigra or locus ceruleus (Pramstaller et al., 2005). There is also increasing evidence suggesting that LB pathology begins in the spinal cord or even in enteric nerve cell plexuses (Hawkes et al., 2007; Kalaitzakis et al., 2008a).

Another staging system that is commonly used alongside Braak staging is the McKeith protocol (McKeith et al., 2005). Like Braak's staging system, this does not take into consideration pathology within the peripheral nervous system. It does however recognise that LB pathology is not always found in every region described by Braak and instead looks at α-synuclein pathology across larger anatomical areas. Thus cases are simply labelled as possessing pathology in Brainstem, Limbic or Neocortical areas.

### 1.1.3.3. Neuropathology of glial cells

In addition to neurons, glial cells can also exhibit various degrees of pathology in PD brain. All three types of glial cells: astrocytes, oligodendrocytes and microglia are likely to be involved in one of two ways; either reacting to existing pathology or being directly affected

by the pathology themselves with evidence to support both (for review see McGeer and McGeer, 2008)

With the seclusion from the rest of the body by the blood-brain barrier, the CNS is protected from the majority of infectious agents that enter the rest of the body. For any that do cross the blood-brain barrier (BBB), it is the role of the microglia to act as the first and main line of defence. They are constantly active, scanning their extracellular environment within the CNS for infectious agents, cytokines, signalling molecules, damaged neurons and plaques (Nimmerjahn et al., 2005). In PD, activated microglia have been found in multiple regions, including the nigra (Wilms et al., 2003). Neuromelanin has been shown to attract microglia. This suggests that microglia act as a protector to dopaminergic neurons in the nigra under normal conditions (Wilms et al., 2003). However in the presence of aggregated α-synuclein activated microglia and their inflammatory components could actually be neurotoxic to dopaminergic neurons (Croisier et al., 2005; Zecca et al., 2008b; Zhang et al., 2005b). This may explain why the typical age of onset for PD in patients who have 3 copies of α-synuclein gene is in the fifties (Chartier-Harlin et al., 2004) whilst it is in the thirties for those that express 4 copies (Singleton et al., 2003). Regular consumption of ibuprofen and anti-inflammatories has been shown to be associated with a 35% lower risk of developing PD (Chen et al., 2005a), possibly by curbing the inflammatory action of microglia. Thus the precise role of microglia and any contribution to PD pathogenesis remains to be clarified.

Astrocytes characteristically thought of as support cells, can also partake in immune/pro-inflammatory responses within the CNS (McGeer and McGeer, 2008) and are then known as reactive astrocytes. Staining of astrocytes with α-synuclein has revealed the presence of positive inclusion in PD brain, though surprisingly a minimal level of reactive astrocytosis is seen within the substantia nigra (Mirza et al., 2000). Like microglia, astrocytes may have a dual role in PD. They have been reported to secrete a number of dopaminergic neurotrophic factors such as glial cell-line-derived neurotrophic factor (Chen et al., 2006; Lin et al., 1993) and brain-derived neurotrophic factor (Knott et al., 2002). Other neuroprotective activity may include increasing the activity of glutathione peroxidise (Ishida et al., 2006) and instigating antioxidant enzymes through expression of NF-E2 related factor (Nrf2) (Jakel et al., 2007). On the other hand, reactive astrocytes can also attract microglia to sites of injury

via the production of interleukin-6 and intracellular adhesion molecule-1 (Klegeris et al., 2008) exacerbating any present inflammatory reaction.

Oligodendrocytes (ODC), the cells that form the myelin sheath around axons have also been found to contain α-synuclein inclusions showing they can be affected by PD pathology in some manner (Shoji et al., 2000; Wakabayashi et al., 2000). There remains little literature on the involvement of ODCs in PD but interestingly ODC pathology is clearly seen in multiple system atrophy; another synucleinopathy (McGeer and McGeer, 2008).

### 1.1.4. PD aetiology

For the majority of the last century the risk of developing PD was thought to be influenced by environment factors. One of the earliest thoughts was that PD resulted from viral infection. This was based on a number of cases where parkinsonian symptoms were caused by a viral infection and similarities between inclusion bodies with PD patients and those caused by rabies virus (Holdorff, 2002). Since then a number of epidemiological studies have shown that environmental factors such as exposure to well water, rural living and certain chemicals are associated with an increased risk of developing PD (Firestone et al., 2005; Tanner and Langston, 1990). On the other hand caffeine and vitamin consumption and smoking have been shown to have an inverse correlation with PD through as yet unknown means (Allam et al., 2004; Baron, 1986; de Lau and Breteler, 2006; Ross et al., 2000).

However, it is thought that environmental factors are unable to solely contribute to the development of PD with many believing that the genetic make-up of an individual has some role to play. Indeed since 1880 inheritance has been touted as a possible cause of PD when 2 of Jean-Martin Charcot students, Leroux and Lhirondel, recorded a familial component to PD. Since then numerous reports have arisen detailing hereditary parkinsonism including the work of Henry Mjönes who in the 1940s studied familial parkinsonism in Sweden and suggested PD was inherited in an autosomal dominant fashion with reduced penetrance (Gosal et al., 2006). Despite this, genetic research in PD remained controversial with some twin studies showing low concordance in mono and dizygotic twins (Marttila et al., 1988; Ward et al., 1983). It was only in the latter part of the last decade that the genetic

component of PD was thrown into the limelight with the discovery of the first form of familial PD caused by a missense mutation in the SNCA gene (Polymeropoulos et al., 1997). Shortly after this the protein α-synuclein which is encoded by the SNCA gene, was found to be the major component of LBs (Spillantini et al., 1997). Since then further evidence has been collected to suggest that numerous genetic loci (termed PARK loci) contribute to the aetiology of PD (Healy et al., 2004). Despite this, around 85% of all PD cases lack any genetic cause and are termed sporadic or idiopathic cases. The cause of idiopathic PD (IPD) remains for the most part unknown. But by studying the few documented cases where a cause can be identified and genetic models, it is hoped a mechanism may be identified and potential risk factors determined.

## 1.1.4.1. Environmental factors

### 1.1.4.1.1. Infectious causes of parkinsonism

A number of disorders leave people suffering from parkinsonian neurological like conditions suggesting that some infections may cause PD in at least a few cases. The basis for this includes Briassauds description of tuberculoma in the substantia nigra of a patient and the post world war one enchepalitis lethargic epidemic where thousands of survivors developed acute parkinsonism. More modern day examples include movement disorders in subsets of AIDS patients, possibly due to HIV infection of nigra and Japanese B encepalitis, which affects around 50,000 people a year in south Asia (for review see Jankovic and Tolosa, 2002). Any possible role for viral/bacterial infection in PD aetiology remains unknown and under debate (Mattson, 2004) though an animal model where viral infection results in PD-like symptoms may shed some light on this (Ogata et al., 1997).

### 1.1.4.1.2. Toxic causes of parkinsonism

A number of epidemiological studies have reported that use of pesticides and herbicides may be a risk factor of PD and that farming, rural residence, well water drinking and chronic low exposure to agricultural chemicals are all linked with an increased risk of PD (Brown et al., 2005). Additionally exposure to a number of exogenous toxins may be connected to the development of parkinsonism including trace metals, notably manganese and lead , lacquer

thinner, cyanide and organic solvents (reviewed in Watts and Koller, 2004). However any relationship between toxic exposure and the development of PD remains poorly defined and in many cases the clinical picture is not typical of LB PD. Furthermore, no specific toxin has been identified in the brain of PD patients.

Possibly the most compelling and conclusive evidence for an environmental component was discovered purely by chance in 1982. In the San Francisco Bay area, a group of young heroin addicts suddenly developed Parkinsonian symptoms (Langston et al., 1983). The source was soon identified as a contamination of a street drug with unintentionally manufactured pyridine 1-methyl-4-phenyl-1,2,3,6-tetrahydropyridine (MPTP). Though the numbers were low, all who had consumed it developed a progressive Parkinsonian disorder that has been replicated in monkeys (Burns et al., 1983). Once it crosses the BBB, MPTP is taken up by astrocytes and oxidised to its pyridinium derivative 1-methyl-4-phenylpyridine (MPP+) by glial monoamine oxidase B. This metabolite is then absorbed into dopaminergic neurons by the specific dopamine transporter (DAT). The mechanism of cell death associated with MPTP toxicity is thought to be via the inhibition of complex I of the mitochondrial respiratory chain (Watts and Koller, 2004). Thus not only did MPTP provide a link between environmental exposure and PD development, it also implicated mitochondrial dysfunction in the development of the disease. Histopathological examination of the brains of humans and primates exposed to MPTP showed severe cell loss within the substantia nigra with other regions including the striatum seemingly unaffected (Burns et al., 1983). Additionally neither showed signs of LB development; meaning they are not an accurate reflection of PD.

Interestingly another complex I inhibitor, rotenone, has been shown to induce parkinson like syndrome with both nigral degeneration and α-synuclein containing inclusion bodies when chronically administered (Betarbet et al., 2000). Rotenone is a pesticide that invokes apoptosis in low doses and necrosis in high doses when applied to rat pheochromocytoma cell lines (Hartley et al., 1994). When systemically administered, it has the ability to uniformly decrease the activity of complex I, as it does not have to rely on any specific uptake transporters (Betarbet et al., 2000). The fact that nigral dopaminergic neurons are selectively vulnerable to neurodegeneration suggests they are particularly sensitive to complex I inhibition (Betarbet et al., 2002). The presence of inclusion bodies reminiscent of

LBs in rotenone models may be due to another mechanism separate to its inhibition of complex I. Rotenone has been shown to hinder the polymerisation of tubulin into microtubules which may disrupt the clearance of other aggregated proteins like α-synuclein (Sherer et al., 2002).

Paraquat, a herbicide structurally similar to MPP+, can also cause dopaminergic cell loss (Brooks et al., 1999). Its mode of action however differs from MPTP in that it induces a specific loss of tyrosine hydroxylase (TH) positive neurons in the substantia nigra (Ossowska et al., 2006). The effects of paraquat are more severe when administered with the fungicide manganese ethylenebisdithiocarbamate (maneb). Maneb which can also induce nigrostriatal damage on its own through mitochondrial dysfunction and increased free radical formation via auto-oxidation of dopamine (Watts and Koller, 2004). 6-hydroxydopamine (6-OHDA), a hydroxylase analogue of dopamine, can also produce degeneration of the nigrostriatal system due to its preferential uptake by dopamine transporter molecules. Once inside the cell it results in the rapid depletion of dopamine and the formation of toxic quinones and reactive oxygen species (ROS) in the presence of iron (Betarbet et al., 2002). In some instances dopamine itself may be neurotoxic as its catalysis by monoamine oxidases produces hydrogen peroxides.

A number of other reports exist detailing the association of other toxins with the development of parkinsonism symptoms. Examples include exposure to carbon disulphide, carbon monoxide, cyanide and solvents such as methanol and lacquer thinner which have all been associated with the development of parkinsonism symptoms e.g. rigidity, shuffling gait, resting tremor etc (Jankovic and Tolosa, 2002; Watts and Koller, 2004). The mechanism of toxicity for these compounds include mitochondrial dysfunction, chelating to metal ions like copper and zinc and deprivation of oxygen to the brain producing anoxic injury to which the globus pallidus is particularly vulnerable (Watts and Koller, 2004).

### 1.1.4.2. Genetic causes of parkinsonism

Since the discovery of the first PD linked gene, α-synuclein (Polymeropoulos et al., 1997) studies of familial PD i.e. where a clear history of the disease is present within a family, have

become more rigorous. With the aid of family based linkage analysis, positional cloning and genome-wide association analysis this has resulted in the identification of 12 genetic loci, termed *PARK* loci and 7 genes being associated with the disorder (table 1.1).

| Locus | Gene | Inheritance | Chomosomal location | Onset | Reference |
|---|---|---|---|---|---|
| PARK 1 | SNCA | AD | 4q21 | Mid-late | Polymeropoulos et al., 1997 |
| PARK 2 | Parkin | AR | 6q25.2-q27 | Early | Kitada et al., 1998 |
| PARK 3 | N/K | AD | 2q13 | Late | Gasser et al., 1998 |
| PARK 4 | SNCA | AD | 4q21 | Late | Singleton et al., 2003 |
| PARK 5 | UCLH1 | AD | 4p13 | Mid-late | Leroy et al., 1998 |
| PARK 6 | PINK1 | AR | 1p36 | Early | Valente et al., 2004 |
| PARK 7 | DJ-1 | AR | 1p36 | Early | Bonifati et al., 2003 |
| PARK 8 | LRRK2 | AD | 12q12 | Late | Paisan-Ruiz et al., 2004 |
| PARK 9 | ATP13A2 | AR | 1p36 | Juvenile | Ramirez et al., 2006 |
| PARK 10 | N/K | AD | 1p | Late | Hicks et al., 2002 |
| PARK 11 | N/K | AD | 2q36-q37 | Late | Pankratz et al., 2002 |
| PARK 12 | N/K | X-Linked | Xq21-q25 | N/K | Hicks et al., 2002 |
| PARK 13 | Htra2 | AD | 2p12 | Late | Strauss et al., 2005 |

**Table 1.1: Gene loci associated with PD.** AD = autosomal dominant, AR = autosomal recessive and N/K = not known.

The familial cases are rare and account for approximately 5-10% of all cases (Dauer and Przedborski, 2003). A family history of PD is second only to age as a predictor of increased risk of the disease (Gosal et al., 2006). Both autosomal dominant and autosomal recessive along with X-linked modes of inheritance have been described (Toulouse and Sullivan, 2008). A dominant mode of inheritance describes the ability of an allele express its phenotype in both the homozygous and heterozygous state, meaning inheritance from a single parent is sufficient for the offspring to be affected. They often result in a "toxic gain of function" and resulting in protein aggregation. Autosomal recessive inheritance means that the offspring will be healthy provided that one normal allele is present i.e. both parents must pass on the mutated variant for the person to be affected. In this situation, it is common for both parents to have a healthy phenotype and they are termed carriers. These mutations lead to a loss of some form of neuroprotection against proteosomal or mitochondrial dysfunctions.

### 1.1.4.2.1. Autosomal dominant genes

The genes that fall under this category include SNCA, UCHL1 and LRRK2. Generally the clinical features of these cases match those presented in sporadic PD cases.

#### SNCA

In 1997, the SNCA 209G>A autosomal point mutation and subsequent A53T missense mutation in the transcribed α-synuclein proteins were identified following genome-wide linkage studies in families expressing autosomal dominant parkinsonisms (Polymeropoulos et al., 1997). The chromosomal position of the *SNCA* gene is 4q21 at the locus named *PARK1*. Since then, the following point mutations; SNCA 88G>C and SNCA 188G>A have been found to cause two missense mutations, A30P and E46K respectively (Kruger et al., 1998; Zarranz et al., 2004). It was the discovery of mutations in the α-synuclein gene that lead to the identification of α-synuclein being a major constituent of LBs (Spillantini et al., 1997). In addition to the missense mutations, genomic multiplications have also been identified recently. In 2003 Singleton et al. reported a genomic triplication of *SNCA* in an autosomal dominant early-onset PD family (Singleton et al., 2003) where four copies of the wild type (WT) *SNCA* gene was found, effectively doubling the amount of protein produced (Miller et al., 2004). Since then a number of α-synuclein duplications containing 3 copies of WT *SNCA* gene, have been found (Chartier-Harlin et al., 2004; Ibanez et al., 2004). Mutations resulting in extra copies of *SNCA* gene are labelled as *PARK4*.

α-synuclein is a 140 amino acid, natively unfolded protein that is expressed throughout the brain, but particularly enriched within presynaptic compartments (Clayton and George, 1998). Its exact function remains unknown, though it has been implicated in synaptic plasticity, vesicle dynamics and dopamine vesicular trafficking amongst other things (Farrer, 2006). The duplications and triplication mutations demonstrate that simple over-expression of WT α-synuclein is enough to induce PD in a dose-dependent manner with triplication cases displaying an earlier age of onset and severity. Over-expression promotes aggregation of α-synuclein protein and the formation of insoluble protein polymers known as fibrils as seen in LBs. Both A53T and E46K also encourage fibril formation (Choi et al., 2004) whilst the A30P mutation promotes the formation of oligomers. (Giasson et al., 1999). It remains

unclear how α-synuclein fibrils and oligomers lead to cell death. Indeed the camp remains divided over whether it is the fibrillar α-synuclein found in LBs or the oligomers that are neurotoxic or whether it depends on the disorder (Cookson, 2005; Xu et al., 2002).

### UCHL1

A year after the identification of *SNCA* mutations, the second autosomal dominant familial PD gene*, ubiquitin C-terminal hydroxylase L1 (UCHL1)*, was discovered (Leroy et al., 1998). The gene located at chromosome 4p14 has been designated *PARK5* and encodes for a deubiquitinating enzyme that cleaves ubiquitin-peptide conjugates freeing monomeric ubiquitin which are necessary for the degradation of abnormal proteins via the ubiquitin protease system (UPS) (Pickart, 2000). The missense mutation identified in the *PARK5* locus produced a I93M substitution in two German siblings (Leroy et al., 1998) No additional mutations have been reported in PD patients and the initial findings have yet to be replicated casting some doubt on the role of these mutations in PD (Healy et al., 2006; Maraganore et al., 2004). In any case if *UCHL1* is a PD gene, then *PARK5* mutations are an extremely rare cause of familial PD (Bertoli-Avella et al., 2004).

UCHL1 mutations reduce deubiquitinating activity in E. coli (Leroy et al., 1998) and lead to the death of cultured dopaminergic neurons and formation of α-synuclein positive inclusions (McNaught et al., 2002). Another mutation in the UCHL1 gene has been reported to be inversely related to PD, suggesting a protective effect (Maraganore et al., 1999) though studies regarding its association with PD remain inconclusive (Healy et al., 2006). As no post-mortem brain tissue is available the role of UCHL1 in PD pathology remains undetermined.

### LRRK2

The *leucine-rich repeat kinase 2 (LRRK2)* gene situated at the *PARK8* locus 12q12 was recently identified as the third autosomal dominant familial PD gene (Paisan-Ruiz et al., 2004; Zimprich et al., 2004). The *LRRK2* 6099 G>A (G2019S) mutation accounts for roughly 5% of familial PD and 1-1.6% idiopathic cases in the Caucasian population (Di Fonzo et al., 2005; Gilks et al., 2005; Nichols et al., 2005). In Jewish and North African Arabic population

this rises to 18-30% of PD cases (Lesage et al., 2006; Ozelius et al., 2006). To date a number of mutations have been identified including I2020T, R1441C, R1441G, T1348N and Y1699C (Morris, 2007). The occurrence of *LRRK2* mutations in sporadic cases and the high incidence and late age of onset in familial cases has made it very appealing to researchers.

The LRRK2 protein, also known as dardarin is a large 280kDa protein made up from 2527 amino acids and in sequence contains leucine-rich repeats, GTPase domain known as a ras of complex protein (ROC), a carboxy-terminal of Ras (COR), a mitogen-activated protein kinase kinase kinase (MAPKKK) domain and a WD40-repeat domain (Thomas and Beal, 2007). Its physiological role remains unknown but the variety of domains present suggests involvement in multiple functions. The point mutations that have been identified give some clue to its operations. Both the G2019S and I2020T mutations are situated at the N-terminal segment of the activation loop in the kinase domain and are associated with an increase in LRRK2 kinase activity (Greggio et al., 2006; West et al., 2005). Whilst over-expressed mutant LRRK2 led to the formation of inclusion bodies suggesting that kinase activity is needed for protein aggregation and cellular toxicity (Greggio et al., 2006). LRRK2 has been shown to reside in LBs (Zhu et al., 2006). It is thought that LRRK2's kinase activity is regulated by the GTPase ROC domain and is supported by the suppressed kinase activity due to GTP binding and hydrolysis as seen in the presence of R1441C and T1348N mutations (Ito et al., 2007; Lewis et al., 2007). Thus mutations in LRRK2 provide evidence of increased kinase activity being a major pathogenic factor in PD, but its *in vivo* substrates are yet to be identified.

#### 1.1.4.2.2. Autosomal Recessive Genes

These genes include *Parkin, PINK1, DJ-1* and *ATP13A2*. Clinically recessive forms of PD are characterised by early age of onset, slow progression and show a good response to L-Dopa (Farrer, 2006).

##### Parkin

Mutation at the *PARK2* locus, 6q25.2-q27, led to the finding of the first gene associated with autosomal recessive familial PD, the *parkin* gene in a Japanese family (Kitada et al., 1998). To date more than 100 *parkin* mutations have been reported consisting of deletions,

duplications, exonic rearrangements and point mutations, with the latter being the most common (Bonifati, 2007). Up to 50% of all early onset (<45 years) familial cases may be attributed to *PARK2* mutations (Mata et al., 2004). In cases where there is a complete loss of parkin due to a homozygous mutation, selective loss of dopaminergic neurons within the substantia nigra and locus ceruleus is evident without the presence of LBs (Hattori et al., 2000; Pramstaller et al., 2005). In the presence of compound heterozygotic mutations, cases with LB pathology have been described (Hattori et al., 2000; Pramstaller et al., 2005). These both suggest that parkin function is involved in LB formation and raises the question of whether LBs are vital for the definition of PD.

Parkin is a E3 ubiquitin ligase that catalyzes the covalent attachment of ubiquitin to target proteins thus marking them for proteosomal degradation via the UPS (Shimura et al., 2000). This activity is abolished by many *PARK2* mutations and supports the notion that accumulation of misfolded parkin substrates results in neuronal cell death in PD (Shimura et al., 2000). Identification of substrates is still ongoing but today includes a glycosylated isoform of α-synuclein, the α-synuclein interacting protein synphilin-1, the synaptic vesicle associated protein CDCrel-1 (cell division control-related protein 1) and the Pael receptor (parkin-associated endothelin-like receptor) (Chung et al., 2001; Imai et al., 2001; Shimura et al., 2001; Zhang et al., 2000). *Parkin* mutations have also been identified in roughly 15% of early onset sporadic PD cases (Bonifati, 2007). Thus *PARK2* mutations appears to be a major cause of early onset familial and sporadic PD and together with UCHL1 provide strong evidence for UPS involvement in PD pathogenesis.

### PINK1

Two homozygous mutations at the *PARK6* locus on chromosome 1p36 led to the identification of the *PTEN-induced kinase 1 (PINK1)* gene being associated with early onset familial PD (Valente et al., 2004a). Both the identified G309D missense and the nonsense truncating mutation occur in the kinase domain coding region. Thereafter a number of other homozygous and heterozygous mutations have also been identified (Abou-Sleiman et al., 2006a; Hatano et al., 2004; Rohe et al., 2004). *PINK1* mutations have also been identified as a rare cause of early onset sporadic PD with approximately 5% of cases being due to a single

heterozygous mutation despite its recessive nature (Bonifati et al., 2005; Valente et al., 2004b).

PINK1 is a ubiquitously expressed 581 amino acid protein containing both a mitochondria targeting motif and a highly conserved serine-threonine kinase domain (Silvestri et al., 2005). The PINK1 kinase is localised at the mitochondrial membrane (Gandhi et al., 2006) and plays a role in mitochondrial biogenesis. The majority of mutations occur in or around the kinase domain making it reasonable to postulate that loss of kinase activity results in PD development (Kubo et al., 2006). The serine-threonine kinase activity of recombinant PINK1 has been shown *in vitro* and this is down-regulated by the G386A and G409V mutations (Sim et al., 2006). Loss of PINK1 function *in vivo*, through expression of disease causing mutations or siRNA knockout results in mitochondrial dysfunction and consequently dopaminergic neuronal death in flies, which is interestingly saved by over-expression of *parkin* (Clark et al., 2006; Yang et al., 2006). This suggests an interaction and possibly a common pathway shared by two AR familial PD genes. It has also been reported that the *PINK1* locus is regulated *in vivo* by non-coding naturally occurring RNA implicating them for the first time in regulating familial PD genes (Scheele et al., 2007).

### DJ-1

Mutations in the *DJ-1* gene were identified in an Italian and Dutch family displaying early onset PD (Bonifati et al., 2003b). The *DJ-1* gene was labelled as PARK7 and has the same chromosome location as *PINK1* (1p36). A homozygous mutation L166P and deletion of exons 1-5 in the *DJ-1* gene are responsible for the development of PD in Italian and Dutch families respectively (Bonifati et al., 2003b). Other missense, truncating, splice site and large deletion mutations have been reported to date including a novel single heterozygous mutation in both the *DJ-1* gene and *PINK1* gene in a Chinese early onset PD family (Tang et al., 2006). This suggests a digenic inheritance and a possible functional interaction between the two PD proteins. Generally speaking, mutations in DJ-1 are quite rare and account for less than 2% of all early onset PD cases (Bonifati, 2007).

The precise function of DJ-1 remains unclear however evidence suggests it works as a chaperone (Shendelman et al., 2004) and/ an oxidative stress response protein (Mitsumoto and Nakagawa, 2001).

### ATP13A2

A homozygous and compound heterozygous mutation were identified in the *ATP13A2* gene from a Jordanian and Chilean family diagnosed with Kufor-Rakeb Syndrome, a juvenile onset parkinsonism (Ramirez et al., 2006). The *ATP13A2* gene is located in the vicinity of *DJ-1* and *PINK1* on chromosome 1p36 and its loci has been designated *PARK9*. ATP13A2 is a large lysosomal transmembrane protein with putative ATPase activity (Bonifati, 2007). The Jordanian homozygous mutation involves a duplication on exon 16 (c.1632_1653dup22) whilst the Chilean compound heterozygous mutation is a splice site mutation in exon 13 (c.1306+5G>A) and a frameshift mutation in exon 26 (c.3057delC) (Ramirez et al., 2006). A homozygotic missense mutation in exon 6 (c.546C>A) in a Japanese kindred and one in exon 15 (c.1510G>C) from a sporadic Brazilian patient with juvenile parkinsonism have also been recently identified (Vilarino-Guell et al., 2009).

The exact role for ATP13A2 is still to be elucidated though its lysosomal localisation suggests a role in lysosomal degradation. The c.3057delC mutation has been shown to promote localisation to the endoplasmic reticulum favouring the notion that lysosomal dysfunction is the underlying mechanism of *PARK9* induced PD (Ramirez et al., 2006).

## 1.2. An overview of DJ-1

DJ-1 was first identified as a novel oncogene that promoted the transformation of NIH3T3 cells in the presence of H-Ras (Nagakubo et al., 1997). Shortly afterwards contraceptive associated protein 1 (CAP1) was reported to be a rat homologue of DJ-1 involved in fertility (Wagenfeld et al., 1998). Then in 2003, following fine mapping studies and a positional cloning strategy in two PARK7 families with homozygous mutations in the DJ-1 gene, a 14kb

deletion in a Dutch family and a L166P substitution in an Italian family, were discovered as causes of AR early-onset PD (Bonifati et al., 2003b).

## 1.2.1. DJ-1 expression and localisation

### 1.2.1.1. Cellular expression

When first identified, Nagakubo et al., (1997) investigated DJ-1 gene expression using northern blotting and showed the presence of DJ-1 mRNA within a range of human tissue groups including brain, heart, skeletal muscle etc. In the human brain, higher levels of DJ-1 mRNA were found in cortical areas than in comparison to subcortical regions like the substantia nigra, caudate nucleus and thalamus (Galter et al., 2007).

Gene expression studies have been complemented by numerous reports on DJ-1 protein expression in human brain. Bandopadhyay and colleagues (2004) first characterised the cellular expression profile of DJ-1 in human brains by performing immunohistochemistry with a monoclonal antibody on frontal cortex sections. They found DJ-1 immunoreactivity (IR) to be predominantly found in astrocytes, though faint staining of a small population of neurons in both PD and control cases was also noted. A similar distribution pattern was reported in the midbrain, but to a lesser degree and with no DJ-1 positive neurons in control cases (Bandopadhyay et al., 2004). In PD midbrain though, DJ-1 weakly stained a small number of dopaminergic neurons. The group also studied DJ-1 localisation to LBs, but DJ-1 IR was found to be a very rare occurrence and only then in the outer halo, indicating DJ-1 is not a fundamental nor typical component of LBs. This pattern of strong astrocytic and weak neuronal staining was also reported in follow-up studies and elsewhere (Bandopadhyay et al., 2005; Baulac et al., 2009; Neumann et al., 2004).

A similar study was also conducted by Rizzu using tissue from a number of patients diagnosed with a variety of parkinsonism/dementia disorders. With the aid of polyclonal antibodies, the group reported moderate neuronal staining for DJ-1 in a number of brain regions and weak astrocytic IR in control tissue. Astrocytic DJ-1 IR was additionally found within the midbrain and cortical regions of PD brains (Rizzu et al., 2004). When examining

DJ-1 IR in the affected brain regions of cases labelled as tauopathies i.e. those displaying an abundance of insoluble tau aggregates, DJ-1 was seen to co-localise with tau in both neuronal and glial pathological inclusions (Rizzu et al., 2004). This hints at a role for DJ-1 in other neurological disorders, though whether the mechanisms involved are similar to those that underlie PD pathogenesis remain to be elucidated.

In mice, DJ-1 protein and mRNA expression is much more robust and is strongly expressed by neurons in both motor and non-motor brain regions (Bader et al., 2005; Kotaria et al., 2005; Shang et al., 2004). By using double labelling experiments, Kotaria et al., (2005) showed that in murine brains, DJ-1 is predominantly expressed by neurons, though DJ-1 was also found in small populations of glial cells particularly within the nigra. A similar abundant neuronal and low glial staining pattern is also observed in rat brains (Bandopadhyay et al., 2005).

A number of reasons have been presented to explain the discrepancy of data obtained from human and murine brains. These include the lack of post-mortem delay and variable tissue fixation/preservation conditions for rodent brains (Lev et al., 2007). Additionally studies on mice and rats have involved healthy animals. Indeed greater neuronal staining is seen in control human brains than pathological tissue (Bandopadhyay et al., 2004; Neumann et al., 2004; Rizzu et al., 2004). It should also be noted that different studies utilised different antibodies meaning any variation between species could be due to the recognition of different epitopes by the numerous DJ-1 antibodies. A more recent study by Olzmann attempted to address a number of these issues by comparing DJ-1 expression in brains from humans, macaque monkeys and rats using an 'in-house' DJ-1 antibody that recognises an evolutionarily conserved epitope. Their findings revealed that in the cortex, DJ-1 was largely found within neurons in rodent brains and glia in primates whilst within subcortical regions like nigra and striatum, staining was primarily neuronal for both humans and macaque in-line with rodents (Olzmann et al., 2007). This difference is unlikely to arise from fixation and/or post-mortem interval due to the similarity in staining pattern seen in human and non-human primate brains. It additionally dispels any notion of variation in DJ-1 expression being due to differences in epitopes and instead suggests an actual species difference (Olzmann et al., 2007).

### 1.2.1.2. Subcellular localisation

Within cells, subcellular distribution studies performed on over-expression models showed DJ-1 to be predominantly localised to the cytoplasm and nucleus of a number of cell lines e.g. COS, M17 and Hela cells (Blackinton et al., 2005; Bonifati et al., 2003b; Macedo et al., 2003; Miller et al., 2003; Nagakubo et al., 1997). These *in vitro* models also showed small amount of DJ-1 in the mitochondria, with levels rising under stress conditions (Blackinton et al., 2005; Canet-Aviles et al., 2004; Miller et al., 2003). Subcellular fractionation and immunogold electron microscopy of mouse brain has shown the presence of an endogenous pool of DJ-1 within the mitochondrial matrix and inter-membrane space (Zhang et al., 2005a)

## 1.2.2. Structure of DJ-1 protein

In humans the DJ-1 gene is located on chromosome 1p36. It spans 24kb and contains 8 exons, the first two $1^a$ and $1^b$ being non-coding and alternatively spliced. The encoded DJ-1 protein is 189 amino acids in length and has been highly conserved throughout evolution and is present in a diverse range of species (Nagakubo et al., 1997). The structure of DJ-1 was originally predicted using computer assisted molecular models based on a bacterial homologue, PH1704 protease (Bonifati et al., 2003b). Gel exclusion chromatography performed with epitope-tagged WT DJ-1 transfected into Hela or Cos cells and followed by SDS-PAGE analysis showed DJ-1 to be eluted at fractions corresponding to a molecular weight range of 35-45kDa (Macedo et al., 2003; Miller et al., 2003). This range is approximately double the 19.9kDa molecular weight of DJ-1 monomer as predicted by Bonifati et al., (2003) and suggests that DJ-1 exists as a dimer under physiological conditions.

Since then, the structure of DJ-1 has been studied in more depth and independent groups have reported the crystal structure of both the monomer and dimer (Honbou et al., 2003; Lee et al., 2003; Tao and Tong, 2003). As a monomer, DJ-1 consists of eight α-helices and 11 β-strands arranged asymmetrically in a helix-strand-helix sandwich (Huai et al., 2003; Wilson et al., 2003). This is similar to a Rossman fold (Honbou et al., 2003). Dimerisation of DJ-1 is

formed by 8 pairs of hydrogen bonds and numerous van der Waal's interactions (Huai et al., 2003).

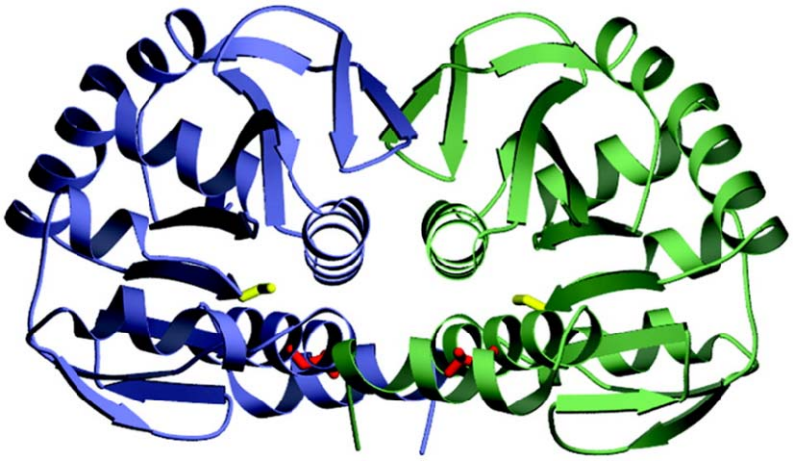

**Figure 1.5: Ribbon representation of the DJ-1 dimer.** One monomer is coloured blue and the other is green.
(Reproduced from Wilson et al., 2003)

## 1.2.3. Exploring the functions of DJ-1

Crystallographic analysis of DJ-1 structure provides certain clues to possible roles for DJ-1. Its homologue PH1704 displays proteolytic activity at a conserved cysteine residue. DJ-1 also has a highly conserved cysteine residue, C106 suggesting a possible role as a protease (Honbou et al., 2003; Huai et al., 2003; Lee et al., 2003). However, the key "catalytic triad" of Cys-His-Glu located in the active site of PH1704 is missing in DJ-1, with C106 instead being neighboured by Ala107 (Huai et al., 2003). Rather than lending itself to proteolytic activity, the yeast homologue of DJ-1, YDR533c is up-regulated in response to oxidative stress (Lee et al., 2003) hinting at a possible role as a ROS scavenger/antioxidant protein. The C106 residue in DJ-1 is able to undergo oxidation which would enable it to fulfil this function (Wilson et al., 2003). PH1704 is a member of the THij/Pfpi superfamily of proteins. These include chaperone proteins like heat shock protein 31 (HSP31) which have also been noted to be structurally similar to DJ-1 (Lee et al., 2003). Indeed dimerisation of DJ-1 produces a hydrophobic patch at the molecular interface, characteristic of chaperone proteins sites of interaction with non-native proteins (Lee et al., 2003). As of yet, the precise role of DJ-1 is

still undetermined, however numerous studies have implicated it in a variety of biological processes.

### 1.2.3.1. DJ-1 and cancer

DJ-1 has been implicated in cancer ever since its discovery in 1997, during Nagakubo and colleagues investigations of NIH3T3 cell transformation. Further study showed that when co-transfected with the oncogene H-Ras, the transforming activity of DJ-1 was greatly enhanced and suggested an involvement in Ras-related signal transduction mechanisms (Nagakubo et al., 1997). The transforming abilities of DJ-1 can also be stimulated by Abstrakt, a RNA helicase that co-localises and binds to DJ-1 in the nucleus (Sekito et al., 2005).

DJ-1 has also been shown to have increased expression in a variety of cancers (Kim et al., 2005a; MacKeigan et al., 2003; Pardo et al., 2006) and is a good biomarker in breast cancers with patients showing elevated levels of anti-DJ-1 auto-antibodies when compared to controls (Le Naour et al., 2001). DJ-1 is also capable of suppressing the activities of PTEN (phosphatise and tensin homologue on chromosome 10), which is one of the most mutated suppressor genes associated with human cancers (Kim et al., 2005a). The activity of protein 53 (p53), another tumour suppressor which regulates the cell cycle, also appears to be modulated by DJ-1 though in what manner is unclear. When overexpressed *in vitro,* DJ-1 can free sumoylated p53 that has been inactivated by topors (Shinbo et al., 2005). However, a similar up-regulation of p53 has also been observed in DJ-1 knockout (KO) zebrafish (Bretaud et al., 2007).

### 1.2.3.2. DJ-1 and fertility

Other early studies also described a role for DJ-1 in male fertility. CAP1 is the rat homologue of DJ-1 and Wagenfeld et al., (1998) showed CAP1 levels in rat epididymal fluid to be positively correlated with male rat infertility. Lower levels of CAP1 were also confirmed in the sperm and epididymis of rat following treatment with spermicide (Klinefelter and Suarez, 1997; Wagenfeld et al., 1998; Yoshida et al., 2003). DJ-1 is also reported to be

capable of affecting sperm production through activation of androgen receptor (AR) that is involved in the development, growth and regulation of male reproductive function. Using yeast two hybrid screening of human testis cDNA identified PIAS-α (protein inhibitor of activated STAT) as a DJ-1 interacting protein (Takahashi et al., 2001). PIAS-α can inhibit AR activity in a dose-dependent manner in co-transfected monkey CV1 cells, but the introduction of DJ-1 into the cells prevents this. A number of proteins in the PIAS family are SUMO E3 ligases which act as modulators of transcriptional activity and Takahashi and colleagues hypothesized that PIAS-α in particular inhibited the transcriptional activity of AR by binding to it. They reported that DJ-1 was able to bind to PIAS-α and remove it from AR-PIAS-α complexes, thereby restoring AR transcriptional activity (Takahashi et al., 2001).

Another negative regulator of AR transcriptional activity is DJ-1 binding protein (DJBP), which was identified by the same group a couple of years later (Niki et al., 2003). DJBP was also reported to repress AR transcriptional activity, though this time in a testosterone dependent manner via the recruitment of histone deacetylase complexes (HDAC) such as HDAC1 and mSin3. DJ-1 disrupts the DJBP-HDAC complex, thus promoting AR transcriptional activity (Niki et al., 2003). The fact DJBP is expressed solely and PIAS-α predominantly in the testis suggests that this is local function of DJ-1.

### 1.2.3.3. DJ-1 and gene expression

In addition to promoting AR transcription activity, DJ-1 may also regulate the expression of several other genes associated with oxidative stress, apoptosis and neurotoxicity. DNA microarray analysis of NIH3T3 containing DJ-1 KO or L166P DJ-1 mutations showed decreased expression of extracellular superoxide dismutase (SOD3) and an increase in tau expression respectively (Nishinaga et al., 2005).

DJ-1 may also be involved in controlling post-translational expression of a number of genes after it was reported to share an almost identical homology with a regulatory subunit (RS) that binds to a RNA-binding protein (RBP) (Hod et al., 1999). The RBP is capable of binding to RNA, a process that is inhibited when bound to a RS. The close homology of DJ-1 to RS

suggests that it too harbours RNA-binding properties and could therefore post-transcriptionally regulate gene expression (Hod et al., 1999; Siomi and Dreyfuss, 1997).

### 1.2.3.4. DJ-1 and oxidative stress

Prior to being implicated in PD, DJ-1 was reported to react to oxidative stress by becoming more acidic, as noted by a shift in its isoelectric point (pI) (Mitsumoto and Nakagawa, 2001; Mitsumoto et al., 2001). Since being associated with PD, 2-dimensional gel electrophoresis (2DGE) studies with post-mortem human control and PD brain tissue have shown an accumulation of acidic DJ-1 pI isoforms in PD cases (Bandopadhyay et al., 2004; Choi et al., 2006). A similar pattern is also seen in neuroblastoma cell lines. Exposure of M17 or SH-SY5Y to toxic agents like rotenone or $H_2O_2$ causes endogenous DJ-1 to undergo a pI shift from 6.2 to 5.8 (Bandopadhyay et al., 2004; Canet-Aviles et al., 2004; Kim et al., 2005b; Shendelman et al., 2004). The formation of more acidic isoforms suggests that DJ-1 is capable of removing ROS from cellular environments and therefore functions as an anti-oxidant (Mitsumoto and Nakagawa, 2001).

The ability of DJ-1 to act as an antioxidant may also enable it to protect against ROS induced cell death. Comparison of normal NIH3T3 cells with DJ-1 KO variant showed the latter to have a much lower cell viability following incubation with $H_2O_2$ (Takahashi-Niki et al., 2004). Transient DJ-1 KO SH-SY5Y cells were also less resistant to MPTP and $H_2O_2$ treatment (Taira et al., 2004) whilst a similar finding was seen when comparing M17 neuroblastoma cells with epitope tagged WT DJ-1 and vector transfected controls (Canet-Aviles et al., 2004). Mice primary cortical neurons cultured in a $H_2O_2$ supplement media also displayed the same phenomenon, with DJ-1 KO cells showing a 20% increase in cell death (Kim et al., 2005b). Cell viability of KO primary cortical neurons in the presence of $H_2O_2$ was increased when transfected with WT DJ-1 and further improved upon over expression of endogenous DJ-1 suggesting a gene dosage effect (Kim et al., 2005b).

The protective action of DJ-1 against oxidative stress can be abolished by mutation of the highly conserved cysteine at amino acid 106 in humans (Canet-Aviles et al., 2004; Meulener et al., 2006). Under mildly oxidising conditions, this residue forms a stable cysteine-sulfinic

acid (Wilson et al., 2003; Witt et al., 2008) which is spatially anchored by a neighbouring glutamate residue, E18. This relationship shows absolute evolutionary conservation in all PfPI family members, from bacteria to humans (Wilson et al., 2005). DJ-1 also possesses two additional cysteine subunits at C46 and C53 which can also be oxidised.

Martinat and colleagues (2004) used 2'.7'-dichlorodihydroflurescein diacetate (DCFH-DA), an indicator for the presence of hydroxyl free radical, and flow cytometry to study the ability of DJ-1 to eliminate ROS when treated with $H_2O_2$. Comparison of normal NIH3T3 and DJ-1 KO cells showed no difference in the accumulation of ROS 15 minutes post treatment with $H_2O_2$, however after 6 hours a significantly higher ROS level and increased apoptosis was seen in DJ-1 KO cells (Martinat et al., 2004). The same procedure was used to show lower accumulation of ROS in SH-SY5Y cells transiently transfected with epitope tagged WT DJ-1 in comparison to the control vector-transfected cells (Taira et al., 2004). Together these results infer that cells lacking DJ-1 are initially capable of dealing with elevated ROS levels, however long term defences against prolonged oxidative stress conditions fail to materialise suggesting DJ-1 functions in a protective role downstream of ROS insult.

Elevated sensitivity to oxidative stress has also been noted *in vivo*. Treatment of WT and DJ-1 null mice with MPTP produces a significant decrease of Tyrosine Hydroxylase (TH) positive neurons in comparison to control counterparts treated with saline. A greater loss was observed in DJ-1 null mice treated with MPTP than in WT mice, a difference that was prevented in by administration of a DJ-1 expressing adenoviral vector to DJ-1 null mice prior to treatment with MPTP (Kim et al., 2005b). Administration of MPTP to WT mice results in a measurable increase in DJ-1 oxidised at C106 (Andres-Mateos et al., 2007). Like DJ-1 null mice, KO of DJ-1 in drosophila results in increased sensitivity of flies fed $H_2O_2$, rotenone or paraquat supplemented food towards oxidative stress (Lavara-Culebras and Paricio, 2007; Meulener et al., 2005). Drosophila express two homologues of human DJ-1; DJ-1α and DJ-1β. Specific KO of DJ-1β results in an acute sensitivity to $H_2O_2$ treatment, however there is some compensatory up-regulation of DJ-1α in the brain (Menzies et al., 2005). Together these show that loss of DJ-1 increases sensitivity towards toxin induced oxidative stress.

### 1.2.3.5. DJ-1 as a chaperone

Structural similarities to HSP31 suggest that DJ-1 may function as a chaperone and the presence of a hydrophobic patch characteristic of chaperone proteins in the DJ-1 dimer complex lends support to this notion (Lee et al., 2003). Evidence of its chaperone activity has been demonstrated *in vitro* by use of chaperone assays. By measuring the suppression of heat-induced aggregation of citrate synthase and glutionione S-transferase, Shendelman et al (2004) were able to show that DJ-1 harbours mild chaperone activity *in vitro*. A separate chaperone assay, targeted towards reduced insulin, also demonstrated that DJ-1 is redox regulated and that its chaperone capabilities are abrogated in a reduced environment (Shendelman et al., 2004). The ability of DJ-1 to suppress heat-induced aggregation of citrate synthase was inhibited in the presence of the reducing agent DTT but could be restored by brief incubation with $H_2O_2$.

α-synuclein aggregation is a hall mark of PD so Shendelman and colleagues then examined DJ-1 chaperone activity toward α-synuclein protofibril formation, a precursor to natural amyloid fibril formation. They found DJ-1 was capable of inhibiting α-synuclein protofibrils formations, but only if the C106 amino acid residue of DJ-1 had been oxidised to sulfinic acid (Shendelman et al., 2004). Further oxidation of DJ-1 causes a loss of secondary structure and diminishes all chaperone activity (Zhou et al., 2006). *In vivo*, over-expression of WT DJ-1 in CAD murine neuroblastoma cells reportedly inhibited the accumulation of Triton X-100 insoluble α-synuclein that had been induced by incubation with $FeCl_2$ (Shendelman et al., 2004).

### 1.2.3.6. DJ-1 and programmed cell death

As mentioned above, DJ-1 may modulate cell apoptosis by regulating the activity of PTEN and p53 (Kim et al., 2005a; Shinbo et al., 2005). PTEN antagonises the phosphatidylinositol 3' kinase (PI3'K) pathway which regulates cell survival (Kim et al., 2005a). Inhibition of DJ-1 in drosophila using RNA interference (RNAi) followed by genetic interaction studies, showed members of PI3'K/Akt signalling pathway as specific modulators of DJ-1 RNAi-induced neurodegeneration (Yang et al., 2005). Exposure of DJ-1 KO zebrafish to $H_2O_2$ reportedly produces an up-regulation of Bax and elevation of dopaminergic neuronal cell death

(Bretaud et al., 2007). Bax induces cell death via activation of caspases and a more recent study using N2a cells has shown DJ-1 to be capable of reducing Bax levels by inhibiting p53 transcriptional activity (Fan et al., 2008b).

In neuronal dopaminergic cells two additional binding partners have been identified; pyrimidine tract-binding protein-associated splicing factor (PSF) and p54nrb (Xu et al., 2005). These nuclear proteins are multifunctional regulators of transcription and mRNA metabolism. In SH-SY5Y cells Xu and colleague (2005) showed that DJ-1 present in the nucleus can work in conjunction with p54nrb to inhibit the transcriptional silencing activity of PSF and prevent PSF induced apoptosis. KO of WT DJ-1 increased the sensitivity of cells towards PSF induced apoptosis. Additionally in collaboration with p54nrb, DJ-1 was also capable of significantly preventing apoptosis in cells exposed to $H_2O_2$ induced oxidative stress and A30P α-synuclein accumulation (Xu et al., 2005).

DJ-1 is further implicated in programmed cell death by its association with Daxx which activates Fas-mediated apoptosis and the Jun N-terminal kinase (JNK) pathway (Junn et al., 2005). Exposure to toxins promotes Daxx translocation from nucleus to cytosol, where it activates and interacts with the apoptosis signal-regulating kinase 1 (ASK1) which mediates cell death (da Costa, 2007). DJ-1 is capable of preventing this by hindering the migration of Daxx into the cytosol (Junn et al., 2005). Down regulation of DJ-1 by MPTP administration has been shown to enhance the migration of Daxx into the cytosol in mice dopaminergic neurons in the substantia nigra (Karunakaran et al., 2007). JNK1 pathway may also be activated by mitogen-activated protein kinase/extracellular signal-regulated kinase kinase kinase 1 (MEPKK1), a process that is inhibited by DJ-1 sequestering MEPKK1 within the cytoplasm as seen in human embryonic kidney 293 (HEK293) cells exposed to UV-induced oxidative stress (Mo et al., 2008). L166P DJ-1 however facilitates the translocation of MEPKK1 to the nucleus thereby promoting the JNK1 signalling cascade and cell death.

### 1.2.3.7. DJ-1 and the dopaminergic system

DJ-1 may also be involved in modulating nigrostriatal dopaminergic function. Age and task dependent motor behavioural deficits have been described in DJ-1 KO mice despite the

presence of a normal number of dopaminergic neurons in the substantia nigra (Andres-Mateos et al., 2007; Chen et al., 2005b; Goldberg et al., 2005; Kim et al., 2005b). Similarly DJ-1 null drosophila show no loss of dopamine neurons, but exhibit locomotor deficits as highlighted by their reduced climbing ability (Park et al., 2005). In mice, the cause of these motor discrepancies has been identified as an increased reuptake rate of dopamine and a consequential decrease in evoked dopamine overflow within the striatum (Chen et al., 2005b). This can be attributed to enhanced DAT activity which produces a greater tissue dopamine content than normal (Chen et al., 2005b). This may prove toxic to neurons as higher dopamine content is associated with increased cellular oxidative stress (Ben-Shachar et al., 2004; Stokes et al., 2000). DJ-1 may protect against dopamine toxicity with *in vivo* striatal administration of 6-OHDA and producing an up-regulation of DJ-1 via the MAP kinase pathway and activation of ERK 1 and 2 (Lev et al., 2009). DAT KO rodents and *C. elegans* are less sensitive to parkinsonism-inducing toxins (Chen et al., 2005b; Nass et al., 2002) suggesting loss of DJ-1 and consequential elevation of DAT function may increase vulnerability to neural toxins.

This data is supplemented by Goldberg et al., (2005) who showed the reduced evoked dopamine overflow in the striatum of DJ-1 KO mice arises from a decreased sensitivity of D2 dopamine autoreceptors (D2R). Binding of dopamine to D2R on presynaptic terminals inhibits DAT activity but in DJ-1 null mice this inhibitory action is impaired producing the observed faster reuptake of dopamine (Goldberg et al., 2005). Activation of somatodendritic D2R inhibits the firing activity of nigral dopaminergic neurons and loss of this inhibition disrupts outputs of nigrostriatal projections resulting in reduced long-term depression (LTD) induction at striatal medium spiny neurons (Goldberg et al., 2005). A similar phenomenon has been observed in the CA1 synapses in the hippocampus of mice (Wang et al., 2008).

## 1.2.4. DJ-1 and familial PD

### 1.2.4.1. Pathogenic mutations

Following the discovery of the L166P mutation and the deletion of exons 1-5 in two *PARK7* families, there was a flurry of genetic analysis involving large groups of familial and

idiopathic PD patients across the world. The aim was to establish the frequency of these two mutations in different ethnic groups and possibly identify new mutations that were not present in control cases. This work has resulted in a number of other mutations being identified to date (Fig. 1.6).

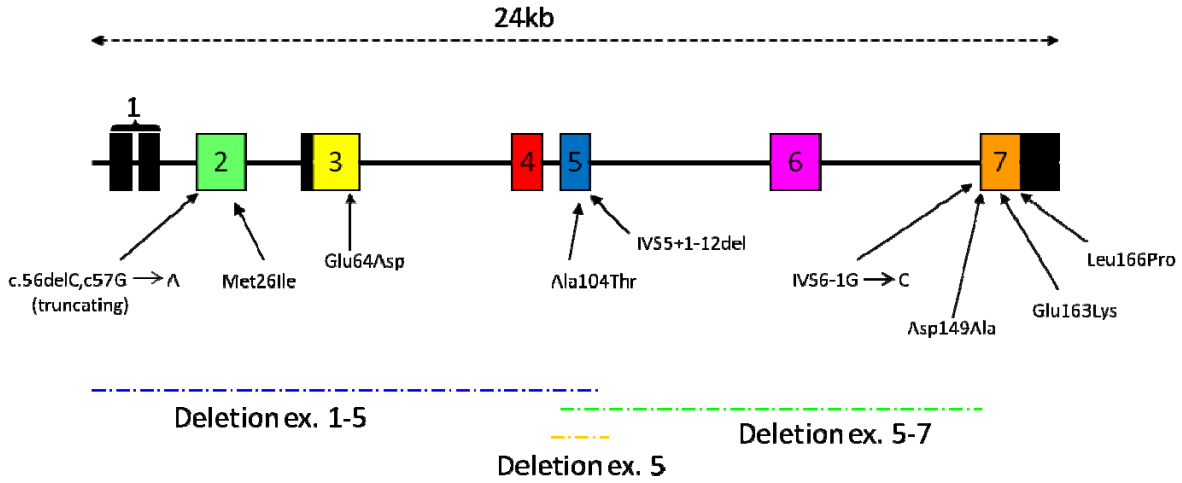


**Figure 1.6: Genomic structure of DJ-1 gene showing parkinsonian mutations.** The PARK7 locus located on chromosome 1p36 spans 24kb and encodes for 7 exons. The position of identified mutations is marked. Black boxes represent non-coding segments.
(adapted from Bonifati et al., 2004)

Study of the Hispanic population led to the discovery of a "double hit" or heterozygous compound mutations, IVS6-1G→C and c.56delC c.57G→A in early-onset patients with no previous familial history (Hague et al., 2003). The first mutation resulted in the formation of a defective transcript due to a nucleotide substitution in the splice acceptor site of intron 6. The c.56delC c.57G→A mutation is resident in exon 2 and involves both a deletion of nucleotide 56 and G→A transition at nucleotide 57, the combined outcome being a frameshift and the introduction of a premature stop codon believed to encode a cropped protein of 18 amino acids (Hague et al., 2003). Within the same population, Hague and colleagues also reported a missense mutation (A104T) in another early-onset PD patient caused by a heterozygous mutation in exon 5 (c.310G→A) (Hague et al., 2003). This mutation was also later reported in an Asian patient with early-onset PD (Clark et al., 2004).

Additional mutations were brought to light by the investigation of other groups. In an early-onset idiopathic PD patient of Ashkenazi-Jewish hereditary, a missense mutation (M26I) resulting from a homozygotic mutation in exon 2 (c.78G→A) was identified (Abou-Sleiman et al., 2003). Simultaneously, a heterozygotic point mutation on exon 7 (c446.A→C) producing a D149A missense mutation and homozygotic point mutation on exon 4 (c.234C→T) yielding a silent G78G change was found in early-onset sporadic PD patients with Afro-caribbean decent (Abou-Sleiman et al., 2003). This synonymous change may eliminate a predicted exonic splice enhancer site. Abou-Sleiman also looked at a population of late-onset patients but only identified a single silent heterozygous mutation (A167A) and two heterozygotic changes in the 3'-untranslated region (3' UTR) (Abou-Sleiman et al., 2003).

A more exhaustive analysis of Caucasian population groups led to the identification of a missense mutation (E64D) in a early-onset IPD patient from Turkey, caused by a homozygous mutation in exon 3 (c.192G→C) (Hering et al., 2004). Furthermore, by using a quantitative fluorescent based gene dosage assay in place of standard sequencing techniques, a heterozygotic deletion of exons 5-7 in DJ-1 was discovered in another Italian patient diagnosed with sporadic early-onset PD (Hedrich et al., 2004a). The same technique was used to discover an additional heterozygotic 11bp deletion in intron 5 (IVs5+2-12del) in a Russian early-onset individual (Hedrich et al., 2004a). This is mutation is thought to interfere with genomic splicing. None of the groups have found additional carriers of the original mutations reported by Bonifati et al (2003).

Recent direct sequencing of DJ-1 exons in two patients from southern Italy diagnosed with early-onset parkinsonism-dementia-amyotrophic lateral sclerosis by Annesi and colleagues (2005) revealed two further novel homozygotic mutations. Both patients carried a sequence duplication in exon 1 (g.168_185dup) hypothesised to affect DJ-1 mRNA levels due to its proximity to the promoter region (Annesi et al., 2005). The second homozygous mutation was a nucleotide substitution (c.487→A) in the last exon, exon 7 (Annesi et al., 2005). All mutations identified to date are summarised in table 1.2.

| Mutation | Inheritance | Onset | Origin | Effect on DJ-1 protein |
|---|---|---|---|---|
| g.168_185dup | Homozygous | Early | Italian | Unknown |
| Ex1-5del | Homozygous | Early | Dutch | Loss of protein |
| c.56delC c57G→A | Compound Heterozygous | Early | Hispanic | Truncated protein |
| M26I | Homozygous | Early | Askenazi Jew | Unknown |
| E64D | Homozygous | Early | Turkish | Unknown |
| | Heterozygous | Early | Hispanic | Unknown |
| A104T | Heterozygous | Mid | Asian | Unknown |
| Ex5-7del | Heterozygous | Mid | Italian | Aberrant protein |
| IVS5+2-12del | Heterozygous | Early | Russian | Aberrant protein |
| D149A | Heterozygous | Early | Afro-Carribbean | Unknown |
| E163K | Homozygous | Early | Italian | Unknown |
| L166P | Homozygous | Early-Mid | Italian | Loss of protein stability |
| IVS6-1G→C | Compound Heterozygous | Early | Hispanic | Unknown |

**Table 1.2: Summary of reported *PARK7* mutations.** The mode of inheritance, term of onset, ethnic origin and effect on protein is listed for each mutation. d. = genomic sequence, dup = duplication, c. = cDNA sequence, Ex = exon, del = deletion and IVS = intervening sequence.

### 1.2.4.2. Consequences of mutations: 'loss of function' theory

When the original 14kb deletion encompassing the first 5 exons, including the promoter region was reported, the development of PD was thought to arise from a lack of DJ-1 expression (Bonifati et al., 2003b). In order to explain the pathogenic nature of the homozygotic L166P mutation computer molecular models of DJ-1 proteins were produced based on a DJ-1 homologue, the PH1704 protease from Pyrococcus horikoshii which is an oligomeric protein. Introduction of the L166P mutation into the wild type model destabilised the DJ-1 protein by disrupting its normal helical conformation and altering its oligermerisation interface. From this, Bonifati reasoned that WT DJ-1 adopts a dimer/oligomer arrangement which is disrupted by the L166P mutation rendering the subsequently produced DJ-1 protein functionally inactive (Bonifati et al., 2003b). Thus under this rationale, a loss of function mechanism was proposed for DJ-1 based PD cases.

As DJ-1 mutations display an autosomal recessive mode of inheritance this loss of function theory readily explains the pathogenic outcome of the numerous homozygotic mutations discovered. However, apart from the compound heterozygotic mutation consisting of the truncated DJ-1 producing c.56delC c.57G→A mutation on one allele and the splice site mutation IVS6-1G→C on the other (Hague et al., 2003), it does not lend itself to an

explanation for the disease phenotype seen in some heterozygotic carriers. As these individuals still express WT DJ-1, albeit at a lower level that controls, they are expected to remain unaffected. A number of ideas have been put forward to explain this, including the suggestion that these individuals may harbour a second unidentified DJ-1 mutation. The conventional method of identifying mutations via direct sequencing of coding exons may overlook alterations in the 5' and 3' UTR sequence as well as genomic variations due to insertions or deletions. (Abou-Sleiman et al., 2003; Hague et al., 2003; Hedrich et al., 2004a). Additionally, the idea that DJ-1 forms dimers has lead to the hypothesis that heterozygotic DJ-1 mutations are similar to dominant-negative mutations where mutant DJ-1 forms a dimer with WT-DJ-1 thereby preventing it from functioning normally (Bonifati et al., 2004; Moore et al., 2003a; Moore et al., 2003b). A final suggestion is that the presence of heterozygotic DJ-1 mutations only results in a disease phenotype when combined with other factors like mutations in other PD genes or external stimulus (Hague et al., 2003).

### 1.2.4.3. Effects of mutations on protein structure and function

The effects of mutations that result in the formation of a truncated version of DJ-1 protein or even no protein formation at all are pretty much self evident. Analysis of DJ-1 proteins that carry substitution mutation however can provide clues as to the normal functional activity of DJ-1. The approximate location of substitution mutations is shown in figure 1.7.

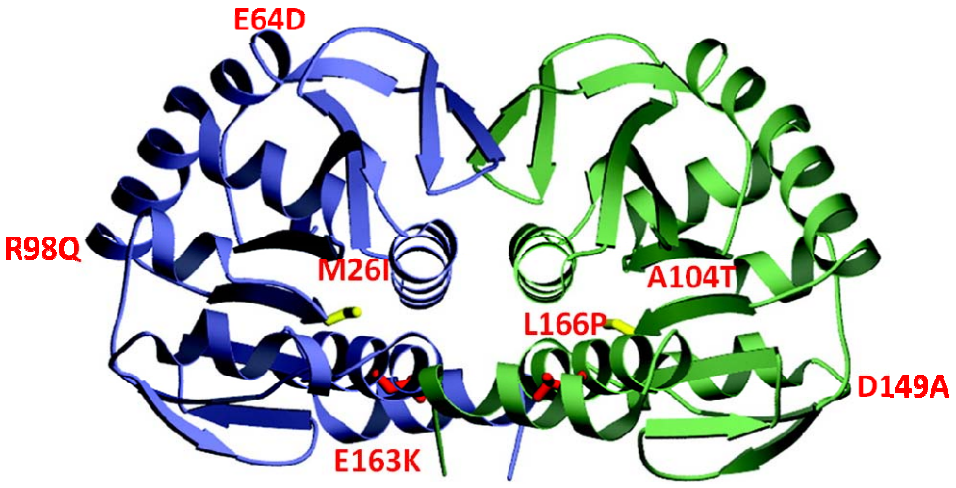


**Figure 1.7: Location of DJ-1 mutations.** Approximate location of substitution mutations on DJ-1 dimer complex are shown. Blue and green ribbon depict separate DJ-1 monomers. (adapted from Wilson et al., 2003)

### L166P

The leucine to proline substitution at amino acid 166 (L166P) was one of the originally reported DJ-1 mutations by Bonifati et al (2003). Amino acid 166 is placed in α-helix 7, a C-terminal helix that forms part of the hydrophobic core found at the dimer interface. The presence of proline disrupts the normal helical conformation, destabilising the dimer interface and impeding DJ-1 dimer formation (Olzmann et al., 2004; Wilson et al., 2003).

Compared to WT DJ-1, L166P DJ-1 expression is relatively low in neuronal and non-neuronal cell lines as well as lymphoblasts cultured from L166P patients (Gorner et al., 2004; Macedo et al., 2003; Miller et al., 2003). This is not due to impaired transcription/translation but rather from rapid degradation of the protein (Gorner et al., 2004; Macedo et al., 2003; Miller et al., 2003). Use of the lysosomal protease inhibitor $NH_4Cl$ and the proteasome inhibitor MG-132 suggests degradation of L166P mutant DJ-1 protein is via the proteasome system (Miller et al., 2003; Moore et al., 2003b). The direct interaction between ubiquitin and L166P DJ-1 was shown by Olzmann et al (2004) in an ubiquitination assay using HeLa cells over-expressing epitope-tagged ubiquitin and L166P DJ-1. The low levels of L166P DJ-1 is not a factor for its inability to dimerise as even when overexpressed to artificially high levels it fails to do so suggesting that its structural alteration is to blame for its instability (Miller et al., 2003; Moore et al., 2003b).

The ability to dimerise appears to be essential for DJ-1 to exert its chaperone function, with oxidation of L166P DJ-1 failing to prevent α-synuclein protofibril formation both *in vitro* and *in vivo* (Shendelman et al., 2004). It has also been noted that there is a significant decrease in its transcriptional activity and its ability to prevent Daxx migration into the cytoplasm (Junn et al., 2005; Xu et al., 2005). This may be influenced by the decreased localisation of L166P DJ-1 to the nucleus compared to WT (Xu et al., 2005). Furthermore, L166P appears to perturb the ability of DJ-1 to eliminate $H_2O_2$ from cells or protect them from $H_2O_2$ induced death (Taira et al., 2004).

### M26I

The methionine residue at amino acid 26 is highly conserved and is located in N-terminal α-helix 1 and contributes to the same hydrophobic core as L166 to which it is spatially close to. Methionine contains a liner non-polar side chain whereas isoleucine contains a branched non-polar side chain which is more suited to β-sheet conformation (Hulleman et al., 2007). In the dimer interface, α-helix 1 is thought to interact with the corresponding α-helix on the partner monomer (Tao and Tong, 2003). However, replacing methionine with an isoleucine residue on DJ-1 does not appear to affect the proteins capacity to dimerise as dramatically as L166P mutation with Takahashi-Niki et al., (2004) showing in yeast two-hybrid system that M26I is able to form a dimer with another M26I DJ-1 monomer or even a WT DJ-1 monomer.

In over-expression models, M26I levels are reported to be less than WT DJ-1 (Blackinton et al., 2005; Takahashi-Niki et al., 2004) suggesting the mutation may compromise protein stability. A recent study reported M26I DJ-1 to have decreased thermal stability and to more readily form aggregates than WT variant (Hulleman et al., 2007). When in a reduced state, this altered structure has little effect. However, it has been reported that two neighbouring residues, D24 and R28 may play a role in maintaining structural integrity when C106 is oxidised to sulfinic acid by forming hydrogen bonds with the sulfinic oxygen molecules (Tao and Tong, 2003). Under conditions of oxidative stress, the branched side chain of isoleucine in oxidised DJ-1 would disrupt this structural network and destabilise the dimer interface, resulting in protein destabilisation and subsequent aggregation (Malgieri and Eliezer, 2008). Thus any DJ-1 protein carrying this mutation would be inept at dealing with elevated oxidative stress conditions. Due to their ineffectiveness, M26I DJ-1 is rapidly degraded by the proteosome system, a process that can be inhibited in vitro by proteosome inhibitors (Blackinton et al., 2005)

Immunofluorescence has shown M26I DJ-1 to have a similar subcellular distribution pattern to WT DJ-1 in NIH3T3 and M17 cells i.e. within the nucleus and cytoplasm with some mitochondrial localisation (Blackinton et al., 2005; Zhang et al., 2005a). Blackinton and colleagues also observed a more pronounced relocation of M26I DJ-1 to the mitochondria

than WT which may possibly be a compensatory mechanism to combat the increased loss of M26I DJ-1 when oxidised.

### E64D

The glutamate at amino acid 64 is found on the surface of DJ-1 protein, away from the dimer interface and is part of the loop connecting α-helix 2 to β-strand 6 (Honbou et al., 2003; Tao and Tong, 2003; Wilson et al., 2003). As such, the replacement of glutamate with an aspartate residue has no effect on DJ-1 dimerisation. Indeed the glutamate residue is not evolutionarily conserved across vertebrates with both mice and rats possessing a glutamine amino acid at this point, suggesting it is not critical in stabilising the structure of DJ-1 (Bandyopadhyay and Cookson, 2004). This coupled with the fact that both glutamate and aspartate are negatively charged and structurally similar, suggests there is minimal disruption to the structure of DJ-1 protein and this is indeed the case with its 3D structure being almost identical to WT DJ-1 (Hering et al., 2004).

Given its close resemblance to WT DJ-1, its lack of evolutionary importance and its remote location from the dimer interface it is difficult to see how E64D mutation disrupts normal DJ-1 functioning. However, its detection in patients with familial PD (Hering et al., 2004) and the observation that it is less able to protect dopaminergic neurons culture models from various PD-related stresses (Hulleman et al., 2007) suggests some functional loss exists. Hulleman et al., (2007) have reported that the E64D mutation makes the α-helical structure of DJ-1 more thermally stable and that it forms a more stable dimer. This may upset the chaperone activity of DJ-1 or its ability to bind to mitochondria. In contrast, Malgieri and Eliezer (2008) observed no significant changes in the thermodynamic stability of E64D and instead attributed functional changes to altered interaction of DJ-1 with cellular partners that are fundamental to its proper functioning.

### A104T

Unlike E64, alanine 104 is another highly conserved residue that is located towards the C-terminal end of β-strand 7 (Malgieri and Eliezer, 2008). Substitution with threonine produces a protein whose secondary structure and dimerisation capabilities remain

unchanged (Lakshminarasimhan et al., 2008). It is however thermodynamically less stable than WT DJ-1 which explains the increased rate of turnover observed by Blackinton et al., (2005) and the subsequent lower steady-state expression levels.

A104 is a small residue that is tightly packed into a hydrophobic core surrounded by L72, P109 and L112. Threonine on the other hand is bulkier and causes the displacement of L72 and L112. As A104 is in the spatial vicinity of C106, it is hypothesised that its substitution upsets the geometric alignment in this region and in doing so, abrogates C106 actions (Lakshminarasimhan et al., 2008; Malgieri and Eliezer, 2008). C106 has been shown to be critical for sensing oxidative stress with its oxidative state being shown to regulate DJ-1 chaperone activity (Zhou et al., 2006) and its binding to mitochondria (Canet-Aviles et al., 2004).

### D149T

The aspartate present at residue 149 is another highly conserved amino acid located at the C-terminus of β-strand 10 of human DJ-1 protein (Wilson et al., 2003). Limited data is available on this mutation, however like A104, this residue is in the spatial vicinity of C106 and substitution with threonine can be assumed to disturb the local structure, thereby affecting C106 activities (Malgieri and Eliezer, 2008). The mutation does not affect its ability to form homodimers or even heterodimers with WT DJ-1 in transfected cells (Blackinton et al., 2005).

### E163K

Rather than inducing PD, E163K substitution mutation is associated with an early onset parkinsonism-dementia-amyotrophic lateral sclerosis complex (Annesi et al., 2005). Here the glutamate 163 residue located towards the edge of α-helix 7 is replaced with a lysine residue. α-helix 7 is also the location of L166 highlighting the importance of this particular α-helix in dimer formation. However, whereas L166P results in the loss of dimer forming property, E163K DJ-1 has been shown to dimerise *in vitro* (Lakshminarasimhan et al., 2008). Lakshminarasimhan and colleagues (2008) also showed that in WT DJ-1 dimer, the negatively charged E163 residue forms a salt bridge (a weak ionic bond between two

oppositely charged amino acids) with the positively charged R145 subunit from the other monomer, enabling the formation of a network of H-bonds at the dimer interface. Replacement of glutamate with a positively charged lysine residue results in an electrostatic conflict with R145 which is repelled and leads to the weakening of H-bonds at the dimer interface. Despite this, under normal conditions E163K DJ-1 has similar properties to WT DJ-1 in terms of dimerisation, subcellular localisation, stability and solubility (Ramsey and Giasson, 2008).

This mutation does however ruin the ability of DJ-1 to protect against oxidative stress but not by altering dimerisation, stability or aggregation properties like other mutations do. Instead it weakens the protective activity against oxidative stress by impairing the relocalisation of DJ-1 to the mitochondrial, a phenomenon that naturally occurs during times of cellular stress (Ramsey and Giasson, 2008). As yet, the mechanisms involved in the redistribution of DJ-1 to the mitochondria remain unknown but the change in residue charge or the arising subtle structural changes may hinder interaction with any partner proteins involved (Ramsey and Giasson, 2008).

## 1.2.5. DJ-1 in idiopathic PD

### 1.2.5.1. DJ-1 polymorphisms

With DJ-1 being the least common cause of AR PD, accounting for less than 2% of all early-onset cases, it was hoped that non-pathogenic mutations that predispose carriers to the development of idiopathic PD could be discovered. A number of DJ-1 polymorphisms have been reported with the most frequent being a silent heterozygous nucleotide substitution in exon 5 (c.293G→A) that produces an arginine to glutamine switch in the protein (R98Q) (Abou-Sleiman et al., 2003; Clark et al., 2004; Hague et al., 2003; Hedrich et al., 2004b). This polymorphism was found to occur in more than 1% of control cases and in a similar amount in IPD cases (Hedrich et al., 2004b). Another polymorphism of note is the reported g.168-185del (Eerola et al., 2003). Given its close closeness to the promoter region of DJ-1 and the previous reports of polymorphisms in the promoter regions of other PD genes like α-synuclein and parkin being a risk factor for IPD (West et al., 2002), this was investigated in

some detail. However screening of late-onset IPD samples showed this not to be the case (Eerola et al., 2003; Morris et al., 2003).

With the genetic make-up of DJ-1 seemingly having no influence on the development of sporadic PD, it remains unclear what role DJ-1 plays in its pathogenesis.

## 1.3. Thesis Objectives

Mutations in *PARK7* highlight the importance of DJ-1 protein in PD. However, occurrences are extremely rare, accounting for less than 2% of all early-onset cases. To date, any involvement of DJ-1 in sporadic PD remains undetermined. The overall objective of this thesis is to investigate any possible role for DJ-1 in the development of IPD and other neurodegenerative disorders. By taking advantage of the extensive collection of human post-mortem brain tissue here at the Queens Square Brain Bank (QSBB), I have attempted to characterise the properties of DJ-1 in human brain tissue. The specific aims of the studies that follow were

1. to characterise DJ-1 expression in human brain and identify any changes in IPD tissue
2. to identify potential *in vivo* interactors that would help explain the diverse range of cellular activities reported for DJ-1.
3. to investigate any possible involvement of DJ-1 in tauopathies.

The relevance of any findings, in terms of the pathogenesis of PD and other neurological disorders will be explored.

# 2. Materials and methods

# 2.1. Pathological material

Demographic data of all tissue used will be detailed in the following chapters. All frozen tissue was procured from the QSBB, following ethical review by the London Multicentre Research Ethics Committee and the National Hospital for Neurology and Neurosurgery/Institute of Neurology Joint Research Ethics Committee. For immunohistochemical studies a number of formalin fixed brain sections were obtained from Professor David Mann with ethical consent from the Manchester Brain Bank. Where possible tissue used in studies were matched for age, post-mortem delay and pH. The latter two can be used to judge tissue breakdown and acidosis.

# 2.2. Protein expression techniques

## 2.2.1. Tissue homogenisation

For protein analysis, approximately 0.5g flash frozen tissue was mechanically homogenised in 10 volumes (w/v) of 50mM Tris-HCL buffer (pH 7.0), containing complete mini protease inhibitor cocktail (PIC) tablets (Roche, UK). Homogenates were then centrifuged at 14,000g for 15min at 4$^{o}$C to remove debris. The resulting pellet was discarded and the supernatant stored for future use at -20$^{o}$C. 20µl of supernatant was kept separately in order to measure the protein concentration via a Bradford protein assay.

## 2.2.2. Bradford protein assay

The Bio-Rad protein assay used to measure protein concentration of homogenates is based on the Bradford dye-binding procedure. Here, a microplate reader is used to assess the colour change of Coomassie brilliant blue G-250 in response to protein concentration. 1µl of each sample was pipetted in triplicate on to a 96 well microtiter. On the same plate 8 known concentrations of bovine serum albumin (BSA) (Sigma, UK) are pipetted in triplicates. The concentration of BSA ranges from 1µg/µl to 10µg/µl. All wells plus an additional 3 empty wells were made up to 10µl using distilled water. 200µl of Bio-rad protein assay dye, diluted to 25% solution, was then added to each well. Wells were then analysed on a plate reader

set at 595nm and a standard curve constructed from BSA readings (Fig. 2.1). Protein concentrations for unknown samples were extrapolated from the curves linear equation.

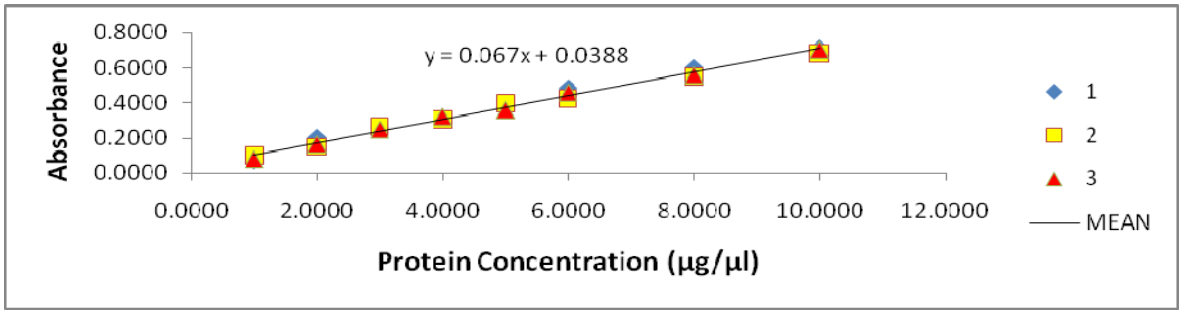


**Figure 2.1: A Bradford assay BSA calibration plot.** Absorbance for each protein standard was measured in triplicate and the resulting equation for the mean line of best fit was used to calculate protein concentrations of samples.

### 2.2.3. Western blotting & chemilluminescent protein detection

In the majority of cases, samples were run under denaturing conditions. Initially samples were run on Invitrogen's Novex gel system. Towards the end stages of the project a Bio-rad Criterion gel system was acquired and this was favoured as double the number of samples could be run on one gel thereby minimising gel-to-gel variances. Both systems use laemmli based tris-glycine gels.

For both systems, samples were prepared by mixing a known concentration of protein with 2x Tris-Glycine SDS sample buffer and 10x reducing agent. Depending on whether Invitrogen or Bio-rad gels were used, double distilled water was used to make the mixture up to 20µl or 25µl respectively. Sample mixtures were heated to 85$^{o}$C for 2 minutes and then loaded onto Tris-Glycine gels placed in a gel tank filled with 1x Tris-glycine running buffer (Invitrogen, UK). 5µl of SeeBlue Plus 2 pre-stained standard marker (Invitrogen, UK) was also loaded into an empty well. Gels were run at 130V for 2 hours. Protein bands were then electroblotted for 2.5 hours on to Hybond-P nylon membrane (GE Healthcare, UK) using 1x Tris-Glycine transfer buffer (Invitrogen, UK) containing 20% methanol (VWR, UK). Proteins

separated using the Invitrogen system were transferred at 30V whilst the Bio-rad system required 90V.

Once transfer was complete, membranes were blocked for 1 hour at room temperature (RT) with 5% milk (Marvel, UK) in PBS containing 0.1% Tween-20 (PBS-Tw). Blots were subsequently incubated with the antibody of interest diluted appropriately in PBS-Tw with 5% milk for 1-3 hours at RT. This was followed by three 10 minute washes with PBS-Tw and then by incubation with an appropriate HRP-conjugated secondary antibody (Santa Cruz) diluted in 5% milk for an hour at RT. Membranes were washed a further three times with PBS-Tw and then exposed to a standard enhanced chemilluminescent substrate (ECL), SuperSignal West Pico Substrate (Pierce, UK), prior to placement in an autoradiograph cassette; protein side up. Immunoreactive (IR) bands were then captured on to Kodak Biomax autoradiography film (Sigma, UK) which was subsequently developed to enable visualisation of bands. For weakly expressed proteins, a more sensitive chemilluminescent substrate, SuperSignal West Dura Substrate (Pierce, UK) was used.

Afterwards, membranes would be stripped for 30 minutes using Restore Plus Western Blot Stripping Buffer (Pierce, UK) and blocked again with 5% milk for an hour at RT before being incubated with β-actin monoclonal antibody (Sigma, UK) for 1 hour at RT. Unbound primary antibody was removed by washing with PBS-Tw and blots were subsequently incubated with goat anti-mouse HRP-conjugated secondary antibody (Santa Cruz, UK). Bands were then detected as described above. Quality One software (Bio-rad, UK) was used to quantify detected bands of the protein of interest and readings for each sample would be normalised to their corresponding β-actin levels. A student's T-test was used to compare control and PD samples.

## 2.2.4. Fluorescent protein detection

One of the main drawbacks of chemilluminescent detection of protein is that it relies on a chemical reaction that produces light imaged on to film. Samples are quantified by measuring the intensity of their bands. However, readings are time dependent as they are based on the accumulation of light absorbed by the films and can become saturated if the

protein concentration is particularly high. This can produce variable results when measuring protein levels. DJ-1 is one such protein that is highly expressed in the brain tissue. To allow for more accurate quantification, the Odyssey infrared imaging system (Li-Cor, UK) and fluorescent protein detection was used. Light produced from excitation of the fluorescent dye is constant and readily comparable to emissions from other samples.

The method for fluorescent protein detection is not too dissimilar to the chemilluminescent procedure described above. For this 15µg of protein from control and PD homogenates of selected regions were run on a 10% Tris-Glycine gel (Invitrogen, UK) at 125V for 90 minutes. Proteins were then transferred from the gel on to Immobilon-FL PVDF membrane (Millipore, UK) as described above. On completion of transfer, membranes were blocked with 5% milk in PBS (without tween) for an hour at room temperature before incubation overnight at 4$^{o}$C with both monoclonal DJ-1 (1:10000; Stressgen, USA) and monoclonal β-actin (1:10000; Sigma, UK). The following day blots were washed three times with PBS-Tw and then IRDye 680 Goat Anti-Mouse Secondary Antibody (1:20000, Li-cor, UK) was applied for an hour at RT. After another series of washes with PSB-Tw protein levels were measure using Odyssey infrared imaging system and bands quantified using the supplied software. DJ-1 levels were normalised to their β-actin readings and a T-test used to compare control and PD groups.

## 2.2.5. DJ-1 ELISA

Enzyme-Linked ImmunoSorbent Assay (ELISA) is another biochemical technique that is commonly used to measure protein levels. A human DJ-1/PARK7 ELISA kit (MBL International, USA) has been developed to measure human DJ-1 protein concentration from human serum/plasma and we aimed to test its suitability for use with human brain homogenate.

The ELISA assay procedure was carried out as directed by the manufacturer. 100µl of recombinant human DJ-1 standard and diluted samples were pipetted in triplicate into the appropriate wells of a 96-well microtitre plate and incubated for an hour at RT on an orbital shaker, shaking at 200 ca. Wells were then washed four times with 300µl wash buffer followed by the addition of 100µl HRP-conjugated detection antibody and incubation at RT

for another hour on the orbital shaker. Wells were then washed a further four times with wash buffer and the then incubated at RT with 100µl of substrate reagent. The reaction was stopped after 15min with 100µl stop solution and the absorbance of each well read at 450 and 540nm on a spectrophotometric microplate reader. The absorbance values of the standards were then plotted and the concentration of unknown samples calculated from the standard curve.

## 2.2.6. Extraction of TBS, SDS and urea soluble DJ-1

This protocol is based on the methods described in Campbell et al., (2000). TBS buffer (50mM Tris-HCl, pH 7.4, 150mM NaCl)) was made up and 1 mini PIC tablet (Roche, UK) and 500µl of 100mM EDTA was added per 10ml before being chilled on ice. Approximately 0.3g of flash frozen frontal cortex tissue from 8 control and 8 PD cases were mechanically homogenised in 10 volumes of TBS buffer. Any non-homogenised material was collected by centrifugation at 1000g for 5min at 4$^{o}$C and discarded. The crude homogenate supernatant was transferred to Beckman tubes and after being carefully balanced, subjected to ultracentrifugation at 100,000g for 1 hour at 4$^{o}$C. The resulting supernatant constituted the TBS-soluble fraction and was frozen for future use. The pellet meanwhile was washed twice with TBS buffer and then resuspended by briefly homogenising in 3 volumes TBS-SDS buffer (TBS plus 5% w/v SDS). This was then ultracentrifuged at RT for 30min at 100,000g after which the supernatant was labelled as the SDS soluble fraction and stored at -20$^{o}$C. The pellet was subjected to two washes with TBS-SDS buffer and resuspension in 150µl TBS-SDS-Urea buffer (TBS plus 8% SDS w/v and 8M urea) and stored as the Urea soluble fraction.

## 2.2.7. BCA protein assay

The standard Bio-Rad protein assay used earlier is incompatible with the SDS and urea present in the buffers used in these protein extractions. To overcome this, we measured the protein concentration of each fraction using a bincinchoninic acid (BCA) protein assay (Pierce, UK). As described by the manufacturer's instructions 50 units of reagent A containing sodium carbonate, sodium bicarbonate, BCA and sodium tartrate in 0.1M sodium hydroxide was mixed with 1 unit regent B containing 4% cupric sulphate to form a working

reagent. At the same time, one vial of Albumin Standard (Pierce, UK) was used to make a set of 8 protein standards ranging from 2000µg/ml down to 25µg/ml using the same buffer present in the homogenates as a dilutant. 25µl of each standard and protein sample was pipetted in triplicate into a 96-well microplate and incubated with 200µl of working reagent for 30min at 37$^{o}$C. The plate was then left to cool before the absorbance of each sample was measured at 562nm on a plate reader. A standard curve was then formed from using the albumin readings and the unknown protein concentration of homogenates calculated.

## 2.2.8. Extraction of sarkosyl insoluble DJ-1

Sarkosyl insoluble proteins were extracted from brain tissue by my supervisor, using the method described in Goedert et al., (1992). This protocol was developed in order to solubilise the tough tau tangles (Goedert et al., 1992).

For the extraction 1g of frontal cortex from control, AD and FTLD-Pick's cases were homogenised in 10vol of buffer consisting of 10mM Tris-HCl (pH 7.4), 0.8M NaCl, 1mM EDTA and 10% sucrose. The homogenate was centrifuged at 20,000g for 20min. the supernatant was retained and the pellet rehomogenised in 5vol of buffer and respun. The resulting supernatant was combined with the first supernatant and incubated for 1 hour with 1% N-laurylsarkosine at RT while shaking. Samples were then subjected to 1 hour ultracentrifugation at 100,000g followed by resuspension of the resulting sarkosyl insoluble pellet in 50mM Tris-HCl pH 7.4 (0.2ml/g starting material). Proteins were then separated on 12% Tris-Glycine gels (Invitrogen) as described above. DJ-1 and tau were detected using monoclonal DJ-1 (Stressgen, USA) and AT8 (Innogenetics, UK) antibodies respectively and visualised on autoradiographic film.

## 2.2.9. Subcellular fractionation of human brain tissue

This protocol is based on (Gandhi et al., 2006). Fresh human brain tissue was weighed and placed on a chilled ground glass beaker on ice. It was thoroughly homogenised on ice in 5ml/g isolation medium (320nM sucrose, 1mM EDTA, 10mM Trizma-base pH 7.4 and PIC tablets) before being centrifuged at 3000g for 5min. The supernatant was collected and

centrifuged again for 10min at 12000g whilst the pellet containing the unhomogenised material was discarded. The resulting supernatant was stored for later use on ice whilst the pellet which constituted the crude mitochondrial fraction was re-suspended in 1ml isolation buffer and subjected to further centrifugation at 3000g to remove nuclear contamination. The pellet was discarded and the supernatant re-centrifuged at 12000g for 10min. The supernatant was discarded and the last two steps were repeated twice more with the pellet in order to further purify the mitochondrial fraction. Eventually the pellet from the 12000g centrifugation was re-suspended in 300µl isolation buffer and labelled as the mitochondrial enriched fraction. The supernatant stored earlier was subjected to ultracentrifugation at 70000g for 60min and the ensuing supernatant made up the soluble cytosolic fraction. The pellet on the other hand consisted of the microsomal (including the endoplasmic reticulum) enriched fraction and was re-suspended in 500µl isolation buffer. All fractions were stored at -70$^{o}$C till use. The protein concentration of each fraction was measured using the Bio-rad Bradford assay. The purity of the fractions was tested by standard chemilluminescent immunoblotting techniques using antibodies against mitochondrial, microsomal and cytosolic markers. All fractions were tested for the presence of DJ-1 in the same manner.

## 2.2.10. Gel exclusion chromatography

Approximately 150mg of tissue was homogenised in 10 volumes of PBS containing 0.1% Triton X-100 and PIC using a glass hand homogeniser. Unhomogenised debris was cleared by centrifugation at 10000g for 10min at 4$^{o}$C and the supernatant containing the soluble protein was loaded by a technician into a FPLC Superdex 200 HR 10/30 (Amersham, USA) set with a flow rate of 0.25ml/min. Soluble protein was eluted in a size dependent manner over 45 250µl fractions into collection tubes. Once all the fractions had been eluted they were run on Invitrogen Bis-tris gel system as previously described and probed with monoclonal anti DJ-1 at a 1:10000 dilution. After chemilluminescent detection of DJ-1, protein band intensities were measured using Image J and plotted in excel against fraction number. Molecular weight of native DJ-1 in brain tissue was then calculated using a standard curve constructed from protein standards; Thyroglobulin, Ferritin, Human IgG, Transferrin, Ovalbumin, Myoglobulin and vitamin $B_{12}$ (Amersham and Sigma, USA) that had been

previously separated on the same column, under the same conditions by other members of Dr Mark Cookson's group.

## 2.2.11. Two-dimensional gel electrophoresis

Two dimensional gel electrophoresis (2DGE) is a method for the separation of proteins in a sample by displacement in 2 dimensions, perpendicular to one another. The first dimension involves separating proteins by their charge via isoelectric focusing. Proteins are then separated in the second dimension by their molecular weight using SDS-Polyacrylamide gel electrophoresis (SDS-PAGE).

### 2.2.11.1. Isoelectric focusing

6µl of de-streak reagent (Amersham, UK) and 4µl of immobilized pH gradient (IPG) pH 4-7 buffer (Amersham, UK) was added to 500µl rehydration buffer (8M urea, 4% CHAPS and 0.002% bromphenol blue) and mixed by vortexing. Soluble homogenate was pipetted into individual tubes and made to 125µl with rehydration/de-streak/IPG buffer mixture and pipetted into ceramic plates. 7 cm pH 4-7 IPG strips (Amersham, UK) were removed from their packaging and placed into ceramic strip holders, gel side down and covered with 300µl mineral oil (Sigma, UK). Strip holders were placed on an Ettan IPGPhor II system (Amersham, UK) set at 20V for 8 hours to allow strips to rehydrate. Proteins were separated by 500V for 1 hour, followed by another hour at 1000V before the voltage was ramped up to 5000V for 2.5 hours and then finally held for 8 hours at 500V. The step-wise increase in voltage minimises sample aggregation and ensures a low current. Strips were then taken through to molecular weight separation using SDS-PAGE.

### 2.2.11.2. SDS-PAGE

After isoelectric focusing, IPG strips were removed from the ceramic plates and washed for 15min with SDS equilibration buffer (50mM Tris-HCl, pH 8.8, 6M urea 30% glycerol, 2% SDS and bromophenol blue) containing 1% w/v DTT and bromophenol blue. This was followed by a 15min wash with SDS equilibration buffer containing 2.5% w/v iodoacetamide. Strips

were then loaded into 1 well, 12% Tris-glycine gels (Invitrogen, UK) and sealed with quick melting agarose. Proteins were then separated by molecular weight and transferred onto Hybond-P membrane as previously described. Blots were probed with DJ-1 monoclonal antibody (Stressgen, USA) 1:2000 and visualised using ECL and autoradiograph film. Quality One software was used to measure DJ-1 pI isoforms distribution.

### 2.2.11.3. Identification of protein carbonyls

Oxidation of proteins leads to an increase in protein carbonyls and these can be detected by forming a hydrazone derivative using 2,4-dinitropheylhydrazine (DNP). These can be detected by immunoblotting with an antibody against the DNP segment of the hydrazone.

In-strip DNP derivation as described by Choi et al., (2006) was performed on 2 samples to establish whether any of the DJ-1 pI isoforms underwent increased oxidation in PD. Proteins were subjected to in-strip derivation following overnight isoelectric focusing by placing the strips into 15ml falcon tubes and incubating for 20min with 2 N HCl containing 10mM DNP at RT. The reaction was neutralised by a subsequent 15min wash with 2M Tris-Base and 30% glycerol solution. Strips were then prepared and processed for second dimension separation as described above. Following blocking in 5% milk, membranes were incubated overnight with rabbit polyclonal anti-DNP-KLH antibody at 1:10000. After extensive washing with PBS-Tw, blots were incubated for an hour at RT with an anti-rabbit HRP conjugated secondary antibody. Immunostained proteins were detected in the usual manner with ECL and autoradiograph film. Membranes were then stripped and probed with anti-DJ-1 antibody as described above.

## 2.2.12. Protein immunoprecipitation

Tissue was mechanically homogenised in lysis buffer (150mM NaCl, 50mM Tris pH7.5, 5mM EDTA, 0.25% NP-40 and PIC tablets). 750µg of homogenised tissue was made up to 500µl with lysis buffer and rotated for two hours at 4$^{o}$C with 100µl protein G sepherose (Amersham, UK). The protein G-slurry had previously been buffered with lysis buffer. After rotation, samples were centrifuged at 10000g at 4$^{o}$C for 10min and the supernatant

transferred to fresh tubes. A 30µl aliquot of the cleared lysate (CL) was stored at -20$^{o}$C. 2.5µg of goat polyclonal anti-DJ-1 antibody (Abcam, UK) was then added to the remaining CL and tubes were returned back to the cold room and rotated over night. The following day 100µl of fresh pre-buffered protein G-slurry was added to each tube. At the same time a mock tube containing 500µl lysis buffer and 100µl protein G-slurry was made and along with the samples were subjected to 2 hours rocking at 4$^{o}$C. Centrifugation at 1000g for 2min at 4$^{o}$C was used to collect the protein G-sepherose complex at the bottom of the tube and they were then washed 5 times with wash buffer (150mM NaCl, 50mM Tris ph 7.5, 5mM EDTA and 0.05% NP-40). Following the removal of all supernatant, 20µl of 8M urea and 5µl of LDS NuPage sample buffer (Invitrogen, UK) was added to the pellet and heated to 65$^{o}$C for 15min to allow protein complexes to dissociate from the beads. Immunoprecipitates and their corresponding CL were resolved on 10% Bis-Tris gels using MES running buffer and probed with antibodies to potential interactors. Blots were also probed with monoclonal anti-DJ-1 to confirm pull-down of DJ-1 protein.

# 2.3. Immunochemical staining techniques

## 2.3.1. Immunohistochemistry

Tissue from regions of interest in human control and diseased wax embedded formalin fixed brains were sectioned at a thickness of 8µm using a microtome and dewaxed in 3 changes of xylene for 5min each before rehydration with graded alcohol (100%, 95% and 70%). Endogenous peroxidise reactions were blocked by treating with 0.3% $H_2O_2$ in methanol for 10min after which sections were pre-treated with either formic acid for 5min or pressure cooking with citrate buffer, pH 6.0 for 10min. Sections were then thoroughly washed in distilled water to ensure removal of all traces of pre-treatment and then incubated with 5% milk in PBS for 30min to block non-specific protein binding. The milk was then replace with primary antibody and incubated for 1 hour at RT or overnight at 4$^{o}$C. Sections were then incubated with the relevant secondary antibody for 30min and then advin-botin complex (ABC) was applied for a further 30min. Antibody concentrations along with the appropriate

pre-treatment and secondary antibody are listed in table 2.1 below. Diaminobenzidine (DAB) staining was used to visualise protein IR followed by light counterstaining with haematoxylin (BDH, UK). After incubation with each reagent, slides where thoroughly washed in tap water to remove any excess. Before being permanently mounted slides were dehydrated in increasing strengths of ethanol and passed through two changes of xylene.

| Protein | Antibody | Source | Pretreatment | Secondary |
|---|---|---|---|---|
| DJ-1 | monoclonal DJ-1 1:1000 | Stressgen | 10min pressure cooking in citrate buffer, pH 6.0 | anti-mouse, 1:200 |
| DJ-1 | polyclonal DJ-1 1:200 | Dr P. Rizzu | 5min in 95% formic acid | Broad Spectrum kit, Zymed |
| 3R tau | monoclonal RD3 1:3000 | Dr R. de Silva | 10min pressure cooking in citrate buffer, pH 6.0 | anti-mouse, 1:200 |
| 4R tau | monoclonal RD4 1:100 | Dr R. de Silva | 10min pressure cooking in citrate buffer, pH 6.0 | anti-mouse, 1:200 |
| Tau | AT8 1:600 | Innogenetics | 10min pressure cooking in citrate buffer, pH 6.0 | anti-mouse, 1:200 |
| Ubiquitin | polyclonal ubiquitin 1:100 | Dako | 10min pressure cooking in citrate buffer, pH 6.0 | ant-rabbit, 1:200 |

**Table 2.1: Antibodies and pre-treatments used for immunohistochemical projects**

## 2.3.2. Double fluorescence confocal microscopy

In order to see co-localisation of DJ-1 and Tau, double immunofluorescence was carried out sequentially with DJ-1 1130 and AT8 antibodies. Sections were first stained with DJ-1 1130 at 1:200 dilution as described above. After administration of streptavidin-peroxidase conjugate, slides were incubated for 15min in the dark at RT with tetramethyl rhodamine fluorescent probe (Perkin Elmer, UK) diluted 1:200 in supplied TSA amplification buffer. Slides were placed in running tap water to thoroughly wash away any unbound probe prior to incubation with AT8 antibody, followed by anti-mouse secondary antibody and then ABC complex. Fluorescein fluorescent probe (Perkin Elmer, UK) was then applied to the sections. After thorough washing in tap water sections were mounted in aquamount (Merck, UK). Fluorescent signals were detected using a Leica TCS40 laser confocal microscope.

# 2.4. mRNA expression techniques

## 2.4.1. Quantitative real-time PCR

### 2.4.1.1. Extraction of RNA

For this study flash frozen tissue from the amygdala, cerebellum, cingulated gyrus, entorinal cortex, frontal cortex, medulla, parietal cortex and striatum were collected from 20 control and 20 IPD cases. Total RNA from all samples were extracted via the standard Trizol method. Small pieces of tissue were homogenised in 2ml eppendorf tubes containing 1ml Trizol reagent (Invitrogen, UK). Homogenates were allowed to settle at RT before 200µl of chloroform (Sigma, UK) was added and mixed vigorously by hand. Samples were then centrifuged at 12,000g for 15min at 4$^{o}$C to separate the mixture. The resulting clear upper aqueous phase was transferred to fresh 1.5ml eppendorf tubes, combined with 500µl isopropanol and left to stand at RT for 10min to promote RNA precipitation. This was followed by centrifugation at 12,000g for 10min at 4$^{o}$C after which the RNA precipitate in the form of a white pellet could be seen at the bottom of the tube. The supernatant was then removed and replaced with 1ml of 75% ethanol. Brief gentle vortexing was used to mix the sample and the RNA collected again, by a 5min 7,500g spin at 4$^{o}$C. The supernatant was then discarded and the RNA pellet air dried before being dissolved in 100µl DEPEC water using a pipette. 5µl were removed and the remainder stored at -80$^{o}$C till use.

### 2.4.1.2. Accessing RNA quality and quantity

Out of the 5µl of RNA kept aside, 1µl was loaded on to a NanoDrop spectrometer and its absorbance at 230, 260 and 280nm was recorded along with the concentration of the RNA. The ratio of A260/A280 was used to indicate contamination of the sample with protein, salts and phenol. Samples whose A260/A280 ratio fell below 1.7 were classed as impure and discarded.

To assess the integrity of collected RNA, a number of the samples were analysed using the Agilent Bioanalyser 2100. This involved loading 1µl of sample of RNA on to an Agilent RNA

6000 nanochip containing a preset gel and allowing it to run against a RNA ladder. RNA is composed of two ribosomal subunits, 28s and 18s and when run on a gel the ratio of these two ribosomal bands gives an indication of the integrity of the RNA collected (Fig. 2.2A and B). For perfect RNA the 28s:18s ratio is 2:1 but as it degrades there is a gradual loss of the 28s ribosomal band and the appearance of smaller degraded products. Samples that were shown to lack a 28s band or for those where it appeared very faintly were discarded as were those that showed the presence of multiple degradation products.

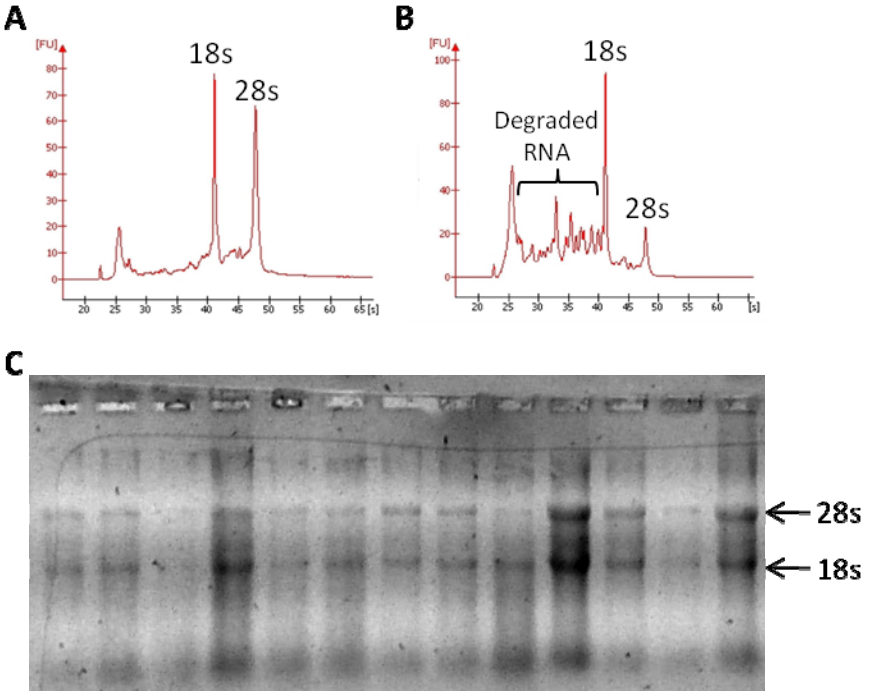


**Figure 2.2: RNA integrity analysis.** A and B) show electropherogram produced by Agilent bioanalyser detailing RNA quality of two samples. Sample A shows RNA of excellent quality whilst sample B shows loss of ribosome 28s and increased degraded RNA products. Samples with an electropherogram similar to B were re-extracted or discarded. C) RNA integrity assessment using 1% formaldehyde gels.

The remainder of the samples were run on a 1.5% formaldehyde agarose gel (Fig. 2.2C). These work on the same principle as the Agilent bioanalyser but are more cost effective and time efficient when dealing with large sample numbers. Their main drawback is the need to use a larger amount of the sample. For these gels, 4µl of RNA was mixed with 12µl loading dye and 2µl of ethidium bromide and heated to 65$^{o}$C for 15min to denature any RNA

secondary structure. Samples were then loaded on to the gel and run ¾ of its length at 80v. Bands were visualised using UV florescence and images stored using Kodak digital camera. Samples were discarded if the 28s and 18s could not be distinctly identified or if they exhibited a great deal of smearing on the gel.

Samples that were shown to be degraded by the bioanalyser and formaldehyde gels were re-extracted. If successful re-extraction was not possible, that tissue sample was dropped from the series. For this reason the medulla was entirely dropped from the study.

### 2.4.1.3. cDNA synthesis

Once the purity and integrity of the extracted RNA was confirmed, Superscript III first-strand synthesis supermix kit (Invitrogen, UK) was used to convert it into first strand cDNA for use in quantitative real-time PCR (RT-PCR). For this 1µg RNA was made up to 20µl using the supermix and left to stand at RT for 10min. It was then incubated at 50$^{o}$C for 30min and the reaction was then terminated by heating the mix to 85$^{o}$C for 5min. 1µl of *E. coli* RNase H was then added to each reaction and incubated at 37$^{o}$C for 20min, to ensure breakdown of remaining RNA. 5µl of the resulting cDNA was removed and converted into a working concentration of 2ng/µl, whilst the rest was stored at -20$^{o}$C for future use.

### 2.4.1.4. Real-time PCR

In order to measure the DJ-1 mRNA levels in human brain regions we decided to use RT-PCR as it is widely considered the most sensitive method for detecting and quantifying mRNA. Reactions were carried out in a volume of 25µl consisting of 12.5µl Power Sybr Green (Applied Biosystems), 10ng cDNA, 0.2µM forward and reverse primers and DEPC water. Primers for our gene of interest, DJ-1 and housekeeper genes, β-actin and β-2-microglobulin (B2M) were designed by imputing the gene transcript into a web based program, Primer3 (http://frodo.wi.mit.edu/). β-actin and B2M were chosen as internal controls due to their stable expression in both control and PD tissue as previously reported (Beyer et al., 2008; Coulson et al., 2008).

Suggested primer sequences were then blasted against the human genome sequence using NCBI blast (http://blast.ncbi.nlm.nih.gov/Blast.cgi) to see how exclusive they were. In order to minimise contamination from genomic DNA amplification, at least one of the primers was designed to fall on an exon-exon boundary.

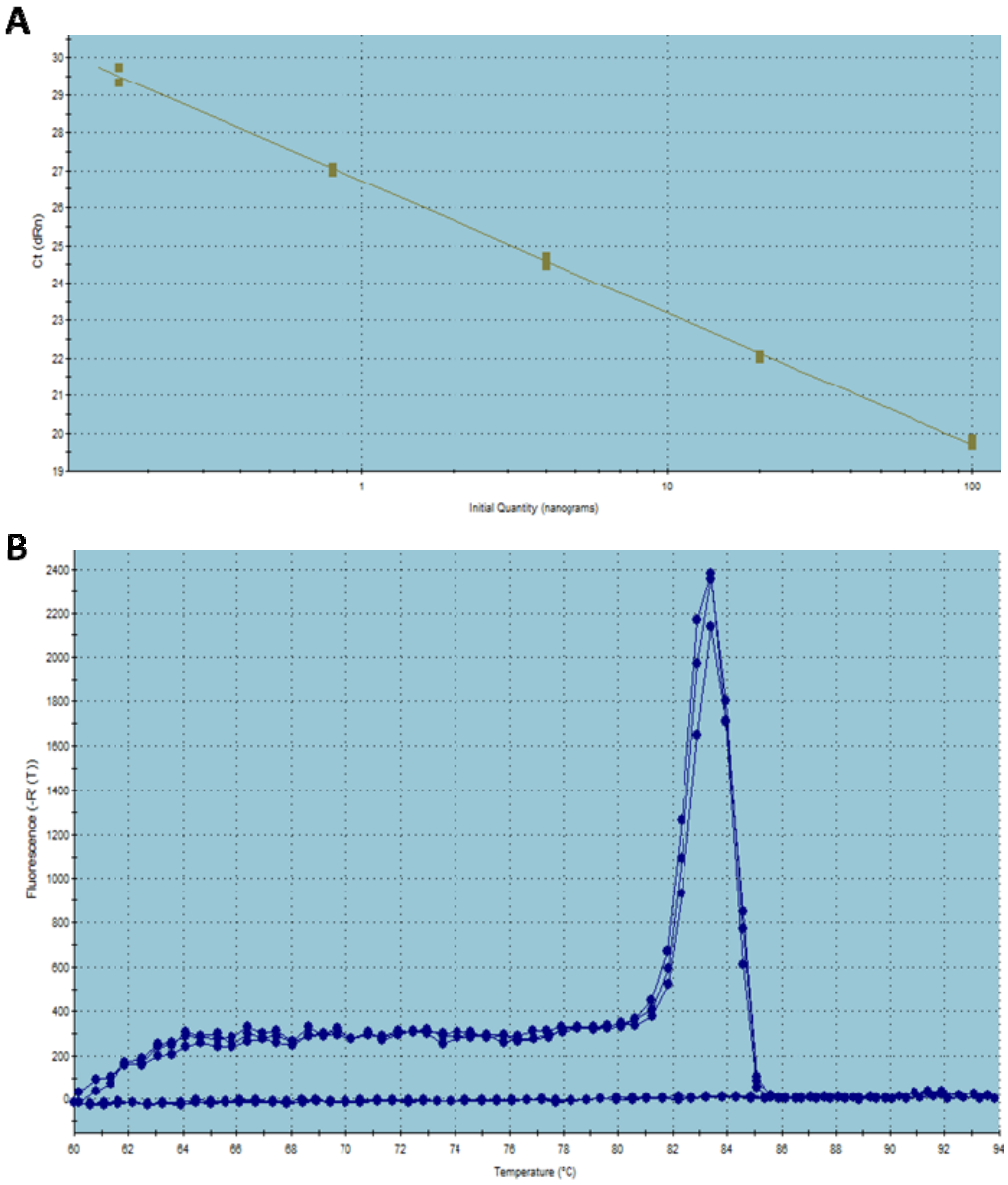


**Figure 2.3: Primer suitability for RT-PCR amplification.** A) Arbitrary concentration of each dilutant on standard curve plotted against Ct value. A line of best fit is constructed from the points, is used to assess the efficiency of the DJ-1 primers. B) Dissociation curve from a RT-PCR run using DJ-1 primers. The single peak indicates the formation of only one PCR product. Peaks at different points of the curves would be indicative of primer dimer formation or non-specific binding of primers.

Suitable primers were tested for their amplification efficiency using a 5 point standard curve constructed from 5-fold dilutions of template cDNA (Fig. 2.3A). Primer pairs for DJ-1, β-actin and B2M were only selected if they had an amplification efficiency greater than 90% and if the dissociation curve for the reaction showed a single peak (Fig. 2.3B), indicating the amplification of only one product. The sequence of the chosen primers is shown in table 2.2. All reactions were run in triplicates on a 96 well Stratagene Mx3000P qPCR system. The cycling protocol consisted of 40 cycles involving a 30s denaturation step at 94$^{o}$C followed by a 1min annealing step at 55$^{o}$C for runs involving β-actin and 60$^{o}$C in the case of DJ-1 and B2M and ending with 30s at 72$^{o}$C for extension. Each plate contained 3 no template controls to ensure there was no contamination of reagents and a dissociation curve analysis was added to the end of each run to confirm amplification specificity.

| Primer Name | Primer Sequence 5' - 3' |
|---|---|
| B2M F | TTTCATCCATCCGACATTGA |
| B2M R | CCTCCATGATGCTGCTTACA |
| β-actin F | AGTACTCCGTGTGGATCGGC |
| β-actin R | GCTGATCCACATCTGCTGGA |
| DJ-1 F | CTGGCTAAAGGAGCAGAGGA |
| DJ-1 R | ATCTTCAAGGCTGGCATCAG |

**Table 2.2: Sequence of primers used to quantify DJ-1 mRNA expression**

## 2.4.1.5. RT-PCR analysis

RT-PCR data was analysed using a variant of the widely used comparative Ct method proposed by M. W. Plaffl (Pfaffl, 2001). This formula allows the efficiency of the PCR amplification for each primer to be taken into account, when calculating gene expression levels for samples without having to run a standard curve of known RNA concentration during each run. Thus it provides a more accurate comparison of mRNA levels without incurring the additional costs that running a standard curve per plate would add if I was to use the standard curve method for analysis.

Ct values for the target gene DJ-1 in each sample was averaged and normalised to the average Ct value of both housekeeper genes. One sample was then chosen to be the internal control and all other readings were normalised to this. A good explanation of the different modes of analysis can be found at http://pathmicro.med.sc.edu/pcr/realtime-home.htm.

## 2.4.2. RNA immunoprecipitation

### 2.4.2.1. Dynabead preparation

For each sample, 100µl of Dynabeads Protein G (Invitrogen, USA) was placed into tubes on a magnetic rack and the initial storage solution was removed once all the beads had stuck to the side wall. Beads were then washed twice with 1ml 150mM NaAc, pH 5.0, in the same manner. 30µg of polyclonal anti-DJ-1 C16 antibody (Santa Cruz, USA) and 150µl of NT2 buffer (50mM Tris. pH 7.4, 150mM NaCl, 1mM $MgCl_2$, 0.05% NP-40) was subsequently added to the beads and rotated for an hour at 4$^{o}$C. They were then washed three times with 1ml ice cold NT2 buffer and stored for use. As a control, 100µl of Dynabeads were prepared in a separate tube in the same manner using 30µg non-specific IgG antibody (Santa Cruz, USA) in place of DJ-1.

### 2.4.2.2. Tissue preparation

Whilst the Dynabeads were being prepared, tissue was homogenised by hand in PLB buffer (0.5% NP-40, 10 mM Hepes, 100 mM KCl, 5 mM MgCl2, 1mM DTT, RNase OUT and protease inhibitors) using a glass homogeniser and left to stand on ice for 10min. Debris was then removed by centrifuging homogenate at 14000g for 15min at 4$^{o}$C. The supernatant was then pre-cleared by rotation with 5µg non-specific IgG (Santa Cruz, UK) and 50µl of Dynabeads for 30min at 4$^{o}$C. Supernatant was then removed and stored for use.

### 2.4.2.3. Immunoprecipitation

To both the prepared DJ-1 and IgG Dynabeads; 700µl NT2 buffer, 10µl 0.1M DTT and 10µl RnaseOUT (Invitrogen, USA) was added along with 250µl of the cleared lysate and rotated overnight at 4°C. The next day the supernatant was removed and stored whilst the beads were washed four times with 1ml cold NT2 buffer. After the last wash 100µl NT2 buffer with 5µl amplification grade DNase (Invitrogen, USA) and incubated for 5min at 37°C. DNase was then replaced with 100µl fresh NT2 buffer containing 0.1% SDS and 2.5µl Proteinase K (Ambion, USA) and incubated at 55°C for 20min. The supernatant was then transferred to a fresh tube and beads washed with another 200µl NT2 which was then added to the first collected supernatant. 300µl of lower layer acid phenol-chloroform (Ambion, USA) was then added and the mixture vortexed. Tubes were then spun for 1min at RT and upper layer transferred to a fresh tube to which 20µl 3M NaAc pH5.2, 625µl 100% ethanol and 5µl glycoblue were added and mixed together. Tubes were placed at -20°C over night to allow RNA to precipitate out. RNA was collected by spinning the tubes the next day at 14000g at 4°C for 30min. Supernatant was removed and pellet washed once with 1ml 70% ethanol, air-dried for 5min and resuspended in 16µl DEPC water.

### 2.4.2.4. cDNA synthesis

The collected RNA was converted into cDNA using SuperScript III First Strand Synthesis System (Invitrogen, USA) as follows. For each reaction, 8µl of RNA was combined with 1µl of 50mM Oligo $(dT)_{20}$ primer and 1µl dNTP mix in a 0.5ml tube and heated to 65°C for 5min. The reaction was stopped by placing on ice for 1min. Next the cDNA synthesis mix was prepared using 2µl 10x RT buffer, 4µl 25nM $MgCl_2$, 2µl 0.1M DTT, 1µl (40 units) RNaseOUT and 1µl (200 units) SuperScript III RT. This was added to the RNA/primer mixture, gently mixed and incubated at 50°C for 50min followed by heating to 85°C for 5min in order to terminate the reaction. Tubes were then briefly centrifuged and placed on ice before 1µl of RNase H was added and left to stand for 20min at 37°C. Like samples were then pooled together and stored at -20°C.

## 2.4.2.5. Identification of mRNA transcripts using RT-PCR

RT-PCR was performed in order to identify selected transcripts under similar principle as before. Reactions were carried out in 384 well plates with a total reaction volume of 10µl consisting of 5µl Sybr Green, 0.3µl forward primer, 0.3µl reverse primer, 1.9µl sterile water and 2.5µl cDNA. Primer sequences for selected transcripts are shown in table 2.3. Reactions were performed using a 7900HT Fast Real Time PCR system (Applied Biosystems, USA) under the following settings: 30s denaturing step at 94$^{o}$C, 1min annealing step at 60$^{o}$C and finally 30s extension step at 72$^{o}$C. All reactions were performed in quadruplicates. Expression of transcripts of interest were normalised to corresponding β-actin levels.

| Primer Name | Primer Sequence 5' - 3' |
|---|---|
| GPx3 F | GTGCTGGACAGTGACAACCCT |
| GPx3 R | GGAGGCAGTGGGAGATGCT |
| GPx4 F | GAGATCAAAGAGTTCGCCGC |
| GPx4 R | GGTGAAGTTCCACTTGATGGC |
| MAPK8IP1 F | TGATGAACCCGACGTCCATT |
| MAPK8IP1 R | CCGTTGATGATGCAGGAGAAC |
| ND1 F | ATGGCCAACCTCCTACTCCT |
| ND1 R | GGTAGATGTGGCGGGTTTTA |
| ND2 F | TAGCCCCCTTTCACTTCTGA |
| ND2 R | ATTTTGCGTAGCTGGGTTTG |
| ND4 F | CCTGACTCCTACCCCTCACA |
| ND4 R | ATCGGGTGATGATAGCCAAG |
| ND5 F | AGCCCTACTCCACTCAAGCA |
| ND5 R | TCGATGATGTGGTCTTTGGA |
| NDUFB1 F | TGGCAGAACTGTAGGCCCC |
| NDUFB1 R | CATTATGCAGGATCGGCCTCA |
| PPP2R2C F | GAACATCATTGCCATCGCC |
| PPP2R2C R | TTGCGGTCGTGAAGGTCAT |
| SEPHS2 F | CTGGCTCTTTCCTGCTCTGG |
| SEPHS2 R | GGGCTCTGAGGCTTGCTCT |
| SEPW1 F | GGACACCTGGTCTTTCCCTGA |
| SEPW1 R | GATGAAACCACGGGACAGGA |

**Table 2.3: Sequence of primers used to identify RNA transcripts bound to DJ-1**

## 2.4.3. Microarray gene expression

Microarrays are one of the latest tools in molecular biology that allows relative quantification of gene expression. This procedure was performed with collaborators at the NIH, Washington USA.

### 2.4.3.1. RNA extraction

Total RNA was extracted from the frontal cortex of 16 control and 14 IPD cases, using the Trizol method described previously. Concentration and purity of extracted RNA was measured using a Nanodrop. RNA integrity was assessed by running 2µg of each sample on a 1.5% TAE agarose gel in the presence of ethidium bromide, in order to separate the 18s and 28s bands in a similar manner to the formaldehyde gels described previously. Samples of poor quality were re-extracted

### 2.4.3.2. Amplification of RNA

Before samples can be used for array analysis they were amplified with the Illumina TotalPrep RNA Amplification Kit (Ambion, USA) in a 96 well plate. This primary involved the synthesis of cDNA from 500ng extracted RNA by incubating with the reverse transcription master mix containing the reverse transcriptase Array Script, for 2hours at 42$^{o}$C. The cDNA was then incubated with 100µl second strand master mix for 2 hours at 16$^{o}$C. Here DNA polymerase is used to synthesise a complementary strand to the cDNA forming double stranded DNA. This was then collected using a filter cartridge, washed with ethanol containing wash buffer and then eluted into 19µl of nuclease-free water. Once cleaned-up the double stranded cDNA is used as a template for *in vitro* transcription to synthesise RNA using a T7 RNA polymerase. This step is performed at 37$^{o}$C for 16hours and is where multiple copies of biotinylated, antisense RNA (aRNA) to each mRNA is generated. The final stage of the amplification process is the aRNA purification step. Here aRNA is washed in 100% ethanol and wash buffer before being eluted in 100µl preheated nuclease water in order to remove salts, inorganic phosphates, enzymes and unincorporated NTPs. The labelled aRNA is now ready for hybridization to array chips.

### 2.4.3.3. Hybridization of aRNA to array chip

750ng of aRNA was mixed with 10µl GEX-HYB reagent (Illumina, USA) and heated to 65$^{o}$C for 5min and allowed to cool to RT. In the meantime HumanRef-8 v2 expression beadchips (chips that allow gene expression profiling of 8 individual samples in parallel) (Illumine, USA) were slid into a hybridisation chamber containing 200µl of GEX-HCB (illumine, USA). 15µl of each sample aRNA/GEX-HYB mix was then pipetted onto each array and chips were incubated in an oven overnight at 58$^{o}$C. The following day the chips were taken from the oven and the coverseal of each array was removed. The chips were then placed immediately into 250ml wash E1BC solution (Illumina, USA) and then transferred into preheated High-Temp wash buffer (Illumina, USA) for 10 min. the chips were next placed into fresh wash E1BC solution and placed on an orbital shaker for 5min. This was followed by 10min on the orbital shaker in 100% ethanol followed by a further 2min in fresh wash E1BC solution. Chips were then placed in supplied wash trays and rock for 10min at a medium speed with 4ml Block E1 buffer (Illumina, USA) before being transferred to fresh wash trays and rocked for a further 10min with 3ml Block E1 buffer containing 3µl streptavidin-Cy3. Chips were subjected to one final 5min wash with Wash E1BC solution before being placed in racks and centrifuged at 275rcf to dry them. They were then stored in the dark at RT till use.

### 2.4.3.4. Reading and analysis of Illumina arrays

Micorarrays were read on an Illumina Bead array reader confocal scanner and a spot intensity was recorded for each probe. The outputted raw data was then loaded into the supplied Illumina Beadstudio software suite and processed to remove any background intensity. Data was then normalised to remove any systemic differences between samples, after which differential gene expression values between control and PD samples could be calculated using the Illumina Custom algorithm.

### 2.4.3.5. Validation of microarray results

It is standard practice to validate microarray findings using an independent technique in order to reduce errors caused by technical inaccuracy of the microarray itself. The technique we used was RT-PCR.

## 2.5. Analysis and representation of data

Where appropriate, data from pathological tissue was compared to data from controls using statistical tests. Before deciding which test to use, data from each group was analysed using a D'Agostino and Pearson omnibus normality test to ascertain whether it followed a Gaussian distribution or not. If the answer was yes, a parametric unpaired student's T-test was used to compare data from the two groups. If the data did not follow a normal distribution, the non-parametric Mann-Whitney test was applied. All statistical calculations were performed using Graphpad Prism 5. Data was plotted using a combination of 3 programs, Graphpad Prism 5, SPSS 16 and Microsoft Excel 2007. Two main graph types were employed: bar graph and box-plots. Bar graphs were plotted showing mean±SEM for each data groups. For box-plots, the mean and interquartile range is illustrated by the bar whilst the whiskers give an indication of the spread of the data. Data points that were at least one and a half and three box lengths away from the interquartile range are labelled as outliers and extreme outliers respectively. Outliers were included in all statistical analysis.

# 3. Comparison of DJ-1 expression in human control and PD brains

# 3.1. Preliminary comparison of DJ-1 protein levels in control and PD

## 3.1.1. Aim

Since the initial discovery of a Dutch and Italian family harbouring homozygous mutations in the DJ-1 gene (Bonifati et al., 2003b) a number of other PD inducing *PARK7* mutations have been identified (Abou-Sleiman et al., 2003; Bonifati et al., 2004; Hedrich et al., 2004a; Hedrich et al., 2004b). These mutations often result in either lack of protein synthesis or formation of aberrant DJ-1 protein and it is the consequential loss of function that results in the development of PD. However, these mutations occur very rarely and account for less than 2% of early-onset cases (Abou-Sleiman et al., 2003; Clark et al., 2004; Hedrich et al., 2004a). Since its contribution towards familial PD is minimal, we decided to investigate any possible involvement in sporadic cases like other PD gene linked proteins e.g. α-synuclein. Using tissue from QSBB we aimed to first learn whether DJ-1 protein levels are altered in PD subjects which would compromise its function.

## 3.1.2. Material and methods

### 3.1.2.1. Pathological material

| Sample | Sex | Age | PMD | pH | Pathology | Regions | | | |
|---|---|---|---|---|---|---|---|---|---|
| | | | | | | Nigra | STR | FCX | CB |
| Con 1 | M | 79 | 56.40 | 6.60 | - | x | x | x | |
| Con 2 | F | 89 | 77.3 | 6.49 | - | x | x | | |
| Con 3 | F | 78 | 51.30 | 6.24 | - | x | | | |
| Con 4 | M | 83 | 117.05 | 6.81 | - | x | | | |
| Con 5 | M | 63 | 42.00 | 6.23 | - | | x | x | |
| Con 6 | F | 73 | 28.00 | 6.38 | - | | x | x | x |
| Con 7 | M | 81 | 40.00 | 6.48 | - | | | | x |
| Con 8 | F | 83 | 20.00 | 6.55 | - | | | | x |
| Mean±SEM | 4M, 4F | 78.6±2.8 | 54.0±10.9 | 6.5±0.1 | | | | | |
| | | | | | | | | | |
| PD 1 | F | 84 | 36.00 | N/A | N | x | x | x | |
| PD 2 | M | 73 | 25.20 | 7.18 | N | x | x | x | |
| PD 3 | M | 75 | 44.15 | 6.73 | N/A | x | x | x | |
| PD 4 | M | 55 | 8.00 | 6.37 | N | x | x | | |
| PD 5 | F | 71 | 50.10 | 6.38 | N | | | | x |
| PD 6 | F | 82 | 24.00 | 6.4 | L | | | | x |
| PD 7 | F | 73 | 40.15 | 6.44 | N/A | | | | x |
| Mean±SEM | 3M, 4F | 73.3±3.6 | 32.5±5.4 | 6.6±0.1 | | | | | |

**Table 3.1: Demographic data of samples used in initial study of DJ-1 protein levels.** N = Neocortical, L = limbic, STR = striatum, FCX = frontal cortex and CB = cerebellum.

For this study a small cohort of samples homogenised in buffer (10mM Tris-HCL, pH7.4, 0.8M NaCl, 1mM EGTA, 10% sucrose and PIC) by my supervisor Dr Bandopadyay prior to the start of the project were used. Sample details are listed in table 3.1.

### 3.1.2.2. DJ-1 chemilluminescent western blotting

10µg of each sample was combined with 4x LDS sample buffer, 10x reducing agent and water and separated on a 10% Bis-Tris gel. Proteins were then transferred and probed with monoclonal DJ-1 antibody diluted 1:5000 for 1 hour overnight at 4$^{o}$C and then incubated with a HRP-conjugated anti-mouse IgG secondary antibody also diluted 1:5000 for 1 hour at RT. ECL and autoradiography film was used to detect DJ-1 immunoreactive bands.

Preliminary results showed DJ-1 expression levels to be high which caused saturation of protein bands on the autoradiograph film, even with short exposure times as shown in figure 3.1.

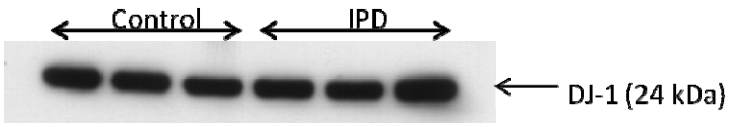


**Figure 3.1 DJ-1 immunoreactive bands from fontal cortex.** Visualisation of DJ-1 protein levels from 10µg of 3 control and 3 PD frontal cortex samples using ECL. Bands become saturated in as little as 10seconds.

This can produce a false intensity reading which makes accurate quantification of protein levels difficult. Two possible ways of overcoming this would be to repeat the run using a lower protein concentration or reduce antibody concentration. A third option that was available to us was to make use of an Odyssey Infrared imaging system which recently became available to us. By replacing the conventional HRP-conjugated secondary antibodies with fluorescent probes, we were able to accurately measure protein levels. Additionally the system allowed us to simultaneously probe for two proteins using a polyclonal and monoclonal antibody thereby removing the side-effects of membrane stripping and re-probing.

### 3.1.2.3. DJ-1 fluorescent western blotting

By taking into account our ECL produced results and the recommended operating guidelines of the Odyssey machine, the total protein load was halved to 5µg. This was separated on a 10% Bis-Tris gel and transferred on to Immobilon-FL PVDF membrane. After blocking with 5% milk, blots were incubated together with monoclonal DJ-1 and polyclonal β-actin antibodies (both 1:5000) overnight at 4$^{o}$C. Blots were then incubated with IRDye 680 Goat Anti-Mouse and IRDye 800 Anti-Rabbit secondary antibodies at 1:20000 dilution for an hour at RT before being scanned on the Odyssey machine. DJ-1 levels were normalised to corresponding β-actin levels and data for control and PD groups were compared via an unpaired student's T-test.

## 3.1.3. Results

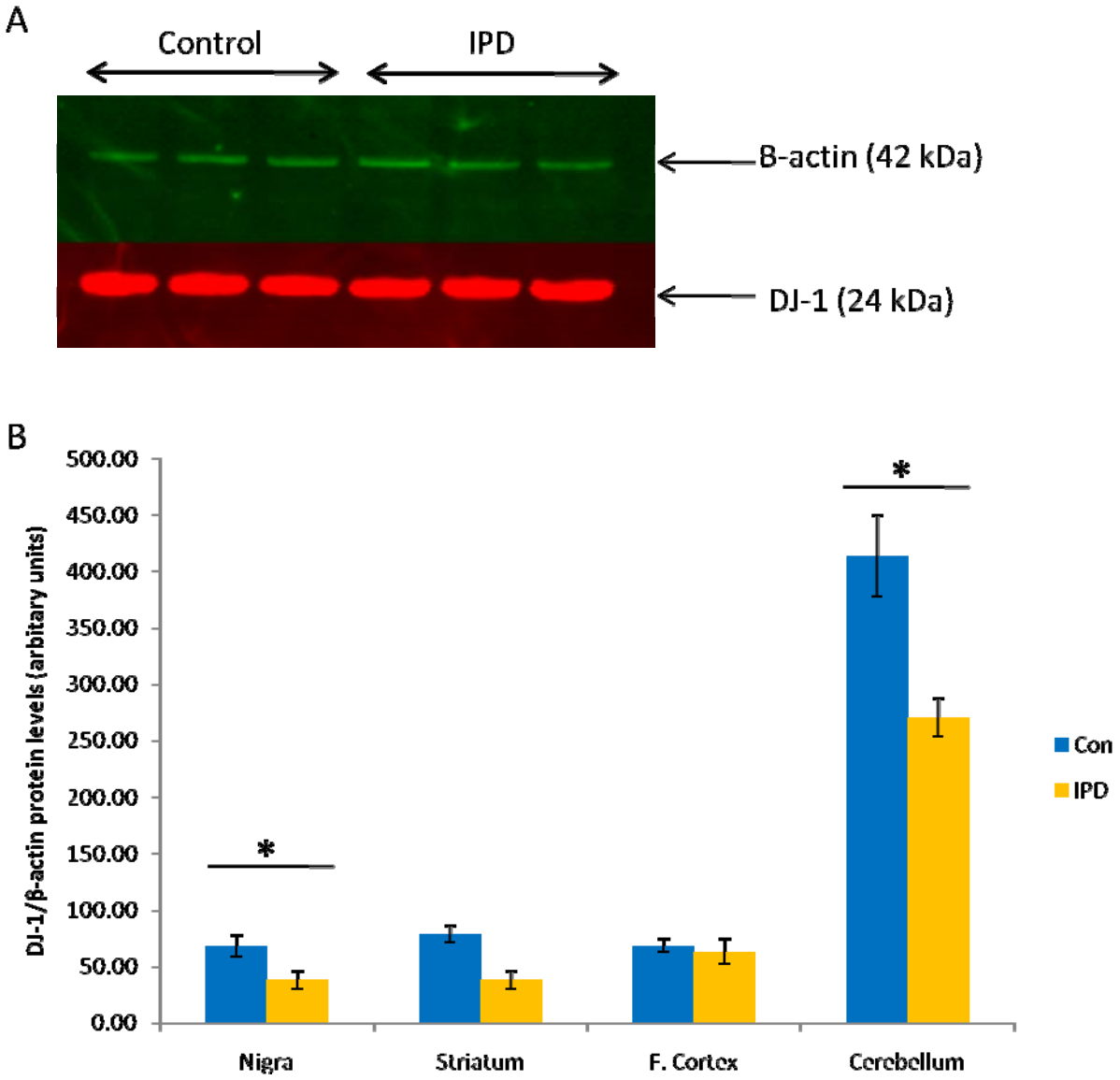


**Figure 3.2: Quantitative western blot analysis of total DJ-1 protein expression in multiple control and PD brain regions.** A) An immunoblot showing DJ-1 (red 700 channel) and β-actin (green 800 channel) protein levels in control and PD cases from frontal cortex n = 3. B) Densitometric quantification of DJ-1 monomer protein levels normalised to β-actin levels in the corresponding brain extract. The bar graph shows the results (mean±SEM) for the nigra (n = 4), striatum (n = 4), frontal cortex (n = 3) and cerebellum (n = 3). * indicates a significant ($p < 0.05$) decrease in total level of DJ-1 protein in PD region versus control, as determined by a student's T-Test.

Western blotting analysis of PD and control samples showed DJ-1 presence in all four regions studied. Quantitative double fluorescent western blotting analysis of DJ-1 protein levels in this small group of samples showed a significant decrease ($p<0.05$) in nigra and cerebellum of PD case when compared to controls (Fig. 3.2). Protein levels were reduced in these two regions by 44% and 35% respectively. A non-significant ($p=0.12$) decrease of 52% was also observed in PD striatum tissue. The PD frontal cortex showed negligible changes in DJ-1 protein levels. Together these results provide an indication for a disease related change in DJ-1 protein levels for a number of regions. Expanding this study using more samples would improve the statistical power of these findings.

# 3.2. Extended analysis of DJ-1 protein levels in control and PD brains

## 3.2.1. Aim

The aim of this study is to expand on preliminary data gathered showing significant PD related decreases of DJ-1 protein in the nigra and cerebellum. By increasing the sample size, we hope to validate these findings and provide more scientifically significant evidence for changes in DJ-1 protein levels in PD brains.

## 3.2.2. Materials and methods

### 3.2.2.1. Pathological material

Tissue group sizes were increased to 8 and homogenised in 50mM Tris-HCL buffer (pH 7.0) as detailed in section 2.2.1. Whilst the nigra is the key pathological region associated with PD, we had difficulty sourcing more tissue and it was therefore dropped. As a replacement we considered the medulla, firstly because it is thought to be affected by PD prior to the nigra and secondly, because it is a relatively understudied region. Details of cases chosen for this study are shown below, in table 3.2.

| Sample | Sex | Age | PMD | pH | Pathology | Regions | | | |
|---|---|---|---|---|---|---|---|---|---|
| | | | | | | Med | Str | FCX | CB |
| Con 1 | F | 85 | 37.10 | n/a | - | | | x | x |
| Con 2 | F | 95 | 39.30 | n/a | - | | | x | |
| Con 3 | M | 79 | 56.40 | 6.60 | - | x | x | x | x |
| Con 4 | M | 85 | 43.35 | 6.68 | - | | | x | |
| Con 5 | M | 86 | 53.00 | 6.65 | - | x | | x | |
| Con 6 | M | 57 | 78.50 | 6.03 | - | x | x | x | x |
| Con 7 | F | 84 | 28.50 | 6.13 | - | x | x | x | x |
| Con 8 | M | 71 | 38.5 | n/a | - | | x | x | |
| Con 9 | M | 63 | 42.00 | 6.23 | - | | x | | x |
| Con 10 | F | 91 | 98.50 | 6.41 | - | | | | x |
| Con 11 | F | 73 | 28.00 | 6.38 | - | | x | | x |
| Con 12 | F | 78 | 23.30 | 6.07 | - | | x | | x |
| Con 13 | F | 83 | 22.00 | 6.25 | - | | x | | |
| Con 14 | F | 64 | 79.00 | 5.88 | - | x | | | |
| Con 15 | F | 86 | 46.50 | 6.17 | - | x | | | |
| Con 16 | F | 85 | 34.00 | 6.31 | - | x | | | |
| Mean±SEM | 6M, 10F | 79.1±2.7 | 46.7±5.4 | 6.3±0.1 | | | | | |
| | | | | | | | | | |
| PD 1 | F | 77 | 80.00 | 6.53 | N | x | x | x | x |
| PD 2 | F | 78 | 75.45 | 6.46 | N | | | x | |
| PD 3 | F | 81 | 24.25 | n/a | L | | | x | |
| PD 4 | M | 70 | 61.20 | 6.29 | L | | | x | |
| PD 5 | M | 55 | 8.00 | 6.37 | N | x | | x | x |
| PD 6 | M | 71 | 40.45 | 6.1 | N | x | | x | |
| PD 7 | M | 79 | 27.25 | 5.88 | N | | | x | |
| PD 8 | M | 71 | 81.30 | 6.76 | N | x | | x | |
| PD 9 | M | 75 | 22.25 | 6.22 | N/A | x | x | | x |
| PD 10 | M | 77 | 28.25 | 6.39 | N/A | | x | | x |
| PD 11 | F | 62 | 46.20 | 5.88 | N | | | | x |
| PD 12 | F | 74 | 48.15 | n/a | N/A | | x | | x |
| PD 13 | F | 69 | 52.45 | 6.14 | N/A | | x | | x |
| PD 14 | M | 76 | 28.45 | n/a | N/A | | x | | x |
| PD 15 | M | 77 | 23.35 | 6.26 | N | | x | | |
| PD 16 | F | 57 | 85.40 | n/a | N/A | | x | | |
| PD 17 | F | 88 | 11.30 | 6.38 | L | x | | | |
| PD 18 | M | 73 | 20.30 | 6.22 | T | x | | | |
| PD 19 | M | 70 | 71.30 | 6.17 | L | x | | | |
| Mean±SEM | 11M, 8F | 72.4±1.9 | 41.9±5.6 | 6.3±0.1 | | | | | |

**Table 3.2 Demographic data for tissue samples used in extended study of DJ-1 protein levels.** N/A = not available, N = Neocortical, T = Transitional, L = Limbic, Med = medulla, Str = striatum, FCX = frontal cortex and CB = cerebellum

### 3.2.2.2. DJ-1 fluorescent western blotting

Western blotting was carried out in a similar manner to that used in the initial study. The key difference being that the polyclonal β-actin antibody was replaced with a monoclonal variant (Sigma, UK) as it provides a stronger and cleaner signal. In addition we increased the total amount of protein loaded to 10µg and reduced the concentration of the primary antibodies to 1:10000 in order to lessen non-specific membrane background. As both the DJ-1 and β-actin antibodies were monoclonal only the IRDye 680 Goat Anti-Mouse secondary antibody was used at 1:20000 dilution. Blots were scanned on the Odyssey machine and DJ-1 protein levels normalised to β-actin before being statistically analysed using an unpaired student's T-test.

### 3.2.2.3. DJ-1 ELISA

In order to independently verify western blotting results, DJ-1 protein levels in the same samples from the frontal cortex, striatum and cerebellum were measured using a commercially available ELISA kit. As the kit was designed for use with plasma, we attempted to standardise it for use with human brain homogenate. This involved finding the optimum homogenate dilution which did not disrupt the standard curve as described in the methods. This was identified as being 1:5000. Samples were then diluted accordingly in PBS and DJ-1 protein levels measured as described in section 2.2.5.

### 3.2.2.4. Results

Our expanded study into PD induced changes in DJ-1 protein levels (Fig. 3.3) confirmed our preliminary findings of a significant decrease in PD cerebellum ($p < 0.02$). Additionally, by increasing the sample size we find PD striatum to now exhibit a significant decrease ($p < 0.04$) in DJ-1 protein. The frontal cortex is another region that now shows a statistically significant decrease in DJ-1 protein in PD tissue compared to control. Indeed, of the four regions examined, the frontal cortex shows the most significant decrease ($p = 0.0005$) of DJ-1 in protein. Following the trend of the other regions, we also find the medulla from PD brains to have a markedly lower ($p = 0.0014$) DJ-1 protein content compared to controls using a 2-tailed T-test. The greatest decrease in protein was found in the cerebellum, where

on average PD tissue contained 70% less DJ-1 protein than control cerebellum. The smallest decrease was 39% in the striatum whilst the medulla and frontal cortex from PD cases contained approximately 60% less DJ-1 protein.

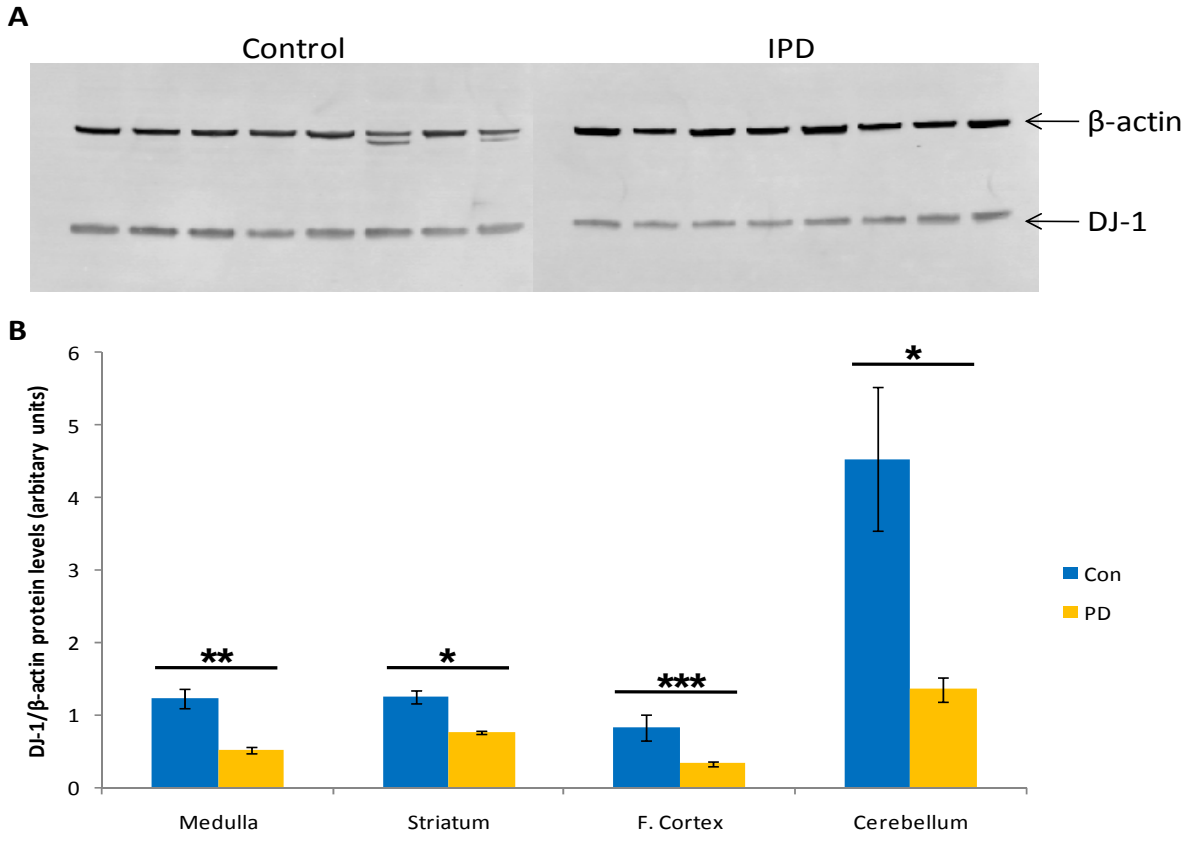


**Figure 3.3: Quantitative western blot analysis of total DJ-1 protein expression in multiple control and PD brain regions.** A) An immunoblot showing DJ-1 and β-actin protein levels in control and PD cases from frontal cortex n = 8 detected together in 700 channel. B) Densitometric quantification of DJ-1 monomer protein levels normalised to β-actin levels in the corresponding brain extract. The bar graph shows the results (mean±SEM) for the medulla, striatum, frontal cortex and cerebellum. * indicates a significant ($p < 0.05$), ** highly significant ($p < 0.01$), *** very significant ($p < 0.001$) decrease in total level of DJ-1 protein in PD region versus control, as determined by a student's T-Test.

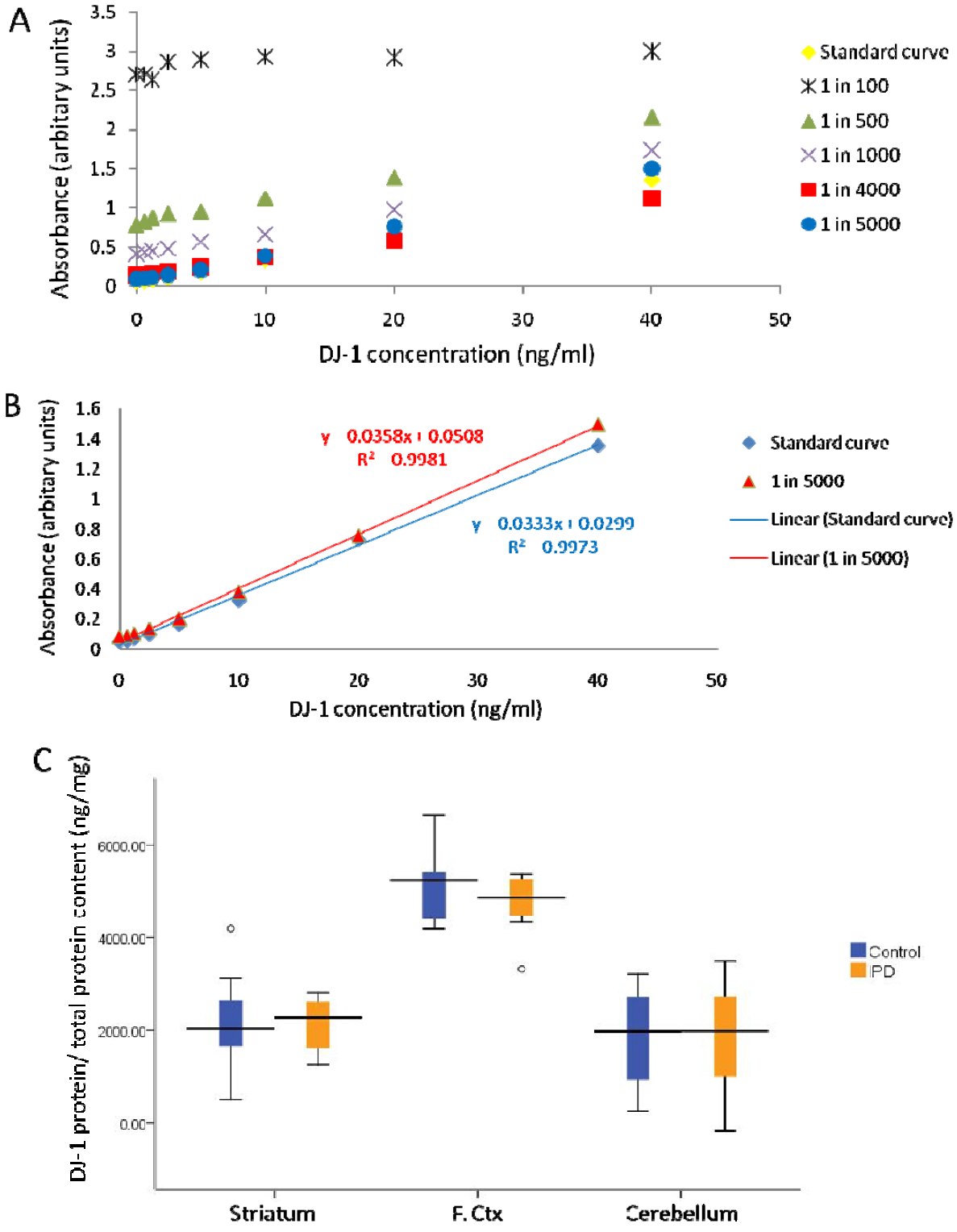


**Figure 3.4: Quantitative analysis of total DJ-1 protein levels in multiple brain control and PD brain regions using ELISA.** A) parallelisms for DJ-1 between calibrant dilution buffer and brain homogenate of varying dilutions. B) Parallelism for DJ-1 between dilution buffer and brain homogenate diluted 1:5000 showing linear regression. C) Levels of soluble DJ-1 in homogenised striatum, frontal cortex and cerebellum control (n = 8) and PD brain (n = 8). $_{o}$ = outliers. F. Ctx = frontal cortex

The commercial ELISA kit is designed for use with human serum/plasma, human cell lines or conditioned medium and had to be adapted for use with human brain homogenate. Parallelisms between the supplied calibrated dilution buffer and brain homogenate were assessed by generating standard curves using different dilutions of brain homogenate spiked with recombinant human DJ-1 (Fig. 3.4A). 1:5000 dilution of brain homogenate displayed the best parallel relationship with the original dilution buffer, as judged by the linear regression line (Fig. 3.4A and B); suggesting interference from brain matrices is minimal at this dilution. Using this dilution factor, we used the ELISA kit to measure soluble DJ-1 protein levels from striatum, frontal cortex and cerebellum of normal control and PD brains. Homogenates for these 3 regions were the same as used in western blotting analysis of DJ-1 protein levels (table 3.2). Contrary to immunoblotting data, no variation in DJ-1 reactivity was detected in any of the regions between control and diseased samples (Fig.3.4C). In both control and PD brains, the region with the greatest amount DJ-1 protein in proportion to total protein was the frontal cortex.

# 3.3. Analysis of DJ-1 insolubility in PD

## 3.3.1. Aim

Having noted soluble DJ-1 protein levels to be significantly reduced in PD brains, we aim to examine whether this is due to a progressive transition towards an insoluble state by sequentially extracting DJ-1 from control and PD cases using buffers of increasing solubilisation strengths.

## 3.3.2. Materials and methods

### 3.3.2.1. Pathological material

As described in Campbell et al., (1999), DJ-1 was sequentially extracted in buffers of increasing solubilisation strengths (TBS soluble, SDS soluble and urea soluble) from the same

frontal cortex tissue used to study soluble DJ-1 protein levels (table 3.2). Frontal cortex tissue was chosen due to its availability and involvement in PD.

#### 3.3.2.2. DJ-1 chemilluminescent western blotting

DJ-1 protein was detected in each fraction using monoclonal DJ-1 antibody after separation on Bio-Rad 10% Tris-HCL gels. For TBS and SDS soluble samples 5µg were separated whilst for urea soluble samples 20µg was used. Density of protein bands were measured using Bio-Rad Quality One software. DJ-1 protein levels were normalised to β-actin and control and PD groups compared using an unpaired student's T-test.

### 3.3.3. Results

In order to study alterations in DJ-1 protein solubility, 8 frontal cortex samples were separated into increasingly insoluble fractions. The most soluble proteins were collected in the TBS buffer, whilst 5% SDS buffer was used to solubilise proteins with an intermediate solubility property, including membrane bound proteins and protein aggregates. The most insoluble protein aggregates were solubilised in 8M urea buffer containing 8% w/v SDS.

Analysis of all samples by western blotting showed DJ-1, for both control and PD cases, to be present in all 3 buffers (Fig. 3.5B). Separation of 5µg of TBS soluble samples on 10% Tris-HCL gels and probing with anti-DJ-1 antibody (dilution 1:5000), revealed PD samples to possess a significantly ($p=0.03$) lower amount of DJ-1 protein than controls samples (Fig. 3.5A). Analysis of DJ-1 protein levels in SDS fractions separated in a similar manner also revealed a highly significant ($p=0.002$) decrease in PD. No DJ-1 immunoreactivity was initially visible in urea fractions. However, after increasing protein load to 20µg and probing with a higher concentration of antibody (1:2000) DJ-1 was detected in all samples. Densitometric quantification followed by normalisation to β-actin showed that like in TBS and SDS fractions, a decreasing trend of DJ-1 protein levels were noted in PD urea samples, though differences to controls were not significant ($p=0.07$). Comparison of immunoblots of all three fractions, suggest DJ-1 protein is largely present in TBS fraction and that only a small proportion resides in the urea soluble homogenate. No higher molecular weight DJ-1

complexes were detected for any of the samples in the 3 fractions with the only observed band corresponding to the 24kDa DJ-1 monomer.

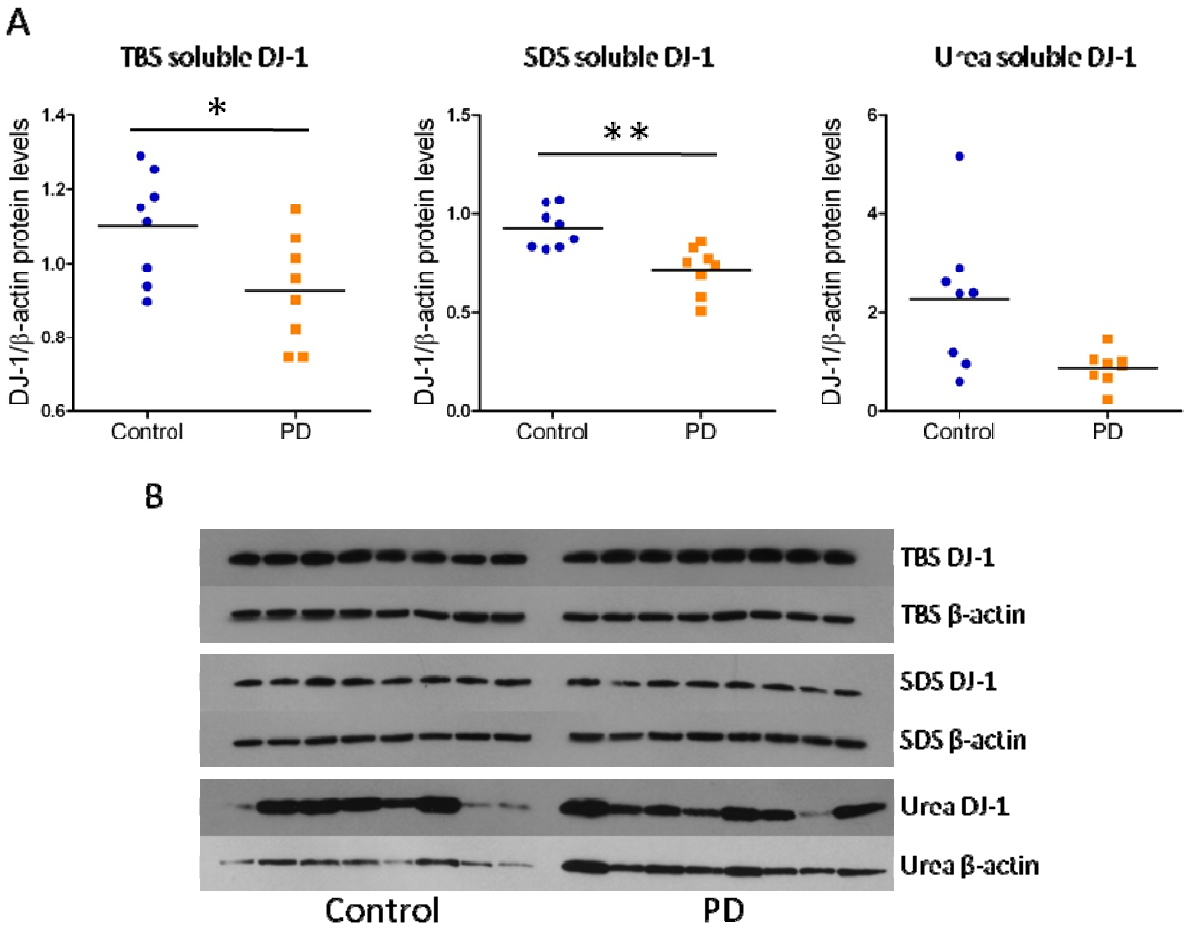


**Figure 3.5: TBS, SDS and Urea soluble DJ-1 protein expression in control and PD frontal cortex.** A) Densitometric quantification of DJ-1 protein levels in TBS, SDS and urea soluble fractions from frontal cortex of control and PD subjects. All samples normalised to corresponding β-actin and control and PD groups compared using unpaired student's T-test. * = $p<0.05$ and **= $p<0.01$. B) Immunoblots of DJ-1 and β-actin from TBS, SDS and urea fractions of 8 control and 8 PD frontal cortex samples.

# 3.4. Comparison of DJ-1 mRNA expression in control and PD brains

## 3.4.1. Aim

Having eliminated disease related aggregation as a cause for the lower soluble DJ-1 protein content found in PD brains, quantitative real-time PCR was used to compare DJ-1 gene expression. Differences between DJ-1 mRNA levels between normal control and PD tissue would suggest the lessened DJ-1 protein levels seen in PD were due to transcriptional changes. However if DJ-1 gene expression is similar in both, post-translational processes such as enhanced protein degradation could be responsible.

## 3.4.2. Materials and methods

### 3.4.2.1. Pathological material

Tissue for this study was collected with the aid of two fellow PhD students, Miss Simone Sharma and Mr Alan Renton, from the medulla, striatum, frontal cortex and cerebellum to correlate with the protein data gathered earlier. Simone and Alan also required RNA from the amygdala, cingulate gyrus, entorhinal cortex and parietal cortex so these regions were also incorporated into my study. Details of cases selected are recorded in table 3.3 below.

| Case | Sex | Age | PMD | pH | Pathology | Regions RNA collected from | | | | | | |
|---|---|---|---|---|---|---|---|---|---|---|---|---|
| | | | | | | CB | FCX | ECX | PCX | AMY | CG | STR |
| Con 1 | F | 77 | 23.0 | 5.60 | - | x | x | x | x | x | x | x |
| Con 2 | F | 86 | 46.5 | 6.17 | - | x | x | x | x | x | x | x |
| Con 3 | F | 84 | 81.5 | 6.28 | - | x | x | x | x | x | x | x |
| Con 4 | M | 85 | 43.4 | 6.68 | - | x | x | x | x | x | x | x |
| Con 5 | M | 86 | 53.0 | 6.65 | - | x | x | x | x | x | x | |
| Con 6 | M | 86 | 23.3 | 6.55 | - | x | x | x | x | x | x | x |
| Con 7 | M | 81 | 40.0 | 6.48 | - | x | x | x | x | | x | x |
| Con 8 | F | 53 | 29.5 | 6.64 | - | x | x | x | x | x | x | x |
| Con 9 | M | 91 | 48.0 | 6.54 | - | x | x | x | x | | x | x |
| Con 10 | F | 88 | 49.3 | 6.23 | - | x | x | x | x | | x | x |
| Con 11 | F | 85 | 34.0 | 6.31 | - | x | x | x | x | x | x | x |
| Con 12 | F | 89 | 77.3 | 6.49 | - | x | x | x | x | x | x | x |
| Con 13 | M | 83 | 117.1 | 6.81 | - | x | x | x | x | x | x | |
| Con 14 | M | 79 | 56.4 | 6.60 | - | x | x | x | x | x | x | x |
| Con 15 | M | 75 | 64.5 | 6.18 | - | x | x | x | x | | x | x |
| Con 16 | F | 81 | 13.5 | 6.39 | - | x | x | x | x | x | x | x |
| Con 17 | M | 63 | 42.0 | 6.23 | - | x | x | x | x | x | x | x |
| Con 18 | M | 57 | 78.5 | 6.03 | - | x | x | x | x | x | x | x |
| Con 19 | F | 78 | 23.3 | 6.07 | - | | x | x | x | x | x | x |
| Con 20 | M | 71 | 38.5 | N/A | - | | x | x | x | x | x | x |
| Mean±SEM | 11M, 9F | 78.9±2.3 | 49.1±5.6 | 6.4±0.1 | | | | | | | | |
| PD 1 | M | 77 | 46.2 | 6.73 | N | x | x | x | x | x | x | x |
| PD 2 | M | 73 | 11.2 | 6.32 | N | x | x | x | x | | x | x |
| PD 3 | F | 62 | 46.2 | 5.88 | N | x | x | x | x | x | x | x |
| PD 4 | F | 78 | 75.5 | 6.46 | N | x | x | x | x | x | x | x |
| PD 5 | F | 87 | 47.5 | 6.62 | T | x | x | x | x | x | x | x |
| PD 6 | F | 81 | 24.3 | N/A | L | x | x | x | x | x | x | x |
| PD 7 | M | 81 | 103.0 | 6.15 | T | x | x | x | x | x | x | x |
| PD 8 | M | 73 | 20.3 | 6.22 | T | x | x | x | x | x | x | x |
| PD 9 | F | 66 | 125.3 | 6.2 | N | x | x | x | x | x | x | x |
| PD 10 | F | 77 | 80.0 | 6.53 | N | x | x | x | x | x | x | x |
| PD 11 | F | 88 | 11.3 | 6.38 | L | x | x | x | x | | x | x |
| PD 12 | M | 70 | 61.2 | 6.29 | L | x | x | x | x | x | x | x |
| PD 13 | M | 55 | 8.0 | 6.37 | N | x | x | x | x | x | x | x |
| PD 14 | M | 71 | 40.5 | 6.10 | N | x | x | x | x | x | x | x |
| PD 15 | M | 79 | 27.3 | 5.88 | N | x | x | x | x | x | x | x |
| PD 16 | M | 71 | 81.3 | 6.76 | N | x | x | x | x | x | x | x |
| PD 17 | M | 70 | 71.3 | 6.17 | L | x | x | x | x | | x | x |
| PD 18 | M | 70 | 51.2 | 6.29 | N | | x | x | x | x | x | x |
| PD 19 | M | 91 | 31.5 | 5.81 | N | x | x | x | x | x | x | x |
| PD 20 | F | 81 | 57.3 | N/A | N | x | x | x | x | x | x | x |
| Mean±SEM | 12M, 8F | 75.1±2.0 | 51.0±7.1 | 6.3±0.1 | | | | | | | | |

**Table 3.3: Demographic data of samples used to study DJ-1 mRNA expression.** x = successful extraction of RNA from that region. N/A = data not available. N = neocortical, T = transitional, L = Limbic, CB = cerebellum, FCX = frontal cortex, ECX = entorhinal cortex, PCX = parietal cortex, AMY = amygdala, CG = cingulate gyrus and STR = striatum.

### 3.4.2.2. RNA extraction

Total RNA was extracted with the help of Simone and Alan using Trizol. RNA integrity was assessed by separation on 1% formaldehyde gels or Agilent bioanalyser. All medulla samples along with a few samples from each of the other regions were dropped from the study due to the poor quality of RNA extracted. RNA concentration was measured using a nanodrop.

### 3.4.2.3. Real-time PCR

1µg RNA from each successful extractions was converted into cDNA using SuperScript III cDNA synthesis kit, as previously described. Expression of DJ-1 was measured using RT-PCR and normalised to corresponding expression of two housekeeper genes, β-actin and B2M. After normalisation, expression of DJ-1 was compared between control and PD samples for each region using a nonparametric Mann-Whitney statistical test.

## 3.4.3. Results

Analysis of DJ-1 mRNA expression, normalised to two housekeeping genes, β-actin and B2M, was performed across multiple control and diseased brain regions using RT-PCR and shown in figure 3.6. Similar to protein expression, the highest average level of DJ-1 mRNA in control brain was found in the cerebellum followed by the frontal and entorhinal cortex. The brain region with the lowest expression of DJ-1 mRNA in normal control was the amygdala. In PD brains the amygdala was also the region with the lowest DJ-1 mRNA expression whilst the entorhinal cortex was where DJ-1 mRNA was most abundant.

Control and PD data were compared using a Mann-Whitney U test. Like protein expression, a statistically significant down-regulation of *DJ-1* mRNA was observed in PD cerebellum ($p=0.0003$), frontal cortex ($p<0.005$) and striatum ($p<0.04$). The largest DJ-1 mRNA expression decrease, at 58%, is seen in the cerebellum (table 3.4). DJ-1 gene expression was significantly elevated in both the entorhinal cortex ($p < 0.005$) and amygdala ($p = 0.0005$) of PD brains in comparison to controls. An increase of 92% nearly doubles the expression of DJ-1 mRNA in PD amygdala compared to control whilst 39% increase was seen in PD

entorhinal cortex. There is no significant difference between the ages, post-mortem delay or pH of control and PD brains which could have influenced DJ-1 gene expression (Fig. 3.7).

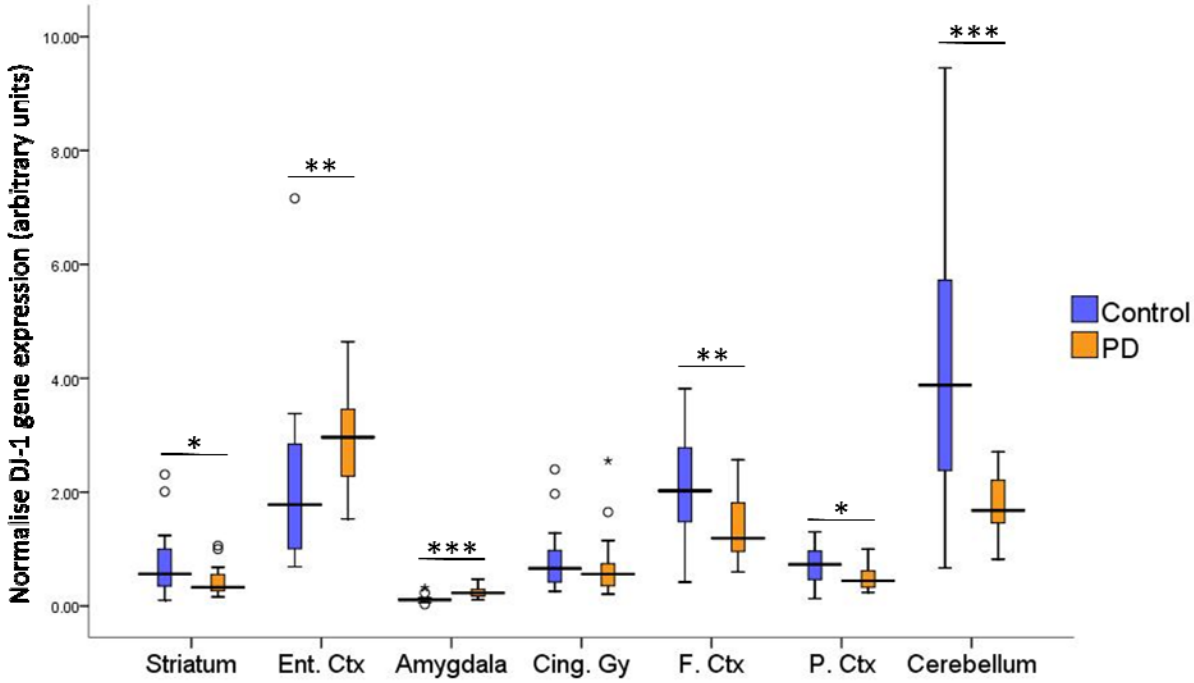


**Figure 3.6: Quantitative real time PCR comparison of human DJ-1 mRNA in multiple human control and PD brain regions.** Data was normalised to β-actin and B2M expression and analysed using a Mann-Whitney U test. Differences between control and PD data considered statistically significant if $p < 0.05$ (*), highly significant if $p < 0.01$ (**) and very significant if $p < 0.001$ (***). $_o$ = outlying readings and + = extreme outliers. Ent Ctx = entorhinal cortex, Cing Gy = cingulated gyrus, F. Ctx = frontal cortex and P. Ctx = parietal cortex. n = 16-20.

| | Striatum | F. Ctx | Cerebellum |
|---|---|---|---|
| Decrease in DJ-1 mRNA expression | 43% | 34% | 58% |
| Decrease in DJ -1 protein expression | 39% | 60% | 70% |

**Table 3.4: DJ-1 mRNA and protein changes in PD tissue compared to control.**

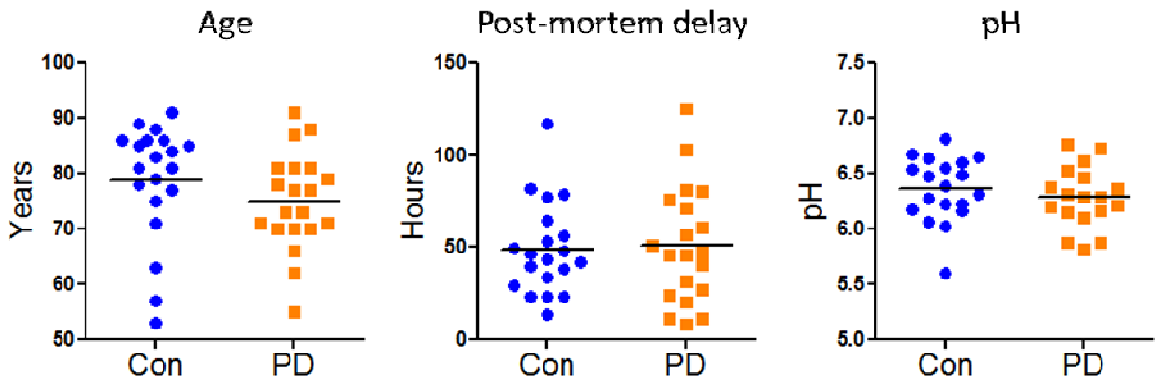


**Figure 3.7: Post-mortem delay, age and pH of control and PD brains included in the real time PCR analysis.** Student's t-test showed no difference between the two groups.

# 3.5. Gender specific changes in DJ-1 expression

## 3.5.1. Aim

DJ-1 has been implicated in male fertility and is homologous to rat CAP1, levels of which can be reduced in sperm and epididymis of rats by treatment with toxic spermicide. This suggests a gender specific role for DJ-1. Using data detailed above, I aim to examine gender related effects on the changes in DJ-1 protein and mRNA expression seen in PD.

## 3.5.2. Material and methods

### 3.5.2.1. Pathological material

Data regarding DJ-1 protein and mRNA levels shown in Fig 3.4 and 3.8 were separated according to gender (table 3.5) and the mean, SD and SEM for each group calculated. An unpaired student's T-test was used to compare gender specific DJ-1 protein changes whilst DJ-1 mRNA data was analysed using a nonparametric Mann-Whitney U test.

DJ-1 protein

| | Striatum | F.Cortex | Cerebellum |
|---|---|---|---|
| Male con | 4 | 5 | 3 |
| Male PD | 4 | 5 | 4 |
| Female con | 4 | 3 | 5 |
| Female PD | 4 | 3 | 4 |

DJ-1 mRNA

| | Striatum | E.Cortex | Amygdala | Cing. Gy | F.Cortex | P.Cortex | Cerebellum |
|---|---|---|---|---|---|---|---|
| Male con | 10 | 11 | 8 | 11 | 11 | 10 | 10 |
| Male PD | 12 | 12 | 9 | 12 | 12 | 12 | 12 |
| Female con | 8 | 9 | 8 | 9 | 9 | 9 | 8 |
| Female PD | 8 | 8 | 7 | 8 | 8 | 8 | 8 |

**Table 3.5: Number of male and female samples used per region for gender specific study on DJ-1 protein and mRNA changes in PD.**

## 3.5.3. Results

Comparison of DJ-1 protein levels in male subjects (Fig. 3.8A) show significantly lower levels in the striatum (p=0.04), frontal cortex (p=0.003) and cerebellum (p=0.04) of PD brains. In control males, the cerebellum contains the greatest amount of DJ-1 protein, at least 3 times more than in striatum and frontal cortex. In males, the cerebellum appears most vulnerable to DJ-1 protein loss, with PD patients having approximately 71% less DJ-1 protein than their control counterparts. The same region also displays a highly significant (p = 0.0007) loss of DJ-1 mRNA which at 64% is the biggest out of all the regions in male PD brains. The striatum, frontal cortex and parietal cortex also all show significant decreases, p=0.03, 0.004 and 0.004 respectively, of around 50% in DJ-1 mRNA in male PD subjects. Analysis of male entorhinal cortex data reveals that the significant increase in DJ-1 mRNA noted in figure 3.8 no longer exists. PD amygdala though still displays a very significant (p=0.0001) increase in DJ-1 mRNA, with average levels more than double those found in controls.

A) Male

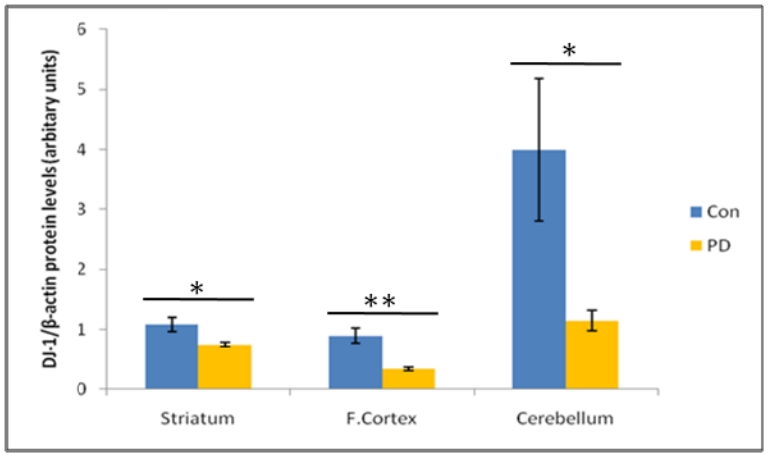


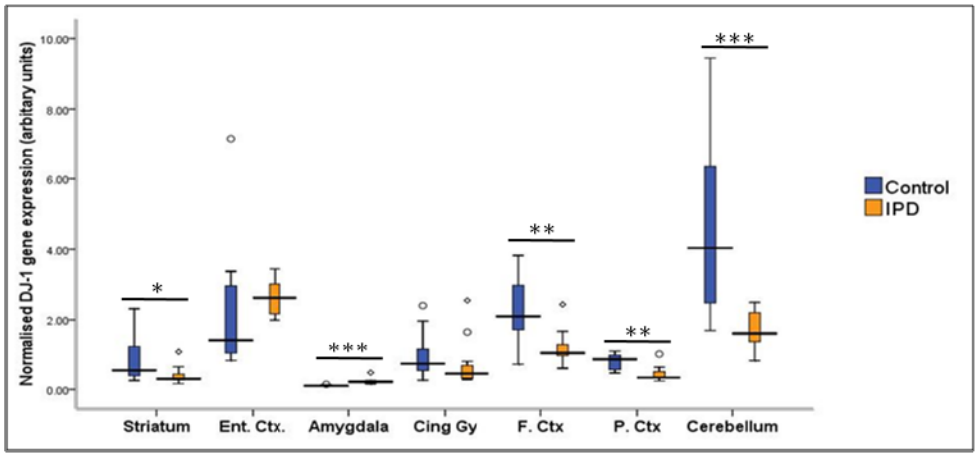


B) Female

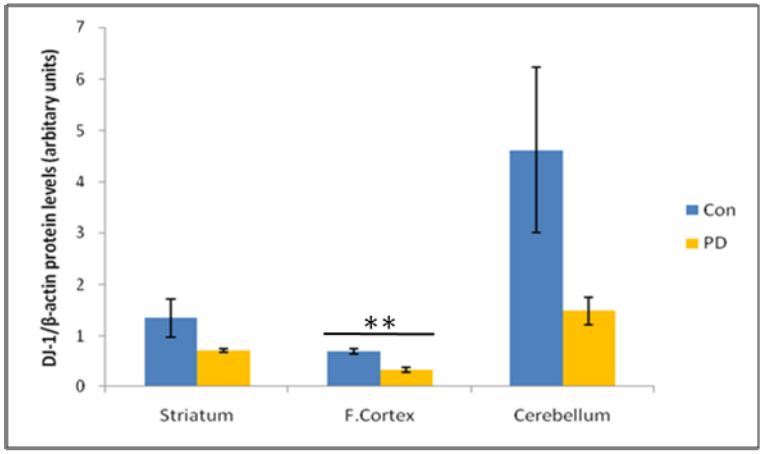


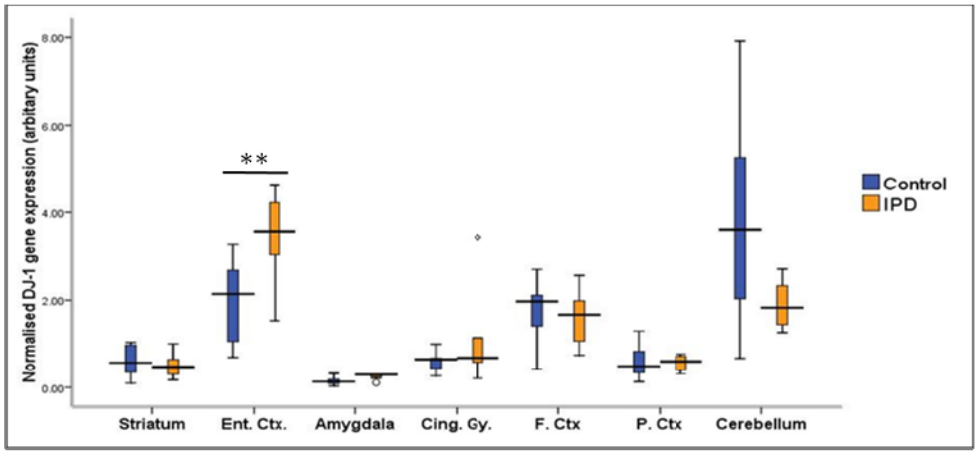


**Fig 3.8: Gender specific comparison of DJ-1 protein and mRNA levels in multiple regions of control and PD brains.** A) Bar graph and boxplot showing DJ-1 protein and mRNA levels in multiple regions of male control and PD brains. B) DJ-1 protein and mRNA levels from multiple brain regions of female control and PD subjects. Bar graph shows mean±SEM. For boxplot ○ outlying readings and ◊ extreme outliers. Student's T Test and Mann Whitney U test used to analyse protein and mRNA data respectively. Differences between control and IPD data considered statistically significant if $p < 0.05$ (*), highly significant if $p < 0.01$ (**) and very significant if $p < 0.001$ (***).

Analysis of data from female brains (Fig. 3.8B) provides some interesting findings. Whilst a highly significant ($p=0.009$) decrease in DJ-1 protein levels is observed in the frontal cortex of female PD subjects, there is no longer any significant variation in the cerebellum and striatum of female control and PD brains. Likewise DJ-1 mRNA levels continue to be significantly elevated in female diseased entorhinal cortex tissue ($p<0.004$). However, no other region shows any statistical differences in DJ-1 mRNA expression between control and PD cases. For both male and female control cases, DJ-1 mRNA appears to be highest in the cerebellum but in PD brains the greatest DJ-1 gene expression is seen in the entorhinal cortex, particularly in females. Medulla protein levels were not examined in this manner, as only two female PD samples were used, making it unsuitable for statistical analysis.

# 3.6. Identification of the native state of DJ-1

## 3.6.1. Aim

Higher molecular weight (HMW) complexes of DJ-1 were noticed on a number of autoradiographs exposed for prolonged periods of time to DJ-1 immunoblots. The following experiments were aimed at identifying the native state of DJ-1 in human control and PD brains.

## 3.6.2. Materials and Methods

### 3.6.2.1. Denaturing western blotting

DJ-1 protein was detected in nigra, striatum, frontal cortex and cerebellum control and PD tissue (table 3.1), using standard western blotting techniques described in section 2.2.3. Briefly, 10µg of each sample was separated on 10% Tris-glycine gels under denaturing conditions. Blots were probed with monoclonal DJ-1 antibody (dilution 1:5000) and protein immunoreactivity detected by exposing a autoradiographic film to activated immunoblots for 4 hours.

### 3.6.2.2. Native, non-denaturing western blotting

Two control cerebellum samples were also separated on a 7% Tris-acetate gel, under native non-denaturing conditions. To achieve this, samples were not mixed with reducing agent or SDS and not heated. After gel electrophoresis, samples were transferred onto membranes, incubated with anti-DJ-1 antibody and visualised using x-ray film.

### 3.6.2.3. Gel-exclusion chromatography

One control and one PD medulla, striatum, frontal cortex and cerebellum tissue sample was homogenised in PBS containing 0.1% Triton-X100 and separated via FPLC gel-exclusion chromatography into 45 fractions by collaborators at the NIH, Washington DC. Each fraction was then screened for the presence of DJ-1 by western blotting. ImageJ, an analysis software similar to Quality One was used to measure the density of DJ-1 bands. These were then expressed as a percentage of total DJ-1 and duly plotted in Microsoft Excel to identify the most abundant DJ-1 complex.

## 3.6.3. Results

10µg of brain homogenate, containing soluble protein, were separated on 10% tris-glycine gels and probed with monoclonal DJ-1 antibody. 2 SDS resistant DJ-1 complexes, in addition to the 24kDa monomer, were seen after prolonged exposure to X-ray film. The 47kDa complex was clearly evident in both the cerebellum and striatum, with a faint immunoreactive band also noticeable in the nigra (Fig. 3.9A). The molecular size of this complex is comparable to DJ-1 dimer. In samples from the cerebellum, a faint immunoreactive band was detected just below the 47kDa dimer complex and may represent a modified/degraded DJ-1 dimer. In addition to the monomeric and dimeric forms of DJ-1, another DJ-1 complex with a molecular weight of 64kDa was seen on all the samples from nigra, cortex, striatum and cerebellum. These HMW complexes appear in both control and PD samples. This band appears to be most prominent in the nigra of control and PD brains and weakest in the frontal cortex.

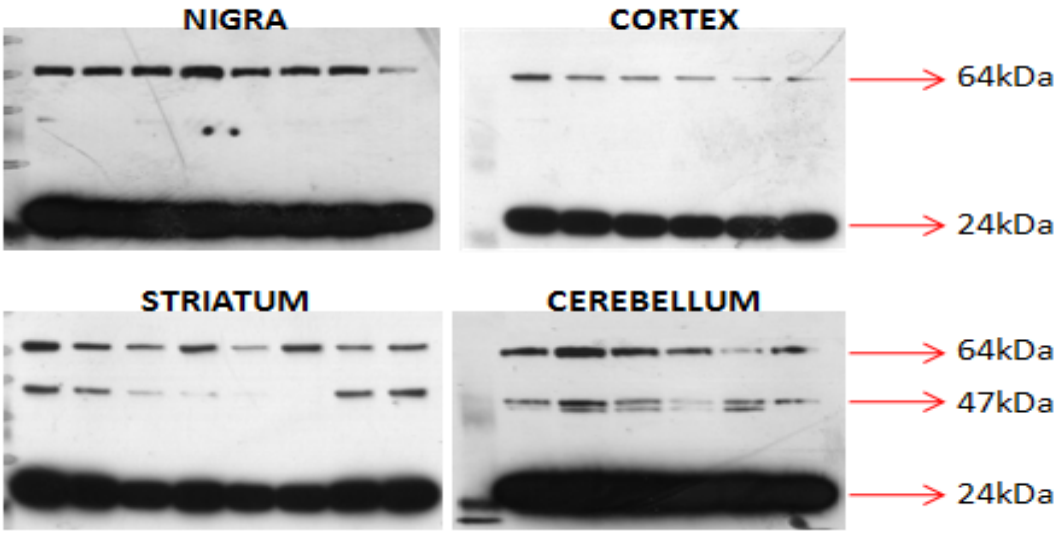


**Figure 3.9: Higher molecular weight DJ-1 complexes.** A) Prolonged exposure of autoradiographic film to DJ-1 immunoblots showing presence of 47 and 64kDa SDS-resistant complexes containing DJ-1. Regions shown are nigra, frontal cortex, striatum and cerebellum First half of samples on each immunoblot are control samples and the latter half are PD samples.

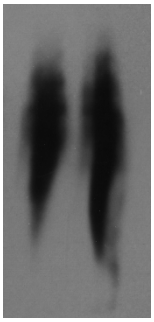

**Figure 3.10: Native DJ-1 expression in cerebellum.** Separation of 5µg control cerebellum homogenate on native gel followed by incubation with anti-DJ-1.

In order to ascertain the native state of DJ-1 in human control and PD brain tissue, 5µg of control cerebellum was separated under native non-denaturing conditions. Probing with monoclonal DJ-1 antibody showed a smear in each sample reflecting the inability of DJ-1 to be resolved under these conditions (Fig. 3.10).

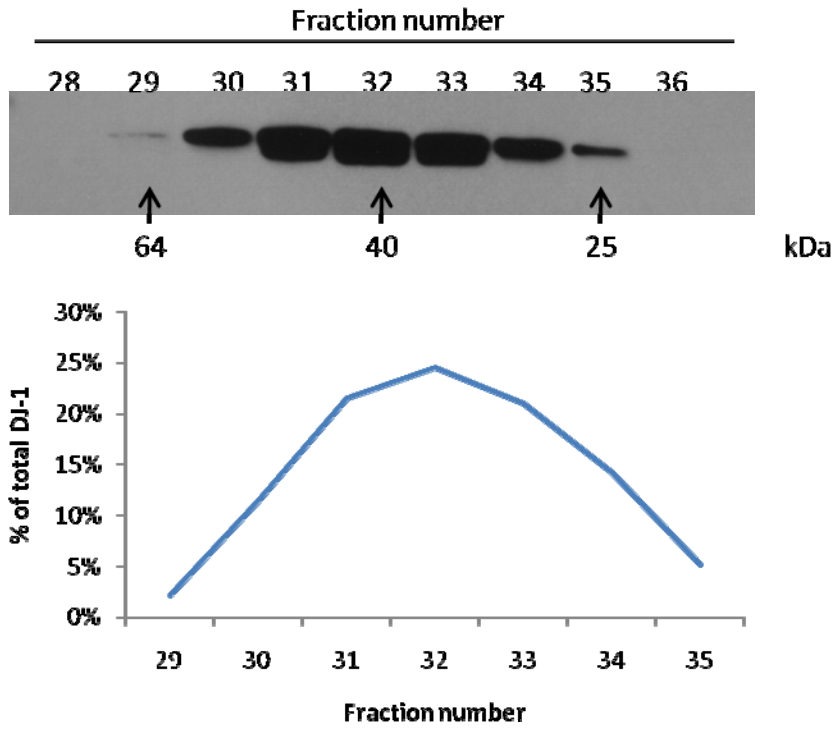


**Figure 3.11: Distribution of human brain DJ-1 from control medulla after gel filtration.** Immunoblot showing distribution of DJ-1 in fractions 29-35 and a graph showing the amount of DJ-1 in each fraction expressed as a % of total DJ-1 present. The majority of DJ-1 is found in fraction 32, which includes molecular complexes with a molecular weight of approximately 40kDa ±15%. This would include the DJ-1 dimer with its predicted weight of 47kDa.

As an alternative, control and PD brain tissue was homogenised in PBS containing 0.1% Triton X100 and subjected to FPLC gel-exclusion chromatography. Analysis of native DJ-1 from multiple control and PD brain regions, via this method revealed a single major peak for all samples in fraction 32 (Fig. 3.11 and table 3.6). This corresponded to a molecular weight range of 39-47kDa. Given the ±15% accuracy of this technique, this is consistent with the predicted size of DJ-1 homodimer and the 47kDa immunoreactive band seen in figure 3.9. For all tissue used, the greatest percentage of DJ-1 was found in this fraction, suggesting the majority of DJ-1 protein in human brain exists as a dimer. DJ-1 also exists as a monomer, though in much lower levels. This can be seen by its elution into fraction 35, which relates to proteins with an approximate size of 25kDa. A tiny percentage of DJ-1 with a calculated size of 63-70kDa was observed in fraction 29 and is consistent with the 64kDa immunoreactive band seen on the denaturing gels in figure 3.9. These results suggest DJ-1 preferentially

exists as a dimer in human brain tissue and that it is capable of forming higher order structures, possibly an oligomer complex.

| Sample | Most abundant complex size (kDa) | Highest complex size (kDa) | Lowest complex size (kDa) |
|---|---|---|---|
| Cerebellum Control | 43.7 | 69.0 | 27.4 |
| Cerebellum PD | 40.6 | 68.7 | 24.9 |
| Frontal Cortex control | 47.2 | 68.7 | 26.2 |
| Frontal cortex PD | 39.0 | 62.7 | 24.0 |
| Medulla control | 40.0 | 63.7 | 25.1 |
| Medulla PD | 43.4 | 64.4 | 24.5 |

**Table 3.6: A table showing the most abundant DJ-1 complex in different control and PD brain region.** The molecular sizes of the highest and lowest complexes are also shown. All molecular weights are ± 15%.

# 3.7. Comparison of DJ-1 pI isoform distribution

## 3.7.1. Aim

Exposure to ROS has been shown to cause a pI shift of DJ-1, resulting in a more acidic isoform. In accordance with this, accumulation of acidic pI isoforms has been documented in PD frontal cortex. As PD pathology is thought to progress up the brainstem into the cortical regions I intend to determine whether DJ-1's pI isoform distribution in control and PD subjects varies between regions.

## 3.7.2. Material and methods

### 3.7.2.1. Pathological material

The regions used in this study were medulla, nigra, striatum, frontal cortex and cerebellum. For each region, DJ-1 pI isoforms were visualised in 4 control and 4 PD samples. Control samples 1-4 and PD samples 1-4 detailed in table 3.2 were used for medulla, striatum,

frontal cortex and cerebellum. Nigra samples were taken from the preliminary DJ-1 protein expression study and are described in table 3.1.

### 3.7.2.2. 2DGE

25µg of protein from each sample underwent isoelectric focusing on a 7cm IPG strip before equilibration in first, SDS equilibration buffer containing 1% w/v DTT and then secondly in the same buffer with 2.5% w/v iodoacetamide in place of DTT. Proteins were subsequently separated by molecular weight on a 12% Tris-glycine gel. Following electroblotting on to PVDF membrane, monoclonal DJ-1 antibody (1:1000 dilution) was used to visualise DJ-1 pI isoforms on autoradiographic film. Intensity of each isoform was measured using Quality One software and expressed as a percentage of total sample DJ-1. After separating the data into control and PD groups for each region, the average and SEM of each isoform was calculated. For each region, the proportion of DJ-1 in each isoform was compared between control and PD using the unpaired T-test.

### 3.7.2.3. 2DGE detection of DJ-1 HMW DJ-1 pI isoforms

In order to try and identify pI isoforms for DJ-1 HMW complexes, the same procedure as above was performed using 65µg starting material. Additionally, activated immunoblots were exposed to autoradiographic film for a period of 4 hours or more, to maximise signal capture.

### 3.7.2.4. Protein derivation

Following separation in the first dimension of 40µg of a PD striatum and frontal cortex sample, proteins on the IPG strip were derivatised by washing IPG strips with 2N HCl containing 10mM DNP, at RT for 20min. Protein samples were then equilibrated and subsequently separated using SDS PAGE before being transferred onto nylon membrane as normal. Anti-DNP antibody, diluted 1:10000, was used to detect the presence of protein carbonyls. Membranes were then stripped with commercially available stripping buffer and then probed for DJ-1.

## 3.7.3. Results

In order to investigate any possible oxidative modifications of DJ-1 in PD vulnerable regions, regional expression patterns of DJ-1 pI isoforms were studied in frontal cortex, striatum, nigra, medulla and cerebellum of 4 control and 4 PD individuals (Fig. 3.12). Separation of 25µg of protein using 2DGE resulted in at least 6 pI isoforms of DJ-1 being resolved (5.3, 5.4, 5.5, 5.6, 5.8 and 6.3) in the medulla, nigra and striatum. All isoforms had a molecular mass equal to that of DJ-1 monomer (24kDa). Two additional isoforms (6.0 and 6.5) were identified in both cortex and cerebellum samples (Fig. 3.12A). To better compare DJ-1 oxidation between control and PD samples, DJ-1 isoforms with a pI value less than or equal to 5.8 were collated together and compared using a student's T-test. pI 5.8 was selected as the cut off value based on based *in vitro* studies showing exposure to ROS causes DJ-1 to undergo a pI shift to 5.8 or below (Bandopadhyay et al., 2004; Canet-Aviles et al., 2004; Mitsumoto et al., 2001).

In the frontal cortex, an accumulation of acidic isoforms (5.8 or below) was noted in PD samples (Fig. 3.12F). In particular, levels of pI 5.4 DJ-1 isoform were elevated in PD. This shift towards more acidic isoforms resulted in a significant decrease in the amount of DJ-1 resolved at isoelectric points greater than 5.8 in the same subjects. A similar pattern was also observed in PD medulla (Fig. 3.12C). No significant alterations in DJ-1 pI isoform distribution were visible between control and PD in the nigra, striatum and cerebellum (Fig. 3.12D, E and G). In all regions, the bulk of DJ-1 adopts a pI state of 5.6, 5.8 or 6.3 regardless of pathological condition. Very faint traces of a more acidic DJ-1 isoform, pI 5.2, were detected in a number of samples, particularly in nigra and cerebellum (Fig. 3.12 D and G). In all cases these accounted for less than 1% of total DJ-1. Separation of frontal cortex and striatum protein samples on a pH 3-10 IPG strip showed no DJ-1 isoforms more basic than 6.5 (Fig. 3.12B).

In addition to monomeric forms of DJ-1, a number of pI isoforms were also observed for the SDS-resistant HMW complexes when a larger amount of protein (65µg) was separated (Fig. 3.13A). For the 64kDa DJ-1 complex, at least 7 different pI isoforms were found at isoelectric points 5.6, 5.7, 5.8, 6.0, 6.3, 6.9 and 7.0 (Fig. 3.13B). Two degraded monomer pI isoforms,

5.8 and 6.3 were also seen. The 47kDa DJ-1 dimer complex is clearly composed of a minimum of 4 pI isoforms; 5.7, 5.8, 6.0 and 6.3 (Fig 3.13C). Though not always clearly resolved, pI isoforms for both the 47 and 64kDa complexes were seen in both control and PD samples. However, their visibility was temperamental which prevented us from establishing the pI isoform makeup of these HMC complexes, as was done for the monomer.

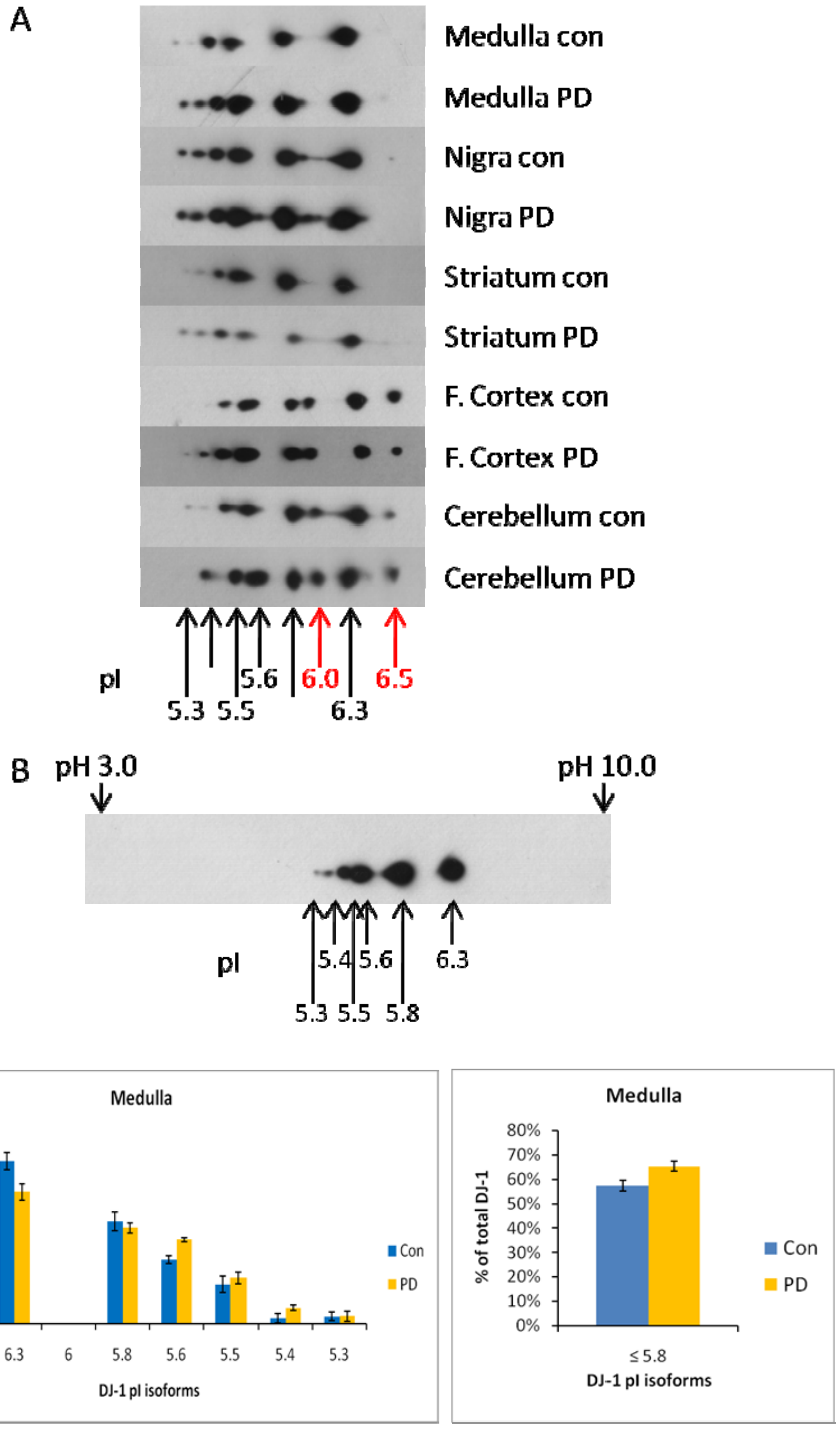

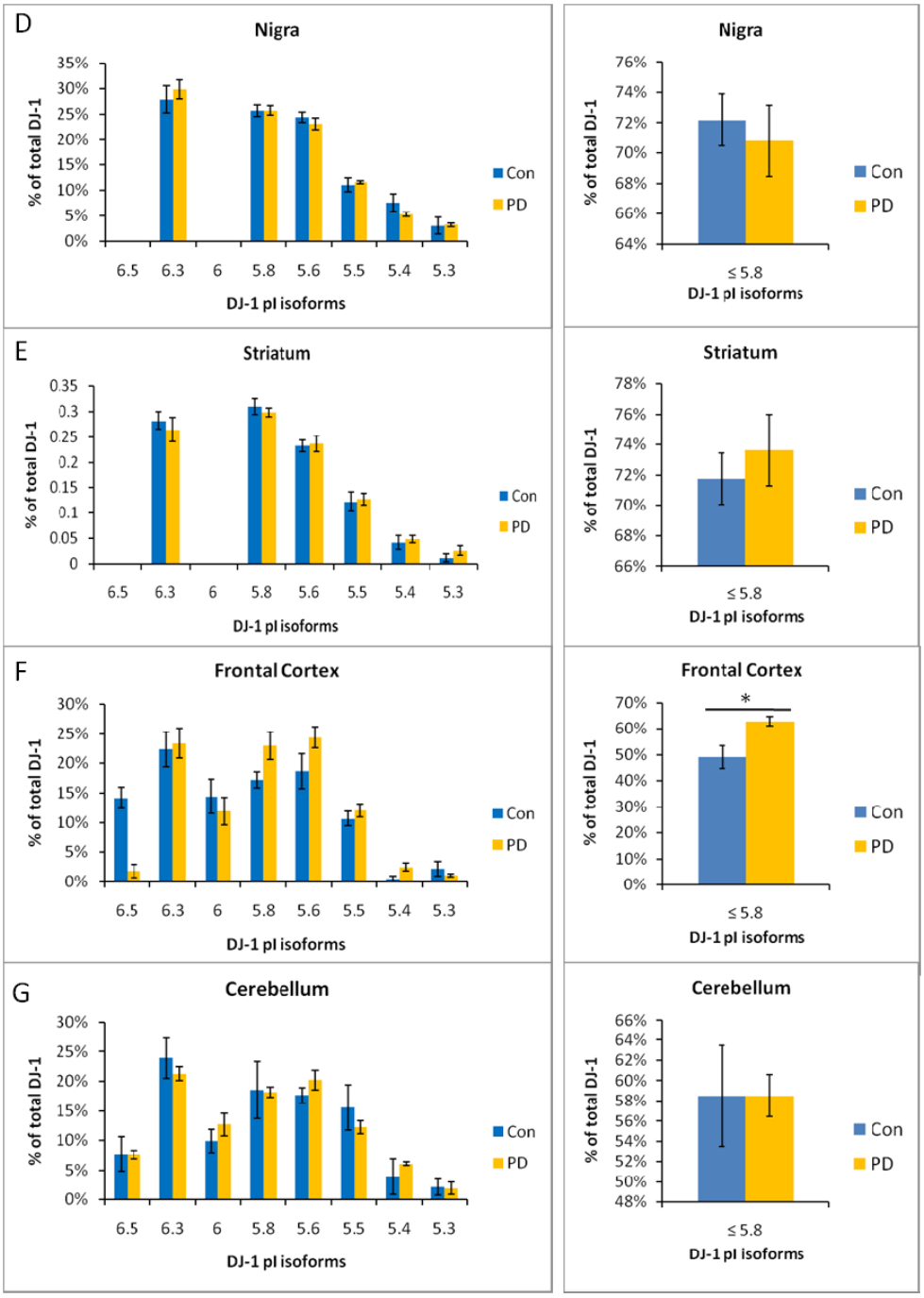


**Figure 3.12: Expression of DJ-1 monomer isoforms in control and PD brain regions.** A) DJ-1 pI isoform expression in multiple control and PD brains regions as revealed by 2-dimensional immunoblot analysis across a 4-7pH range. Arrows indicated approximate pI value. Red arrow highlights pI isoforms predominantly found within frontal cortex and cerebellum. B) DJ-1 pI expression in striatum across 3-10 pH range. C-G) pI distribution of DJ-1 in multiple control and PD brain regions and comparison oxidised DJ-1 levels below pI 5.8. Values represent mean±SEM for 4 controls (blue) and 4 PD (orange) cases for C) medulla, D) nigra, E) striatum, F) frontal cortex and G) cerebellum. Data compared using unpaired student's T-test. Differences between control and PD considered statistically significant if $p<0.05$ (*).

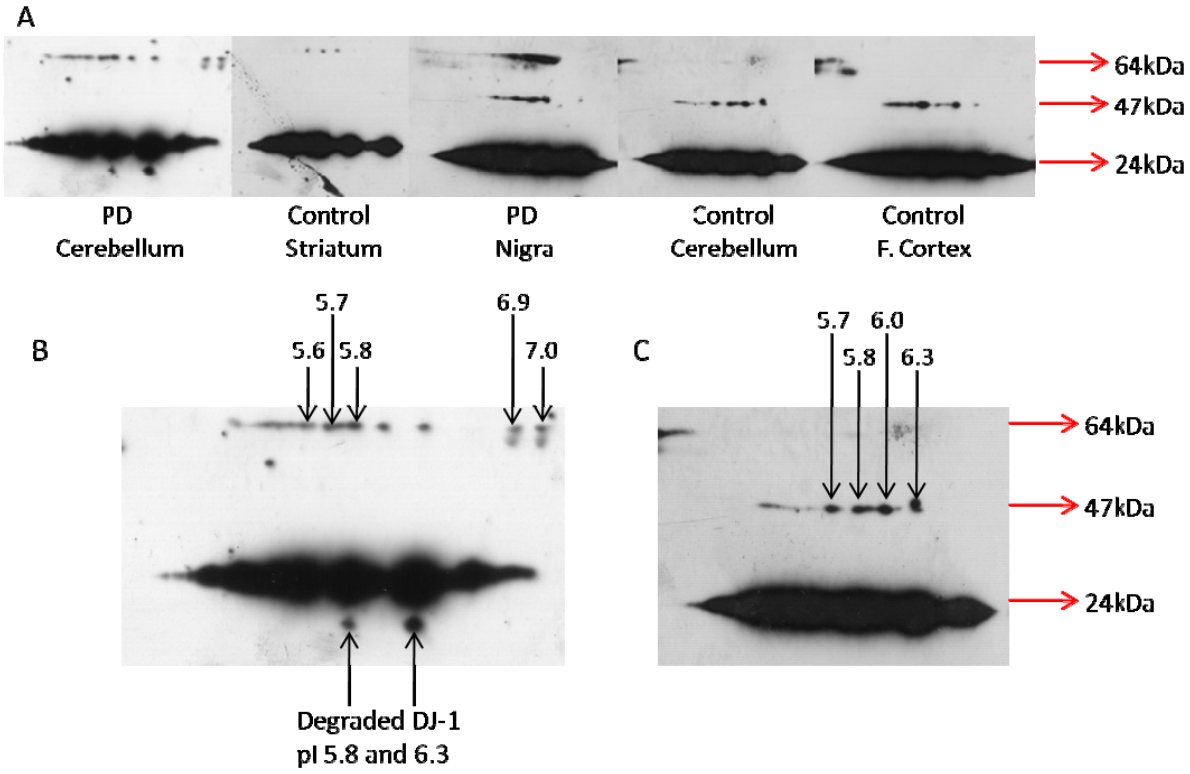


**Figure 3.13: pI isoforms of DJ-1 higher molecular weight complexes.** A) Multiple DJ-1 pI isoforms for DJ-1 dimer and other HMC in multiple brain regions as revealed by separation of 50µg of brain homogenate by 2DGE and probing with anti-DJ-1 antibody. B) Identification of pI isoforms present in 64kDa DJ-1 complex from PD cerebellum. 2 degraded pI isoforms of DJ-1 monomer also shown. C) DJ-1 47kDa homodimer pI expression in a control cerebellum.

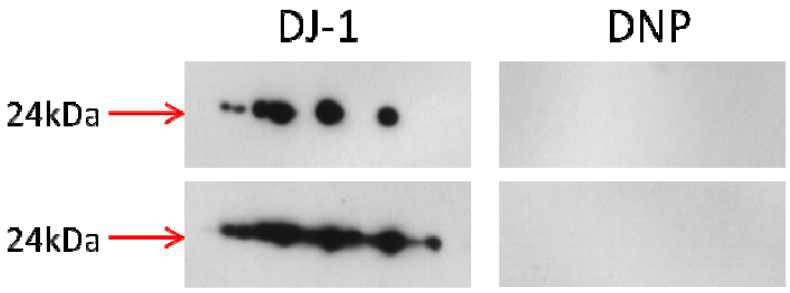


**Figure 3.14: Presence of protein carbonyls in DJ-1 monomer pI isoforms.** 40ug of PD striatum (top) and PD frontal cortex (bottom) were separated using 2DGE and probed with anti-DJ-1 and anti-DNP antibodies to detect presence of DJ-1 protein and protein carbonyls respectively.

In order to establish the extent of oxidative damage to DJ-1 protein, we tried to detect protein carbonyls in the DJ-1 pI isoforms. After treating the samples with 2, 4-

dinitrophenylhydrazine to derivitise the carbonyls, the samples underwent gel electrophoresis and were subsequently probed with an anti-DNP antibody. However, no immunoreactivity was detected in the blot area corresponding to the DJ-1 monomer (24kDa), suggesting that no DJ-1 pI isoforms undergo carbonylation in the striatum or frontal cortex of PD subjects (Fig. 3.13). Blots were then stripped and immunoblotted with DJ-1 to confirm protein presence and validate protein separation and transfer.

# 3.8. Cellular localisation of DJ-1

## 3.8.1. Aim

The aim of this project is to detail the cellular distribution pattern of DJ-1 in different regions of control and PD brains.

## 3.8.2. Methods

### 3.8.2.1. Pathological material

Cellular expression in the following regions: medulla, striatum, entorhinal cortex, hippocampus, cingulate gyrus, frontal cortex, parietal cortex, amygdala and cerebellum were studied in 3 control and PD subjects detailed below (table 3.7).

| Case | Sex | Age | PMD | pH | Pathology |
|---|---|---|---|---|---|
| Con 1 | M | 83 | 117.1 | 6.81 | - |
| Con 2 | M | 79 | 56.4 | 6.60 | - |
| Con 3 | M | 75 | 64.5 | 6.18 | - |
| Mean±SEM | 3M, 0F | 79.0±2.3 | 79.3±19.0 | 6.5±0.2 | |
| | | | | | |
| PD 1 | M | 77 | 46.2 | 6.73 | N |
| PD 2 | M | 73 | 11.2 | 6.32 | N/A |
| PD 3 | F | 77 | 80.0 | 6.53 | N |
| Mean±SEM | 2M, 1F | 75.7±1.3 | 45.8±19.9 | 6.5±0.1 | |

**Table 3.7: Demographic data for subjects use in DJ-1 cellular expression study.** N = neocortical and N/A = not available.

### 3.8.2.2. Immunohistochemistry

Sections were incubated overnight with DJ-1 monoclonal antibody (1:1000) following pretreatment with boiling citrate buffer. DAB was used to identify DJ-1 positive structures. Semi-quantitative assessment was carried out independently by my supervisor and me. Staining of neurons and astrocytes were graded using the following scale; - negative, 0/+rare, + few, ++ moderate, +++many and ++++ numerous.

## 3.8.3. Results

DJ-1 IR was observed in all regions of control and PD brains. Semi-quantitative assessment of DJ-1 positive neuronal and astrocytic structure are summarised in table 3.8.

| Area of brain | Region | Neurons | | Astrocytes | |
|---|---|---|---|---|---|
| | | Control | PD | Control | PD |
| Brainstem | Medulla | + to ++ | ++ | +++ to ++++ | +++ to ++++ |
| Basal Ganglia | Midbrain | 0/+ | 0/+ | +++ | +++ |
| | Striatum | - to + | - to + | ++++ | ++++ |
| Medial-temporal lobe | Hippocampus | - | - to ++ | +++ to ++++ | +++ to ++++ |
| | Entorhinal cortex | 0/+ to + | + to ++ | +++ | ++++ |
| | Amygdala | + to ++ | + to ++ | ++++ | ++++ |
| Neocortex | Frontal cortex | 0/+ to + | 0/+ to + | ++++ | ++++ |
| | Temporal cortex | 0/+ | 0/+ | ++++ | ++++ |
| | Parietal cortex | 0/+ | 0/+ | ++++ | ++++ |
| | Cingulate gyrus | 0/+ | 0/+ | ++++ | ++++ |
| Cerebellum | Cerebellar cortex | - to 0/+ | - to 0/+ | ++++ | ++++ |

**Table 3.8: Semi-quantitative comparison of DJ-1 immunoreactive neurons and astrocytes in control and PD brain.** Neuronal and astrocytic immunoreactivity was independently semi-quantified using the following scale: - = absent, 0/+ = rare, + = few, ++ = moderate, +++ = many and ++++ = numerous.

For all regions, regardless of pathological state, the majority of DJ-1 IR was located within astrocytes. Differences between astrocytic staining in control and PD tissue were largely negligible, with the entorhinal cortex being the only region where a noticeable difference was observed. Neuronal staining was largely minimal in all regions and when present was weaker than in astrocytes.

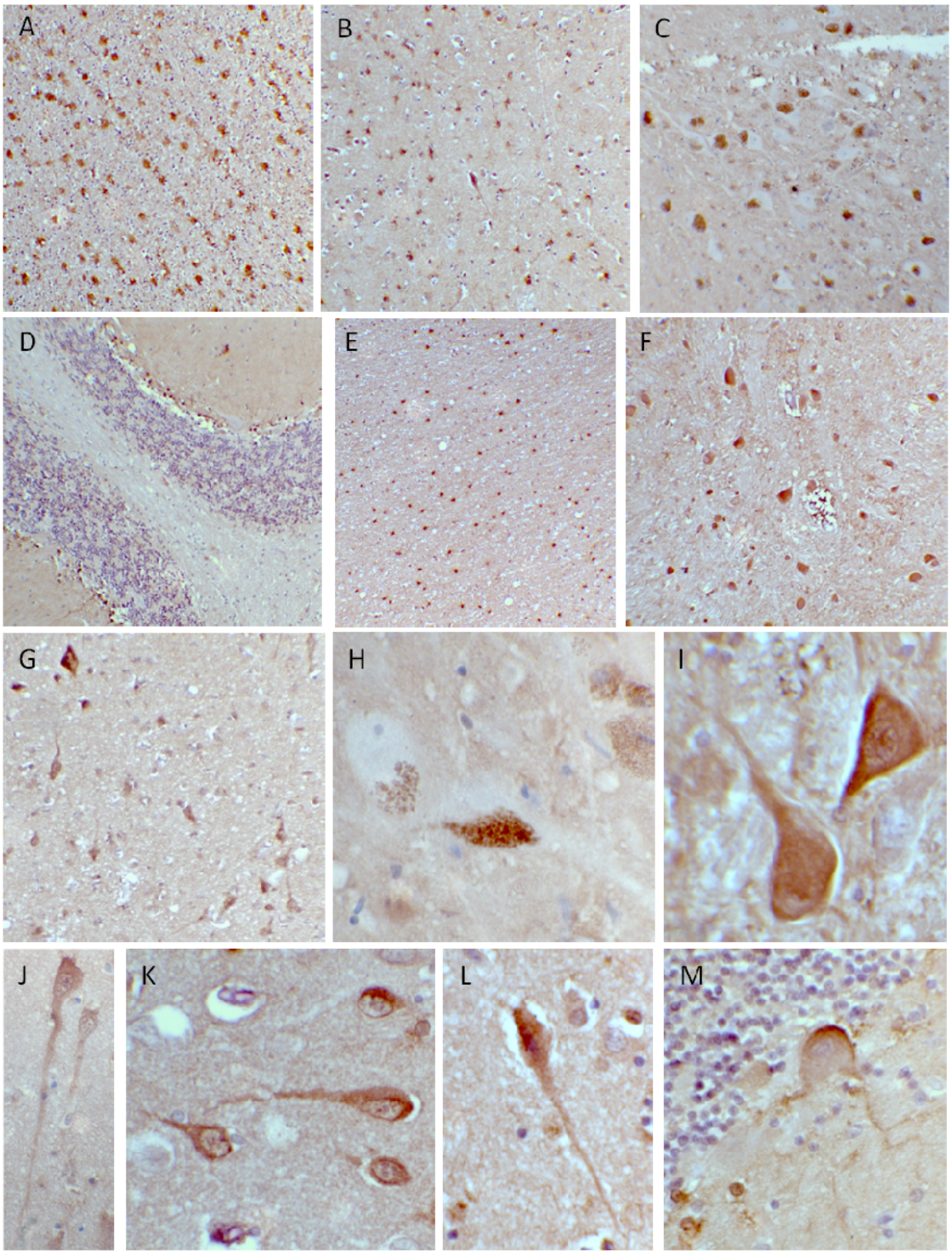


**Figure 3.15: Cellular expression of DJ-1 protein in the human brain.** Abundant astrocytic expression of DJ-1 in control amygdala (A) and frontal cortex (B). C) Reactive astrocytes in control substantia nigra. D) Immunoreactive Bergmann glia in molecular layer of PD cerebellum and DJ positive astrocytes from PD cingulate gyrus (E). Neuronal staining in PD medulla (F) and entorhinal cortex (G). DJ-1 negative dopaminergic neuron in control substantia nigra. Variable high powered immunolabelling of neurons with DJ-1 in control medulla (I), cingulate gyrus (J), amygdala (K) and frontal cortex (L). An extremely rare DJ-1 positive purkinje neuron from control cerebellum. A – G are low powered 10x images and H – M are high powered 40x.

For both normal and diseased individuals, neocortical areas displayed abundant DJ-1 immunoreactive astrocytes (Fig. 3.15B and E) with the occasional DJ-1 positive neuron also being observed. (Fig. 3.15J and L). These were sparsely distributed throughout the cortical areas. A similar pattern was seen in the basal ganglia (Fig. 3.15C). There was no discernible difference between DJ-1 IR in caudate and putamen regions of the striatum, whilst dopaminergic neurons in the substantia nigra were DJ-1 negative (Fig. 3.15C and H). Astrocytic expression of DJ-1 was widespread throughout regions of the medial temporal lobe (Fig 3.15A). In controls, no DJ-1 positive neurons were seen in the hippocampus and only a few were found in the amygdala and entorhinal cortex. In PD however, neuronal staining was elevated to moderate levels in the hippocampus and entorhinal cortex (Fig. 3.15G) whilst numbers in the amygdala (Fig. 3.15E) remained on par with those observed in controls. The main subcortical area where DJ-1 positive neurons were observed was the medulla (Fig. 3.15F and I), in particular the inferior olivary nucleus. Neuronal staining was slightly more prominent in both the dorsal motor nucleus of the vagus and nucleus cuneatus for PD cases. Within control and PD cerebellum, the DJ-1 was mainly localised to Bergmann glia (Fig. 3.15G), with the occasional granule cell within the granular layer also staining positive. The large purkinje neurons are mostly negative for DJ-1, though a couple of exceptions were observed (Fig. 3.15H).

# 3.9. Subcellular localisation of DJ-1

## 3.9.1. Aim

To identify the subcellular location of DJ-1 protein in human brain tissue.

# 3.10. Methods

## 3.10.1. Pathological material

Fresh cerebellum and striatum tissue were taken from a control subject detailed below in table 3.9 and homogenised in 5 volumes of isolation medium. Fresh tissue was used in order eliminate disruption of subcellular organelle membranes caused by freeze thaw processes.

| Sample | Sex | Age | PMD | pH |
|---|---|---|---|---|
| 1 | F | 68 | 44.55 | n/a |

**Table 3.9: Demographic data of control subject used for subcellular fractionation study**

### 3.10.1.1. Subcellular fractionation

Material was separated into subcellular organelles as described in Gandhi et al., (2006). Briefly, debris was removed by 5min centrifugation at 3000g followed by a second 10min centrifugation of the supernatant at 12000g. The resulting supernatant was then subjected to ultracentrifugation for an hour at 70000g to separate the soluble cytosolic fraction (supernatant) and the enriched microsomal pellet, which was immediately resuspended in 500µl isolation buffer. Meanwhile, the pellet formed from the previous 12000g spin contained the crude mitochondria fraction. This was washed three times in isolation medium to remove nuclear contamination, before being finally resuspended in 500µl of buffer.

### 3.10.1.2. Western blotting

Fractions were separated on 10% Bis-tris gels and immunoblotted with DJ-1 (1:5000) and following stripping, β-actin (1:5000). A second gel was run in order to detect cytochrome C (1:1000) and PDI (1:1000), which are mitochondria and endoplasmic reticulum markers respectively.

## 3.10.2. Results

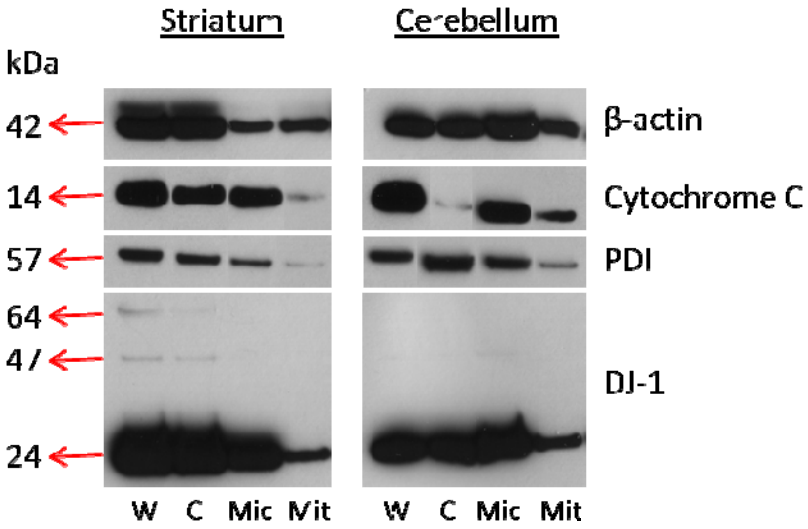


**Figure 3.16: Detection of DJ-1 in subcellular fractions of human control brain.** DJ-1 antibody was used for western blotting of different fractions from normal cerebellum and striatum tissue. This demonstrated that DJ-1 is present in the cytosolic fraction (C), microsomal fraction (Mic) and mitochondrial fraction (Mit). Whole homogenate (W) was run alongside these fractions as a positive control. Antibodies against mitochondrial marker cytochrome C and the microsomal specific PDI were used to check the purity of the fractions. β-actin was used as a cytosolic marker.

Immunoblotting with monoclonal DJ-1 antibody revealed positive immunoreactivity in the cytoplasmic, microsomal and mitochondrial fractions with the latter containing the least amount (Fig. 3.16). Weak DJ-1 positive bands, representing the 64kDa DJ-1 complex, were detected in the cytosolic and whole fractions from the striatum. DJ-1 dimer was also observed to different degrees in all fractions of the cerebellum and striatum, except the crude mitochondria fraction.

Probing for cytochrome C revealed contamination of cytosolic and microsomal fraction with mitochondrial proteins. Likewise, the microsomal enzyme PDI was detected in the cytoplasmic fraction and to a lesser extent the mitochondrial fraction. The cross contamination of both cytochrome C and PDI and their failure to be enriched in their respective fractions indicate that the separation of subcellular organelles was unsuccessful, even after high speed ultracentrifugation.

# 3.11. Discussion

*PARK7* mutations induce the development of PD through the loss of DJ-1 (Bonifati et al., 2003b) and it stands to reason that any changes in DJ-1 expression and consequential alterations in functional activity may contribute to the development of sporadic PD. Under this rationale, a comprehensive study of DJ-1 protein and gene expression in multiple brain regions was performed using a cohort of closely matched controls and PD cases.

Our analysis of DJ-1 mRNA revealed a robust presence in all regions of control and PD brains showing that, like α-synuclein and parkin, it is not just restricted to the dopaminergic system (Solano et al., 2000). In controls, DJ-1 mRNA expression was highest in the cerebellum, followed by the frontal cortex, with the lowest levels recorded in the amygdala. This is in good agreement with a recent report by, Galter and colleagues who used *in situ* hybridisation to show DJ-1 mRNA levels to be greater in cortical regions than sub-cortical areas (Galter et al., 2007).

Of the regions typically associated with PD pathology, the striatum of PD subjects showed the greatest loss of DJ-1 mRNA (43%), possibly reflecting its early involvement in PD pathogenesis and the loss of dopaminergic cell innervations. According to Braak staging, both the medulla and substantia nigra are affected prior to the appearance of striatal pathology (Braak et al., 2003). We attempted to study DJ-1 mRNA expression in these regions but were restricted by the poor quality of RNA extracted from the medulla and the lack of available nigral samples. Screening of the substantia nigra, using custom designed Agilent microarrays, has shown DJ-1 mRNA expression to be 30% lower in PD subjects compared to controls (Bossers et al., 2009). Due to the extent of cell loss in PD nigra, this data may be misleading However, using laser captured dopaminergic neurons, a separate study reported an 8 fold decrease in DJ-1 mRNA within the nigra of PD patients (Simunovic et al., 2008).

Within the frontal cortex, real-time PCR showed DJ-1 expression to be almost a third lower in diseased tissue. This significant decrease ($p<0.01$) may reflect cell loss or neuroplastic changes, induced by the pathological process of PD. Significant reductions were also

observed in the parietal cortex and a decreasing trend noted in the cingulate gyrus in PD subjects. Together, this is suggestive of a widespread down-regulation in PD of DJ-1 mRNA for cortical regions, possibly due to common disease related and/or levodopa responsive changes.

Parallel to DJ-1 mRNA reductions, a significant loss of DJ-1 protein in PD, compared to age matched controls, was found in both the striatum and frontal cortex after western blotting. Similar analysis of medulla and a small number of nigra tissue also revealed DJ-1 protein levels to be significantly diminished in PD. A previous study showed no variability in DJ-1 protein levels in the cingulate cortex of control and PD samples, consistent with our real-time PCR data for the region (Moore et al., 2005). In contrast, Choi et al., (2006) have reported DJ-1 levels to be elevated in the frontal cortex of PD patients. Though unclear, this discrepancy may be down to variations in sample cohort or methodologies. The majority of tissue used in our study was derived from subjects who displayed neocortical LBs (Lashley et al., 2008). Thus, the decrease in DJ-1 protein observed by us may be reflective of the end stages of PD, whilst the increases described by Choi and colleagues could occur during the early stages of PD development. Furthermore, our use of a monoclonal DJ-1 antibody and a protein loading concentration of 15µg as opposed to the polyclonal antibody and 50µg of protein employed by them, may also account for the lack of agreement between the two studies. Of note we were unable to replicate their reported increase in soluble DJ-1 in AD frontal cortex, though we did observe an up-regulation of insoluble DJ-1 (Kumaran et al., 2007).

For both DJ-1 mRNA and protein, the largest significant decrease in PD brains was found in the cerebellum. This is surprising and intriguing as the cerebellum is not traditionally associated with PD pathology due to the absence of LBs. Nevertheless, neuroimaging studies have shown hyperactivation of cerebellum in PD patients (Rascol et al., 1997; Yu et al., 2007), suggestive of a functional compensatory mechanism for defective basal ganglia functioning. Increased activity may expose the cerebellum to the same DJ-1 diminishing factors seen in the basal ganglia and cortex. It may also explain the recently reported significant decrease of ATP13A2 (*PARK9*) mRNA in PD cerebellum (Vilarino-Guell et al., 2009). A number of studies have also documented a decrease in α-synuclein protein and

mRNA in the same region of PD brains (Fuchs et al., 2008; Westerlund et al., 2008). Additionally, levels of $D_1$ and $D_3$ receptor mRNA and tyrosine hydroxylase mRNA are also notably reduced in PD cerebellum (Hurley et al., 2003), further suggesting that the role of this region in PD may be underestimated.

We were unable to replicate our DJ-1 immunoblot data with a commercially available ELISA kit. For the three measured regions (striatum, frontal cortex and cerebellum), no difference between control and PD samples were detected. Additionally, the ELISA indicated the frontal cortex and not the cerebellum contained the most DJ-1 protein. Whilst this data is contrary to our previous findings, it must be remembered that this assay was designed for use with serum and plasma and not brain homogenate which is much "dirtier". Attempts were made to minimise the effects of the brain matrix on assay performance by constructing multiple standard curves with different brain homogenate concentrations. In total, 5 dilutions were compared to the standard curve formed using the supplied calibrant buffer and 1:5000 was selected as having the best parallel relationship. A closer fit may have been found if more dilutions were tested, but it was uneconomical to do so. The use of a frontal cortex sample to generate the standard curve also raises questions about its suitability in measuring DJ-1 content from striatal and cerebellar samples. Given DJ-1's tendency to form homodimers, one could also question the validity in using an ELISA to measure its levels. Binding of DJ-1 to itself or other endogenous proteins may sterically restrict antibody access to the binding site, resulting in a false reading. During western blotting this scenario is avoided as proteins are subjected to denaturation.

In contrast to the other regions, the two areas studied from the medial temporal lobe; entorinal cortex and amygdala, showed very significant increases of 39% and 92% in DJ-1 mRNA levels in PD. It would have been interesting to see whether this correlated with an increase in DJ-1 protein, but unfortunately tissue was not available for protein analysis due to the small nature of these regions. It is currently unclear as to why an increase in DJ-1 mRNA expression occurs in these regions. One explanation could be that different areas of the brain express different transcripts of DJ-1 mRNA, which are independently regulated. Exon 1 of DJ-1 is non-coding but consists of two parts that undergo alternative splicing (Bonifati et al., 2003a). This could result in the formation of two transcripts with different

transcriptional enhancers or other cis-regulatory elements. Using the same group of PD cases, Lashley et al., (2008) found LB count to be more than 6 times denser in the entorinal cortex than in either the frontal and parietal cortex. It is therefore plausible that DJ-1 is up-regulated in these regions to combat the greatly elevated LB pathology. Regions of the medial lobe that express PD pathology are also associated with cognitive function and memory and their affliction provides an explanation for the development of hallucinations and dementia by PD patients (Braak et al., 2002; Braak et al., 2003). It is not uncommon for AD pathology to be found alongside PD pathology in these areas, providing a rationale for these non-motor symptoms (Jellinger, 2006). In our PD cases, both tau and Aβ pathology were found within these regions (Lashley et al., 2008), meaning that the up-regulation of DJ-1 mRNA may be a response to the onset of AD pathology rather than PD. Ourselves and others have previously reported co-localisation of DJ-1 with tau in numerous tauopathies (Kumaran et al., 2007; Neumann et al., 2004; Rizzu et al., 2004). In lieu with this, a very recent study in regions CA1-4 showed immunostaining of DJ-1 in AD, but not controls (Baulac et al., 2009). We too have noticed a slight increase in neuronal staining in the hippocampus of PD patients. LRRK2 has also been found to associate with hyperphosphorylated tau in neurofibrillary tangles and threads in AD (Miklossy et al., 2006) and it would be interesting to see whether LRRK2 mRNA and protein levels are up-regulated in the medial temporal lobe of PD individuals.

When taking patients' gender into account during our analysis of DJ-1 expression, we found PD induced alterations to be more pronounced in males. Protein down-regulation was seen in all three regions and analysis of gene expression data revealed the entorinal cortex to be the only region no longer displaying significant changes. In females though, the entorinal cortex was the only region to exhibit a considerable difference amongst control and PD groups. Additionally, the frontal cortex was the only region where a significant loss of DJ-1 was noted. Before its role in PD was discovered, interactions with androgen receptors and a positive correlation with male rat infertility linked DJ-1 to male fertility (Takahashi et al., 2001; Wagenfeld et al., 1998) and this role lead to the rat homologue being named CAP1). DJ-1 null mice have been shown to be viable and fertile without any major abnormalities (Chen et al., 2005b; Goldberg et al., 2005; Kim et al., 2005b). One group reported that over an 11 month period only male KO mice showed motor behavioural deficits in the adhesive

tape removal task (Chen et al., 2005b). The intricate nature of movement required for this task is a sensitive measure of nigrostriatal dysfunction. These results suggest that lack of DJ-1 in males results in a more accelerated development of PD. Whilst DJ-1 appears to have a gender specific role in fertility, it is unclear whether this conforms some sort of gender bias towards the development of PD. Intriguingly in humans the incidence of PD is higher in males than females (Van Den Eeden et al., 2003).

Whilst we have demonstrated changes in mRNA levels in PD tissue, the technique used is unable to ascertain whether they occur in neurons, astrocytes or a combination of the two. Unfortunately, *in-situ* hybridisation was beyond the scope of this project but would be an interesting point to pursue. Semi-quantitative immunohistochemistry was attempted to depict regional protein cellular distribution in which the pattern of strong astrocytic and weak neuronal staining was seen, as previously described by ourselves and others (Bandopadhyay et al., 2004; Neumann et al., 2004; Olzmann et al., 2007; Rizzu et al., 2004). These studies described neuronal staining to be greater in control tissue than pathological tissue. Since the majority of tissue was sourced from regions in the cortex and basal ganglia this may be attributed to the lower amount of DJ-1 that may be present in pathological tissue as we report. Olzmann et al., (2007) showed more DJ-1 positive neurons in subcortical basal ganglia than cortical regions. Whilst we did not find neuronal staining to be greatly elevated in the midbrain and striatum, it was noticeable within the medulla. Baulac and colleagues have demonstrated that neuronal staining with antibodies raised against C-terminal or whole length DJ-1, like the Stressgen one we used, are less robust than N-terminal variants. They postulated that the C and mid-terminal part of DJ-1 is involved in dimerisation, effectively making it inaccessible to the antibody whilst the N-terminal is left exposed. This does not explain why astrocytes are so vividly expressed or why some neurons are detected (Baulac et al., 2009). They additionally showed greater neuronal staining in tissue that had been fixed for shorter periods of time, though again it remains unclear why this would only affect neurons. It is possible that the morphology of DJ-1 differs between neurons and astrocytes. If this is indeed the case, it may explain why the cerebellum no noticeable increase in DJ-1 staining was observed despite western blotting showing it to have the highest DJ-1 content. The large purkinje neurons present of the

cerebellum many contain a significant amount of DJ-1 that is only freed for detection following cell lysis and subsequent immunoblotting.

It is also possible that whilst DJ-1 is abundantly expressed in neurons in murine brains (Kotaria et al., 2005), human neurons may have evolved to delegate DJ-1's neuroprotective role to astrocytes. Over-expression of DJ-1 in astrocytes has been shown to be more neuroprotective towards rotenone toxicity *in vitro* (Mullett and Hinkle, 2009). Conversely, DJ-1 KO in astrocytes results in increased nitric oxide production which is harmful to neurons (Waak et al., 2009). Whilst DJ-1 is not directly secreted by astrocytes, it may regulate the release of a number of astrocytic derived protective substances (e.g. neurotrophic factors, anti-oxidant molecules, cytokines etc) into the microenvironment (Mullett and Hinkle, 2009).

We were unable to determine the subcellular locations of DJ-1 in either the striatum or cerebellum of a human control subject. Though we found DJ-1 to be present in cytoplasmic, microsomal and mitochondrial fractions, probing with relevant fraction markers showed poor separation of organelles. Our use of fresh tissue rules out disruption of organelle membranes through freeze-thaw, however this may still have occurred during the post-mortem period. Subcellular fractionation using mice brains showed endogenous DJ-1 to be present in the cytoplasm and mitochondria. Further evaluation of mitochondrial fraction found that within mitochondria, DJ-1 is resident in the mitochondrial matrix and inner mitochondrial space (Zhang et al., 2005a). *In vitro* studies have revealed that under oxidative stress conditions DJ-1 can migrate towards the mitochondria (Blackinton et al., 2005; Canet-Aviles et al., 2004). This translocation was not observed by Zhang and colleagues for endogenous DJ-1 in mice and may only occur in over-expressed models or at undetectable levels.

In order to identify whether degrees of DJ-1 oxidation in PD varies amongst regions, DJ-1 pI isoforms were analysed. This provided no compelling evidence for increased oxidation within the nigra or any other region in PD. In fact, whilst the frontal cortex showed a significant accumulation of acidic isoforms as previously documented (Bandopadhyay et al., 2004; Blackinton et al., 2009; Choi et al., 2006) no other region except the medulla displayed

this property. The pI isoform distribution of DJ-1 in nigra and striatal tissue was similar in both control and PD, possibly owing to the high dopamine content in these regions and its associated toxicity. The presence of acidic isoforms in controls may be a consequence of aging with a similar accumulation observed in old mice compared to young (van der Brug et al., 2008). Acidic DJ-1 isoforms were additionally seen to accrue with age in drosophila and human cortex (Meulener et al., 2006). We also noted that DJ-1 pI isoforms differed in the subcortical regions to the cortex and cerebellum, with pI isoforms 6.0 and 6.5 almost exclusively restricted to the frontal cortex and cerebellum. This may indicate that in subcortical areas, both the 6.0 and 6.5 pI isoforms are permanently oxidised to 5.8 and 6.3 respectively or that responses to oxidative stress are unique to each region culminating in the formation of different DJ-1 pI isoforms.

DJ-1 has been proposed to be functionally active in a dimeric state (Bonifati et al., 2003b). We attempted to decipher the native conformation of DJ-1 in the human brain, but our efforts with a non-denaturing native gel were unsuccessful. Our gel filtration studies however, showed that in both control and PD brain regions the majority of DJ-1 protein adopts a complex with a molecular weight representative of a dimer structure (40-47kDa). The remainder of endogenous DJ-1 is present as a monomer (24-27kDa) and a small fraction as a HMW complex with an approximate molecular weight of 63-69kDa ± 15%. Prolonged exposure of soluble DJ-1 immunoblots to x-ray film produced faint immunoreactive bands at 47 and 67kDa, providing a more accurate molecular size measurement of DJ-1 dimer and HMW complex respectively. The HMW complex possibly represents DJ-1 oligomer/aggregate. DJ-1 belongs to a superfamily of proteins that form different oligomeric species e.g. Hsp31 forms dimers (Quigley et al., 2003) whilst PH1704 forms hexamers (Bonifati et al., 2003a). Thus, DJ-1 may also have the capacity to form trimers and other oligomers, particularly when its structural integrity has been compromised (Miller et al., 2003).

DJ-1 protein lacking amino acid residues 173-189 or harbouring the L166P mutation have both been reported to exhibit a tendency to form HMW structures *in vitro* (Herrera et al., 2007; Tao and Tong, 2003). Gel filtration of endogenous L166P DJ-1 sourced from lymphoblast cells belonging to an individual with L166P mutation, was also eluted into the

fraction corresponding to the protein marker BSA (68kDa) (Macedo et al., 2003). This evidence is supportive of HMW complexes being formed in response to alterations in DJ-1 protein structure/stability. Thus, the small amount visualised by us may be due to a loss of structural stability through modifications, possibly induced by oxidative stress. Not all modifications to protein structure result in the formation of HMW aggregates e.g. E163K substitution (Ramsey and Giasson, 2008). Unlike the L166P mutation, E163K substitution does not compromise protein structure dramatically (Gorner et al., 2007). Another mutation that affects protein structure, though to a lesser extent than L166P mutations, is the M26I substitution and this has been reported to display an increased tendency to aggregate (Hulleman et al., 2007). The M26 subunit in DJ-1 has been shown to undergo oxidation (Choi et al., 2006) which may have a similar effect. Aggregation of DJ-1 in human brains is reportedly favoured by elevated levels of inorganic phosphate (Cha et al., 2008).

DJ-1 monomer and dimer are soluble complexes; however aggregation of DJ-1 would make them increasingly insoluble. To establish whether DJ-1 aggregation contributed to our observed reduction of soluble DJ-1 in PD frontal cortex, DJ-1 protein levels were measured in buffers of increasing solubilisation strength, in the same region. Soluble DJ-1 levels in TBS buffer supported our earlier findings of decreased DJ-1 levels in PD frontal cortex. Insoluble DJ-1 was detected in both SDS soluble and urea-soluble fractions for both control and PD samples. Similar to soluble DJ-1, SDS-soluble DJ-1 levels were significantly reduced in PD compared to controls whilst a downward trend was also seen for urea-soluble DJ-1. Collectively this is suggestive of a general down-regulation of DJ-1 in the frontal cortex of PD patients. Together with our real-time data for this region, it suggests that the lower levels of DJ-1 protein observed in PD tissue are a direct result of mRNA down-regulation and not disease related aggregation.

DJ-1 protein has been shown to be neuroprotective *in vitro* (Liu et al., 2008a), with both antioxidant and chaperone activity being reported (Shendelman et al., 2004; Taira et al., 2004; Zhou et al., 2006). Additional evidence supporting its defensive role in neurons includes up-regulation of the antioxidant glutathione (Zhou and Freed, 2005) and tyrosine hydroxylase enzyme (Zhong et al., 2006). In *PARK7* patients, PD is the consequence of a loss of DJ-1 function through either lack of protein synthesis or the formation of an aberrant

protein (Bonifati et al., 2003b). In line with this, the down-regulation of DJ-1 protein that we observe in multiple IPD regions could be interpreted as a reduction in DJ-1's neuroprotective activity, thereby making the tissue more susceptible to PD pathology.

## 3.12. Conclusions

In this chapter, differences between DJ-1 protein and gene expression in multiple PD and normal control brain regions are described. We show that DJ-1 protein levels are reduced in PD medulla, nigra, striatum, frontal cortex and cerebellum. Parallel reductions within PD striatum, frontal cortex and cerebellum of DJ-1 mRNA suggest that protein down-regulation is transcriptionally induced. Our data indicates that DJ-1's neuroprotective functions are diminished in PD. The robust staining of astrocytes with DJ-1 also implies that the neuroprotective effects of DJ-1 are exerted from here.

# 4. Identification of DJ-1 interactors

# 4.1. Identification of DJ-1 interactors in the human brain

## 4.1.1. Aim

To identify interactors of DJ-1 in the human brain to help explain the functional activity of DJ-1 *in vivo*. This will be tackled on two fronts. First, we will try to confirm protein interactions that have been reported in over-expression cell models. Our second approach will draw on the reported close homology of DJ-1 with a regulatory component of a RBP (Hod et al., 1999). Working with collaborators at the NIH we will examine whether DJ-1 itself harbours the capacity to bind to RNA in human brain and compare binding partners in both control and PD tissue.

## 4.1.2. Material and methods

### 4.1.2.1. Pathological material

Interactions were studied using flash frozen control and PD frontal cortex samples detailed in table 4.1.

| Sample | Sex | Age | PMD | pH | Pathology |
|---|---|---|---|---|---|
| Con 1 | F | 78 | 23.30 | 6.07 | - |
| Con 2 | F | 84 | 28.50 | 6.13 | - |
| Con 3 | F | 73 | 28.00 | 6.38 | - |
| Mean±SEM | 0M, 3F | 78.3±3.2 | 26.6±1.7 | 6.2±0.1 | |
| | | | | | |
| PD 1 | F | 87 | 47.45 | 6.62 | T |
| PD 2 | F | 62 | 46.20 | 5.88 | N |
| PD 3 | M | 76 | 28.45 | N/A | N/A |
| Mean±SEM | 1M, 2F | 75±7.2 | 40.7±6.1 | 6.3±0.3 | |

**Table 4.1: Demographic data of samples used to investigate DJ-1's association with RNA *in vivo*.** T= transitional, N = neocortical and N/A = not available.

### 4.1.2.2. Protein co-immunoprecipitation

Co-IP of DJ-1 and associating proteins was performed as described in section 2.2.12. Briefly, 100µl of buffered protein G sepherose and 2.5µg of polyclonal DJ-1 antibody was used to pull down DJ-1 from brain homogenate containing 750µg soluble protein. After dissociation of protein complexes from sepherose beads into 8M urea, immunoprecipitates were resolved alongside corresponding cleared lysate using SDS PAGE and subsequently probed with antibodies to potential interactors. Blots were also probed with monoclonal anti-DJ-1 to confirm pull-down of DJ-1 protein.

### 4.1.2.3. RNA co-immunoprecipitation and identification of mRNA transcripts

RNA was immunoprecipitated using either a specific DJ-1 antibody or a non-specific IgG antibody from frozen tissue as described in the methods. Collected RNA was initially amplified using the Illumina TotalPrep RNA Amplification Kit (Ambion, USA) with the aim of identifying transcripts using Illumina expression chips. However nanodropping of the amplified RNA showed its concentration to be too low for hybridisation on to a microarray chip. Instead following immunoprecipitation, RNA was converted to cDNA and RT-PCR using specific primers (table 2.3) was used to detect select RNA species that our colleagues at the NIH had found to associate strongly with DJ-1 *in vitro*. Association between DJ-1 and RNA transcripts was shown by normalising to β-actin and comparing to non-specific association with IgG using an unpaired student's T-test.

## 4.1.3. Results

### 4.1.3.1. *In vivo* protein interactors of DJ-1

After confirming pull down of DJ-1 by polyclonal DJ-1 antibody, immunoprecipitates were probed for Nrf2, mortalin, Daxx and Sumo-1 (Fig. 4.1). Nrf2 and Sumo-1 showed no IR in frontal cortex lysate or IP samples. A faint immunoreactive band for Daxx was seen in the cleared lysate of one PD case at 81kDa, but not in any of the IP fractions. Probing with mortalin revealed a single band in all cleared lysate samples at 74kDa. For IP samples, heavy

smearing was present at the equivalent molecular weight, though signs of a mortalin immunoreactive band were visible in the second PD IP sample.

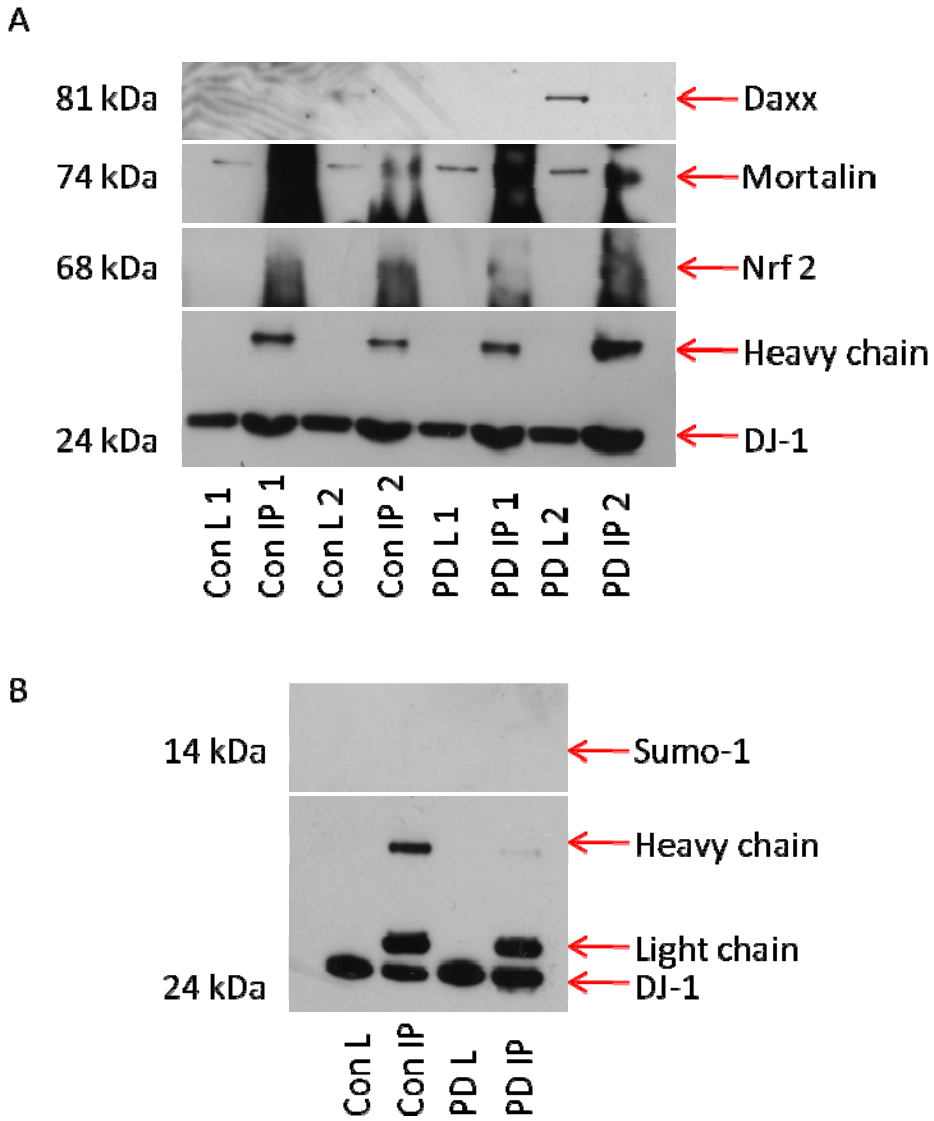


**Figure 4.1: immunoblots of potential interactors of DJ-1 protein in frontal cortex of control and PD brains.** A) Immunoblots showing successful pull-down of DJ-1 and presence/absence of Nrf2, mortalin and Daxx in immunoprecipitate (IP) and cleared lysate (L) from two control and 2 PD individuals. B) Successful pull down of DJ-1 in 1 control and 1 PD frontal cortex case. Probing for Sumo-1 showed no positive IR in either the cleared lysate or immunoprecipitate fractions.

### 4.1.3.2. In vivo RNA interactors of DJ-1

Following RNA IP from control frontal cortex using DJ-1 specific or non-specific IgG antibodies, western blotting was used to confirm the presence of DJ-1 in DJ-1 IP samples and its absence from IgG IP samples (Fig. 4.2A). β-actin was then confirmed to be non-specifically pulled down by both antibodies. Using RT-PCR we found the amount of β-actin mRNA collected was consistent in both sets (Fig. 4.2B). Amplification of β-actin passed the detection threshold on average at PCR cycle 35 in both DJ-1 and IgG IP samples. This allowed us to utilize β-actin as a measure for non-specific RNA IP and subsequently the expression of all other transcripts was corrected to this. RT-PCR using specific probes for transcripts encoding mitochondrial complex 1 subunits showed significant enrichment in DJ-1 IP samples of ND1 ($p=0.0004$), ND2 ($p=0.0025$), ND4 ($p=0.0001$) and ND5 ($p=0.0108$). These mitochondrial transcripts were between 2.5 and 4 times greater in DJ-1 IP fractions (Fig. 4.2D-G). Levels of another mitochondrial transcript, NDUFB1 did not differ between antibody IPs ($p=0.5617$) (Fig. 4.2C). Pull down of mRNA for selenoproteins GPx4 ($p=0.0036$), GPx3, SEPW1 ($p=0.0078$) and SEPHS2 (Fig. 4.2H-K) were also markedly elevated in DJ-1 IPs with SEPW1 in particular being 6 times higher than in control IPs. Levels of transcripts for PTEN/Akt modifiers MAPK8IP1, JunD, PPP2R2C and BAD (Fig. 4.2L-O) were also measured. However whilst we were able to detect them in DJ-1 IP samples, they failed to be detected after 40 amplification cycles in IgG IP samples. We also failed to detect any RNA in any of the PD IP samples after RT-PCR (Fig. 4.3B-G). This was despite successfully immunoprecipitating DJ-1 from the all 3 PD cases (Fig. 4.3A).

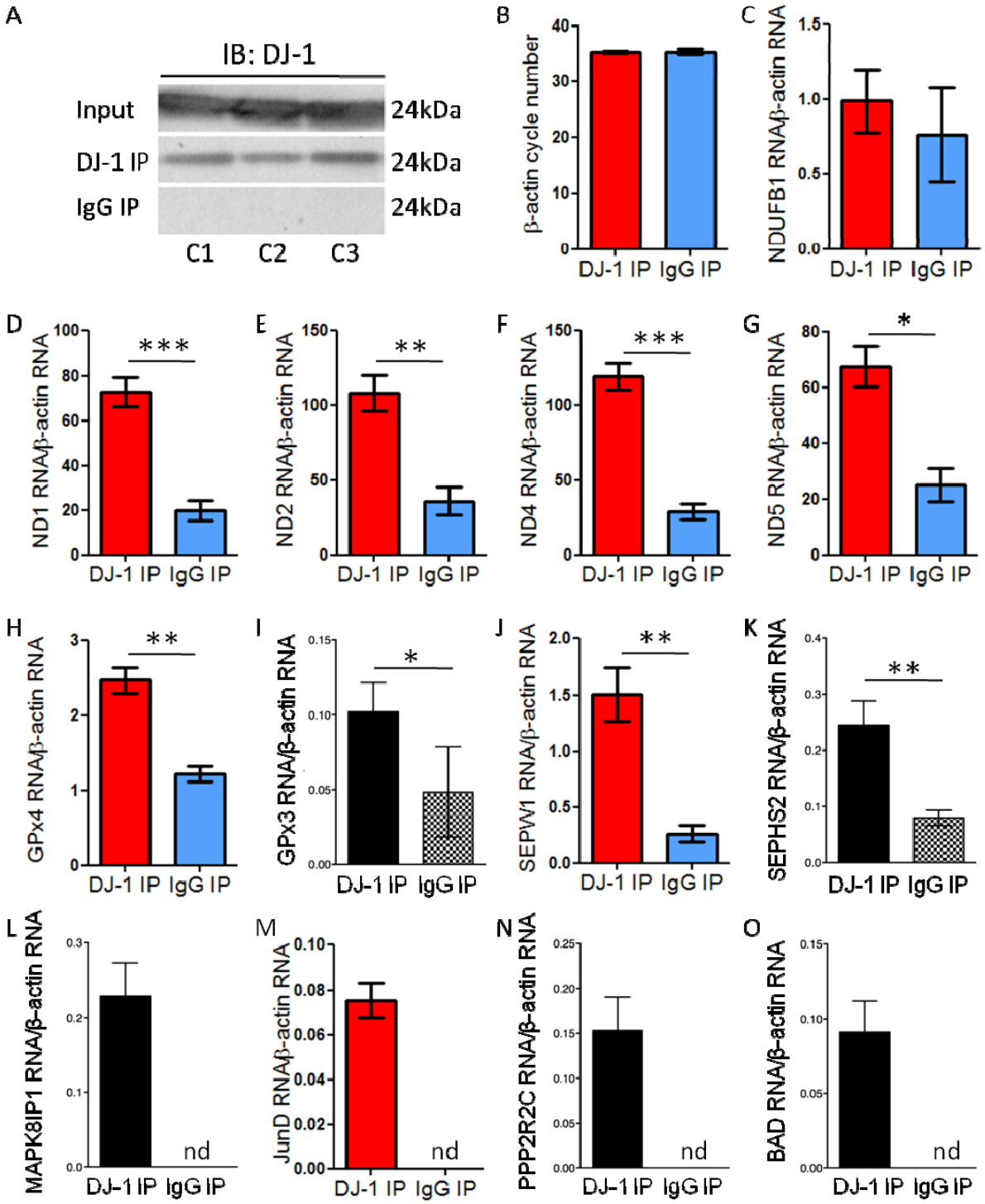


**Figure 4.2: Immunoprecipitation of RNA transcripts that interact with DJ-1 in control human brain.** A) Immunoblot of 3 control frontal cortex samples showing positive DJ-1 IR in whole lysate and DJ-1 IP. No IR was seen in IgG IP samples. B) Amplification of β-actin was similar for both DJ-1 and IgG IPs illustrating it could be used as an internal control for non-specific pull down of RNA. C-O) comparison of transcripts levels collected from DJ-1 and IgG IP samples following normalisation to β-actin. Statistical significance was determined by student's T-test: * = $p<0.05$, ** = $p<0.01$ and *** = $p<0.001$. nd indicates no detection of transcript. Black/grey graphs were kindly provided by collaborator Jeff Blackington.

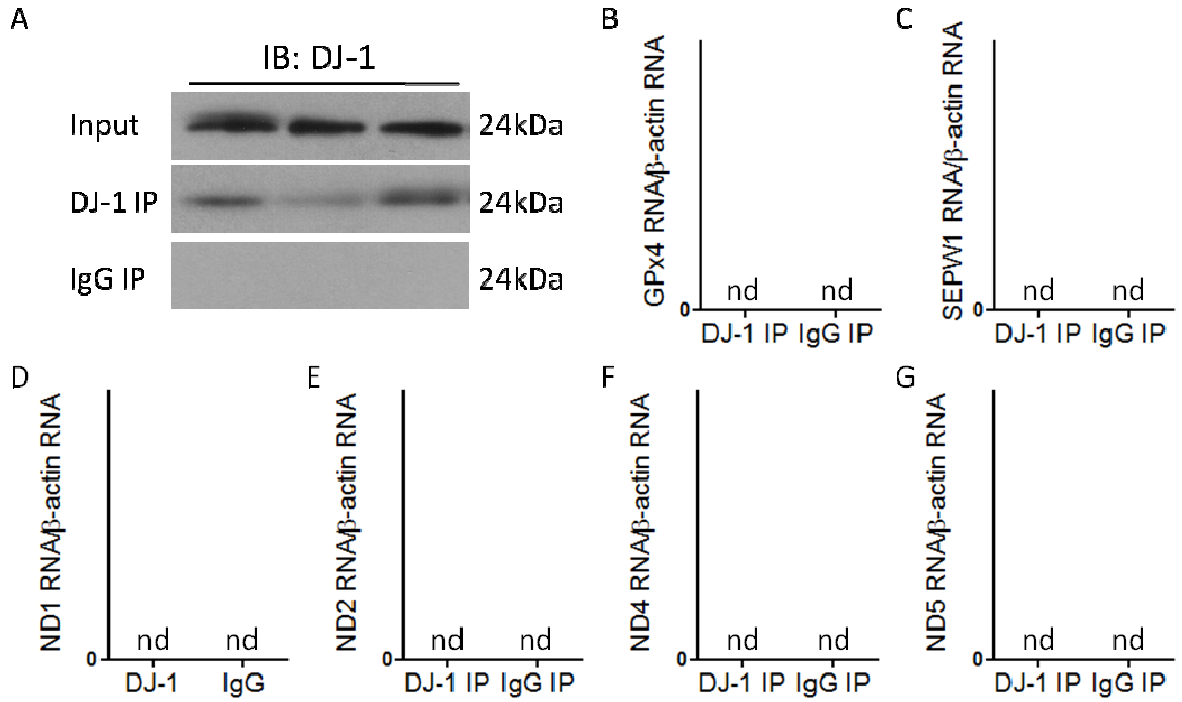


**Figure 4.3: Immunoprecipitation of select RNA transcripts following immunoprecipitation of DJ-1 from human PD brain.** A) Immunoblot of 3 PD frontal cortex samples showing positive DJ-1 IR in whole lysate and DJ-1 IP but not in IgG IP samples. B-G) screening of collected RNA for selenoproteins and mitochondrial transcripts failed to show amplification of any transcript. nd indicates no detection of transcript.

To rule out degradation of RNA by IgG antibody as a cause for enrichment in DJ-1 IP samples, total RNA extracted from the frontal cortex was separated on a 1.5% TAE gel in the presence of either DJ-1 or IgG antibody (Fig. 4.4). Whilst some smearing of RNA was noted, both the 28s and 18s RNA bands were clearly resolved showing neither antibody had a greater effect on RNA integrity that could influence RNA immunoprecipitation.

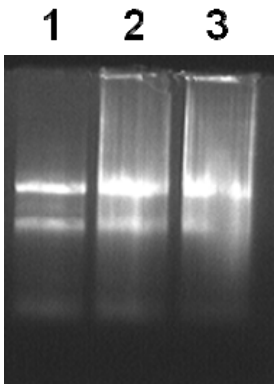


**Figure 4.4: Effects of antibodies used for IP on RNA integrity.** Lane 1 shows RNA without any antibody. Lane 2 shows RNA with DJ-1 antibody. Lane 3 shows RNA with IgG antibody.

# 4.2. Expression of DJ-1 binding transcripts in control and PD brain

## 4.2.1. Aim

Having shown that DJ-1 can associate with RNA species in the human brain, we examined the role of DJ-1 as a post-transcriptional regulator of protein expression by comparing expression of identified transcripts between control and PD cases.

## 4.2.2. Materials and methods

### 4.2.2.1. Pathological material

For microarray procedure RNA was extracted from the frontal cortex of 16 control and 14 PD cases detailed in table 4.2. RT-PCR was performed using previously synthesised cDNA from the frontal cortex of the first 16 control and PD samples listed in table 3.3. Additionally, protein levels were measured in the frontal cortex homogenates used previously in DJ-1 protein expression study (table 3.2).

### 4.2.2.2. Quantifying gene expression

Due to the large number of transcripts, microarray was adopted as the technique for measuring gene expression as it allows simultaneous measurement of multiple genes. This technique, detailed in section 2.4.3, was carried out with the help of Jeff Blackington and Marcel van der Brug at the NIH. Probes against the mitochondrial transcripts, ND1, ND2, ND4 and ND5 were not present on the array chip and were instead measured using RT-PCR using the primers in table 2.3. As before gene expression was normalised to both β-actin and B2M. Real-time PCR was also used to measure GPx4 as a means of validating array data.

| Sample | Sex | Age | PMD | pH | Pathology |
|---|---|---|---|---|---|
| Con 1 | M | 85 | 43.35 | 6.68 | - |
| Con 2 | M | 86 | 53.00 | 6.65 | - |
| Con 3 | M | 81 | 40.00 | 6.48 | - |
| Con 4 | M | 83 | 117.05 | 6.81 | - |
| Con 5 | M | 79 | 56.40 | 6.60 | - |
| Con 6 | M | 63 | 42.00 | 6.23 | - |
| Con 7 | M | 57 | 78.50 | 6.03 | - |
| Con 8 | F | 78 | 23.30 | 6.07 | - |
| Con 9 | M | 71 | 38.5 | N/A | - |
| Con 10 | F | 68 | 44.55 | N/A | - |
| Con 11 | F | 91 | 98.50 | 6.41 | - |
| Con 12 | F | 84 | 28.50 | 6.13 | - |
| Con 13 | F | 95 | 39.30 | N/A | - |
| Con 14 | F | 73 | 28.00 | 6.38 | - |
| Con 15 | M | 93 | 19.00 | 6.80 | - |
| Con 16 | F | 85 | 37.10 | 5.7 | - |
| Mean±SEM | 9M, 7F | 79.5±2.7 | 49.2±6.8 | 6.4±0.1 | |
| | | | | | |
| PD 1 | F | 62 | 46.20 | 5.88 | N |
| PD 2 | F | 87 | 47.45 | 6.62 | T |
| PD 3 | M | 81 | 103 | 6.15 | T |
| PD 4 | F | 77 | 80.00 | 6.53 | N |
| PD 5 | M | 70 | 51.20 | 6.29 | N |
| PD 6 | F | 73 | 70.00 | 6.63 | N/A |
| PD 7 | M | 76 | 28.45 | N/A | N/A |
| PD 8 | M | 77 | 23.35 | 6.26 | N |
| PD 9 | M | 75 | 22.25 | 6.22 | N/A |
| PD 10 | M | 77 | 28.25 | 6.39 | N/A |
| PD 11 | F | 69 | 52.45 | 6.14 | N/A |
| PD 12 | M | 72 | 27.00 | 6.32 | L |
| PD 13 | F | 74 | 48.15 | N/A | N/A |
| PD 14 | F | 74 | 35.05 | 6.11 | N |
| Mean±SEM | 7M, 7F | 74.6±1.5 | 47.3±6.3 | 6.3±0.1 | |

**Table 4.2: Demographic data of samples used in gene expression study.** N = neocortical, T = transitional, L = limbic, N/A = not available.

### 4.2.2.3. Protein expression

Protein levels of ND1, ND2, ND4, ND5 and SEPW1 were measured in control and PD cases using western blotting with chemiluminescent detection. Antibody concentrations are listed

below. Expression of two additional proteins, GPx4 and MAPK8IP1, were measured by Jeff Blackington at the NIH in an independent cohort of 9 control and 9 PD frontal cortex samples.

| Antibody | Dilution | Source |
|---|---|---|
| monoclonal anti-ND1 | 1:500 | Santa Cruz |
| polyclonal anti-ND2 | 1:1000 | Santa Cruz |
| polyclonal anti-ND4 | 1:500 | Abcam |
| polyclonal anti-ND5 | 1:1000 | Santa Cruz |
| polyclonal anti-SEPW1 | 1:500 | Santa Cruz |

**Table 4.3: Details of antibodies used to measure protein expression of DJ-1 associated transcripts.**

## 4.2.3. Results

Gene expression profiles for control and PD frontal cortex groups were compared in order to establish similarities between the two. Frontal cortex region was also compared against profiles for 3 other distinct regions (medulla, striatum and cerebellum) that our collaborators had previously obtained. Unsupervised clustering of liked group samples using Beadstudio software showed clear separation of both regions and disease states (Fig. 4.5A). Independent comparison of control and PD frontal cortex samples via the same technique identified 2 control (con 5 and 13) and 3 PD (PD 7, 10 and 13) samples that had different gene expression profiles to the rest of the group (Fig. 4.5B and C). These samples were duly excluded from any subsequent analysis.

We next compared the expression of transcripts we had found to associate with DJ-1 *in vivo* between PD and control frontal cortex. Using RT-PCR and microarray technology we found no statistically significant difference in the RNA expression of the previously identified selenoproteins (GPx4, SEPW1, GPx3, SEPHS2), PTEN/AKT modulators (MAPK8IP1, PPP2R2C, JunD, BAD) or mitochondrial subunits (ND1, ND2, ND4, ND5) (Fig. 4.6, 4.7A and 4.8). We also compared the expression of additional transcripts that were reported to interact with DJ-1 *in vitro* (van der Brug et al., 2008). Selonoprotein related transcripts SELT, SEPX1 and SELH

along with the Akt/PTEN pathway transcripts BCL2L1, RSP6KB2 and EIF4EBP1 and the mitochondrial complex one associated transcript NDUFB1 all showed no difference in their expression levels between PD and controls. Both control and PD tissue used for gene expression analysis were matched for age, post-mortem delay and pH (Fig. 4.9A and Fig. 3.7).

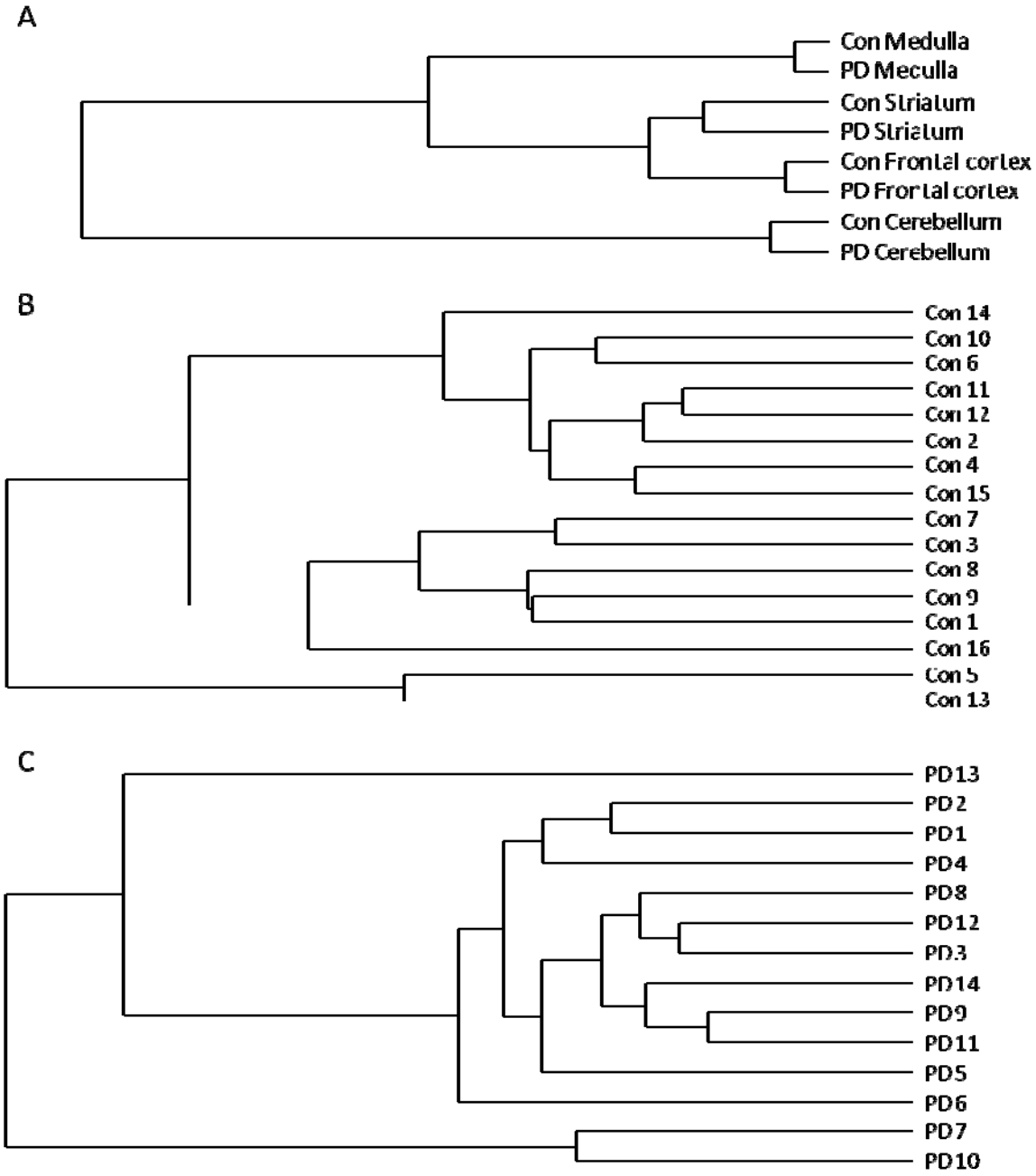


**Figure 4.5: Dendrogram showing clustering of samples.** A) Clustering of samples from PD cases and matched controls across 4 distinct regions. B and C) Gene profile comparison of control and PD frontal cortex sample groups.

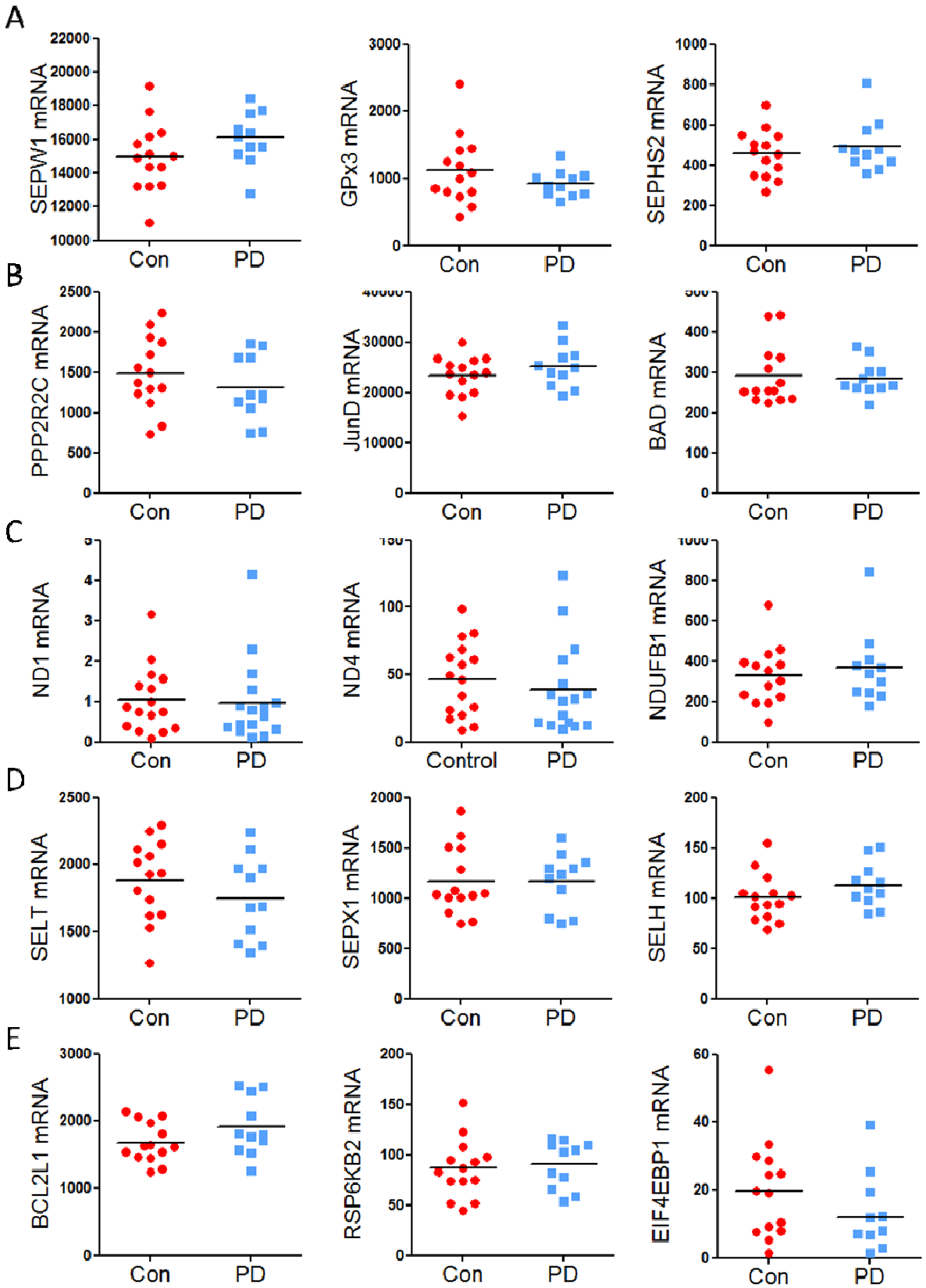


**Figure 4.6: Gene expression of DJ-1 associating mRNA species in control and PD subjects.** Expression of selenoproteins (A), PTEN/Akt pathway modulators (B) and mitochondrial (C) transcripts we found to interact with DJ-1 in vivo. Expression of additional selenoproteins (D) and PTEN/Akt (E) associated transcripts reported to interact with DJ-1 in vitro.

In order to show that microarray and RT-PCR are complimentary techniques for measuring gene expression we measured the expression of GPx4 in frontal cortex of PD and control subjects and found no significant difference between the two confirming the array data (Fig. 4.7A). The array chip contained a probe for *PARK7* and subsequent analysis showed a down-regulation of DJ-1 gene expression in PD frontal cortex, in line with our RT PCR data (Fig. 4.7B). However, in this case the decrease was not significant ($p<0.09$).

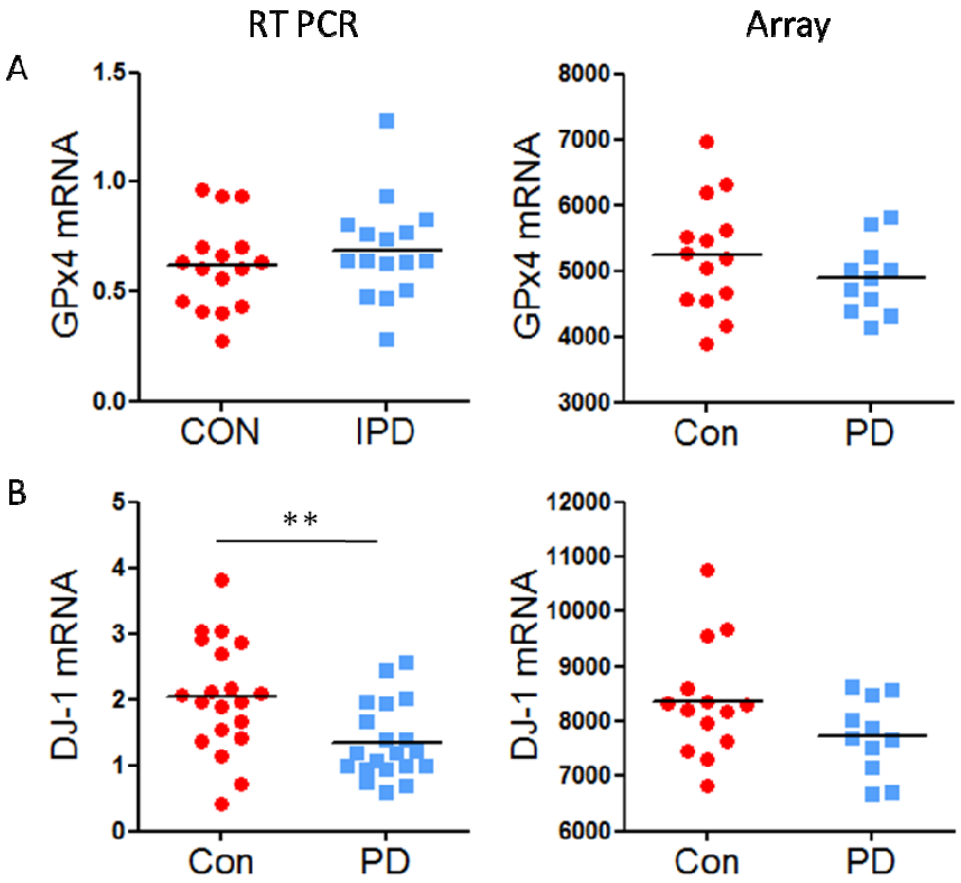


**Figure 4.7: Comparison of RT-PCR and microarray gene expression in the frontal cortex.** A) No difference in GPx4 gene expression between control and PD case was found by both RT-PCR and microarray techniques. B) Both techniques showed average DJ-1 gene expression to be lower in PD frontal cortex than matched controls.

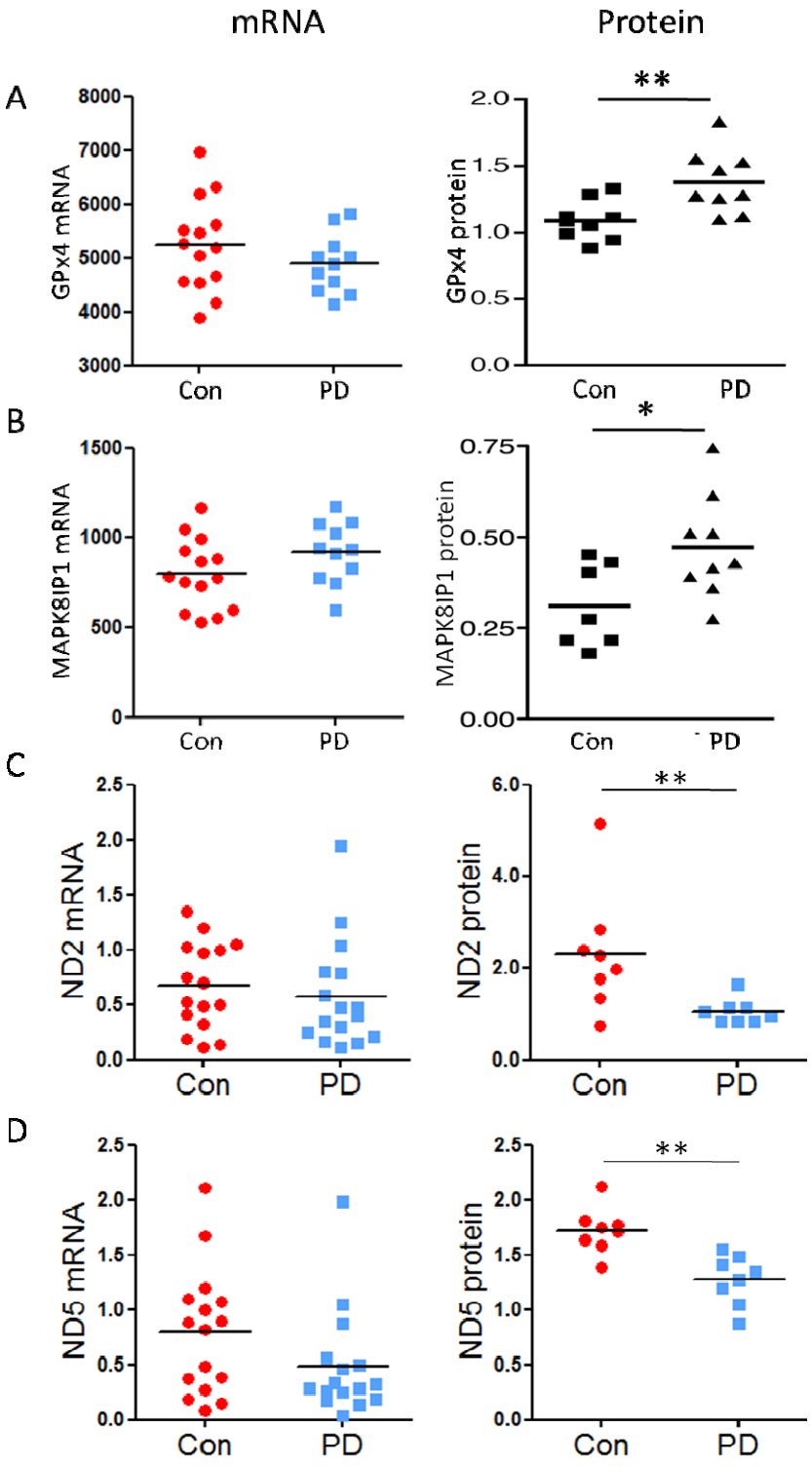


**Figure 4.8: Gene and protein expression in control and PD frontal cortex of transcripts that interact with DJ-1 in vivo.** For both GPx4 (A) and MAPK8IP1 (B) no differences in mRNA levels were observed between control and PD cases, but both showed elevated protein levels in PD. Likewise no difference in the amount of ND2 (C) and ND5 (D) mRNA levels was found. However protein levels were lower in PD compared to controls. Statistical significance determined by student's T-test, * = $p<0.05$ and ** = $p<0.01$. Protein data for GPx4 and MAPK8IP1 was provided by Jeff Blackington, a collaborator at the NIH.

With no observed difference in mRNA abundance for multiple transcripts we examined protein levels for the GPx4, SEPW1, MAPK8IP1, ND1, ND2, ND4 and ND5 (Fig. 4.8) using western blotting. No positive immunoreactivity was found for SEPW1, ND1 and ND4 in frontal cortex tissue. Both GPx4 and MAPK8IP1 protein levels were significantly increased in PD patients. Similarly, gene expression of both mitochondrial ND2 and ND5 were alike but for both protein levels were significantly lower in PD (Fig. 4.8C and D). No significant difference in post-mortem delay, age or tissue pH was noted that could account for altered protein expression in PD subjects (Fig. 4.9B).

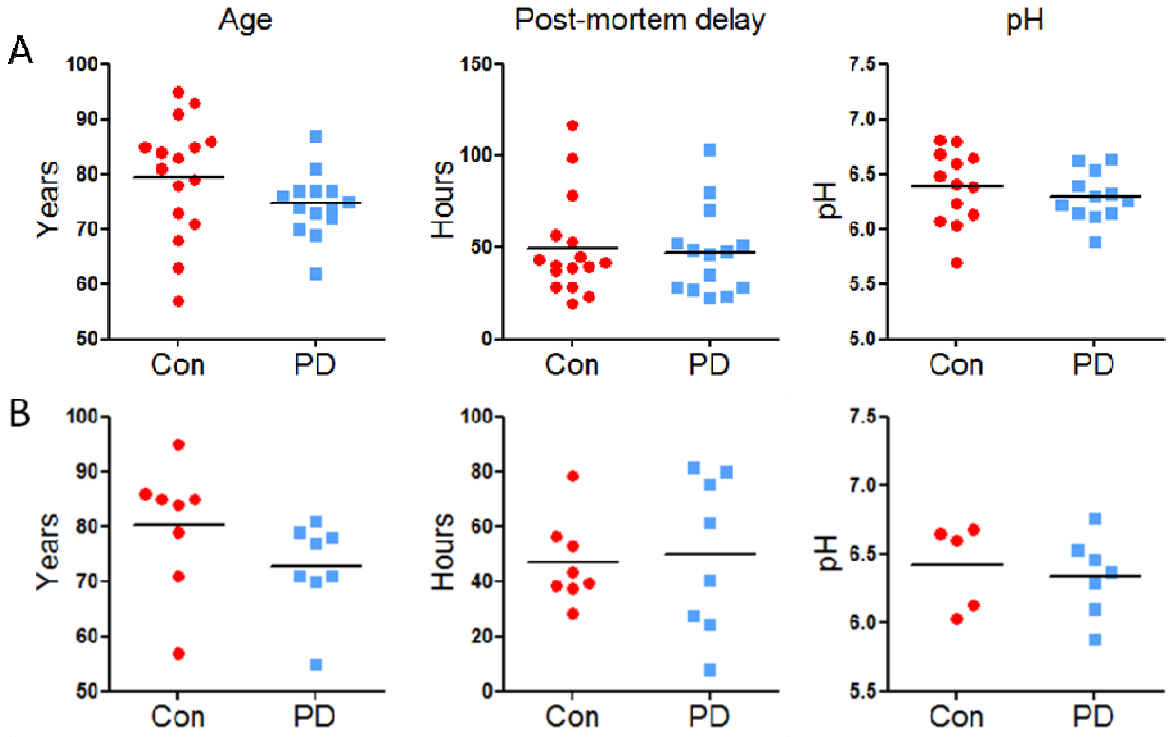


**Figure 4.9: Comparison of demographic data for control and PD brains.** Post-mortem delay, age and pH of control and PD tissue used for A) array and B) protein analysis in expression studies of DJ-1 associated transcripts.

# 4.3. Discussion

DJ-1 is reportedly a participant in multiple biological processes including oxidative response (Canet-Aviles et al., 2004; Taira et al., 2004), transcriptional regulation (Niki et al., 2003; Takahashi et al., 2001), fertility (Wagenfeld et al., 1998; Yoshida et al., 2003) and apoptosis (Fan et al., 2008a; Kim et al., 2005a). Using *in vitro* and yeast two hybrid models, a number

of interactors have been identified that would explain the varied activity of DJ-1. By performing DJ-1 IPs we tried to confirm some of these interactions in human frontal cortex brain tissue.

We failed to show positive IR in either the IP or lysate fractions for Nrf2. DJ-1 has been shown to stabilise Nrf2, a transcription factor that regulates the expression of genes in multiple anti-oxidant pathways (Clements et al., 2006). The absence of Nrf2 IR could be due to a number of reasons. First, Nrf2 may not be highly expressed in human frontal cortex or secondly, the specificity of the antibody is particularly poor. We also failed to co-IP Sumo-1 with DJ-1 or detect it in normal lysate, possibly for the same reasons. *In vitro*, DJ-1 has been found to undergo sumoylation at residue K130 in the presence of ROS, with failure to do so resulting in a loss of anti-apoptotic activity (Shinbo et al., 2006). Sumoylation inhibits apoptosis in neuroblastoma cells by causing translocation of DJ-1 to the nucleus where it represses p53 transcriptional activity and reduces Bax expression (Fan et al., 2008a). In addition to lowering Bax activity, translocation of DJ-1 to the nucleus hinders Daxx migration from the nucleus to the cytosol where it activates ASK1 and resulting in apoptosis (Junn et al., 2005; Karunakaran et al., 2007). Again we were unable to confirm previous reports of an interaction between DJ-1 and Daxx using human tissue, though some IR was noted in one PD lysate, suggesting the antibody was suitable for use with human cortical tissue. Our failure to confirm any of these protein interactions may be explained by possible differences in the reported subcellular location of DJ-1. Interactions between DJ-1 and Nrf2, Sumo-1 and Daxx primarily occurs in the nucleus (Clements et al., 2006; Junn et al., 2005; Shinbo et al., 2006), an organelle where multiple groups have shown DJ-1 to reside. (Blackinton et al., 2005; Bonifati et al., 2003b; Macedo et al., 2003; Nagakubo et al., 1997). In mouse brains however, no DJ-1 immunoreactivity was noted in the nucleus following subcellular fractionation (Zhang et al., 2005a). This discrepancy may be due to differences in methodologies or it could highlight a difference between endogenous DJ-1 localisation in mammalian brain tissue and over-expression cell models.

Though no interaction was found with Nrf2, Sumo-1 or daxx, our co-IP experiments may have identified a tentative association with mortalin. This would confirm a previous report of an association between the two *in vitro* (Jin et al., 2007). Mortalin is a member of the

HSP70 family of proteins. It is native to the mitochondria, but has also been found to reside at other subcellular sites including endoplasmic reticulum, plasma membrane, cytoplasmic vesicles and cytosol (Kaul et al., 2002). In the mitochondria, mortalin forms a translocation system for importing nuclear encoded proteins from the surrounding cytosol (Deocaris et al., 2006). As a chaperone, mortalin would be able to unfold bulky proteins, shuttle them into the mitochondria and then refold them back to their native conformation. This activity could account for the endogenous pool of DJ-1 present in mammalian mitochondria (Zhang et al., 2005a). Migration of DJ-1 to the mitochondria has been demonstrated under conditions of oxidative stress and is a feature that is crucial to its protective activity (Canet-Aviles et al., 2004; Junn et al., 2009). Therefore during times of stress, mortalin may help boost mitochondrial DJ-1 levels with the aim of minimising oxidative damage. Mortalin has also been reported to associate with α-synuclein *in vitro* (Jin et al., 2007) and may offer a passage for its import into the mitochondria as seen in dopaminergic neurons of post-mortem human brains (Devi et al., 2008).

When first cloned, DJ-1 was noted to be almost identical to a regulatory component of a RBP (Hod et al., 1999). Subsequently, DJ-1 was reported to interact *in vitro* with two nucleic acid binding proteins, PSF and p54nrb (Xu et al., 2005) and the RNA helicase Abstrakt (Sekito et al., 2005). As we had relatively little success identifying DJ-1 protein interactions, we decided to investigate whether DJ-1 associates with RNA *in vivo* as a means of explaining its pleiotropic effects. Co-IP of endogenous DJ-1 from 3 controls and subsequent identification of RNA species via real-time PCR showed DJ-1 binds to several RNA transcripts in human frontal cortex. Due to the minute amount of RNA isolated, we were unable to amplify a sufficient quantity with the Illumina RNA amplification kit. This prevented us from identifying novel RNA interactors with a microarray gene expression chip. Instead, real-time PCR was used to validate interactions with RNA transcripts that our collaborators had previously shown to bind to DJ-1 *in vitro* (van der Brug et al., 2008). In total, we tried to confirm interactions between DJ-1 and 13 transcripts and found all but one to be enriched in DJ-1 IP fractions. Transcripts were grouped into 3 categories: those that encode for selenoproteins, those involved in PTEN/Akt pathway and those for subunits of mitochondria complex 1. These transcripts are distinct from those reported to associate with other

proteins like FMR-1 (Brown et al., 2001) and HuR (Lopez de Silanes et al., 2004) highlighting their specificity as targets for DJ-1.

Selenoproteins are proteins that contain a selenocysteine amino acid as their catalytically active residue. We identified 4 transcripts that interacted with DJ-1 in human frontal cortex; GPx4, GPx3, SEPW1 and SEPHS2. Both GPx4 and GPx3 are glutathione peroxidises (GPx) whose functional role is to reduce peroxides. Not much is known about GPx3, but GPx4 has been studied in some detail and found to have the unique ability to reduce phospholipid hyperoxides (Brigelius-Flohe, 2006). This characteristic makes GPx4 vital in maintaining mitochondrial integrity. Within mitochondria, GPx4 prevents the extensive oxidation of cardiolipin, a mitochondria exclusive phospholipid that strongly associates with cytochrome c (Imai and Nakagawa, 2003). Formation of cardiolipin hyperoxide causes cytochrome c to dissociate, leaving it free to seek a path into the cytosol. GPx4 reduces cardiolipin hyperoxides, keeping cytochrome c firmly bound to the mitochondrial membrane (Imai and Nakagawa, 2003). GPx4 has also been noted to be up-regulated in glial cells of PD subjects and provides protection against inflammatory responses (Brigelius-Flohe, 2006). SEPW1 also display anti-oxidant properties, but like GPx3 its actions have not been well documented (Chen and Berry, 2003). Unlike the other 3 proteins, SEPHS2 is not an antioxidant, instead it is an enzyme that donates selenium in the synthesis of selenocysteine residues in selenoproteins like glutathione peroxidises.

We also identified 4 components of the PTEN/Akt survival pathway, namely JunD, MAPK8IP1, PPP2R2C and BAD. JunD has been shown to be cytoprotective against UV induced apoptosis and to protect cells from oxidative stress by regulating the genes involved in antioxidant defence (Tsuji, 2005). MAPK8IP1 is the human homologue of JIP-1 which represses apoptosis by inhibiting the JNK pathway. Elevated JIP-1 has been shown to protect dopaminergic neurons from MPTP damage which promotes cell death via JNK activation (Hashimoto et al., 2002). During apoptosis, Bax facilitates the opening of mitochondrial permeability transition pores allowing cytochrome c to leak into the cytosol (Hartmann et al., 2001). This process is inhibited by Bcl-1 which is released upon phosphorylation of BAD (Chao and Korsmeyer, 1998).

The last group of transcripts, ND1, ND2, ND4 and ND5 were categorized as mitochondria encoded subunits of complex 1. Mitochondria complex 1 (NADH ubiquinone oxireductase) is the first and largest member of the mitochondrial respiratory system. It establishes an electrochemical ion gradient by oxidising NADH and pumping protons ($H^+$) across the inner mitochondria membrane into the inner mitochondria space whilst the freed electrons are transferred to complex III by ubiquone (Fato et al., 2008). It consists of 46 subunits, 7 of which including ND1, ND2, ND4 and ND5 are encoded by the mitochondrial genome (Antonicka et al., 2003). These 7 subunits combine with 7 nuclear encoded subunits in the inner mitochondria membrane to form the catalytic core that shows evolutionary conservation down to bacteria (Fato et al., 2008).

Though we were unable to identify a broader range of transcripts, our collaborators at the NIH found DJ-1 could bind to over 500 transcripts in mouse brains (unpublished observations). DJ-1's association with RNA appears to be governed by its oxidative state, with it showing a drastically reduced affinity for RNA when oxidised (van der Brug et al., 2008). DJ-1 has been reported to be more oxidised in the frontal cortex of PD subjects (Bandopadhyay et al., 2004; Blackinton et al., 2009) which suggests that interactions between DJ-1 and RNA are limited in PD. We found protein levels of both GPx4 and MAPK8IP1 to be significantly elevated in PD frontal cortex. No comparable change in mRNA levels was noticed signifying that some post-trancriptional mechanism is responsible for the increased protein levels. MAPK8IP1 protein levels are also elevated in aged mice which also display a greater degree of DJ-1 oxidation in comparison to younger mice (van der Brug et al., 2008). These results demonstrate that DJ-1 binds to RNA in its reduced form and acts as a repressor of translation. Under conditions of oxidative stress, such as that seen in PD, DJ-1 is oxidised and released RNA strands rapidly undergo translation (Fig. 4.10). This would explain why no discernable difference in RNA quantity was noted between PD and control post-mortem tissue and why both GPx4 and MAPK8IP1 protein levels are elevated in PD. In line with this, levels of both proteins were found to be greater in DJ-1 null mice compared to WT, thought steady state levels of RNA were constant (van der Brug et al., 2008).

Van der Brug and colleagues also showed that for GPx4, DJ-1 binds to the 5' untranslated region (UTR). Binding at this site may be enough to prevent the binding of the small (40s)

ribosomal unit of the cap-binding protein complex, which scans the mRNA transcript in the 5' → 3' direction till it locates the AUG initiation codon (reviewed in Gebauer and Hentze, 2004). Given the dynamic nature of cells in the brain, it is important a mechanism exists that allows rapid responses to changes in the microenvironment. DJ-1 appears to fulfil this role in a quintessential manner by keeping a portion of RNA in storage, making it available for translation in response to changes in physiological conditions. Thus, responses to cellular stress can be immediately instigated without wasting time or energy on the synthesis, processing and export of new RNA transcripts and would ensure that only the required proteins are up-regulated (Holcik and Sonenberg, 2005).

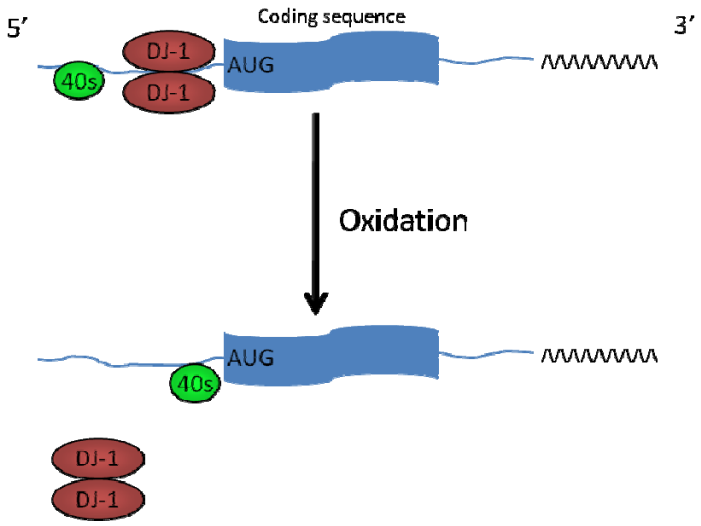


**Figure 4.10: Oxidative-dependent regulation of protein translation by DJ-1.** In its reduced form DJ-1 binds to 5' UTR region and prevents 40s ribosome unit from reaching the AUG start codon. In the presence of oxidative stress, DJ-1 becomes oxidised and dissociates from the mRNA strand allowing the 40s ribosome unit to initiate translation.

DJ-1 may also provide a mode of transport for RNA, conveying it from the nucleus to other areas of the cell where a localised translation of protein can occur. Relocation of DJ-1 to mitochondria has been observed (Blackinton et al., 2005) and it is plausible that DJ-1 could also migrate towards other organelles. Within neurons DJ-1 may even carry RNA towards synaptic terminals to combat the effects of neurotransmitter re-uptake or calcium influx. In this manner DJ-1 may provide protection against dopamine toxicity in dopaminergic neurons.

Six of the twelve transcripts that we found to be preferentially enriched in DJ-1 IPs appear to be involved in maintaining mitochondrial integrity and well being. Mitochondrial dysfunction has been implicated in PD pathogenesis for some time now, with the evidence first emerging following the discovery that MPTP induces parkinsonian symptoms through inhibition of mitochondria complex 1 (Abou-Sleiman et al., 2006b). Rotenone is another neurotoxin that inhibits complex 1 activity and even produces LB like inclusion bodies that contain α-synuclein (Henchcliffe and Beal, 2008). A place for disrupted complex 1 functioning in the development of sporadic PD was established following reports that levels are decreased in post-mortem PD substantia nigra (Schapira et al., 1990) and frontal cortex (Parker et al., 2008). Subunits of complex 1, in particular those that constitute the main catalytic core display a higher protein carbonyl content in PD compared to controls, indicating that they suffer greater oxidative damage (Keeney et al., 2006). Keeney et al., (2006) also reported that the protein levels of a number of these subunits were lower in the frontal cortex of PD subjects. This corroborates previous reports of reduced levels of multiple subunits of complex 1 in PD striatum (Mizuno et al., 1989) and our data showing down-regulation of both ND2 and ND5 in PD is in agreement with this.

Superoxides are an unfortunate by product of complex 1 activity and is thought to be the principle architect of oxidative damage to subunits (Keeney et al., 2006) which results in structural defects that increase electron leakage and ROS production. Rapid replacement of damaged subunits would minimise any deleterious effects and the presence of DJ-1 in the mitochondria along with its association with ND1, ND2, ND4 and ND5 provide a means for this to occur. Furthermore, oxidation of mitochondrial DJ-1 would initiate an up-regulation of antioxidants like GPx4 that would help combat the increased levels of ROS and minimise cytochrome c dissociation from the mitochondrial membrane. At the same time, cytosolic DJ-1 could also translocate to the mitochondria where it may augment antioxidant levels and up-regulate BAD which following phosphorylation would inhibit the opening of mitochondrial pores.

The decrease in complex 1 subunit protein levels observed in PD suggests that damaged subunits are unable to be replaced as efficiently. This would initiate a vicious cycle where elevated ROS production would exacerbate any oxidative damage, leading to the formation

of even more ROS. It is unclear why this down-regulation occurs as we found no corresponding reduction in mRNA levels of ND1, ND2, ND4 and ND5. Cybrid studies, where mitochondria from control and PD patients are transfected into mitochondria depleted cultured cells, have shown that PD cybrids develop molecular features typical of PD phenotype and are more likely to undergo apoptosis (Gu et al., 1998; Trimmer and Bennett, 2009). This strongly hints at a role for PD mitochondria DNA (mtDNA) in mitochondrial dysfunction and PD pathogenesis. Exhaustive screening of the mitochondrial genome however has yet to identify any mutations that consistently associate with PD (Fato et al., 2008). Instead, a high frequency of somatic mutations have been noted in the PD mitochondria located in the substantia nigra (Bender et al., 2006; Kraytsberg et al., 2006) and frontal cortex (Smigrodzki et al., 2004). Compared to nuclear DNA, mutation rates are 10-20 times higher for mtDNA due to the absence of introns and failure of proofreading by mitochondrial polymerase (Leonard and Schapira, 2000). Both ND2 and ND5 genes in particular show a higher mutation load in PD (Parker and Parks, 2005; Smigrodzki et al., 2004) that could affect protein production and explain the observed decreases. Smigrodzki et al., (2004) reported that the PD exclusive ND2 and ND5 amino acid changing mutations occurred in regions outside the segment of RNA we amplified, which would explain the similar levels measured in control and PD.

Pathogenic mutations of DJ-1 such as L166P, M26I and D149A do not prevent translocation towards the mitochondria and indeed this is increased under conditions of oxidative stress, however this is insufficient to protect cells from toxic insults (Blackinton et al., 2005). This failure can be attributed to the mutants reduced affinity for mRNA (van der Brug et al., 2008) which makes the role of DJ-1 as an RNA storage facility redundant. Consequently it would be unable to induce a rapid up-regulation of cell survival protein, with cells being forced to depend on conventional transcription and translation processes. Loss of this defence mechanism would make cells more susceptible to oxidative damage and lower the threshold of tolerable stress accounting for the early onset of PD seen in PARK7 families. In sporadic cases, it can be reasoned that the increased oxidation of DJ-1 caused by aging and PD pathology provides less opportunity for DJ-1 to revert back to its reduced form and replenish its supply of transcripts. Additionally it has been reported that a proportion of DJ-1 is irreversibly oxidised in PD (Choi et al., 2006), which make them incapable of binding to

RNA again, rendering them functionally inactive. Unfortunately, we were unable to study DJ-1's association with RNA in PD brains as RNA collected from immunoprecipitated DJ-1 failed to amplify. It is unclear why this was, but may be due to disease specific changes or variability in post-mortem tissue quality.

## 4.4. Conclusions

In this chapter, DJ-1 interactors were explored using human frontal cortex tissue. We found that DJ-1 associates with mRNA transcripts encoding for a number of stress response and mitochondrial proteins. The data presented here supports a role for DJ-1 as an oxidation-dependent regulator of translation which would be essential in the early stages of limiting the development of PD. Mortalin was also identified as a potential *in vivo* interactor of DJ-1 and maybe involved in its import into the mitochondria. DJ-1 therefore appears to be key for keeping oxidative stress within tolerable levels whilst maintaining mitochondrial activity.

# 5. Exploring DJ-1's role in tauopathies

# 5.1. An introduction to tauopathies

Tau, named after the Greek letter τ (tau) is a microtubule-associated protein (MAP) that was found to facilitate microtubule assembly *in vitro* (Weingarten et al., 1975). It is ubiquitously expressed in the adult brain. Within neurons it is primarily localised to the axon where it modulates binding and stabilisation of cellular microtubule, neurite extension and axonal transport (Ishihara et al., 1999). These functions are performed by different tau isoforms that are all encoded from the tau gene, located at chromosome 17q21. In total, 6 different isoforms exist in the adult human brain (Fig. 5.1) produced by alternative splicing of exons 2 and 3 at the N-terminal and exon 10 at the C-terminal of tau mRNA (Andreadis et al., 1992; Buee et al., 2000). Exon 10 contains a tubulin binding domain that is repeated 3 times elsewhere in the C-terminal region. Thus if exon 10 is spliced out only 3 repeat (3R) regions are present and 3R tau is formed, but if exon 10 is present then 4R tau is encoded. In normal cerebral cortex, 3R tau is slightly more predominant than 4R tau isoforms (Buee and Delacourte, 1999).

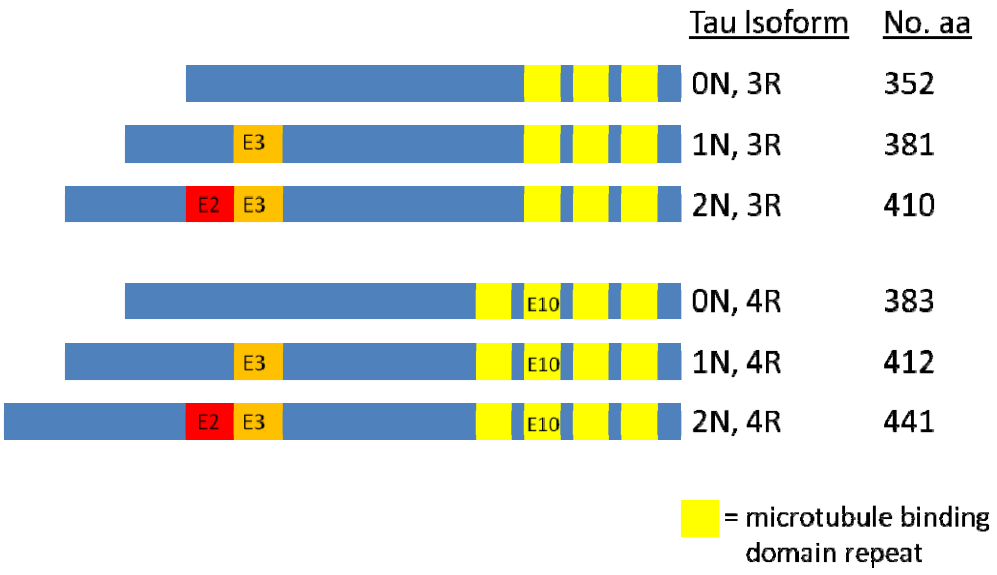


**Figure 5.1: Tau isoforms.** 6 tau isoforms are produced by alternative splicing of exons 2 (E2), 3 (E3) and 10 (E10). Splicing in of exon 10 results in inclusion of a 4$^{th}$ microtubule binding domain in the tau protein that is consequently termed 4R tau. Exclusion of exon 10 leads to 3R tau formation.

(Adapted from Buée et al., 2000)

Kinases and phosphatases negatively regulate Tau's activity by mediating phosphorylation of sites clustered around the tubulin binding repeats (Robert and Mathuranath, 2007). Under conditions that remain unclear, tau can become abnormally phosphorylated and hyperphosphorylated resulting in insoluble filamentous species that dissociate from microtubule surfaces and collect in the cell body (Abraha et al., 2000; Goedert, 2005). Accumulation of insoluble tau aggregates is the defining pathological feature of neurodegenerative disorders classified as tauopathies. These include Alzheimer's disease (AD), progressive supranuclear palsy (PSP), corticobasal degeneration (CBD), Pick's disease (PiD) and Frontotemporal lobe dementia (FTLD). Immnohistochemical and biochemical studies have shown that disease pathogenesis for some tauopathies is linked to aberrations in the levels of tau isoforms suggesting abnormal splicing and/or selective sequestration of insoluble tau species plays a role in these disease (Buee and Delacourte, 1999). Clues to the disease inducing mechanisms may be gathered from a number of identified genetic mutations which cause the dissociation of tau from microtubules, the formation of insoluble filamentous tau or alter the ratio of 3R:4R tau (Goedert, 2005; Pittman et al., 2006).

### *5.1.1.* Alzheimer's disease

AD was the first neurodegenerative disorder to be associated with tau aggregation. It is the most common neurodegenerative disorder and is characterised by tau aggregation, Aβ containing plaques, decreased synaptic density and neuronal loss in selected brain regions. The formation of abnormal tau filaments and amyloidosis (extracellular aggregation of Aβ into amyloid plaques) reflect the two degenerative processes of AD, with interactions between the two still not fully understood.

Phosphorylated normal tau contains 2 or 3 phosphate groups, however in AD hyperphosphorylated tau contains between 5 and 9 groups. These aggregate and are found in intracellular neurofibrillary lesions (NFL) that consist of neurofibrillary tangles (NFTs) and the dendritic process derived neuropil threads (NTs). All 6 tau isoforms contribute to tau pathology in AD which is largely confined to neurons, with glial tau pathology being a minor feature. The majority of tau present in NFL's exists in a paired-helical filament structure (PHL), though some straight filaments (SF) are also present. Formation of NFL is thought to

arise from the accumulation of phosphorylated tau in the cytoplasm which forms polymers and then globular particles. These in turn promote the formation of tau fibrils and PHF.

### 5.1.2. Progressive supranuclear palsy

Though a tauopathy, PSP is defined as a sporadic parkinsonian disorder and is today the second most common form of degenerative parkinsonism. It is also known as Steele-Richardson-Olszewski disease. It is clinically characterised by vertical supranuclear gaze palsy, akinetic-rigid syndrome, pseudobulbar palsy and frontolimbic cognitive decline (Litvan et al., 1996). Pathological changes that account for clinical manifestations occur mostly in the subcortical regions including: globus pallidus, substantia nigra, subthalamic nucleus and midbrain/pontine reticular formation. Additionally the frontal cortex may also be afflicted accounting for cognitive decline.

Unlike AD where all 6 tau isoforms are involved, the NFTs and NTs formed in PSP are predominantly 4R and formed from SF (Buee and Delacourte, 1999). Tau pathology is also not exclusive to neurons as it is in AD and can be found in glial cells in the form of star shaped tufted astrocytes (TA) or the comma shaped oligodendroglial coiled bodies (OCB).

### 5.1.3. Corticobasal degeneration

CBD is yet another sporadic degenerative parkinsonian tauopathy featuring deposition of 4R tau, though it is rarer than PSP. It was first described as corticodentatonigral degeneration with neuronal achromasia by Rebeiz and colleagues in 1967 (Buee and Delacourte, 1999). The clinically observed symptoms include limb rigidity, aphasia, apraxia and alien limb syndrome – where the patient is unable to control the movement of a limb and it feels 'foreign'.

Like PSP, CBD is pathologically defined as a 4R tauopathy with inclusions in both neurons and glial cells. However in CBD they are formed predominantly by the PHF variety associated with AD (Buee and Delacourte, 1999; Robert and Mathuranath, 2007). Similar to PSP, pathological damage is seen in the globus pallidus and the substantia nigra whilst a

greater cortical distribution is observed. CBD is also distinguishable from PSP by the additional presence of tau positive astrocytic plaques and 'ballooned' neurons that display weak immunoreactivity to tau (Komori, 1999).

### 5.1.4. Frontotemporal lobe dementia

FTLD patients clinically display altered behaviour, language and motor disturbances. It can be classed as either a tauopathy or a nontauopathy, the latter termed FTLD-ubiquitin (FTLD-U) as they possess ubiquitin-positive neuronal inclusions that could include TDP-43 (Arai et al., 2006). FTLD cases that exhibit tau pathology usually harbour mutations in the MAPT gene, resulting in alterations in tau isoform ratio or abnormal tau protein (Goedert, 2005) and as a result termed FTLD-MAPT. In total about 40 MAPT mutations have been identified with the majority found within exons, particularly exons 9-12 and take the form of missense, deletions and silent mutations (Fig. 5.2). Mutations also frequently occur in the introns surrounding exon 10 (Gasparini et al., 2007).

Mutations located on exon 10 such as N279K affect splicing of exon 10. By disrupting the splicing regulatory sequence, exon 10 becomes spliced in leading to overproduction of 4R tau isoforms. N279K in fact strengthens the splicing-enhancer element present at the beginning of exon 10, facilitating 4R tau mRNA and protein production. 4R tau formation is also promoted by mutations in the non-coding region that follows exon 10 (Gasparini et al., 2007). Intronic mutations such as exon 10+16 are proposed to disrupt the stem-loop RNA structure that usually obscures the exon 10 splice site. This exposes the splice site, inviting in splicing machinery and leading to increased splicing in of exon 10 (Ingram and Spillantini, 2002).

Mutations that occur away from exon 10 like R406W affect microtubule assembly resulting in a predominantly neuronal based pathology. Mutations affect all 6 isoforms which form PHF and SF within inclusions that are similar to those found in AD.

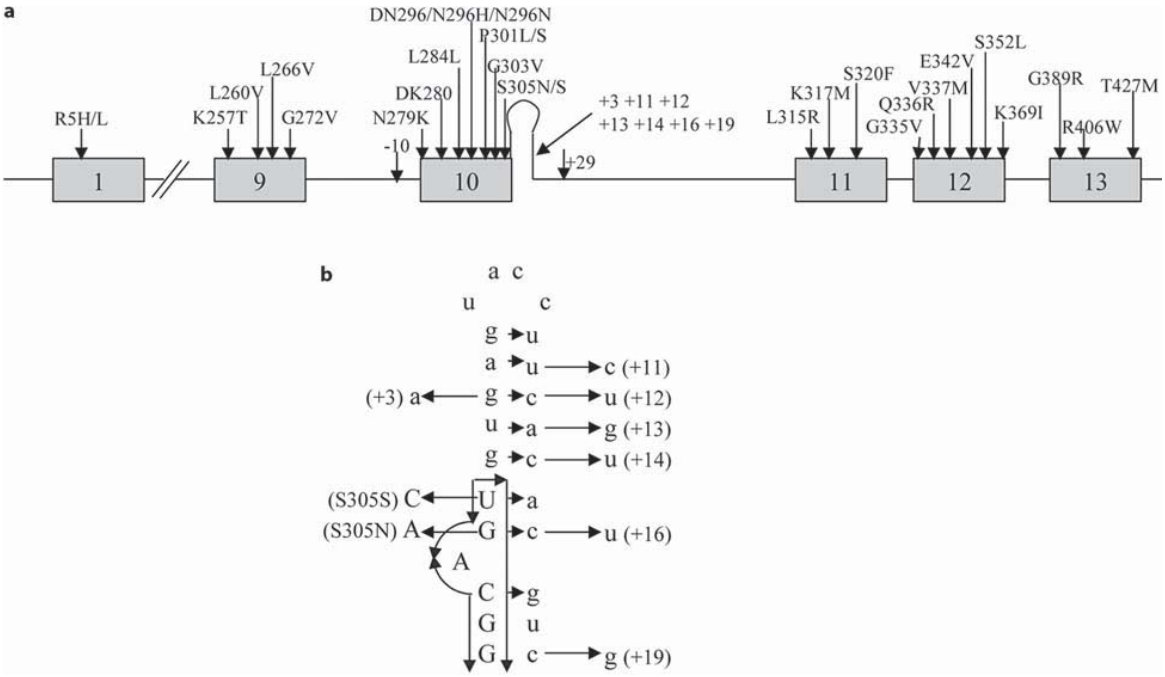


**Figure 5.2: Mutations in tau gene associated with FTLD-MAPT.** A) Mutations in exons 1 and 9-13 of the tau gene are shown along with intronic mutations in the stem-loop structure between exon 10 and 11. B) more detailed image of the stem-loop structure showing locations of mutations that destabilise it thereby increasing splicing in of the preceding exon 10. Exon sequence represented by uppercase with lower case denoting intron sequence. (Reproduced from Gasparini et al., 2007).

## 5.1.5. Pick's Disease

PiD was first described by Arnold Pick in 1892. It is characterised by frontal and temporal lobe dysfunction that induces behavioural changes and aphasia. Unlike other parkinsonism's, the substantia nigra is relatively well spared with the main pathology being asymmetrical atrophy of the frontal and temporal lobes, severe neuronal loss, ballooned achromatic neurons (Pick cells), gliosis and superficial cortical spongiosis (Kertesz, 2003; Uchihara et al., 2003). Degeneration of frontal and temporal lobes brings it under the umbrella of FTLD disorders and it may also be referred to as FTLD-Picks.

There are no NFTs or NTs found in PiD. Instead, neuronal cytoplasmic tau inclusions are spherical and are termed Pick bodies (PBs). They are comprised of randomly coiled and SF tau aggregates (Buee and Delacourte, 1999). Whilst inclusions are largely neuronal based,

OCBs and astrocytic inclusions can be present to a lesser extent (Komori, 1999). Interestingly, unlike PSP and CBD, 3R tau is the predominant tau isoform found in PiD aggregates. However, a number of cases have been described with 4R tau pathology and in some instances 4R tau has even been the most abundant isoform found in PBs (Kertesz et al., 2003; Munoz et al., 2003).

# 5.2. Characterisation of DJ-1 positive tau inclusions in tauopathies

## 5.2.1. Aim

Shortly after DJ-1 was identified as a cause of AR PD, two studies showed it to co-localise with tau inclusions, indicting it in the pathogenesis of tauopathies (Neumann et al., 2004; Rizzu et al., 2004). Here we aim to further our understanding of DJ-1 in tauopathies by examining its association with both 3R and 4R tau isoforms,

## 5.2.2. Materials and methods

### 5.2.2.1. Pathological material

Immunohistochemistry was performed on 8µm formalin-fixed wax-embedded sections from cases detailed in table 5.1 below. Regions used were frontal cortex, temporal cortex, hippocampus, basal ganglia and pons where appropriate or available.

| Case No. | Diagnosis | Sex | Age (years) | Disease Length (years) | PMD (hrs) | Main Pathology |
|---|---|---|---|---|---|---|
| 1 | Control | F | 83 | - | 20 | Minor age related NFT in hippocampus |
| 2 | Control | M | 86 | - | 53 | Normal with some vascular pathology |
| 3 | Control | F | 77 | - | 23 | Normal with some vascular pathology |
| 4 | Control | F | 81 | - | 14 | Normal with some vascular pathology |
| 5 | Control | M | 81 | - | 40 | Minor age related NFT in hippocampus |
| 6 | Control | M | 67 | - | 22 | Normal with some vascular pathology |
| 7 | Control | F | 83 | - | 49 | Normal with some vascular pathology |
| 8 | AD | F | 92 | 7 | 24 | AD pathology Braak Stage VI |
| 9 | AD | M | 64 | n/a | 64 | AD pathology Braak Stage V |
| 10 | AD | F | 91 | n/a | n/a | AD pathology Braak Stage VI |
| 11 | AD | F | 94 | n/a | 28 | AD pathology |
| 12 | AD | F | 57 | 11 | 26 | NFT, massive tau accumulation |
| 13 | AD | M | 82 | 10 | 38 | AD pathology |
| 14 | CBD | M | 80 | 5 | 66 | NFT, NT, CB |
| 15 | CBD | M | 64 | 4 | 42 | NFT, NT, gliosis |
| 16 | CBD | M | 69 | n/a | 7 | Numerous astrocytic plaques, mild NFT |
| 17 | CBD | M | 65 | n/a | 24 | NFT, NT, glial inclusions |
| 18 | FTLD-U | F | 78 | 3 | 37 | Ubiquitin inclusions |
| 19 | FTLD-U | M | 69 | 5 | 28 | Ubiquitin inclusions |
| 20 | FTLD-U | F | 55 | 5 | 44 | Ubiquitin inclusions |
| 21 | FTLD-U | M | 70 | 3 | 24 | Ubiquitin inclusions |
| 22 | PSP | M | 90 | 23 | 36 | NFT, NT, TA, CB |
| 23 | PSP | F | 78 | 9 | 33 | NFT, NT, TA, CB |
| 24 | PSP | M | 62 | 7 | n/a | NFT, NT, TA, CB |
| 25 | PSP | F | 63 | 2 | 51 | NFT, NT, TA, CB |
| 26 | PSP | F | 90 | 33 | 37 | NFT, NT, TA, CB |
| 27 | PSP | M | 78 | 6 | 66 | NFT, NT, TA, CB |
| 28 | PSP | M | 72 | 21 | 27 | NFT, NT, TA, CB |
| 29 | PSP | M | 69 | 6 | 44 | NFT, NT, TA, CB |
| 30 | PSP | M | 80 | 24 | 70 | NFT, NT, TA, CB |
| 31 | PSP | M | 74 | 13 | 37 | NFT, NT, TA, CB |
| 32 | FTLD-Pick's | F | 69 | 10 | 48 | PBs |
| 33 | FTLD-Pick's | M | 56 | 10 | 26 | PBs |
| 34 | FTLD-Pick's | F | 62 | 10 | 46 | PBs |
| 35 | FTLD-Pick's | M | 74 | 11 | 23 | PBs |
| 36 | FTLD-Pick's | M | 68 | 8 | 31 | PBs |
| 37 | FTLD-Pick's | F | 60 | 7 | 24 | PBs |
| 38 | FTLD-Pick's | M | 61 | 13 | 36 | PBs |
| 39 | FTLD-Pick's | F | 50 | 8 | 26 | PBs |
| 40 | FTLD-MAPT R406W | M | 70 | 7 | n/a | NFT |
| 41 | FTLD-MAPT R406W | F | 71 | 13 | n/a | NFT |
| 42 | FTLD-MAPT N279K | F | 53 | 8 | n/a | NFT, glial cell tangles |
| 43 | FTLD-MAPT Ex10+16 | M | 55 | 5 | 34 | NFT, glial cell tangles |
| 44 | FTLD-MAPT Ex10+16 | F | 65 | 13 | 23 | NFT, glial cell tangles |

**Table 5.1: Demographic data of cases used to examine DJ-1 IR in tauopathies.**

## 5.2.2.2. Immunohistochemical analysis

Immunoreactions were performed, as described in chapter 2, using polyclonal DJ-1 1130 and monoclonal tau antibodies AT-8. A semi-quantitative assessment, comparing DJ-1 immunoreactive inclusions with tau inclusions, was carried out independently by my supervisor and me using a scale ranging from - = none to ++++ = numerous. Monoclonal RD3

and RD4 tau antibodies were used to show the presence/absence of the two groups of tau isoforms depending on case diagnosis. The same cases were then used for double immunofluorescence study using both DJ-1 1130 and AT-8 antibodies, also described previously. This was performed with the help of Dr Lashley. In all cases control slides were produced without incubation with primary antibody to ensure no artificial or significant background staining arose. Trial runs were also performed to identify the appropriate pre-treatment for each antibody and the effects of double staining.

## 5.2.3. Results

Immunohistochemistry using a DJ-1 antibody showed all AD and FTLD cases contained DJ-1 positive inclusions. DJ-1 positive inclusions were also observed in CBD and PSP cases, but to a lesser extent. No DJ-1 immunoreactive inclusions were noted in the FTLD-U cases. Staining with AT8 for tau positive inclusions was robust for all samples. Table 5.2 above provides semi-quantitative assessment of DJ-1 immunoreactive structures in relation to AT8 tau positive inclusions and also cites the presence of 3R and 4R tau pathology for all the cases.

Within the frontal cortex of AD patients, DJ-1 IR was largely restricted to neuronal inclusions, particularly NTs with glial inclusions being largely absent (Fig. 5.4). It was also seen in abnormal neurites and NFTs associated with extracellular plaques. DFCM using DJ-1 and AT8 confirmed co-localisation of the two proteins in extracellular plaques and standalone NFTs (Fig. 5.5). RD3 and RD4 antibodies were used to show all AD cases contained both 3R and 4R tau inclusions. 4R tau was predominantly found within NFTs whilst RD3 stained numerous NTs and to a lesser degree NFTs.

FTLD-Pick cases were characterised by the abundant presence of AT8 positive PBs in the frontal cortex and for one case the hippocampus and temporal cortex (Fig. 5.6). In comparison, staining with DJ-1 revealed the presence of DJ-1 in PBs ranged from slight to moderate. Use of RD3 and RD4 antibodies showed that AT8 positive PBs were only positive for 3R tau and not 4R. DFCM confirmed co-localisation of DJ-1 and hyperphosphorylated tau in PBs (Fig. 5.7).

| Disease/case no. | | Region | AT8 IR | Type of DJ-1 IR | | | | RD3 IR | RD4 IR |
|---|---|---|---|---|---|---|---|---|---|
| | | | | PBs | NFTs | NTs | GIs | | |
| AD | 8 | FC | ++++ | - | ++ | +++ | 0/+ rare | +ve | +ve |
| | 9 | FC | ++++ | - | ++ | ++ | - | +ve | +ve |
| | 10 | FC | +++ | - | ++ | +++ | 0/+ rare | +ve | +ve |
| CBD | 14 | FC | +++ | - | - | - | 0/+ (APs) | -ve | +ve |
| | 15 | FC | +++ | - | - | - | 0/+ (APs) | -ve | +ve |
| | 16 | FC | +++ | - | - | - | 0/+ (APs) | -ve | +ve |
| | 17 | FC | +++ | - | - | - | + | -ve | +ve |
| PSP | 22 | Po, FC, Hi | ++++ | - | 0/+ | 0/+ | 0/+ (TA, CB) | -ve | +ve |
| | 23 | Po | ++++ | - | 0/+ | - | 0/+ (CB) | -ve | +ve |
| | 24 | Po, Fc | ++++ | - | 0/+ | 0/+ | 0/+ (TA, CB) | -ve | +ve |
| | 25 | Po | ++++ | - | 0/+ | 0/+ | 0/+ (CB) | -ve | +ve |
| | 26 | Po | ++++ | - | 0/+ | 0/+ | 0/+ (CB) | -ve | +ve |
| | 27 | Po | ++++ | - | 0/+ | - | 0/+ (CB) | -ve | +ve |
| | 28 | Po, FC, Hi | ++++ | - | 0/+ | 0/+ | 0/+ (CB) | -ve | +ve |
| | 29 | Po, FC | ++++ | - | 0/+ | 0/+ | 0/+ (TA, CB) | -ve | +ve |
| | 30 | Po | ++++ | - | 0/+ | 0/+ | 0/+ (CB) | -ve | +ve |
| | 31 | Po | ++++ | - | 0/+ | 0/+ | 0/+ (CB) | -ve | +ve |
| FTLD-Pick's | 32 | FC, TC, Hi | ++++ | +/++/++ | - | - | - | +ve | -ve |
| | 33 | FC | ++++ | ++ | - | - | - | +ve | -ve |
| | 34 | FC | ++++ | + | - | - | - | +ve | -ve |
| | 35 | FC | ++++ | ++ | - | - | - | | |
| | 36 | FC | ++++ | ++ | - | - | - | +ve | -ve |
| | 37 | FC | ++++ | ++ | - | - | - | +ve | -ve |
| | 38 | FC | ++++ | ++ | - | - | - | +ve | -ve |
| | 39 | FC | ++++ | + | - | - | - | +ve | -ve |
| FTLD-R406W | 40 | FC | +++ | - | ++ | ++ | + | +ve | +ve |
| | 41 | FC | +++ | - | ++ | ++ | + | +ve | +ve |
| FTLD-N279K | 42 | FC | ++++ | - | - | 0/+ | ++ | -ve | +ve |
| FTLD-Ex 10+16 | 43 | FC | ++++ | - | - | 0/+ | ++ | -ve | +ve |
| | 44 | FC | ++++ | - | - | 0/+ | ++ | -ve | +ve |

**Table 5.2: Semi-quantitative analysis of tau and DJ-1 neurolesions in neurological disorders with 3R and/or 4R tau pathology.** +ve (present) or –ve (absent) used to denote RD3 IR and RD4 IR. Following scale used to assess DJ-1 IR: - = absent, 0/+ = rare, + = few, ++ = moderate, +++ = many and ++++ = numerous. GI = glial inclusions, AP = astrocytic plaque, CB = coiled bodies, TA = tufted astrocytes, FC = frontal cortex, TC = temporal cortex, Po = Pons and Hi = hippocampus.

For PSP, DJ-1 positive structures were rare in occurrence in comparison to the numerously stained AT8 tau inclusions. DJ-1 IR was evenly associated with NFTs, NTs and glial inclusions in both the pontine base and frontal cortex (Fig. 5.8). Some tufted astrocytes were also seen in the latter region. DJ-1 was found to co-localise with tau in both neuronal and glial structures (Fig. 5.9). Screening with both RD3 and RD4 resulted in visualisation of only 4R tau positive structures. In CBD, DJ-1 IR was even rarer than in PSP and typically located in astrocytic plaques in the frontal cortex where it could seen in several NTs (Fig. 5.3).

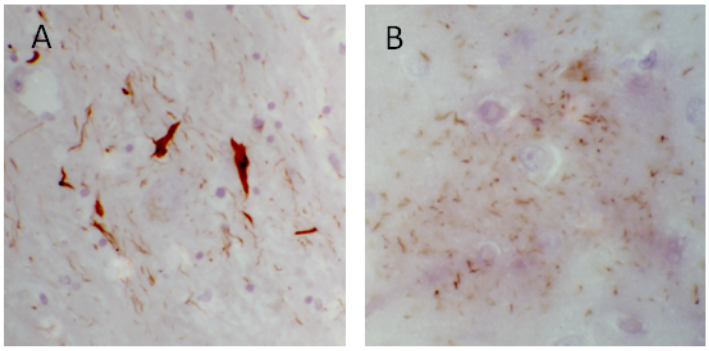


**Figure 5.3: Astrocytic plaques from frontal cortex of CBD cases.** Plaques stained with AT8 (A) and DJ-1 (B).

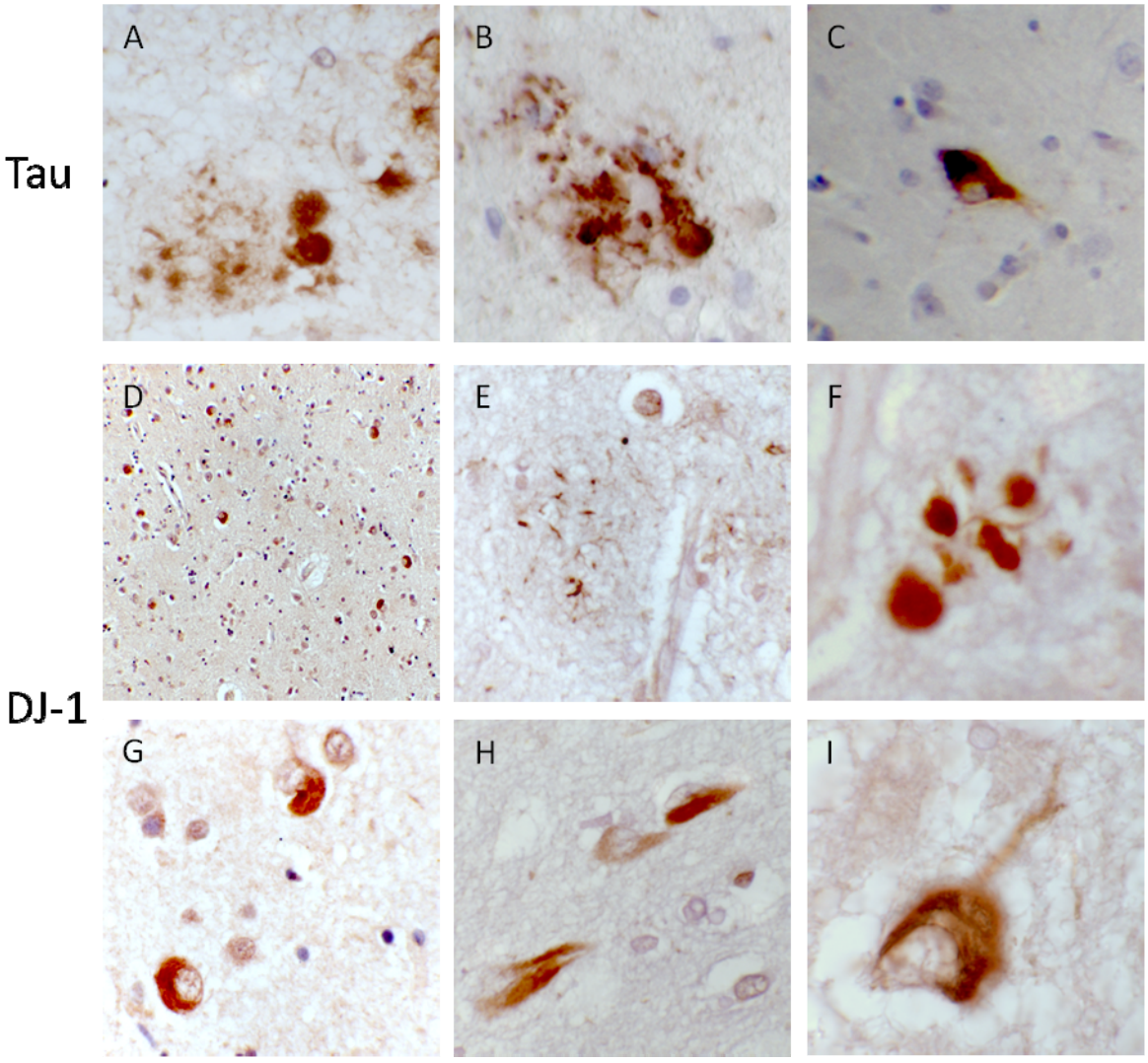


**Figure 5.4: DJ-1 IR in AD frontal cortex.** A, B) AT8 IR in extracellular plaque in AD. C) AT8 IR in an NFT. D, E) low power image of numerous DJ-1 IR NFTs in AD. F) DJ-1 IR NFTs and NTs in an extracellular plaque in AD. G-I) DJ-1 IR NFTs in AD.

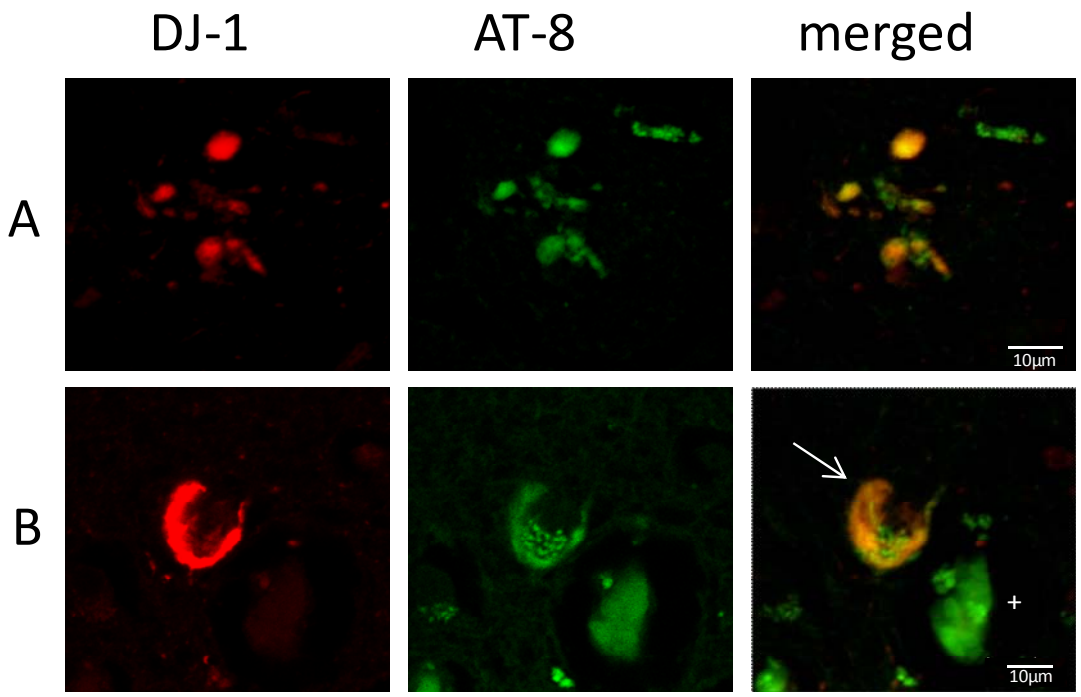


**Figure 5.5: Double confocal immunofluorescence of DJ-1 and tau in AD frontal cortex.** DJ-1 is depicted in red, tau AT8 in green and yellow represents a merged co-localisation of the two. A) Shows co-localisation of the two in NTs and NFTs in an extracellular plaque. B) an NFT containing both proteins (arrow) and one that is only tau positive (+).

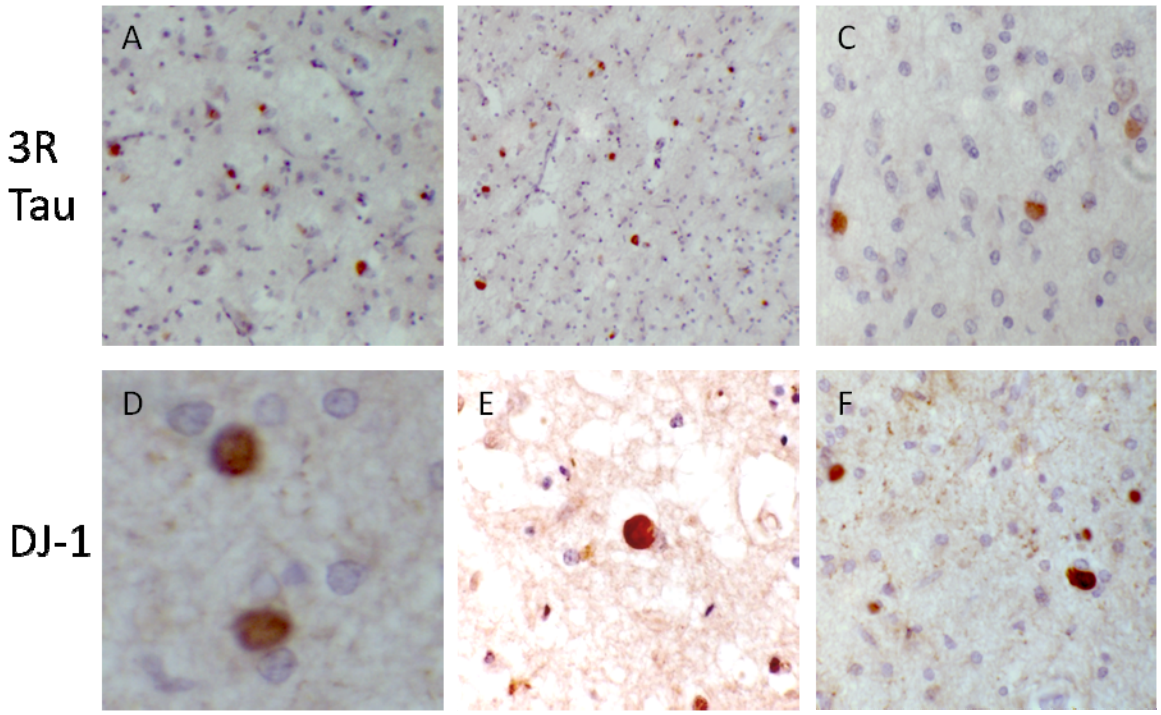


**Figure 5.6: DJ-1 IR in frontal cortex of FTLD-Pick's cases that exclusively display 3R tau pathology**. A-C) 3R-tau positive PBs. D-F) Positive staining of PBs with DJ-1.

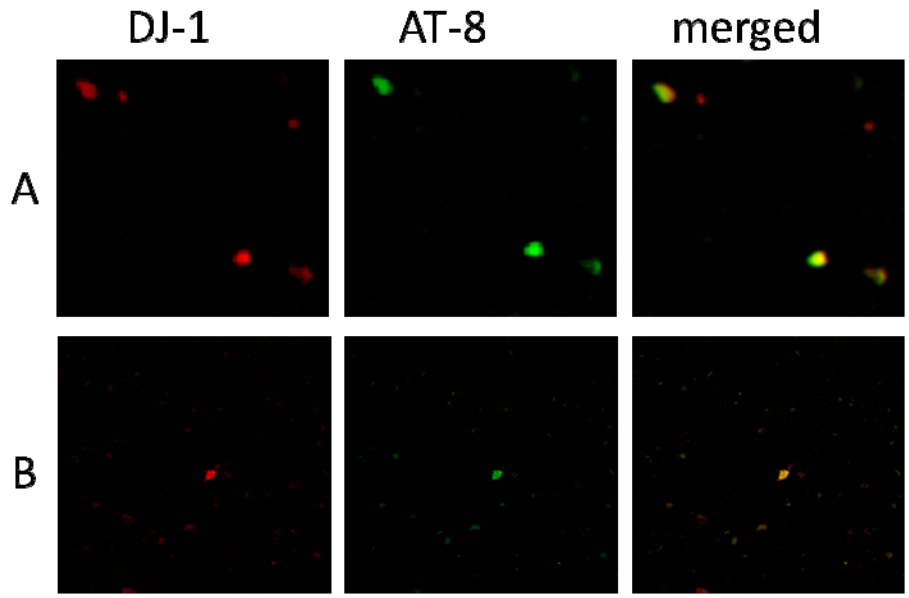


**Figure 5.7: Double confocal immunofluorescence of DJ-1 and tau in frontal cortex FTLD-Pick's case.** DJ-1 is depicted in red, tau AT8 in green and yellow represents a merged co-localisation of the two. Both A and B show co-localisation of DJ-1 and 3R tau proteins in PBs.

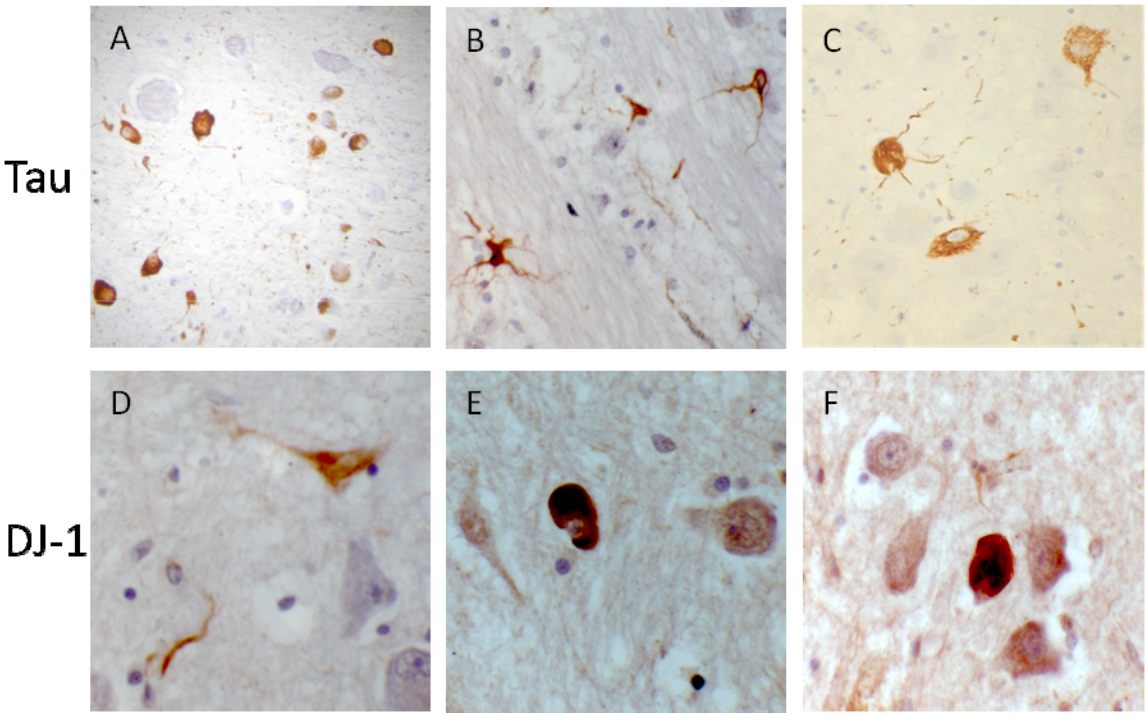


**Figure 5.8: Immunohistochemistry from basal pons of PSP cases demonstrating AT8 tau and DJ-1 IR.** A-C) AT8 positive NFTs and tufted astrocytes from PSP. D-F) Glial cell inclusions and NFTs from PSP displaying DJ-1 IR.

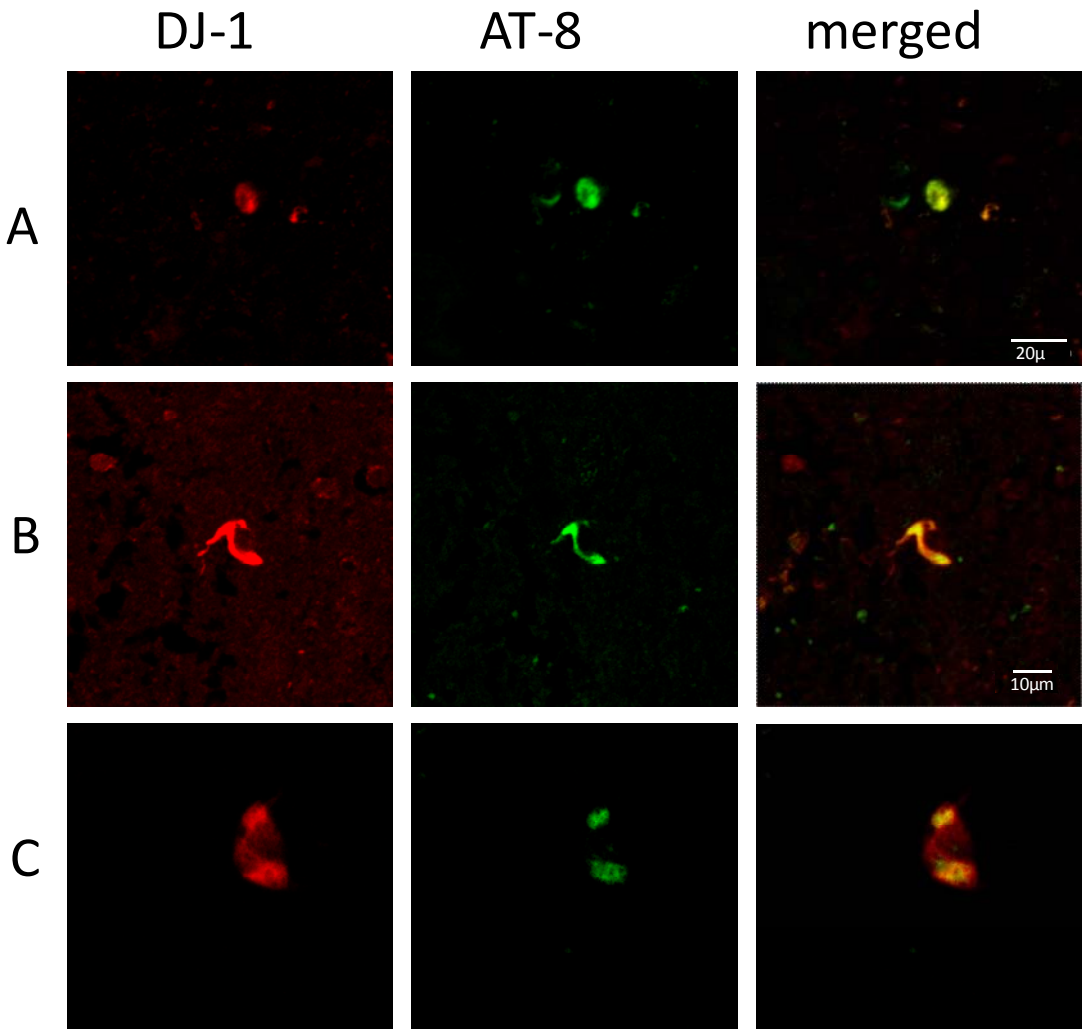


**Figure 5.9: Double confocal immunofluorescence of DJ-1 and tau in PSP frontal cortices.** DJ-1 is depicted in red, tau AT8 in green and yellow represents a merged co-localisation of the two. Co-localisation of the DJ-1 and 4R tau is shown in A) a NFT, B and C) glial inclusion coiled body.

DJ-1 IR was also assessed in a number of tauopathies induced by mutations in the MAPT gene and are summarised in table 5.2. The FTLD-MAPT cases with a R406W mutation displayed many AT8 positive tau inclusions in the frontal cortex. Both NFTs and NTs stained positive for 3R and 4R tau (Fig. 5.10). The same region from the 2 cases also exhibited moderate DJ-1 IR in NFTs and NTs. Co-localisation was again shown using DFCM, in this case a peri-nuclear rim seems to be formed by the DJ-1 and tau inclusions. DFCM also showed that both inclusions may be present within the same spatial vicinity of a neuron, but not co-localised (Fig. 5.11).

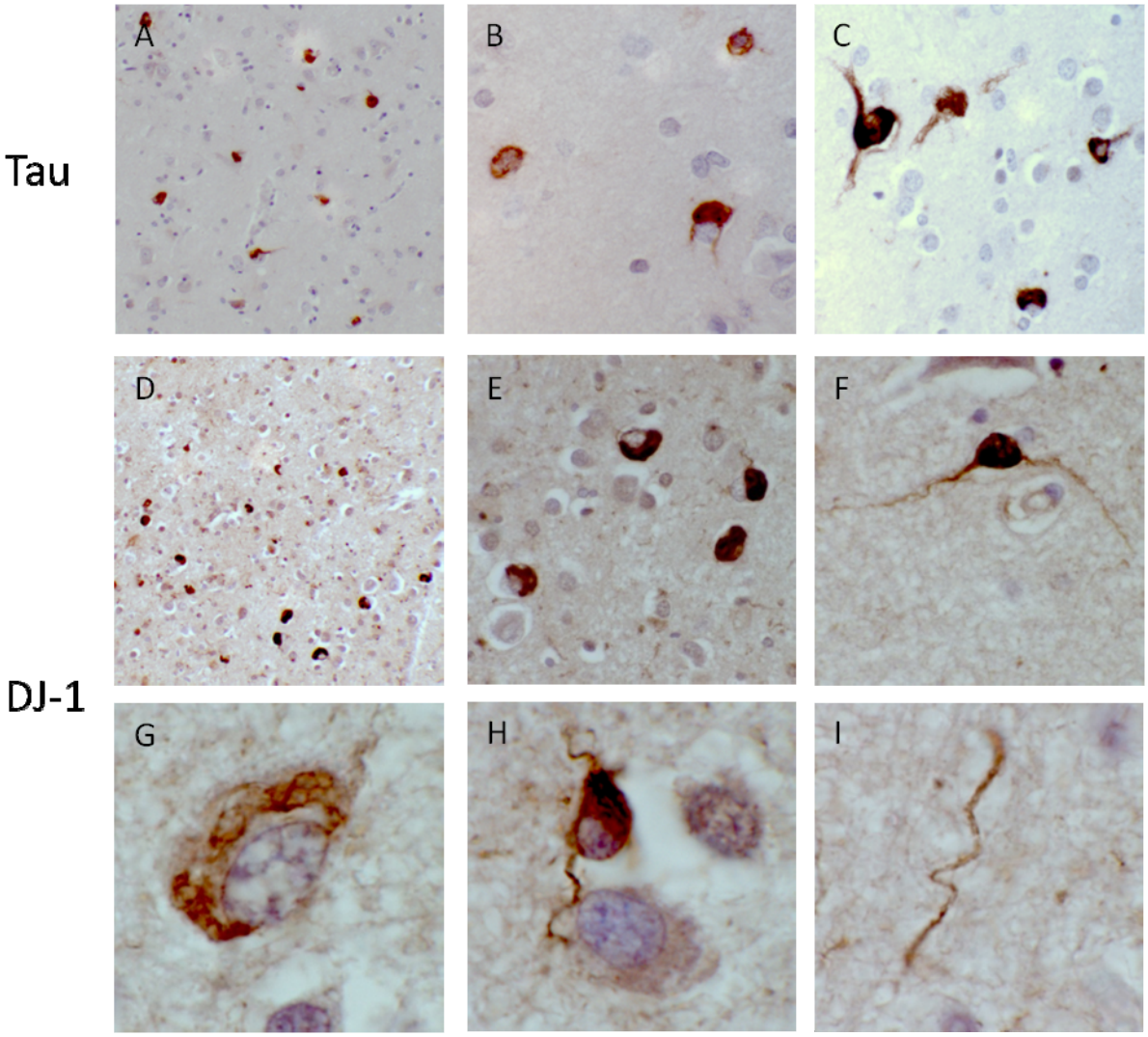


**Figure 5.10: Tau and DJ-1 immunoreactivity from FTLD-MAPT R406W cases which possess both 3R and 4R tau pathology.** A, B) 3R positive tau NFTs. C) 4R tau positive inclusions. D) Low power (10x) image of numerous DJ-1 positive NFTS. E, F) 40x image of DJ-1 positive NFTs. G, H) High power (100x) images of DJ-1 IR NFTs and NT (I). All images from frontal cortex.

For the single case with a N279K mutation, tau inclusions were found to be present within the frontal cortex in greater numbers than in the R406W case and like PSP and CBD were only positive for 4R tau (Fig. 5.12). A moderate number of glial cell inclusions that resembled coiled bodies showed DJ-1 IR in the cortical white matter. No DJ-1 positive NFTs were seen and NTs were rarely stained.

Both the FTLD cases with a MAPT exon 10+16 mutation showed a similar distribution of DJ-1 and tau positive inclusions to the N279K case. Additionally, like the N279K mutation, all tau inclusion in the exon 10+16 cases stained positive for 4R tau and negative for 3R tau (Fig. 5.12).

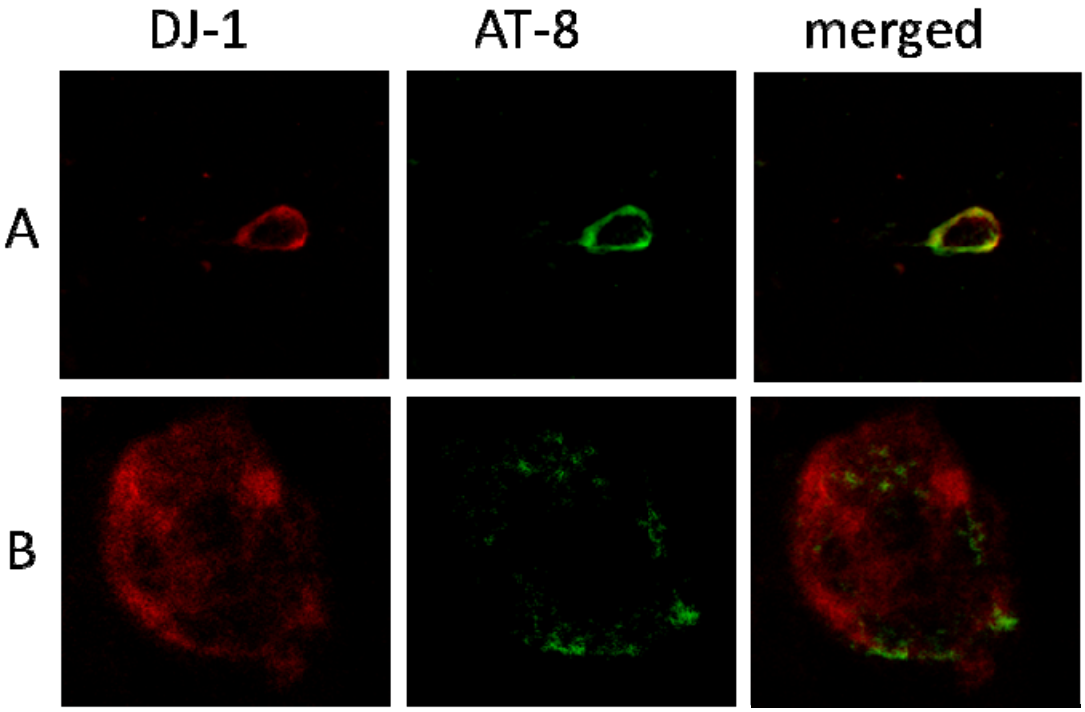


**Figure 5.11: Double confocal immunofluorescence of DJ-1 and tau in frontal cortex of FTLD-R406W case.** DJ-1 is depicted in red, tau AT8 in green and yellow represents a merged co-localisation of the two. A) Shows a ring-like peri-nuclear deposition of DJ-1 and tau. B) An NFT where both DJ-1 and tau are present but not co-localised.

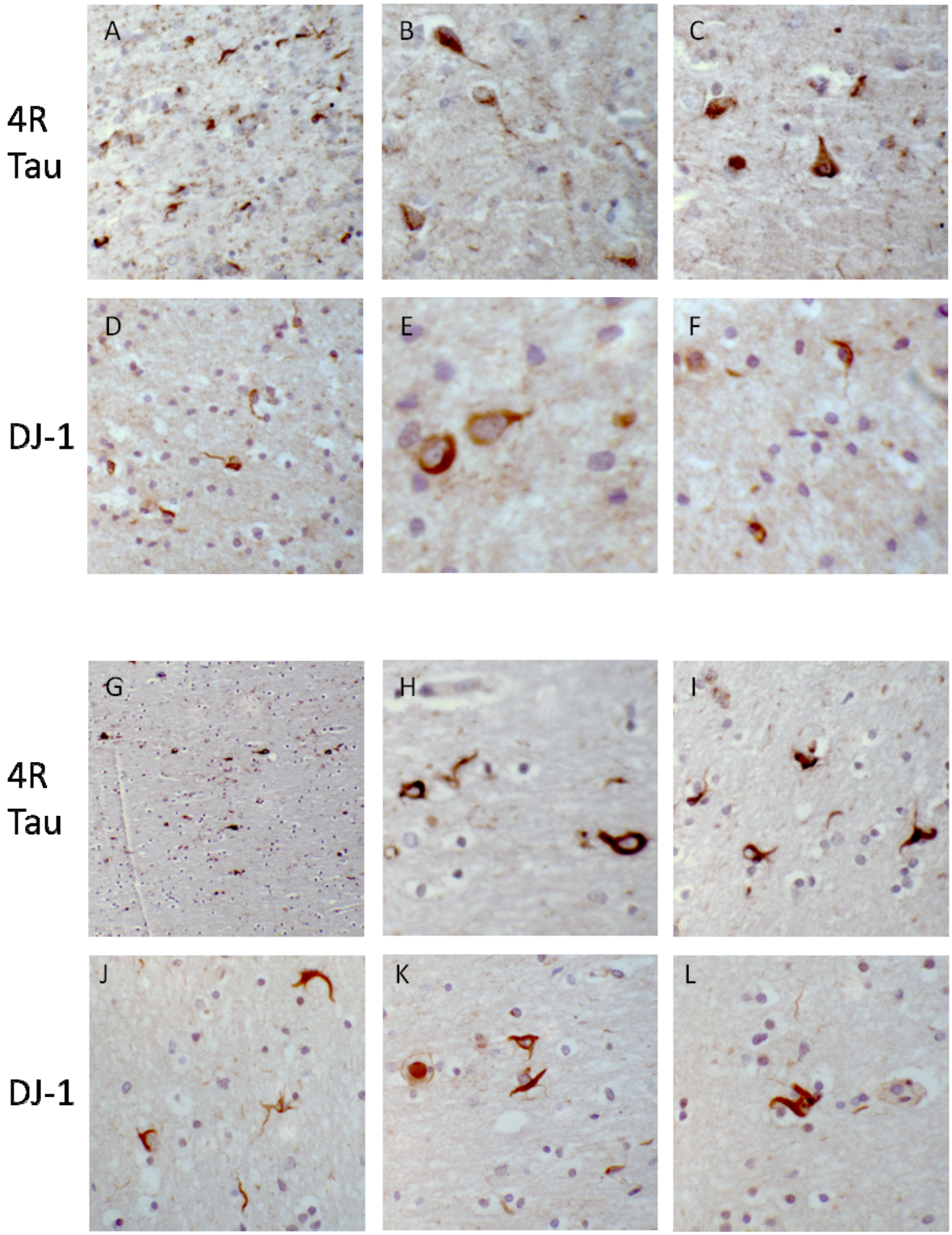


**Figure 5.12: DJ-1 IR in frontal cortex of FTLD-MAPT cases with 4R-tau pathology.** A-C) 4R-tau positive coiled bodies from FTLD-MAPT Ex. 10+16 cases. D-F) DJ-1 positive coiled bodies from the same cases. Coiled bodies from a FTLD-MAPT N279K case, showing 4R-tau IR (G-I) and DJ-1 IR (J-L).

# 5.3. Comparison of DJ-1 expression between tauopathies and controls

## 5.3.1. Aim

To determine whether DJ-1 mRNA and protein levels are compromised in tau related neurodegenerative disorders.

## 5.3.2. Materials and methods

### 5.3.2.1. Pathological material

| Case | Sex | Age | PMD | pH | mRNA | Protein |
|---|---|---|---|---|---|---|
| Con 1 | F | 77 | 23.0 | 5.60 | *x* | x |
| Con 2 | F | 86 | 46.5 | 6.17 | *x* | |
| Con 3 | F | 84 | 81.5 | 6.28 | *x* | |
| Con 4 | M | 85 | 43.4 | 6.68 | *x* | x |
| Con 5 | M | 86 | 53.0 | 6.65 | | |
| Con 6 | M | 86 | 23.3 | 6.55 | *x* | |
| Con 7 | M | 81 | 40.0 | 6.48 | *x* | |
| Con 8 | F | 85 | 34.0 | 6.31 | *x* | x |
| Con 9 | M | 83 | 117.1 | 6.81 | | |
| Con 10 | M | 79 | 56.4 | 6.60 | *x* | x |
| Con 11 | M | 75 | 64.5 | 6.18 | *x* | |
| Con 12 | F | 81 | 13.5 | 6.39 | *x* | x |
| Con 13 | M | 63 | 42.0 | 6.23 | *x* | |
| Con 14 | M | 57 | 78.5 | 6.03 | *x* | x |
| Con 15 | F | 78 | 23.3 | 6.07 | *x* | x |
| Con 16 | M | 71 | 38.5 | N/A | *x* | x |
| Mean±SEM | | 78.6±2.1 | 48.6±6.7 | 6.3±0.1 | | |
| | | | | | | |
| PSP 1 | M | 78 | 66.10 | 6.45 | *x* | *x* |
| PSP 2 | M | 72 | 27-39 | 6.19 | *x* | *x* |
| PSP 3 | F | 90 | 35.50 | 6.75 | *x* | |
| PSP 4 | F | 79 | 27.35 | 6.38 | *x* | *x* |
| PSP 5 | M | 76 | 46.55 | 6.46 | *x* | *x* |
| PSP 6 | M | 79 | 32.15 | 5.93 | *x* | *x* |
| PSP 7 | M | 67 | 28.30 | 6.5 | *x* | |
| PSP 8 | M | 73 | 48.00 | 6.23 | *x* | |
| PSP 9 | F | 81 | 10 | 5.88 | *x* | |
| PSP 10 | F | 80 | 66.10 | | *x* | *x* |
| PSP 11 | M | 70 | 14.40 | 5.96 | *x* | |
| PSP 12 | M | 62 | 50.40 | 6.62 | *x* | |
| PSP 13 | F | 75 | 74.30 | 6.06 | *x* | *x* |
| PSP14 | M | 79 | 44.00 | 6.21 | *x* | *x* |
| Mean±SEM | | 75.8±1.8 | 41.8±5.2 | 6.2±0.1 | | |

**Table 5.3: Demographic data of caudate tissue used to study DJ-1 expression.**

DJ-1 protein levels were compared in frontal cortex of 3 control cases (#1, 5 and 7), 3 AD cases (#11-13) and 3 FTLD-Pick's cases (#37-39) from Table 5.1. Levels of soluble DJ-1 protein in the caudate (striatum) of 8 PSP cases were compared against 8 controls. 14 PSP and 16 control cases were also used to compare DJ-1 gene expression in the same regions. Details of cases where caudate was extracted from are listed in table 5.3.

#### 5.3.2.2. Biochemical comparison of DJ-1 expression levels

Protein separation on a 12% Tris-glycine gel and chemilluminescent protein detection was used to measure soluble DJ-1 protein levels in control, AD and FTLD-Pick's frontal cortex. DJ-1 was detected using a monoclonal DJ-1 antibody and protein levels were normalised to β-actin. Sarkosyl insoluble DJ-1 protein levels, extracted from the same cases using the method described in the methods chapter and reproduced from Goedert et al., (1992) were also measured in a similar manner. Monoclonal AT-8 and monoclonal DJ-1 were used to detect insoluble tau and DJ-1 protein respectively. Fluorescent western blotting on the Li-cor Odyssey scanner was used to compare soluble DJ-1 protein levels in PSP and control caudate. Comparison of DJ-1 protein levels in AD, FTLD-Pick's with control cases was performed by my supervisor, Dr Bandopadhyay. Real-time PCR as described previously was performed to measure DJ-1 mRNA expression in 14 PSP and 16 control caudate (striatum) samples. Expression levels were normalised to both β-actin and B2M and compared using an unpaired student's T-test.

### 5.3.3. Results

Real-time PCR was used to study DJ-1 gene expression in PSP striatum (caudate) (Fig. 5.13C). Comparison with controls using an unpaired student's T-test showed no significant difference ($p = 0.262$). Similarly, western blotting of soluble proteins from the same region of 8 PSP and control cases showed no significant ($p = 0.667$) difference in DJ-1 protein expression between the two groups (Fig. 5.13A and B). On a smaller scale, no statistical change in soluble DJ-1 protein was noted in AD and FTLD-Pick's frontal cortex when compared with control homogenate (Fig. 5.13D and E).

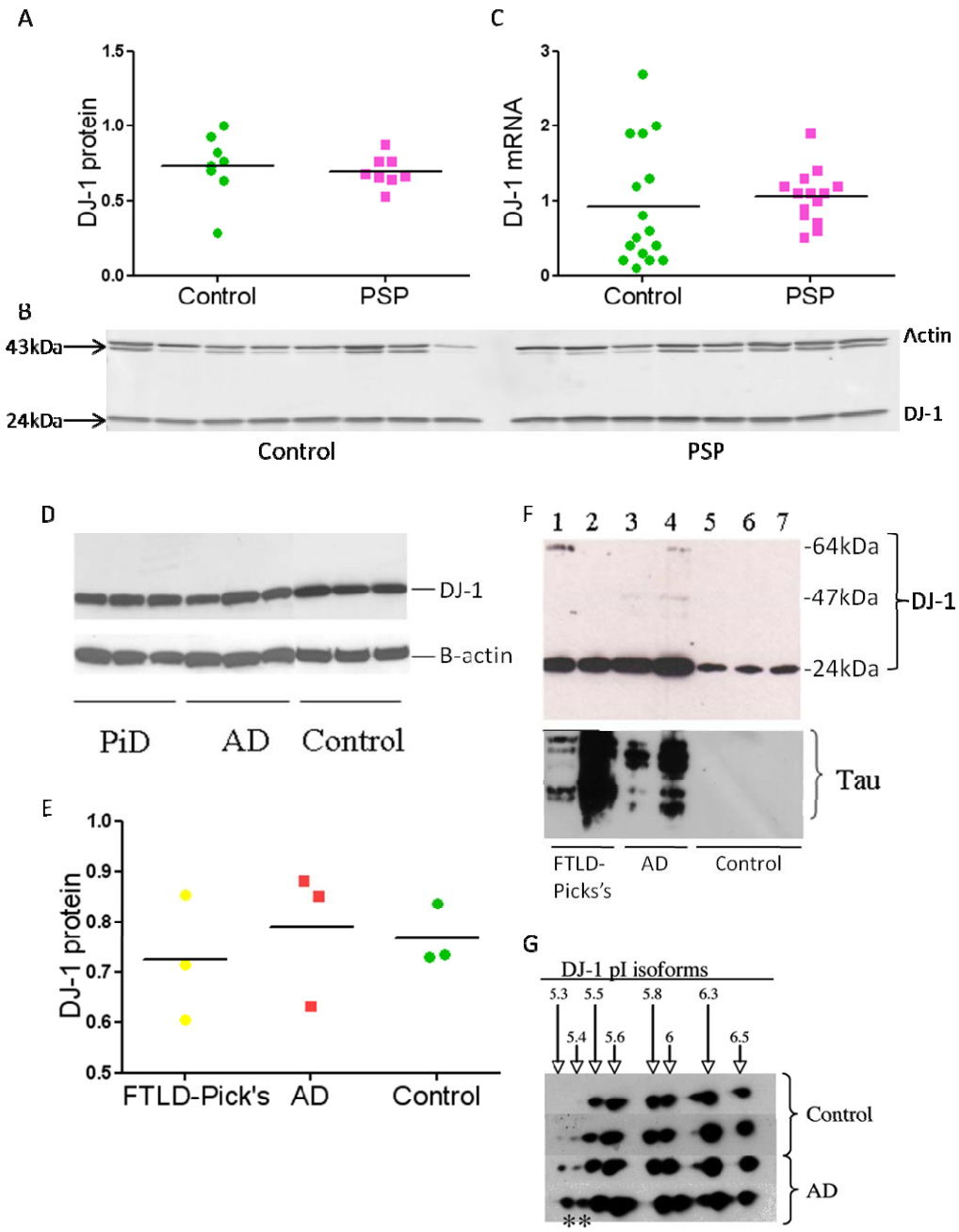


**Figure 5.13: Expression of DJ-1 in sporadic tauopathies.** A, B) Soluble DJ-1 protein levels in PSP and control striatum show no significant difference after normalisation to β-actin and comparison using unpaired student's T-test. C) Quantitative analysis of DJ-1 gene expression from PSP and control striatum. D) Soluble DJ-1 protein level in frontal cortex of three FTLD-Pick's cases, three AD cases and three control cases. E) Comparison of soluble DJ-1 protein levels normalised to β-actin of samples in D show no difference between the three groups. F) Insoluble DJ-1 and phosphorylated tau from sarkosyl-insoluble fractions of FTLD-Pick's (lanes 1 and 2), AD (lanes 3 and 4) and control (lanes 5-7) frontal cortices. Intersecting line on graphs represents mean of group. G) Frontal cortex DJ-1 pI isoform distribution from soluble fraction of 2 AD and 2 control cases. * highlight increased presence of acidic DJ-1.

Sarkosyl-insoluble homogenates were then formed from frontal cortex of two AD, two FTLD-Pick's cases and 3 control cases and separated on Tris-glycine gels. Immunoblotting with DJ-1 monoclonal antibody revealed the presence of small amounts of sarkosyl insoluble DJ-1 in control cases (Fig. 5.13F). Insoluble DJ-1 levels were elevated in both AD and FTLD-Pick's sarkosyl insoluble fractions which are enriched with tau PHF and tau SF respectively. Faint bands representing higher molecular weight isoforms of DJ-1 were also noted in the diseased homogenates but not control. Insoluble fractions were also probed with tau AT8 antibody and the typical tau bands were seen in both AD and FTLD-Pick's but not control tissue.

# 5.4. Discussion

In "lower" vertebrates such as rodents, both DJ-1 protein and mRNA expression can be seen in glial and neuronal cell types (Bader et al., 2005; Bandopadhyay et al., 2005; Kotaria et al., 2005). In contrast early reports on human control and IPD post-mortem brains reported DJ-1 to be predominantly expressed by astrocytes, with some neuronal presence noticed (Bandopadhyay et al., 2004). More recently, DJ-1 IR has been shown in striatal and dopaminergic neurons in human and primate brains (Olzmann et al., 2007) suggesting DJ-1 is expressed by and functions in both cell groups.

In PD, the disease DJ-1 mutations are associated with, staining of LBs is highly uncommon (Bandopadhyay et al., 2004; Rizzu et al., 2004). DJ-1 has however, been found within pathological tau inclusions of AD and FTLD cases (Rizzu et al., 2004). These latter findings have been confirmed by this study, which was extended to demonstrate DJ-1's involvement in a more comprehensive range of tauopathies.

The finding of this study show DJ-1 associates with the pathological features of PSP, CBM, FTLD-Pick's and FTLD with MAPT mutations, but displays a greater affiliation with the tau inclusion of AD. DJ-1 IR was seen in a variety of inclusions including NFTs, NTs, glial, PBs and extracellular amyloid plaques with the precise locations being dependent on the disease type. DCFM confirmed co-localisation of DJ-1 with hyperphosphorylated tau in these

structures. The inability to use formic acid pre-treatment with RD3 and RD4 antibodies prevented us from directly showing co-localisation of DJ-1 with 3R and 4R tau isoforms. Nevertheless its ability to associate with both tau groups can be surmised from the co-localisation demonstrated in FTLD-Pick's, a 3R tauopathy and the PSP cases which exclusively exhibit 4R tau pathology.

Studying DJ-1 IR in FTLD cases with MAPT mutations reveal various DJ-1 staining patterns that are of interest. Cases with R406W MAPT mutations displayed 3R and 4R staining of diffuse cytoplasmic deposits in nerve cells and well formed NFTs shown previously (de Silva et al., 2006) and confirmed by ourselves. In frontal cortex tissue from these cases, DJ-1 was found to positively stain a significant portion of NFTs and NTs. Tissue sourced from the individual with the N279K MAPT mutation, displayed no DJ-1 IR in NFTs. It was instead restricted to glial cell inclusions within the cortical white matter which are reminiscent of coiled bodies. Similarly, tissue from individuals harbouring MAPT exon 10+16 splice site mutations also displayed a moderate number of DJ-1 IR glial cell inclusions. Both N279K and exon10+16 mutations are exclusively 4R tauopathies as previously documented (de Silva et al., 2006) and their tau pathology may be characterised by presence of NFTs with glial inclusions in white matter.

Reasons for the association of DJ-1 with both 3R and 4R tau are not exactly clear. However observations within the department that DJ-1 antibody fails to recognise recombinant tau on immunoblots appears to rule out any non-specific 'sticking' of DJ-1 antibody to tau molecules. Instead, our collected data supports the notion of a chaperone role for DJ-1 towards both 3R and 4R tau. It was recognised early on that DJ-1 resembles the E. coli molecular chaperone HSP31 (Lee et al., 2003). Its chaperone activity was further investigated *in vitro* and *in vivo* using α-synuclein as the substrate (Shendelman et al., 2004; Zhou et al., 2006). Shendelman and colleagues specifically reported that the chaperone activity of DJ-1 is dependent on C53 oxidation. To date, no chaperone assay has been performed using tau as a substrate though it has been conjectured that DJ-1 may function to offset tau misfolding (Neumann et al., 2004). This would infer that DJ-1 should be found within all tau inclusions which we have seen is not the case for at least AD, FTLD, PSP and CBD. With this in mind we speculate that DJ-1 initially associates with tau as it undergoes β-

sheet formation, aiming to facilitate its unwinding it, but as the disease progresses DJ-1 becomes sequestered and trapped with tau inclusions. Co-transfection of DJ-1 and tau into COS-1 cells followed by immunoprecipitation showed no co-immunoprecipitation of the two, suggesting association between the two is dependent on the hyperphosphorylation state of tau (Macedo et al., 2003). Zhou et al., (2006) reported that over oxidation of DJ-1 perturbs its anti-aggregation properties against α-synuclein and we have found that there is a greater abundance of oxidised DJ-1 in AD frontal cortex compared to controls. This considered alongside our data showing DJ-1 can undergo irreversible oxidation in AD (Choi et al., 2006), may be a sign that DJ-1's chaperone activity towards tau diminishes with disease progression. The absence of DJ-1 from LBs casts a shadow over the idea that DJ-1 interacts with α-synuclein in human neurons. However, the two have been shown to co-localise in a subset of oligodendroglial inclusions in MSA cases (Neumann et al., 2004). Any chaperone activity exerted by DJ-1 may be specific towards certain substrates such as tau and α-synuclein as highlighted by its absence from ubiquitin inclusions present in FTLD-U cases.

In addition to a chaperone role, other reasons for DJ-1 to associate with tau inclusions include oxidative stress or age-related modifications in the structure and properties of DJ-1 (Bandopadhyay et al., 2004; Meulener et al., 2006). It has also been reported that DJ-1 is capable of down-regulating the tumour suppressor PTEN (Kim et al., 2005a) which exerts its activity by inhibiting PkB/Akt which mediates a number of intracellular signalling pathways and Akt can phosphorylate tau (Ksiezak-Reding et al., 2003). A number of other reports have linked PTEN/Akt pathway with AD pathology (Griffin et al., 2005; Pei et al., 2003) whilst inactivation of DJ-1 in Drosophila results in impaired PI3'K/Akt signalling (Yang et al., 2005). Thus DJ-1 could affect PTEN/Akt/tau phosphorylation pathways via direct or indirect means and so account for its detection in tau inclusions inside vulnerable cell populations in tauopathies like those studied here. Of note, DJ-1 is not the only FPD linked protein found to associate with hyperphosphorylated tau. LRRK2 (*PARK8*) has recently been found in NFTs and NTs of AD and other tauopathies (Miklossy et al., 2006). This could be indicative of a common neurodegenerative pathway shared by PD and tauopathies, for which DJ-1 and LRRK2 are part of.

*PARK7* mutations results in PD due to a loss of DJ-1 protein function. Thus it can be speculated that changes in protein expression may have detrimental effects in sporadic tauopathies. With the aid of western blotting techniques we showed that in the frontal cortex of AD, FTLD-Pick's and control subjects there was no changes in levels of soluble DJ-1 monomer. Due to the small number of cases (n=3) for each group these results are only preliminary. A larger comparison (n=8) was performed using PSP and control striatal tissue which also showed soluble DJ-1 levels to be consistent in the two groups. In line with this, no change in DJ-1 gene expression was detected meaning there are no pre or post-translational modifications to DJ-1 protein in PSP striatum. A previous study had reported that soluble DJ-1 levels are increased in the frontal cortex of AD patients (Choi et al., 2006) but we feel this difference may be down to experimental discrepancies including protein loading and antibody selection.

Analysis of sarkosyl-insoluble fractions from FTLD-Pick's, AD and control frontal cortex showed an enrichment of DJ-1 in the diseased fractions. Additionally, small quantities of HMW complexes of DJ-1 at 47 and 64kDa were detected in diseased factions. Traces of the 47kDa isoform were also seen in MSA cerebellum (Neumann et al., 2004). The nature of these DJ-1 species remains unknown, but it is possible that these refer to an insoluble form of DJ-1 dimer whilst the 64kDa isoform is an even higher order oligomer/aggregate. Probing of sarkosyl-insoluble homogenates with AT8 antibody revealed the presence of multiple tau bands in all samples except control, showing that the fractionation process was successful. Again, the use of 2 samples for each disease group means these findings are provisional. Nevertheless it can be seen that the amount of insoluble DJ-1 in FTLD-Pick's and AD groups are 3-4 times greater than for control tissue. DJ-1 may naturally become insoluble with aging, which may explain the small amounts seen in control subjects. The elevated levels in diseased tissue may arise from inactivation of DJ-1 due to oxidative damage, which causes it to aggregate and become insoluble. The presence of HMW isoforms in diseased tissue could support this. It has been noted that the mutant L166P DJ-1 protein also forms higher-order structures of a similar size (Macedo et al., 2003). Our 2DGE analysis of DJ-1 pI isoforms in AD frontal cortex show that DJ-1 is subject to a greater degree of oxidative stress than in control with the accumulation of acidic pI isoforms 5.3 and 5.4. Choi et al., (2006) showed a similar accumulation of DJ-1 pI isoform 5.5 in AD frontal cortex. It is also feasible that if DJ-1

is trapped within tau tangles it will be drawn into the sarkosyl-insoluble fraction by the hyperphosphorylated tau. The denaturing conditions present in western blotting protocols would subsequently free it for detection by immunoblotting.

## 5.5. Conclusions

In this chapter we confirmed earlier work by Rizzu and colleagues (2004) and Neumann et al., (2004) showing DJ-1 to co-localise with tau. We extended this to show co-localisation occurred with both 3R and 4R tau isoforms and that DJ-1 has a differential expression profile in pathological inclusions of various neurodegenerative disorders. It also proposes a role for DJ-1 in the pathogenesis of AD, FTLD-Pick's, FTLD-MAPT and to a lesser degree PSP and CBD with no involvement in FTLD-U.

# 6. Final Discussion

# 6.1. Discussion

Though rare, mutations in *PARK7* result in early-onset PD due to the severe and sometimes total loss of DJ-1 protein function. It is therefore likely that in sporadic PD cases the functional activity of DJ-1 may also be disrupted, albeit to a lesser degree, contributing to the development of the disorder. Under this rationale, the research presented in this thesis was undertaken with the intention of exploring altered DJ-1 functioning *in vivo*, for common forms of PD. By using post-mortem human brain tissue, a number of key findings were uncovered. First, in PD DJ-1 appears to undergo a transcriptionally regulated decrease in protein expression in areas associated with motor symptoms. Second, regions associated with non-motor symptoms like dementia display an increase in DJ-1 gene expression. These regions are associated with AD pathology and in light of this we found DJ-1 to co-localise with 3R and 4R tau. The third key finding is that DJ-1 is able to interact with multiple RNA species *in vivo*, the majority of which are of importance to the mitochondria. Based on these observations, we propose that under normal conditions DJ-1 is neuroprotective and that its defensive activity is largely directed towards mitochondrial well-being. In PD however, this protective activity becomes attenuated, resulting in mitochondrial dysfunction and eventually the onset of apoptosis.

DJ-1 belongs to the PfPI superfamily of proteins which encompasses antioxidants, proteases and chaperones. Based on homology comparisons, similar functions have been proposed for DJ-1. Evidence in the literature that has mainly arisen from *in vitro* studies indicates that DJ-1 primarily functions as an oxidative stress response protein. Crystallographic analysis of DJ-1 protein structure shows that mildly oxidising conditions induce the formation of a stable cysteine-sulfinic acid at C46, C53 and in particular, C106 (Wilson et al., 2003). A similar phenomenon occurs at methionine residues (Choi et al., 2006). This purported peroxiredoxin-like FR scavenging activity (Andres-Mateos et al., 2007) is what reportedly confers protection against neurotoxins *in vitro* and *in vivo*. Though no protease activity for DJ-1 has been found, a weak oxidation dependent chaperone activity towards α-synuclein has been reported (Shendelman et al., 2004; Zhou et al., 2006). These findings however are unlikely to fully explain the protective effects of DJ-1 as unlike other thiol containing antioxidants e.g. glutathione, DJ-1 is less abundantly expressed and additionally, the

scavenging activity of DJ-1 is a lot lower than other FR scavengers like catalase (Andres-Mateos et al., 2007).

Instead, the identification of transcripts encoding for selenoproteins that function as antioxidants suggest DJ-1 is a translational mediator of oxidative stress responses. By freeing transcripts like GPx4 etc upon oxidation by ROS (Fig. 6.1), DJ-1 would instigate a response that is more rapid and localised in nature than would be possible if mediated by transcription. Indeed, up-regulation of antioxidants and components of the PTEN/Akt pathway is in line with the observed effects of DJ-1 over-expression including elevated glutathione synthesis (Zhou and Freed, 2005) and inhibition of Bax and other proapoptotic proteins (Bretaud et al., 2007; Fan et al., 2008b). Given the viability of DJ-1 KO mice, these cellular functions of DJ-1 do not appear vital for cellular functioning. Rather the early-onset of PD in carriers of *PARK7* mutations and the increased vulnerability of models to neurotoxins suggests that cells simply have a lower threshold for acceptable oxidative injury. With the time taken for transcription of mRNA strands, it is logical that some other mechanism be in place to enable quick and localised responses to changes in the microenvironment. It is this function that DJ-1 appears to hold, acting as a reservoir of transcripts essential for cell survival and homeostasis.

It is less clear how DJ-1 interactions with mitochondrial transcripts for subunits of complex 1 contribute to PD pathogenesis. Mitochondria are a key source of ROS and numerous subunits of complex 1 become oxidatively damaged during the production of the mitochondrial membrane potential that is essential for the formation of ATP (Keeney et al., 2006). Under oxidative stress conditions, logic dictates that mitochondrial activity would be abated to minimise any further production of ROS. In this scenario, oxidised DJ-1 may actually bind to transcripts for complex 1 subunits, preventing their translation. Once oxidative stress levels become more acceptable, DJ-1 would be reduced to its normal state thereby releasing mitochondrial transcripts which are then utilised to replace any damaged subunits, enabling mitochondrial activity to return to normal.

However, this strategy may lead to ATP shortfalls and the presence of damaged subunits may increase electron leakage which would further fuel the production of FR. Additionally

there would be a decrease in ATP production which would make cells vulnerable to the weak excitotoxic effects of glutamate. ATP depletion would also impair UPS functioning causing an accumulation of oxidised proteins that would promote further ROS generation and may ultimately induce LB formation (Fig. 6.2). Dopamine release and re-uptake may also be compromised by energy reductions and may result in dopamine toxicity. Reductions in the mitochondrial membrane potential would also diminish the mitochondria's capacity for $Ca^{2+}$, leading to cytosolic $Ca^{2+}$ overload. Thus, replacement of damaged subunits in times of oxidative stress would provide energy for other oxidative stress responses and normal cellular activities.

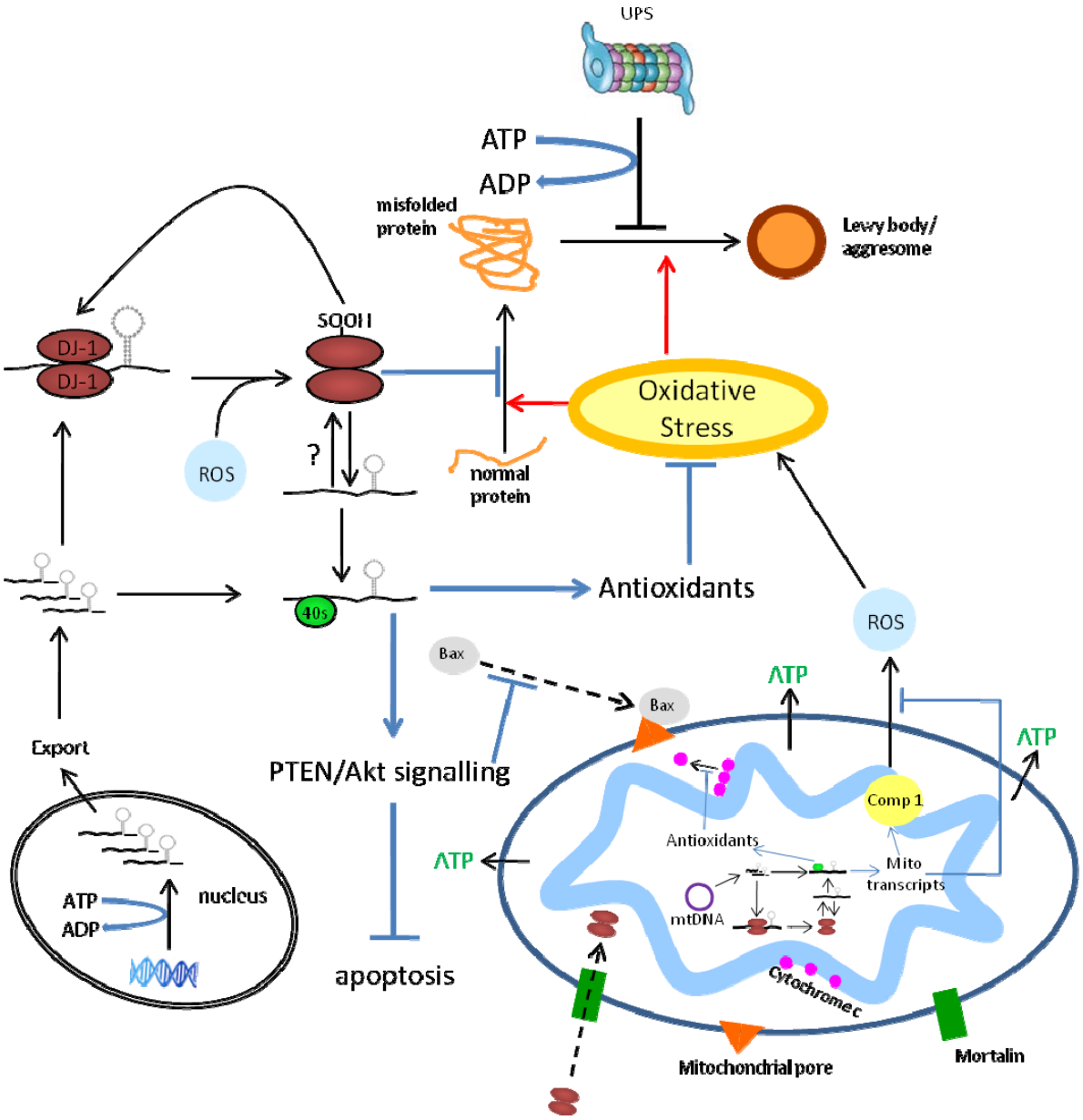

**Figure 6.1: Neuroprotective actions of DJ-1.** Mitochondria are the powerhouse of the cells and during the production of ATP, ROS are generated as a harmful waste product. If not properly disposed of, ROS can damage components of the ETC and inhibit further energy production. In mammals, a small amount of DJ-1 is resident within the mitochondria where they act as oxidative stress sensors. If oxidative conditions reach a certain threshold, DJ-1 acts in 3 ways to return conditions back to basal levels. Firstly, DJ-1 acts as a free radical scavenger by undergoing oxidation at multiple cysteine and methionine residues. This then induces its most effective neuroprotective actions. In its reduced state, DJ-1 represses the translation of protein by binding to a proportion of RNA transcripts. These are released following oxidation of C106, and immediately induce an up-regulation of antioxidants which work rapidly to reduce ROS levels within the mitochondria. One such antioxidant, GPx4, also prevents the dissociation of cytochrome c from the inner mitochondrial membrane. Other transcripts that are released by mitochondrial DJ-1 include those encoding for subunits of complex 1 (comp 1). This ensures energy production is not compromised by replacing any oxidatively damaged subunits. FR's that manage to escape into the cytosol would initiate a similar response for cytosolic DJ-1. In addition to raising cytoplasmic levels of antioxidants, oxidised DJ-1 also releases transcripts involved in PTEN/Akt signalling resulting in an up-regulation of anti-apoptotic proteins. In particular this inhibits the opening of mitochondrial pores by BAX, preventing the escaped of free dissociated cytochrome c. It is also possible that in its oxidised state, DJ-1 may bind to other groups of transcripts eg those that are pro-apoptotic in nature. Furthermore, oxidation of cytosolic DJ-1 initiates a translocation into the mitochondria, possibly through mortalin, to tackle ROS production at the source. The last protective mode of action for DJ-1 is as a chaperone. Following oxidation when oxidised, DJ-1 may possess some chaperone activity and assist it the unfolding of misfolded proteins which may include α-synuclein and tau. Once oxidative stress conditions have subsided, DJ-1 is reduced through unknown means.

Mitochondria are able to instigate apoptosis through activation of caspases and are therefore mediators of cell survival. The identification of transcripts for complex 1 subunits, GPx4 and PTEN/Akt components like BAD suggests a role for DJ-1 in minimising ROS activity and cytochrome c release. In healthy controls these would work in tandem to prevent mitochondrial dysfunction and fragmentation. Our unsuccessful attempts to isolate DJ-1 bound transcripts in PD frontal cortex could be due to the observed reduction and increased oxidation of DJ-1 which together suggests that DJ-1 function have been compromised. PD is an ongoing progressive disorder and the tissue used by us displayed neocortical pathology

highlighting a prolonged disease duration. We have suggested that DJ-1 acts as a rapid response protein towards oxidative stress. If this is true then it is likely that DJ-1 is unsuitable to combat sustained assault by ROS and oxidative stress and is intentionally down-regulated once it has served its purpose, thereby allowing long-term strategies to be implemented.

Such strategies could involve other PD proteins. DJ-1 has been shown to negatively regulated PTEN (Kim et al., 2005a) which in turn induces Pink1 expression (Unoki and Nakamura, 2001). Pink1 reportedly confers protection against rotenone and MPTP toxicity *in vitro* (Deng et al., 2005) and has both a mitochondrial and cytoplasmic localisation like DJ-1 (Gandhi et al., 2006; Weihofen et al., 2008). Pink1 also specifically phosphorylates the mitochondrial chaperone protein TRAP1 to protect against oxidative stress induced apoptosis (Pridgeon et al., 2007). Pink1 may additionally interact with HSP90 and HtrA2 (Plun-Favreau and Hardy, 2008), both of which also display chaperone activity. Interestingly a single heterozygous mutation in the *DJ-1* and *PINK1* gene has been described in a Chinese family, suggesting a possible digenic mode of inheritance and further supporting some form of functional interaction between the two proteins (Tang et al., 2006). Pink1 has also been shown to have a genetic association with parkin (Clark et al., 2006; Park et al., 2006), with KO of either in drosophila producing similar defects. Further investigation showed over-expression of parkin could rescue Pink1 phenotype in *PINK1* deficient flies (Yang et al., 2006). However, the opposite was not true suggesting that the two share a common pathway with Pink1 upstream of parkin. DJ-1 is unable to rescue either phenotype (Dodson and Guo, 2007; Exner et al., 2007) indicating that DJ-1 may act upstream of both Pink1 and parkin. Overexpression of parkin increases mtDNA transcription and replication whilst parkin null mice reportedly have lower levels of complex 1 subunits. Similarly, *PINK1* silencing also results in decreased levels of mtDNA and mtDNA synthesis (Gegg et al., 2009). Thus DJ-1 may indirectly regulate the activity of two other PD proteins, Pinl1 and parkin and that in the latter stages of PD, DJ-1's protective activity is sacrificed in order to promote the combined protective effects of Pink1, parkin and other pro-survival proteins.

It could also be hypothesised that the down regulation of DJ-1 we observed in some PD regions could occur in order to prime cells for apoptosis. Reduced levels of DJ-1 may result

in an up-regulation of members of proapoptotic pathways and would also favour the release of cytochrome c into the cytoplasm where it would activate caspases (Fig. 6.2). DJ-1 KO in zebrafish results in up-regulation of Bax and p53 transcriptional activity which promote apoptosis via the opening of pores on the outer mitochondria membrane (Bretaud et al., 2007). By promoting apoptosis, cell death via necrosis would be minimised and enable salvaging of cellular components whilst simultaneously preventing cytoplasmic contamination of the extracellular space and inflammatory responses that would be harmful to neighbouring cells. In support of this hypothesis, cancerous tissue where apoptotic mechanisms have been switched off often display elevated levels of DJ-1 (Le Naour et al., 2001; Liu et al., 2008b; MacKeigan et al., 2003) and indeed the original description of DJ-1 was as an oncogene that enhanced transformation of cells (Nagakubo et al., 1997).

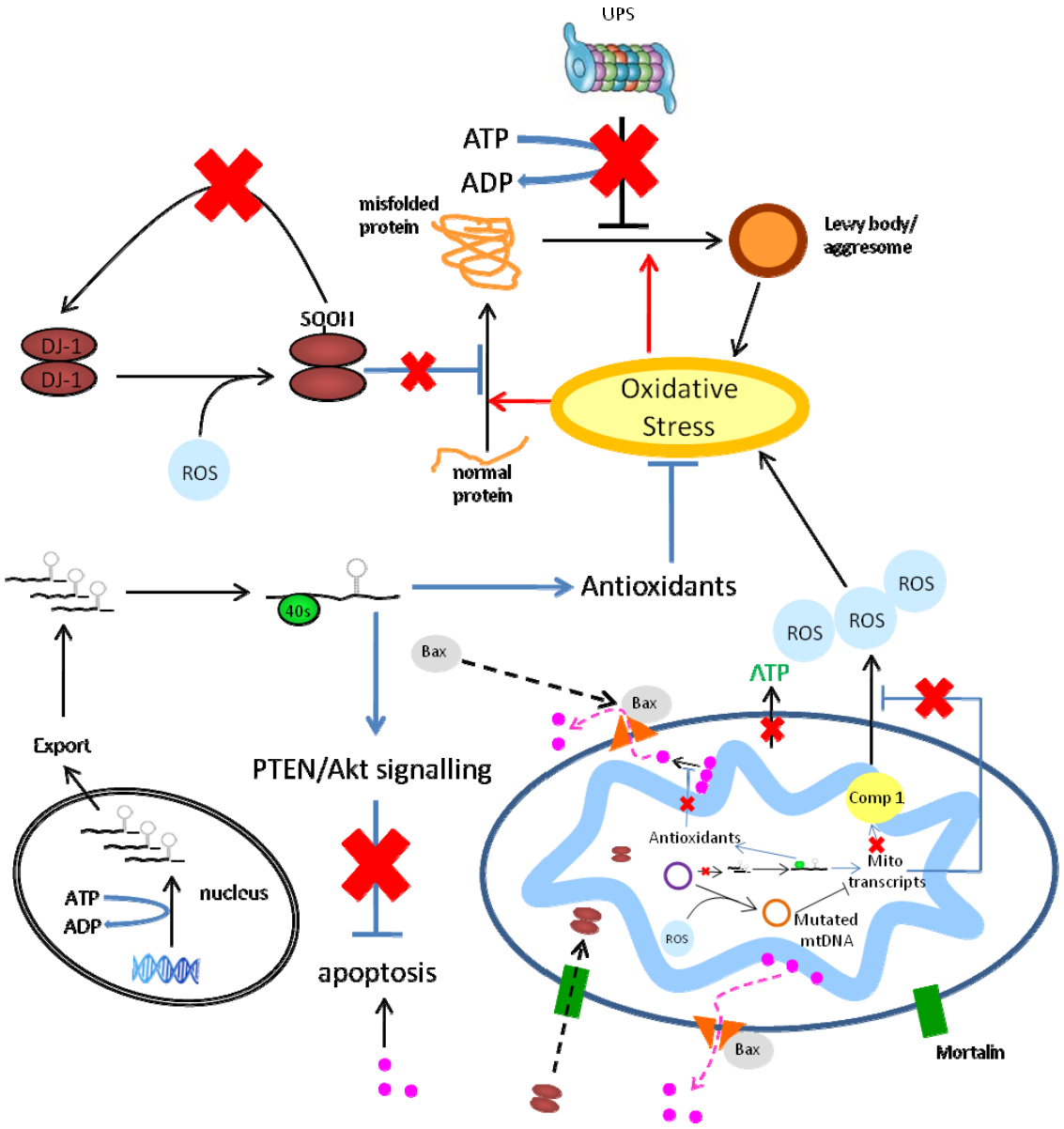

**Figure 6.2: Compromised DJ-1 functioning in PD.** In a number of PD brain regions, DJ-1 levels are significantly lower than in controls and the relatively small amount that is present is often in an oxidised state due to the constant elevated oxidative stress conditions. Thus in PD tissue, the neuroprotective actions of DJ-1 are minimal. As DJ-1 is already oxidised, it is unable to act as an antioxidant. Additionally, if DJ-1 is constantly oxidised, it would be unable to induce translation of antioxidants, anti-apoptotic proteins and component of the ETC. Instead, responses to elevated oxidative stress would be transcriptionally mediated by both the nuclear and mitochondrial genome. Within the mitochondria, this would mean an increase in the time taken to replace damaged subunits of the ETC which would result in greater FR production. With no DJ-1 induced rapid up-regulation of antioxidants, the extra FR would play havoc within the mitochondria resulting in cytochrome c dissociation and further damage to ETC machinery. The increased presence of ROS within the mitochondria may also produce mutation in the mtDNA. In the cytosol, increased ROS levels would cause greater protein damage, of which DJ-1 itself may be a victim of. Though in an oxidised state, the chaperone activity of DJ-1 may also be compromised to degree, which would place more burden on the UPS system. Unfortunately, reduced energy production by the mitochondria may result in proteasome dysfunction and favour the formation of LB like inclusion bodies. Accumulation of aggresomes would further exacerbate cellular stress condition and possibly overload cell-survival mechanisms. Reduced ATP levels may also impair the energy dependent process of transcription. Finally BAX induced opening of mitochondrial pores would allow cytochrome c to enter the cytosol and initiate apoptosis. X indicates processes that are likely to be compromised in PD.

DJ-1 protein expression is not completely abolished in PD tissue, suggesting it still exerts some functional effect. It is possible that this is based on its potential capacity to act as a chaperone. We found DJ-1 to co-localise with tau in a number of pathological inclusions in various tauopathies. This may explain our observed up-regulation of DJ-1 mRNA in PD regions that reportedly have a high density of LBs and AD pathology (Lashley et al., 2008). It is also hypothesized that NFTs confers some form of protection against ROS, with oxidative stress levels found to be inversely correlated to levels of Aβ pathology and NFT numbers (Eggers, 2009). If this assumption is true, it may augment the protective effects of DJ-1 and help extend its “shelf-life”, thereby providing an alternative explanation as to why decreased DJ-1 levels were not seen in transentorhinal regions of PD brains nor in either the caudate or frontal cortex of tauopathies. The stable state of DJ-1 in tauopathies may also highlight the different processes involved in PD and tau based disorders. Though

mitochondrial dysfunction has been reported in AD, it is thought to be only a casual contributor to pathology which is in stark contrast to its principle role in PD.

The data presented here provides evidence for a loss of DJ-1 activity in the development of IPD cases. Down-regulation in certain regions of PD brain further implicates a vicious cycle of mitochondrial dysfunction and oxidative stress as the primary instigators of PD pathogenesis. DJ-1's proclivity to interact with RNA provides a simple biochemical mechanism that helps explain its involvement in multiple cellular activities. Moreover, it delineates a role for DJ-1 as a "first at the scene" response protein that works quickly to bring oxidative stress conditions under control without compromising cellular energy production. Oxidative stress and mitochondrial dysfunction is a common theme in a range of neurodegenerative disorders including PD, AD, ALS and HD. Thus further defining interactions between DJ-1 and RNA, particularly those associated with the mitochondria may not only unravel a common pathway for neurodegeneration, but also provide invaluable insight into therapeutic approaches for the protection of neurons.

## 6.2. Future work

The data presented in this thesis raises a number of interesting points that would be suitable for further investigation. Dependent on tissue availability, it would be worthwhile analysing DJ-1 protein levels in amygdala and entorhinal cortex to determine whether protein expression mirrors DJ-1 mRNA and shows an up-regulation in PD. Given that these two regions display AD pathology and that we have shown DJ-1 to co-localise with both 3R and 4R tau, a chaperone assay directed towards tau may provide a functional explanation for the observed increase in DJ-1 mRNA. Another approach that may explain the bidirectional changes in DJ-1 gene expression would be to analyse the expression of the alternatively spliced exon $1^a$ and $1^b$ in multiple control and diseased brains.

We used real-time PCR to detect differences in gene expression. *In situ* hybridisation could be employed to help determine whether changes in expression are uniform or restricted to

particular cell groups. In a similar manner, immunohistochemistry on flash frozen sections may identify population specific changes in DJ-1 protein expression. A recent paper reported that neuronal staining is more prominent in tissue that has been fixed for shorter periods of time (Baulac et al., 2009), by using flash frozen tissue this issue can be alleviated.

Our data regarding binding of RNA transcripts with DJ-1 *in vivo* provided another avenue for future research. The techniques we used to co-IP RNA were unsuccessful in PD tissue. An alternative method that might have more success is the cross-linking and IP (CLIP) method (Ule et al., 2003). Here brain tissue is irradiated with UV light in order to induce the formation of covalent bonds between proteins and their associated RNA transcripts. This would help increase the amount of RNA collected and minimise any none specific pull-down. It may also be possible to utilise RNA amplification kits like MessageAmp™ II aRNA Amplification Kit from Ambion to increase RNA levels prior to cDNA synthesis and real-time PCR. If sufficient RNA was isolated, it may also be possible to examine transcripts on an array chip which would allow cellular pathways to be identified. RNA-IPs should also be performed in astrocytic cell lines and compared to transcripts isolated in neuronal cell lines. Data suggests that DJ-1 KO in astrocytes is detrimental to neuronal well-being and comparing transcripts from both cell groups may shed some light on this.

Lastly we have speculated that DJ-1 forms a first line of defence against oxidative stress and other changes to the microenvironment and that once its beneficial effects have been exhausted, it is down-regulated to boost Pink1 and parkin function. Comparison of protein and gene expression of these two PD associated proteins between IPD and normal control brains may support this theory. Examination of whether either parkin or Pink1 could rescue the phenotype of DJ-1 KO models would further support this theory and moreover may uncover a single mechanism that explains the pathogenesis of recessive parkinsonisms.

# 7. References

Abbott A. Neuroscience: while you were sleeping. Nature 2005; 437: 1220-2.
Abou-Sleiman PM, Healy DG, Quinn N, Lees AJ, Wood NW. The role of pathogenic DJ-1 mutations in Parkinson's disease. Ann Neurol 2003; 54: 283-6.
Abou-Sleiman PM, Muqit MM, McDonald NQ, Yang YX, Gandhi S, Healy DG, et al. A heterozygous effect for PINK1 mutations in Parkinson's disease? Ann Neurol 2006a; 60: 414-9.
Abou-Sleiman PM, Muqit MM, Wood NW. Expanding insights of mitochondrial dysfunction in Parkinson's disease. Nat Rev Neurosci 2006b; 7: 207-19.
Abraha A, Ghoshal N, Gamblin TC, Cryns V, Berry RW, Kuret J, et al. C-terminal inhibition of tau assembly in vitro and in Alzheimer's disease. J Cell Sci 2000; 113 Pt 21: 3737-45.
Allam MF, Campbell MJ, Hofman A, Del Castillo AS, Fernandez-Crehuet Navajas R. Smoking and Parkinson's disease: systematic review of prospective studies. Mov Disord 2004; 19: 614-21.
Andreadis A, Brown WM, Kosik KS. Structure and novel exons of the human tau gene. Biochemistry 1992; 31: 10626-33.
Andres-Mateos E, Perier C, Zhang L, Blanchard-Fillion B, Greco TM, Thomas B, et al. DJ-1 gene deletion reveals that DJ-1 is an atypical peroxiredoxin-like peroxidase. Proc Natl Acad Sci U S A 2007; 104: 14807-12.
Annesi G, Savettieri G, Pugliese P, D'Amelio M, Tarantino P, Ragonese P, et al. DJ-1 mutations and parkinsonism-dementia-amyotrophic lateral sclerosis complex. Ann Neurol 2005; 58: 803-7.
Antonicka H, Ogilvie I, Taivassalo T, Anitori RP, Haller RG, Vissing J, et al. Identification and characterization of a common set of complex I assembly intermediates in mitochondria from patients with complex I deficiency. J Biol Chem 2003; 278: 43081-8.
Arai T, Hasegawa M, Akiyama H, Ikeda K, Nonaka T, Mori H, et al. TDP-43 is a component of ubiquitin-positive tau-negative inclusions in frontotemporal lobar degeneration and amyotrophic lateral sclerosis. Biochem Biophys Res Commun 2006; 351: 602-11.
Attems J, Jellinger KA. The dorsal motor nucleus of the vagus is not an obligatory trigger site of Parkinson's disease. Neuropathol Appl Neurobiol 2008; 34: 466-7.
Bader V, Ran Zhu X, Lubbert H, Stichel CC. Expression of DJ-1 in the adult mouse CNS. Brain Res 2005; 1041: 102-11.
Bandopadhyay R, Kingsbury AE, Cookson MR, Reid AR, Evans IM, Hope AD, et al. The expression of DJ-1 (PARK7) in normal human CNS and idiopathic Parkinson's disease. Brain 2004; 127: 420-30.
Bandopadhyay R, Miller DW, Kingsbury AE, Jowett TP, Kaleem MM, Pittman AM, et al. Development, characterisation and epitope mapping of novel monoclonal antibodies for DJ-1 (PARK7) protein. Neurosci Lett 2005; 383: 225-30.
Bandyopadhyay S, Cookson MR. Evolutionary and functional relationships within the DJ1 superfamily. BMC Evol Biol 2004; 4: 6.
Baron JA. Cigarette smoking and Parkinson's disease. Neurology 1986; 36: 1490-6.
Baulac S, Lu H, Strahle J, Yang T, Goldberg MS, Shen J, et al. Increased DJ-1 expression under oxidative stress and in Alzheimer's disease brains. Mol Neurodegener 2009; 4: 12.
Ben-Shachar D, Zuk R, Gazawi H, Ljubuncic P. Dopamine toxicity involves mitochondrial complex I inhibition: implications to dopamine-related neuropsychiatric disorders. Biochem Pharmacol 2004; 67: 1965-74.

Bender A, Krishnan KJ, Morris CM, Taylor GA, Reeve AK, Perry RH, et al. High levels of mitochondrial DNA deletions in substantia nigra neurons in aging and Parkinson disease. Nat Genet 2006; 38: 515-7.

Berendse HW, Booij J, Francot CM, Bergmans PL, Hijman R, Stoof JC, et al. Subclinical dopaminergic dysfunction in asymptomatic Parkinson's disease patients' relatives with a decreased sense of smell. Ann Neurol 2001; 50: 34-41.

Bertler A, Rosengren E. Occurrence and distribution of catechol amines in brain. Acta Physiol Scand 1959; 47: 350-61.

Bertoli-Avella AM, Oostra BA, Heutink P. Chasing genes in Alzheimer's and Parkinson's disease. Hum Genet 2004; 114: 413-38.

Betarbet R, Sherer TB, Greenamyre JT. Animal models of Parkinson's disease. Bioessays 2002; 24: 308-18.

Betarbet R, Sherer TB, MacKenzie G, Garcia-Osuna M, Panov AV, Greenamyre JT. Chronic systemic pesticide exposure reproduces features of Parkinson's disease. Nat Neurosci 2000; 3: 1301-6.

Beyer K, Domingo-Sabat M, Humbert J, Carrato C, Ferrer I, Ariza A. Differential expression of alpha-synuclein, parkin, and synphilin-1 isoforms in Lewy body disease. Neurogenetics 2008; 9: 163-72.

Blackinton J, Ahmad R, Miller DW, van der Brug MP, Canet-Aviles RM, Hague SM, et al. Effects of DJ-1 mutations and polymorphisms on protein stability and subcellular localization. Brain Res Mol Brain Res 2005; 134: 76-83.

Blackinton J, Kumaran R, van der Brug MP, Ahmad R, Olson L, Galter D, et al. Post-transcriptional regulation of mRNA associated with DJ-1 in sporadic Parkinson disease. Neurosci Lett 2009; 452: 8-11.

Bonifati V. Genetics of parkinsonism. Parkinsonism Relat Disord 2007; 13 Suppl 3: S233-41.

Bonifati V, Oostra BA, Heutink P. Linking DJ-1 to neurodegeneration offers novel insights for understanding the pathogenesis of Parkinson's disease. J Mol Med 2004; 82: 163-74.

Bonifati V, Rizzu P, Squitieri F, Krieger E, Vanacore N, van Swieten JC, et al. DJ-1( PARK7), a novel gene for autosomal recessive, early onset parkinsonism. Neurol Sci 2003a; 24: 159-60.

Bonifati V, Rizzu P, van Baren MJ, Schaap O, Breedveld GJ, Krieger E, et al. Mutations in the DJ-1 gene associated with autosomal recessive early-onset parkinsonism. Science 2003b; 299: 256-9.

Bonifati V, Rohe CF, Breedveld GJ, Fabrizio E, De Mari M, Tassorelli C, et al. Early-onset parkinsonism associated with PINK1 mutations: frequency, genotypes, and phenotypes. Neurology 2005; 65: 87-95.

Bossers K, Meerhoff G, Balesar R, van Dongen JW, Kruse CG, Swaab DF, et al. Analysis of gene expression in Parkinson's disease: possible involvement of neurotrophic support and axon guidance in dopaminergic cell death. Brain Pathol 2009; 19: 91-107.

Braak H, Del Tredici K. Neuroanatomy and pathology of sporadic Parkinson's disease. New York: Springer, 2009.

Braak H, Del Tredici K, Bratzke H, Hamm-Clement J, Sandmann-Keil D, Rub U. Staging of the intracerebral inclusion body pathology associated with idiopathic Parkinson's disease (preclinical and clinical stages). J Neurol 2002; 249 Suppl 3: III/1-5.

Braak H, Del Tredici K, Rub U, de Vos RA, Jansen Steur EN, Braak E. Staging of brain pathology related to sporadic Parkinson's disease. Neurobiol Aging 2003; 24: 197-211.

Braak H, Ghebremedhin E, Rub U, Bratzke H, Del Tredici K. Stages in the development of Parkinson's disease-related pathology. Cell Tissue Res 2004; 318: 121-34.

Bretaud S, Allen C, Ingham PW, Bandmann O. p53-dependent neuronal cell death in a DJ-1-deficient zebrafish model of Parkinson's disease. J Neurochem 2007; 100: 1626-35.

Brigelius-Flohe R. Glutathione peroxidases and redox-regulated transcription factors. Biol Chem 2006; 387: 1329-35.

Brooks AI, Chadwick CA, Gelbard HA, Cory-Slechta DA, Federoff HJ. Paraquat elicited neurobehavioral syndrome caused by dopaminergic neuron loss. Brain Res 1999; 823: 1-10.

Brown RC, Lockwood AH, Sonawane BR. Neurodegenerative diseases: an overview of environmental risk factors. Environ Health Perspect 2005; 113: 1250-6.

Brown V, Jin P, Ceman S, Darnell JC, O'Donnell WT, Tenenbaum SA, et al. Microarray identification of FMRP-associated brain mRNAs and altered mRNA translational profiles in fragile X syndrome. Cell 2001; 107: 477-87.

Buee L, Bussiere T, Buee-Scherrer V, Delacourte A, Hof PR. Tau protein isoforms, phosphorylation and role in neurodegenerative disorders. Brain Res Brain Res Rev 2000; 33: 95-130.

Buee L, Delacourte A. Comparative biochemistry of tau in progressive supranuclear palsy, corticobasal degeneration, FTDP-17 and Pick's disease. Brain Pathol 1999; 9: 681-93.

Burns RS, Chiueh CC, Markey SP, Ebert MH, Jacobowitz DM, Kopin IJ. A primate model of parkinsonism: selective destruction of dopaminergic neurons in the pars compacta of the substantia nigra by N-methyl-4-phenyl-1,2,3,6-tetrahydropyridine. Proc Natl Acad Sci U S A 1983; 80: 4546-50.

Canet-Aviles RM, Wilson MA, Miller DW, Ahmad R, McLendon C, Bandyopadhyay S, et al. The Parkinson's disease protein DJ-1 is neuroprotective due to cysteine-sulfinic acid-driven mitochondrial localization. Proc Natl Acad Sci U S A 2004; 101: 9103-8.

Carlsson A, Lindqvist M, Magnusson T, Waldeck B. On the presence of 3-hydroxytyramine in brain. Science 1958; 127: 471.

Cha SS, Jung HI, Jeon H, An YJ, Kim IK, Yun S, et al. Crystal structure of filamentous aggregates of human DJ-1 formed in an inorganic phosphate-dependent manner. J Biol Chem 2008; 283: 34069-75.

Chao DT, Korsmeyer SJ. BCL-2 family: regulators of cell death. Annu Rev Immunol 1998; 16: 395-419.

Chartier-Harlin MC, Kachergus J, Roumier C, Mouroux V, Douay X, Lincoln S, et al. Alpha-synuclein locus duplication as a cause of familial Parkinson's disease. Lancet 2004; 364: 1167-9.

Chaudhuri KR, Y. N. Early Parkinson's disease and non-motor issues. J Neuol 2008; 255: 33-8.

Chen H, Jacobs E, Schwarzschild MA, McCullough ML, Calle EE, Thun MJ, et al. Nonsteroidal antiinflammatory drug use and the risk for Parkinson's disease. Ann Neurol 2005a; 58: 963-7.

Chen J, Berry MJ. Selenium and selenoproteins in the brain and brain diseases. J Neurochem 2003; 86: 1-12.

Chen L, Cagniard B, Mathews T, Jones S, Koh HC, Ding Y, et al. Age-dependent motor deficits and dopaminergic dysfunction in DJ-1 null mice. J Biol Chem 2005b; 280: 21418-26.

Chen PS, Peng GS, Li G, Yang S, Wu X, Wang CC, et al. Valproate protects dopaminergic neurons in midbrain neuron/glia cultures by stimulating the release of neurotrophic factors from astrocytes. Mol Psychiatry 2006; 11: 1116-25.

Choi J, Sullards MC, Olzmann JA, Rees HD, Weintraub ST, Bostwick DE, et al. Oxidative damage of DJ-1 is linked to sporadic Parkinson and Alzheimer diseases. J Biol Chem 2006; 281: 10816-24.

Choi W, Zibaee S, Jakes R, Serpell LC, Davletov B, Crowther RA, et al. Mutation E46K increases phospholipid binding and assembly into filaments of human alpha-synuclein. FEBS Lett 2004; 576: 363-8.

Chung KK, Zhang Y, Lim KL, Tanaka Y, Huang H, Gao J, et al. Parkin ubiquitinates the alpha-synuclein-interacting protein, synphilin-1: implications for Lewy-body formation in Parkinson disease. Nat Med 2001; 7: 1144-50.

Clark IE, Dodson MW, Jiang C, Cao JH, Huh JR, Seol JH, et al. Drosophila pink1 is required for mitochondrial function and interacts genetically with parkin. Nature 2006; 441: 1162-6.

Clark LN, Afridi S, Mejia-Santana H, Harris J, Louis ED, Cote LJ, et al. Analysis of an early-onset Parkinson's disease cohort for DJ-1 mutations. Mov Disord 2004; 19: 796-800.

Clayton DF, George JM. The synucleins: a family of proteins involved in synaptic function, plasticity, neurodegeneration and disease. Trends Neurosci 1998; 21: 249-54.

Clements CM, McNally RS, Conti BJ, Mak TW, Ting JP. DJ-1, a cancer- and Parkinson's disease-associated protein, stabilizes the antioxidant transcriptional master regulator Nrf2. Proc Natl Acad Sci U S A 2006; 103: 15091-6.

Cookson MR. The biochemistry of Parkinson's disease. Annu Rev Biochem 2005; 74: 29-52.

Coulson DT, Brockbank S, Quinn JG, Murphy S, Ravid R, Irvine GB, et al. Identification of valid reference genes for the normalization of RT qPCR gene expression data in human brain tissue. BMC Mol Biol 2008; 9: 46.

Croisier E, Moran LB, Dexter DT, Pearce RK, Graeber MB. Microglial inflammation in the parkinsonian substantia nigra: relationship to alpha-synuclein deposition. J Neuroinflammation 2005; 2: 14.

da Costa CA. DJ-1: a newcomer in Parkinson's disease pathology. Curr Mol Med 2007; 7: 650-7.

Dauer W, Przedborski S. Parkinson's disease: mechanisms and models. Neuron 2003; 39: 889-909.

de Lau LM, Breteler MM. Epidemiology of Parkinson's disease. Lancet Neurol 2006; 5: 525-35.

de Rijk MC, Launer LJ, Berger K, Breteler MM, Dartigues JF, Baldereschi M, et al. Prevalence of Parkinson's disease in Europe: A collaborative study of population-based cohorts. Neurologic Diseases in the Elderly Research Group. Neurology 2000; 54: S21-3.

de Silva R, Lashley T, Strand C, Shiarli AM, Shi J, Tian J, et al. An immunohistochemical study of cases of sporadic and inherited frontotemporal lobar degeneration using 3R- and 4R-specific tau monoclonal antibodies. Acta Neuropathol 2006; 111: 329-40.

Deng H, Jankovic J, Guo Y, Xie W, Le W. Small interfering RNA targeting the PINK1 induces apoptosis in dopaminergic cells SH-SY5Y. Biochem Biophys Res Commun 2005; 337: 1133-8.

Deocaris CC, Kaul SC, Wadhwa R. On the brotherhood of the mitochondrial chaperones mortalin and heat shock protein 60. Cell Stress Chaperones 2006; 11: 116-28.

Devi L, Raghavendran V, Prabhu BM, Avadhani NG, Anandatheerthavarada HK. Mitochondrial import and accumulation of alpha-synuclein impair complex I in human dopaminergic neuronal cultures and Parkinson disease brain. J Biol Chem 2008; 283: 9089-100.

Di Fonzo A, Rohe CF, Ferreira J, Chien HF, Vacca L, Stocchi F, et al. A frequent LRRK2 gene mutation associated with autosomal dominant Parkinson's disease. Lancet 2005; 365: 412-5.

Dodson MW, Guo M. Pink1, Parkin, DJ-1 and mitochondrial dysfunction in Parkinson's disease. Curr Opin Neurobiol 2007; 17: 331-7.

Eerola J, Hernandez D, Launes J, Hellstrom O, Hague S, Gulick C, et al. Assessment of a DJ-1 (PARK7) polymorphism in Finnish PD. Neurology 2003; 61: 1000-2.

Eggers AE. Why do Alzheimer's disease and Parkinson's disease target the same neurons? Med Hypotheses 2009; 72: 698-700.

Ehringer H, Hornykiewicz O. [Distribution of noradrenaline and dopamine (3-hydroxytyramine) in the human brain and their behavior in diseases of the extrapyramidal system.]. Klin Wochenschr 1960; 38: 1236-9.

Exner N, Treske B, Paquet D, Holmstrom K, Schiesling C, Gispert S, et al. Loss-of-function of human PINK1 results in mitochondrial pathology and can be rescued by parkin. J Neurosci 2007; 27: 12413-8.

Factor SA, Weiner WJ. Parkinson's disease : diagnosis and clinical management. New York: Demos, 2008.

Fan J, Ren H, Fei E, Jia N, Ying Z, Jiang P, et al. Sumoylation is critical for DJ-1 to repress p53 transcriptional activity. FEBS Lett 2008a; 582: 1151-6.

Fan J, Ren H, Jia N, Fei E, Zhou T, Jiang P, et al. DJ-1 decreases Bax expression through repressing p53 transcriptional activity. J Biol Chem 2008b; 283: 4022-30.

Farrer MJ. Genetics of Parkinson disease: paradigm shifts and future prospects. Nat Rev Genet 2006; 7: 306-18.

Fato R, Bergamini C, Leoni S, Strocchi P, Lenaz G. Generation of reactive oxygen species by mitochondrial complex I: implications in neurodegeneration. Neurochem Res 2008; 33: 2487-501.

Fearnley JM, Lees AJ. Ageing and Parkinson's disease: substantia nigra regional selectivity. Brain 1991; 114 ( Pt 5): 2283-301.

Finger S. Origins of neuroscience : a history of explorations into brain function. New York ; Oxford: Oxford University Press, 1994.

Firestone JA, Smith-Weller T, Franklin G, Swanson P, Longstreth WT, Jr., Checkoway H. Pesticides and risk of Parkinson disease: a population-based case-control study. Arch Neurol 2005; 62: 91-5.

Fuchs J, Tichopad A, Golub Y, Munz M, Schweitzer KJ, Wolf B, et al. Genetic variability in the SNCA gene influences alpha-synuclein levels in the blood and brain. FASEB J 2008; 22: 1327-34.

Galter D, Westerlund M, Belin AC, Olson L. DJ-1 and UCH-L1 gene activity patterns in the brains of controls, Parkinson and schizophrenia patients and in rodents. Physiol Behav 2007; 92: 46-53.

Gandhi S, Muqit MM, Stanyer L, Healy DG, Abou-Sleiman PM, Hargreaves I, et al. PINK1 protein in normal human brain and Parkinson's disease. Brain 2006; 129: 1720-31.

Gasparini L, Terni B, Spillantini MG. Frontotemporal dementia with tau pathology. Neurodegener Dis 2007; 4: 236-53.

Gebauer F, Hentze MW. Molecular mechanisms of translational control. Nat Rev Mol Cell Biol 2004; 5: 827-35.

Gegg ME, Cooper JM, Schapira AH, Taanman JW. Silencing of PINK1 expression affects mitochondrial DNA and oxidative phosphorylation in dopaminergic cells. PLoS ONE 2009; 4: e4756.

Gerlach M, Double KL, Ben-Shachar D, Zecca L, Youdim MB, Riederer P. Neuromelanin and its interaction with iron as a potential risk factor for dopaminergic neurodegeneration underlying Parkinson's disease. Neurotox Res 2003; 5: 35-44.

Giasson BI, Uryu K, Trojanowski JQ, Lee VM. Mutant and wild type human alpha-synucleins assemble into elongated filaments with distinct morphologies in vitro. J Biol Chem 1999; 274: 7619-22.

Gibb WR. Melanin, tyrosine hydroxylase, calbindin and substance P in the human midbrain and substantia nigra in relation to nigrostriatal projections and differential neuronal susceptibility in Parkinson's disease. Brain Res 1992; 581: 283-91.

Gibb WR, Scott T, Lees AJ. Neuronal inclusions of Parkinson's disease. Mov Disord 1991; 6: 2-11.

Gilks WP, Abou-Sleiman PM, Gandhi S, Jain S, Singleton A, Lees AJ, et al. A common LRRK2 mutation in idiopathic Parkinson's disease. Lancet 2005; 365: 415-6.

Goedert M. Tau gene mutations and their effects. Mov Disord 2005; 20 Suppl 12: S45-52.

Goedert M, Spillantini MG, Cairns NJ, Crowther RA. Tau proteins of Alzheimer paired helical filaments: abnormal phosphorylation of all six brain isoforms. Neuron 1992; 8: 159-68.

Goetz CG, Fahn S, Martinez-Martin P, Poewe W, Sampaio C, Stebbins GT, et al. Movement Disorder Society-sponsored revision of the Unified Parkinson's Disease Rating Scale (MDS-UPDRS): Process, format, and clinimetric testing plan. Mov Disord 2007; 22: 41-7.

Goldberg MS, Pisani A, Haburcak M, Vortherms TA, Kitada T, Costa C, et al. Nigrostriatal dopaminergic deficits and hypokinesia caused by inactivation of the familial Parkinsonism-linked gene DJ-1. Neuron 2005; 45: 489-96.

Goldman JE, Yen SH, Chiu FC, Peress NS. Lewy bodies of Parkinson's disease contain neurofilament antigens. Science 1983; 221: 1082-4.

Gonzalez-Hernandez T, Barroso-Chinea P, De La Cruz Muros I, Del Mar Perez-Delgado M, Rodriguez M. Expression of dopamine and vesicular monoamine transporters and differential vulnerability of mesostriatal dopaminergic neurons. J Comp Neurol 2004; 479: 198-215.

Gorner K, Holtorf E, Odoy S, Nuscher B, Yamamoto A, Regula JT, et al. Differential effects of Parkinson's disease-associated mutations on stability and folding of DJ-1. J Biol Chem 2004; 279: 6943-51.

Gorner K, Holtorf E, Waak J, Pham TT, Vogt-Weisenhorn DM, Wurst W, et al. Structural determinants of the C-terminal helix-kink-helix motif essential for protein stability and survival promoting activity of DJ-1. J Biol Chem 2007; 282: 13680-91.

Gosal D, Ross OA, Toft M. Parkinson's disease: the genetics of a heterogeneous disorder. Eur J Neurol 2006; 13: 616-27.

Greenfield JG, Bosanquet FD. The brain-stem lesions in Parkinsonism. J Neurol Neurosurg Psychiatry 1953; 16: 213-26.

Greggio E, Jain S, Kingsbury A, Bandopadhyay R, Lewis P, Kaganovich A, et al. Kinase activity is required for the toxic effects of mutant LRRK2/dardarin. Neurobiol Dis 2006; 23: 329-41.

Griffin RJ, Moloney A, Kelliher M, Johnston JA, Ravid R, Dockery P, et al. Activation of Akt/PKB, increased phosphorylation of Akt substrates and loss and altered distribution of Akt and PTEN are features of Alzheimer's disease pathology. J Neurochem 2005; 93: 105-17.

Gu M, Cooper JM, Taanman JW, Schapira AH. Mitochondrial DNA transmission of the mitochondrial defect in Parkinson's disease. Ann Neurol 1998; 44: 177-86.

Hague S, Rogaeva E, Hernandez D, Gulick C, Singleton A, Hanson M, et al. Early-onset Parkinson's disease caused by a compound heterozygous DJ-1 mutation. Ann Neurol 2003; 54: 271-4.

Halliday G, Hely M, Reid W, Morris J. The progression of pathology in longitudinally followed patients with Parkinson's disease. Acta Neuropathol 2008; 115: 409-15.

Hartley A, Stone JM, Heron C, Cooper JM, Schapira AH. Complex I inhibitors induce dose-dependent apoptosis in PC12 cells: relevance to Parkinson's disease. J Neurochem 1994; 63: 1987-90.

Hartmann A, Michel PP, Troadec JD, Mouatt-Prigent A, Faucheux BA, Ruberg M, et al. Is Bax a mitochondrial mediator in apoptotic death of dopaminergic neurons in Parkinson's disease? J Neurochem 2001; 76: 1785-93.

Hashimoto M, Hsu LJ, Rockenstein E, Takenouchi T, Mallory M, Masliah E. alpha-Synuclein protects against oxidative stress via inactivation of the c-Jun N-terminal kinase stress-signaling pathway in neuronal cells. J Biol Chem 2002; 277: 11465-72.

Hatano Y, Li Y, Sato K, Asakawa S, Yamamura Y, Tomiyama H, et al. Novel PINK1 mutations in early-onset parkinsonism. Ann Neurol 2004; 56: 424-7.

Hattori N, Shimura H, Kubo S, Kitada T, Wang M, Asakawa S, et al. Autosomal recessive juvenile parkinsonism: a key to understanding nigral degeneration in sporadic Parkinson's disease. Neuropathology 2000; 20 Suppl: S85-90.

Hawkes CH, Del Tredici K, Braak H. Parkinson's disease: a dual-hit hypothesis. Neuropathol Appl Neurobiol 2007; 33: 599-614.

Healy DG, Abou-Sleiman PM, Casas JP, Ahmadi KR, Lynch T, Gandhi S, et al. UCHL-1 is not a Parkinson's disease susceptibility gene. Ann Neurol 2006; 59: 627-33.

Healy DG, Abou-Sleiman PM, Wood NW. PINK, PANK, or PARK? A clinicians' guide to familial parkinsonism. Lancet Neurol 2004; 3: 652-62.

Hedrich K, Djarmati A, Schafer N, Hering R, Wellenbrock C, Weiss PH, et al. DJ-1 (PARK7) mutations are less frequent than Parkin (PARK2) mutations in early-onset Parkinson disease. Neurology 2004a; 62: 389-94.

Hedrich K, Schafer N, Hering R, Hagenah J, Lanthaler AJ, Schwinger E, et al. The R98Q variation in DJ-1 represents a rare polymorphism. Ann Neurol 2004b; 55: 145; author reply 145-6.

Henchcliffe C, Beal MF. Mitochondrial biology and oxidative stress in Parkinson disease pathogenesis. Nat Clin Pract Neurol 2008; 4: 600-9.

Hering R, Strauss KM, Tao X, Bauer A, Woitalla D, Mietz EM, et al. Novel homozygous p.E64D mutation in DJ1 in early onset Parkinson disease (PARK7). Hum Mutat 2004; 24: 321-9.

Herrera FE, Zucchelli S, Jezierska A, Lavina ZS, Gustincich S, Carloni P. On the oligomeric state of DJ-1 protein and its mutants associated with Parkinson Disease. A combined computational and in vitro study. J Biol Chem 2007; 282: 24905-14.

Hicks AA, Petursson H, Jonsson T, Stefansson H, Johannsdottir HS, Sainz J, et al. A susceptibility gene for late-onset idiopathic Parkinson's disease. Ann Neurol 2002; 52: 549-55.

Hod Y, Pentyala SN, Whyard TC, El-Maghrabi MR. Identification and characterization of a novel protein that regulates RNA-protein interaction. J Cell Biochem 1999; 72: 435-44.

Holcik M, Sonenberg N. Translational control in stress and apoptosis. Nat Rev Mol Cell Biol 2005; 6: 318-27.

Holdorff B. Friedrich Heinrich Lewy (1885-1950) and his work. J Hist Neurosci 2002; 11: 19-28.

Honbou K, Suzuki NN, Horiuchi M, Niki T, Taira T, Ariga H, et al. The crystal structure of DJ-1, a protein related to male fertility and Parkinson's disease. J Biol Chem 2003; 278: 31380-4.

Huai Q, Sun Y, Wang H, Chin LS, Li L, Robinson H, et al. Crystal structure of DJ-1/RS and implication on familial Parkinson's disease. FEBS Lett 2003; 549: 171-5.

Hulleman JD, Mirzaei H, Guigard E, Taylor KL, Ray SS, Kay CM, et al. Destabilization of DJ-1 by familial substitution and oxidative modifications: implications for Parkinson's disease. Biochemistry 2007; 46: 5776-89.

Hurley MJ, Mash DC, Jenner P. Markers for dopaminergic neurotransmission in the cerebellum in normal individuals and patients with Parkinson's disease examined by RT-PCR. Eur J Neurosci 2003; 18: 2668-72.

Ibanez P, Bonnet AM, Debarges B, Lohmann E, Tison F, Pollak P, et al. Causal relation between alpha-synuclein gene duplication and familial Parkinson's disease. Lancet 2004; 364: 1169-71.

Imai H, Nakagawa Y. Biological significance of phospholipid hydroperoxide glutathione peroxidase (PHGPx, GPx4) in mammalian cells. Free Radic Biol Med 2003; 34: 145-69.

Imai Y, Soda M, Inoue H, Hattori N, Mizuno Y, Takahashi R. An unfolded putative transmembrane polypeptide, which can lead to endoplasmic reticulum stress, is a substrate of Parkin. Cell 2001; 105: 891-902.

Ingram EM, Spillantini MG. Tau gene mutations: dissecting the pathogenesis of FTDP-17. Trends Mol Med 2002; 8: 555-62.

Ishida Y, Nagai A, Kobayashi S, Kim SU. Upregulation of protease-activated receptor-1 in astrocytes in Parkinson disease: astrocyte-mediated neuroprotection through increased levels of glutathione peroxidase. J Neuropathol Exp Neurol 2006; 65: 66-77.

Ishihara T, Hong M, Zhang B, Nakagawa Y, Lee MK, Trojanowski JQ, et al. Age-dependent emergence and progression of a tauopathy in transgenic mice overexpressing the shortest human tau isoform. Neuron 1999; 24: 751-62.

Ito G, Okai T, Fujino G, Takeda K, Ichijo H, Katada T, et al. GTP binding is essential to the protein kinase activity of LRRK2, a causative gene product for familial Parkinson's disease. Biochemistry 2007; 46: 1380-8.

Jakel RJ, Townsend JA, Kraft AD, Johnson JA. Nrf2-mediated protection against 6-hydroxydopamine. Brain Res 2007; 1144: 192-201.

Jankovic J, Tolosa E. Parkinson's disease and movement disorders. Philadelphia, Pa. ; London: Lippincott Williams & Wilkins, 2002.

Jellinger KA. Lewy body-related alpha-synucleinopathy in the aged human brain. J Neural Transm 2004; 111: 1219-35.

Jellinger KA. Neuropathology of dementia in Parkinson's disease. Ann Neurol 2006; 59: 727.

Jin J, Li GJ, Davis J, Zhu D, Wang Y, Pan C, et al. Identification of novel proteins associated with both alpha-synuclein and DJ-1. Mol Cell Proteomics 2007; 6: 845-59.

Junn E, Jang WH, Zhao X, Jeong BS, Mouradian MM. Mitochondrial localization of DJ-1 leads to enhanced neuroprotection. J Neurosci Res 2009; 87: 123-9.

Junn E, Taniguchi H, Jeong BS, Zhao X, Ichijo H, Mouradian MM. Interaction of DJ-1 with Daxx inhibits apoptosis signal-regulating kinase 1 activity and cell death. Proc Natl Acad Sci U S A 2005; 102: 9691-6.

Kalaitzakis ME, Graeber MB, Gentleman SM, Pearce RK. Controversies over the staging of alpha-synuclein pathology in Parkinson's disease. Acta Neuropathol 2008a; 116: 125-8; author reply 129-31.

Kalaitzakis ME, Graeber MB, Gentleman SM, Pearce RK. The dorsal motor nucleus of the vagus is not an obligatory trigger site of Parkinson's disease: a critical analysis of alpha-synuclein staging. Neuropathol Appl Neurobiol 2008b; 34: 284-95.

Karunakaran S, Diwakar L, Saeed U, Agarwal V, Ramakrishnan S, Iyengar S, et al. Activation of apoptosis signal regulating kinase 1 (ASK1) and translocation of death-associated protein, Daxx, in substantia nigra pars compacta in a mouse model of Parkinson's disease: protection by alpha-lipoic acid. FASEB J 2007; 21: 2226-36.

Kaul SC, Taira K, Pereira-Smith OM, Wadhwa R. Mortalin: present and prospective. Exp Gerontol 2002; 37: 1157-64.

Keeney PM, Xie J, Capaldi RA, Bennett JP, Jr. Parkinson's disease brain mitochondrial complex I has oxidatively damaged subunits and is functionally impaired and misassembled. J Neurosci 2006; 26: 5256-64.

Kertesz A. Pick Complex: an integrative approach to frontotemporal dementia: primary progressive aphasia, corticobasal degeneration, and progressive supranuclear palsy. Neurologist 2003; 9: 311-7.

Kertesz A, Hillis A, Munoz DG. Frontotemporal degeneration, Pick's disease, Pick complex, and Ravel. Ann Neurol 2003; 54 Suppl 5: S1-2.

Kim RH, Peters M, Jang Y, Shi W, Pintilie M, Fletcher GC, et al. DJ-1, a novel regulator of the tumor suppressor PTEN. Cancer Cell 2005a; 7: 263-73.

Kim RH, Smith PD, Aleyasin H, Hayley S, Mount MP, Pownall S, et al. Hypersensitivity of DJ-1-deficient mice to 1-methyl-4-phenyl-1,2,3,6-tetrahydropyrindine (MPTP) and oxidative stress. Proc Natl Acad Sci U S A 2005b; 102: 5215-20.

Kitada T, Asakawa S, Hattori N, Matsumine H, Yamamura Y, Minoshima S, et al. Mutations in the parkin gene cause autosomal recessive juvenile parkinsonism. Nature 1998; 392: 605-8.

Klegeris A, Pelech S, Giasson BI, Maguire J, Zhang H, McGeer EG, et al. Alpha-synuclein activates stress signaling protein kinases in THP-1 cells and microglia. Neurobiol Aging 2008; 29: 739-52.

Klinefelter GR, Suarez JD. Toxicant-induced acceleration of epididymal sperm transit: androgen-dependent proteins may be involved. Reprod Toxicol 1997; 11: 511-9.

Knott C, Stern G, Kingsbury A, Welcher AA, Wilkin GP. Elevated glial brain-derived neurotrophic factor in Parkinson's diseased nigra. Parkinsonism Relat Disord 2002; 8: 329-41.

Komori T. Tau-positive glial inclusions in progressive supranuclear palsy, corticobasal degeneration and Pick's disease. Brain Pathol 1999; 9: 663-79.

Kotaria N, Hinz U, Zechel S, von Bohlen Und Halbach O. Localization of DJ-1 protein in the murine brain. Cell Tissue Res 2005; 322: 503-7.

Kraytsberg Y, Kudryavtseva E, McKee AC, Geula C, Kowall NW, Khrapko K. Mitochondrial DNA deletions are abundant and cause functional impairment in aged human substantia nigra neurons. Nat Genet 2006; 38: 518-20.

Kruger R, Kuhn W, Muller T, Woitalla D, Graeber M, Kosel S, et al. Ala30Pro mutation in the gene encoding alpha-synuclein in Parkinson's disease. Nat Genet 1998; 18: 106-8.

Ksiezak-Reding H, Pyo HK, Feinstein B, Pasinetti GM. Akt/PKB kinase phosphorylates separately Thr212 and Ser214 of tau protein in vitro. Biochim Biophys Acta 2003; 1639: 159-68.

Kubo S, Hattori N, Mizuno Y. Recessive Parkinson's disease. Mov Disord 2006; 21: 885-93.

Kumaran R, Kingsbury A, Coulter I, Lashley T, Williams D, de Silva R, et al. DJ-1 (PARK7) is associated with 3R and 4R tau neuronal and glial inclusions in neurodegenerative disorders. Neurobiol Dis 2007; 28: 122-32.

Kuzuhara S, Mori H, Izumiyama N, Yoshimura M, Ihara Y. Lewy bodies are ubiquitinated. A light and electron microscopic immunocytochemical study. Acta Neuropathol 1988; 75: 345-53.

Lakshminarasimhan M, Maldonado MT, Zhou W, Fink AL, Wilson MA. Structural impact of three Parkinsonism-associated missense mutations on human DJ-1. Biochemistry 2008; 47: 1381-92.

Langston JW, Ballard P, Tetrud JW, Irwin I. Chronic Parkinsonism in humans due to a product of meperidine-analog synthesis. Science 1983; 219: 979-80.

Lashley T, Holton JL, Gray E, Kirkham K, O'Sullivan SS, Hilbig A, et al. Cortical alpha-synuclein load is associated with amyloid-beta plaque burden in a subset of Parkinson's disease patients. Acta Neuropathol 2008; 115: 417-25.

Lavara-Culebras E, Paricio N. Drosophila DJ-1 mutants are sensitive to oxidative stress and show reduced lifespan and motor deficits. Gene 2007; 400: 158-65.

Le Naour F, Misek DE, Krause MC, Deneux L, Giordano TJ, Scholl S, et al. Proteomics-based identification of RS/DJ-1 as a novel circulating tumor antigen in breast cancer. Clin Cancer Res 2001; 7: 3328-35.

Lee SJ, Kim SJ, Kim IK, Ko J, Jeong CS, Kim GH, et al. Crystal structures of human DJ-1 and Escherichia coli Hsp31, which share an evolutionarily conserved domain. J Biol Chem 2003; 278: 44552-9.

Leonard JV, Schapira AH. Mitochondrial respiratory chain disorders I: mitochondrial DNA defects. Lancet 2000; 355: 299-304.

Leroy E, Boyer R, Auburger G, Leube B, Ulm G, Mezey E, et al. The ubiquitin pathway in Parkinson's disease. Nature 1998; 395: 451-2.

Lesage S, Durr A, Tazir M, Lohmann E, Leutenegger AL, Janin S, et al. LRRK2 G2019S as a cause of Parkinson's disease in North African Arabs. N Engl J Med 2006; 354: 422-3.

Lev N, Ickowicz D, Barhum Y, Lev S, Melamed E, Offen D. DJ-1 protects against dopamine toxicity. J Neural Transm 2009; 116: 151-60.

Lev N, Roncevich D, Ickowicz D, Melamed E, Offen D. Role of DJ-1 in parkinson's disease. J Mol Neurosci 2007; 31: 307.

Lewis PA, Greggio E, Beilina A, Jain S, Baker A, Cookson MR. The R1441C mutation of LRRK2 disrupts GTP hydrolysis. Biochem Biophys Res Commun 2007; 357: 668-71.

Lin LF, Doherty DH, Lile JD, Bektesh S, Collins F. GDNF: a glial cell line-derived neurotrophic factor for midbrain dopaminergic neurons. Science 1993; 260: 1130-2.

Litvan I, Agid Y, Calne D, Campbell G, Dubois B, Duvoisin RC, et al. Clinical research criteria for the diagnosis of progressive supranuclear palsy (Steele-Richardson-Olszewski syndrome): report of the NINDS-SPSP international workshop. Neurology 1996; 47: 1-9.

Liu F, Nguyen JL, Hulleman JD, Li L, Rochet JC. Mechanisms of DJ-1 neuroprotection in a cellular model of Parkinson's disease. J Neurochem 2008a.

Liu H, Wang M, Li M, Wang D, Rao Q, Wang Y, et al. Expression and role of DJ-1 in leukemia. Biochem Biophys Res Commun 2008b; 375: 477-83.

Lopez de Silanes I, Zhan M, Lal A, Yang X, Gorospe M. Identification of a target RNA motif for RNA-binding protein HuR. Proc Natl Acad Sci U S A 2004; 101: 2987-92.

Macedo MG, Anar B, Bronner IF, Cannella M, Squitieri F, Bonifati V, et al. The DJ-1L166P mutant protein associated with early onset Parkinson's disease is unstable and forms higher-order protein complexes. Hum Mol Genet 2003; 12: 2807-16.

MacKeigan JP, Clements CM, Lich JD, Pope RM, Hod Y, Ting JP. Proteomic profiling drug-induced apoptosis in non-small cell lung carcinoma: identification of RS/DJ-1 and RhoGDIalpha. Cancer Res 2003; 63: 6928-34.

Malgieri G, Eliezer D. Structural effects of Parkinson's disease linked DJ-1 mutations. Protein Sci 2008; 17: 855-68.

Maraganore DM, Farrer MJ, Hardy JA, Lincoln SJ, McDonnell SK, Rocca WA. Case-control study of the ubiquitin carboxy-terminal hydrolase L1 gene in Parkinson's disease. Neurology 1999; 53: 1858-60.

Maraganore DM, Lesnick TG, Elbaz A, Chartier-Harlin MC, Gasser T, Kruger R, et al. UCHL1 is a Parkinson's disease susceptibility gene. Ann Neurol 2004; 55: 512-21.

Martinat C, Shendelman S, Jonason A, Leete T, Beal MF, Yang L, et al. Sensitivity to oxidative stress in DJ-1-deficient dopamine neurons: an ES- derived cell model of primary Parkinsonism. PLoS Biol 2004; 2: e327.

Marttila RJ, Kaprio J, Koskenvuo M, Rinne UK. Parkinson's disease in a nationwide twin cohort. Neurology 1988; 38: 1217-9.

Mata IF, Lockhart PJ, Farrer MJ. Parkin genetics: one model for Parkinson's disease. Hum Mol Genet 2004; 13 Spec No 1: R127-33.

Mattson MP. Infectious agents and age-related neurodegenerative disorders. Ageing Res Rev 2004; 3: 105-20.

McGeer PL, McGeer EG. Glial reactions in Parkinson's disease. Mov Disord 2008; 23: 474-83.

McKeith IG, Dickson DW, Lowe J, Emre M, O'Brien JT, Feldman H, et al. Diagnosis and management of dementia with Lewy bodies: third report of the DLB Consortium. Neurology 2005; 65: 1863-72.

McNaught KS, Mytilineou C, Jnobaptiste R, Yabut J, Shashidharan P, Jennert P, et al. Impairment of the ubiquitin-proteasome system causes dopaminergic cell death and inclusion body formation in ventral mesencephalic cultures. J Neurochem 2002; 81: 301-6.

Menzies FM, Yenisetti SC, Min KT. Roles of Drosophila DJ-1 in survival of dopaminergic neurons and oxidative stress. Curr Biol 2005; 15: 1578-82.

Meulener M, Whitworth AJ, Armstrong-Gold CE, Rizzu P, Heutink P, Wes PD, et al. Drosophila DJ-1 mutants are selectively sensitive to environmental toxins associated with Parkinson's disease. Curr Biol 2005; 15: 1572-7.

Meulener MC, Xu K, Thomson L, Ischiropoulos H, Bonini NM. Mutational analysis of DJ-1 in Drosophila implicates functional inactivation by oxidative damage and aging. Proc Natl Acad Sci U S A 2006; 103: 12517-22.

Miklossy J, Arai T, Guo JP, Klegeris A, Yu S, McGeer EG, et al. LRRK2 expression in normal and pathologic human brain and in human cell lines. J Neuropathol Exp Neurol 2006; 65: 953-63.

Miller DW, Ahmad R, Hague S, Baptista MJ, Canet-Aviles R, McLendon C, et al. L166P mutant DJ-1, causative for recessive Parkinson's disease, is degraded through the ubiquitin-proteasome system. J Biol Chem 2003; 278: 36588-95.

Miller DW, Hague SM, Clarimon J, Baptista M, Gwinn-Hardy K, Cookson MR, et al. Alpha-synuclein in blood and brain from familial Parkinson disease with SNCA locus triplication. Neurology 2004; 62: 1835-8.

Mirza B, Hadberg H, Thomsen P, Moos T. The absence of reactive astrocytosis is indicative of a unique inflammatory process in Parkinson's disease. Neuroscience 2000; 95: 425-32.

Mitsumoto A, Nakagawa Y. DJ-1 is an indicator for endogenous reactive oxygen species elicited by endotoxin. Free Radic Res 2001; 35: 885-93.

Mitsumoto A, Nakagawa Y, Takeuchi A, Okawa K, Iwamatsu A, Takanezawa Y. Oxidized forms of peroxiredoxins and DJ-1 on two-dimensional gels increased in response to sublethal levels of paraquat. Free Radic Res 2001; 35: 301-10.

Mizuno Y, Ohta S, Tanaka M, Takamiya S, Suzuki K, Sato T, et al. Deficiencies in complex I subunits of the respiratory chain in Parkinson's disease. Biochem Biophys Res Commun 1989; 163: 1450-5.

Mo JS, Kim MY, Ann EJ, Hong JA, Park HS. DJ-1 modulates UV-induced oxidative stress signaling through the suppression of MEKK1 and cell death. Cell Death Differ 2008; 15: 1030-41.

Moore DJ, Dawson VL, Dawson TM. Genetics of Parkinson's disease: what do mutations in DJ-1 tell us? Ann Neurol 2003a; 54: 281-2.

Moore DJ, Zhang L, Dawson TM, Dawson VL. A missense mutation (L166P) in DJ-1, linked to familial Parkinson's disease, confers reduced protein stability and impairs homo-oligomerization. J Neurochem 2003b; 87: 1558-67.

Moore DJ, Zhang L, Troncoso J, Lee MK, Hattori N, Mizuno Y, et al. Association of DJ-1 and parkin mediated by pathogenic DJ-1 mutations and oxidative stress. Hum Mol Genet 2005; 14: 71-84.

Morris CM, O'Brien KK, Gibson AM, Hardy JA, Singleton AB. Polymorphism in the human DJ-1 gene is not associated with sporadic dementia with Lewy bodies or Parkinson's disease. Neurosci Lett 2003; 352: 151-3.

Morris HR. Autosomal dominant Parkinson's disease and the route to new therapies. Expert Rev Neurother 2007; 7: 649-56.

Mullett SJ, Hinkle DA. DJ-1 knock-down in astrocytes impairs astrocyte-mediated neuroprotection against rotenone. Neurobiol Dis 2009; 33: 28-36.

Munoz DG, Dickson DW, Bergeron C, Mackenzie IR, Delacourte A, Zhukareva V. The neuropathology and biochemistry of frontotemporal dementia. Ann Neurol 2003; 54 Suppl 5: S24-8.

Nagakubo D, Taira T, Kitaura H, Ikeda M, Tamai K, Iguchi-Ariga SM, et al. DJ-1, a novel oncogene which transforms mouse NIH3T3 cells in cooperation with ras. Biochem Biophys Res Commun 1997; 231: 509-13.

Nass R, Hall DH, Miller DM, 3rd, Blakely RD. Neurotoxin-induced degeneration of dopamine neurons in Caenorhabditis elegans. Proc Natl Acad Sci U S A 2002; 99: 3264-9.

Neumann M, Muller V, Gorner K, Kretzschmar HA, Haass C, Kahle PJ. Pathological properties of the Parkinson's disease-associated protein DJ-1 in alpha-synucleinopathies and tauopathies: relevance for multiple system atrophy and Pick's disease. Acta Neuropathol 2004; 107: 489-96.

Nichols WC, Pankratz N, Hernandez D, Paisan-Ruiz C, Jain S, Halter CA, et al. Genetic screening for a single common LRRK2 mutation in familial Parkinson's disease. Lancet 2005; 365: 410-2.

Niki T, Takahashi-Niki K, Taira T, Iguchi-Ariga SM, Ariga H. DJBP: a novel DJ-1-binding protein, negatively regulates the androgen receptor by recruiting histone deacetylase complex, and DJ-1 antagonizes this inhibition by abrogation of this complex. Mol Cancer Res 2003; 1: 247-61.

Nimmerjahn A, Kirchhoff F, Helmchen F. Resting microglial cells are highly dynamic surveillants of brain parenchyma in vivo. Science 2005; 308: 1314-8.

Nishinaga H, Takahashi-Niki K, Taira T, Andreadis A, Iguchi-Ariga SM, Ariga H. Expression profiles of genes in DJ-1-knockdown and L 166 P DJ-1 mutant cells. Neurosci Lett 2005; 390: 54-9.

Ogata A, Tashiro K, Nukuzuma S, Nagashima K, Hall WW. A rat model of Parkinson's disease induced by Japanese encephalitis virus. J Neurovirol 1997; 3: 141-7.

Olzmann JA, Bordelon JR, Muly EC, Rees HD, Levey AI, Li L, et al. Selective enrichment of DJ-1 protein in primate striatal neuronal processes: implications for Parkinson's disease. J Comp Neurol 2007; 500: 585-99.

Olzmann JA, Brown K, Wilkinson KD, Rees HD, Huai Q, Ke H, et al. Familial Parkinson's disease-associated L166P mutation disrupts DJ-1 protein folding and function. J Biol Chem 2004; 279: 8506-15.

Ossowska K, Smialowska M, Kuter K, Wieronska J, Zieba B, Wardas J, et al. Degeneration of dopaminergic mesocortical neurons and activation of compensatory processes induced by a long-term paraquat administration in rats: implications for Parkinson's disease. Neuroscience 2006; 141: 2155-65.

Ozelius LJ, Senthil G, Saunders-Pullman R, Ohmann E, Deligtisch A, Tagliati M, et al. LRRK2 G2019S as a cause of Parkinson's disease in Ashkenazi Jews. N Engl J Med 2006; 354: 424-5.

Paisan-Ruiz C, Jain S, Evans EW, Gilks WP, Simon J, van der Brug M, et al. Cloning of the gene containing mutations that cause PARK8-linked Parkinson's disease. Neuron 2004; 44: 595-600.

Pankratz N, Nichols WC, Uniacke SK, Halter C, Rudolph A, Shults C, et al. Genome screen to identify susceptibility genes for Parkinson disease in a sample without parkin mutations. Am J Hum Genet 2002; 71: 124-35.

Pardo M, Garcia A, Thomas B, Pineiro A, Akoulitchev A, Dwek RA, et al. The characterization of the invasion phenotype of uveal melanoma tumour cells shows the presence of

MUC18 and HMG-1 metastasis markers and leads to the identification of DJ-1 as a potential serum biomarker. Int J Cancer 2006; 119: 1014-22.
Park J, Kim SY, Cha GH, Lee SB, Kim S, Chung J. Drosophila DJ-1 mutants show oxidative stress-sensitive locomotive dysfunction. Gene 2005; 361: 133-9.
Park J, Lee SB, Lee S, Kim Y, Song S, Kim S, et al. Mitochondrial dysfunction in Drosophila PINK1 mutants is complemented by parkin. Nature 2006; 441: 1157-61.
Parker WD, Jr., Parks JK. Mitochondrial ND5 mutations in idiopathic Parkinson's disease. Biochem Biophys Res Commun 2005; 326: 667-9.
Parker WD, Jr., Parks JK, Swerdlow RH. Complex I deficiency in Parkinson's disease frontal cortex. Brain Res 2008; 1189: 215-8.
Parkinson J. An essay on the shaking palsy. 1817. J Neuropsychiatry Clin Neurosci 2002; 14: 223-36; discussion 222.
Pei JJ, Khatoon S, An WL, Nordlinder M, Tanaka T, Braak H, et al. Role of protein kinase B in Alzheimer's neurofibrillary pathology. Acta Neuropathol 2003; 105: 381-92.
Pfaffl MW. A new mathematical model for relative quantification in real-time RT-PCR. Nucleic Acids Res 2001; 29: e45.
Pickart CM. Ubiquitin in chains. Trends Biochem Sci 2000; 25: 544-8.
Pittman AM, Fung HC, de Silva R. Untangling the tau gene association with neurodegenerative disorders. Hum Mol Genet 2006; 15 Spec No 2: R188-95.
Plun-Favreau H, Hardy J. PINK1 in mitochondrial function. Proc Natl Acad Sci U S A 2008; 105: 11041-2.
Polymeropoulos MH, Lavedan C, Leroy E, Ide SE, Dehejia A, Dutra A, et al. Mutation in the alpha-synuclein gene identified in families with Parkinson's disease. Science 1997; 276: 2045-7.
Pramstaller PP, Schlossmacher MG, Jacques TS, Scaravilli F, Eskelson C, Pepivani I, et al. Lewy body Parkinson's disease in a large pedigree with 77 Parkin mutation carriers. Ann Neurol 2005; 58: 411-22.
Pridgeon JW, Olzmann JA, Chin LS, Li L. PINK1 protects against oxidative stress by phosphorylating mitochondrial chaperone TRAP1. PLoS Biol 2007; 5: e172.
Quigley PM, Korotkov K, Baneyx F, Hol WG. The 1.6-A crystal structure of the class of chaperones represented by Escherichia coli Hsp31 reveals a putative catalytic triad. Proc Natl Acad Sci U S A 2003; 100: 3137-42.
Raab W, Gigee W. Concentration and distribution of "encephalin" in the brain of humans and animals. Proc Soc Exp Biol Med 1951; 76: 97-100.
Ramirez A, Heimbach A, Grundemann J, Stiller B, Hampshire D, Cid LP, et al. Hereditary parkinsonism with dementia is caused by mutations in ATP13A2, encoding a lysosomal type 5 P-type ATPase. Nat Genet 2006; 38: 1184-91.
Ramsey CP, Giasson BI. The E163K DJ-1 mutant shows specific antioxidant deficiency. Brain Res 2008.
Rascol O, Sabatini U, Fabre N, Brefel C, Loubinoux I, Celsis P, et al. The ipsilateral cerebellar hemisphere is overactive during hand movements in akinetic parkinsonian patients. Brain 1997; 120 ( Pt 1): 103-10.
Rizzu P, Hinkle DA, Zhukareva V, Bonifati V, Severijnen LA, Martinez D, et al. DJ-1 colocalizes with tau inclusions: a link between parkinsonism and dementia. Ann Neurol 2004; 55: 113-8.
Robert M, Mathuranath PS. Tau and tauopathies. Neurol India 2007; 55: 11-6.

Rohe CF, Montagna P, Breedveld G, Cortelli P, Oostra BA, Bonifati V. Homozygous PINK1 C-terminus mutation causing early-onset parkinsonism. Ann Neurol 2004; 56: 427-31.
Ross GW, Abbott RD, Petrovitch H, Morens DM, Grandinetti A, Tung KH, et al. Association of coffee and caffeine intake with the risk of Parkinson disease. JAMA 2000; 283: 2674-9.
Roy S, Wolman L. Ultrastructural observations in Parkinsonism. J Pathol 1969; 99: 39-44.
Sano I, Gamo T, Kakimoto Y, Taniguchi K, Takesada M, Nishinuma K. Distribution of catechol compounds in human brain. Biochim Biophys Acta 1959; 32: 586-7.
Schapira AH, Cooper JM, Dexter D, Clark JB, Jenner P, Marsden CD. Mitochondrial complex I deficiency in Parkinson's disease. J Neurochem 1990; 54: 823-7.
Scheele C, Petrovic N, Faghihi MA, Lassmann T, Fredriksson K, Rooyackers O, et al. The human PINK1 locus is regulated in vivo by a non-coding natural antisense RNA during modulation of mitochondrial function. BMC Genomics 2007; 8: 74.
Sekito A, Taira T, Niki T, Iguchi-Ariga SM, Ariga H. Stimulation of transforming activity of DJ-1 by Abstrakt, a DJ-1-binding protein. Int J Oncol 2005; 26: 685-9.
Shah M, Deeb J, Fernando M, Noyce A, Visentin E, Findley LJ, et al. Abnormality of taste and smell in Parkinson's disease. Parkinsonism Relat Disord 2008.
Shang H, Lang D, Jean-Marc B, Kaelin-Lang A. Localization of DJ-1 mRNA in the mouse brain. Neurosci Lett 2004; 367: 273-7.
Shendelman S, Jonason A, Martinat C, Leete T, Abeliovich A. DJ-1 is a redox-dependent molecular chaperone that inhibits alpha-synuclein aggregate formation. PLoS Biol 2004; 2: e362.
Sherer TB, Betarbet R, Stout AK, Lund S, Baptista M, Panov AV, et al. An in vitro model of Parkinson's disease: linking mitochondrial impairment to altered alpha-synuclein metabolism and oxidative damage. J Neurosci 2002; 22: 7006-15.
Shimura H, Hattori N, Kubo S, Mizuno Y, Asakawa S, Minoshima S, et al. Familial Parkinson disease gene product, parkin, is a ubiquitin-protein ligase. Nat Genet 2000; 25: 302-5.
Shimura H, Schlossmacher MG, Hattori N, Frosch MP, Trockenbacher A, Schneider R, et al. Ubiquitination of a new form of alpha-synuclein by parkin from human brain: implications for Parkinson's disease. Science 2001; 293: 263-9.
Shinbo Y, Niki T, Taira T, Ooe H, Takahashi-Niki K, Maita C, et al. Proper SUMO-1 conjugation is essential to DJ-1 to exert its full activities. Cell Death Differ 2006; 13: 96-108.
Shinbo Y, Taira T, Niki T, Iguchi-Ariga SM, Ariga H. DJ-1 restores p53 transcription activity inhibited by Topors/p53BP3. Int J Oncol 2005; 26: 641-8.
Shoji M, Harigaya Y, Sasaki A, Ueda K, Ishiguro K, Matsubara E, et al. Accumulation of NACP/alpha-synuclein in lewy body disease and multiple system atrophy. J Neurol Neurosurg Psychiatry 2000; 68: 605-8.
Silvestri L, Caputo V, Bellacchio E, Atorino L, Dallapiccola B, Valente EM, et al. Mitochondrial import and enzymatic activity of PINK1 mutants associated to recessive parkinsonism. Hum Mol Genet 2005; 14: 3477-92.
Sim CH, Lio DS, Mok SS, Masters CL, Hill AF, Culvenor JG, et al. C-terminal truncation and Parkinson's disease-associated mutations down-regulate the protein serine/threonine kinase activity of PTEN-induced kinase-1. Hum Mol Genet 2006; 15: 3251-62.

Simunovic F, Yi M, Wang Y, Macey L, Brown LT, Krichevsky AM, et al. Gene expression profiling of substantia nigra dopamine neurons: further insights into Parkinson's disease pathology. Brain 2008.

Singleton AB, Farrer M, Johnson J, Singleton A, Hague S, Kachergus J, et al. alpha-Synuclein locus triplication causes Parkinson's disease. Science 2003; 302: 841.

Siomi H, Dreyfuss G. RNA-binding proteins as regulators of gene expression. Curr Opin Genet Dev 1997; 7: 345-53.

Smigrodzki R, Parks J, Parker WD. High frequency of mitochondrial complex I mutations in Parkinson's disease and aging. Neurobiol Aging 2004; 25: 1273-81.

Solano SM, Miller DW, Augood SJ, Young AB, Penney JB, Jr. Expression of alpha-synuclein, parkin, and ubiquitin carboxy-terminal hydrolase L1 mRNA in human brain: genes associated with familial Parkinson's disease. Ann Neurol 2000; 47: 201-10.

Spillantini MG, Crowther RA, Jakes R, Hasegawa M, Goedert M. alpha-Synuclein in filamentous inclusions of Lewy bodies from Parkinson's disease and dementia with lewy bodies. Proc Natl Acad Sci U S A 1998; 95: 6469-73.

Spillantini MG, Schmidt ML, Lee VM, Trojanowski JQ, Jakes R, Goedert M. Alpha-synuclein in Lewy bodies. Nature 1997; 388: 839-40.

Stokes AH, Lewis DY, Lash LH, Jerome WG, 3rd, Grant KW, Aschner M, et al. Dopamine toxicity in neuroblastoma cells: role of glutathione depletion by L-BSO and apoptosis. Brain Res 2000; 858: 1-8.

Strauss KM, Martins LM, Plun-Favreau H, Marx FP, Kautzmann S, Berg D, et al. Loss of function mutations in the gene encoding Omi/HtrA2 in Parkinson's disease. Hum Mol Genet 2005; 14: 2099-111.

Taira T, Saito Y, Niki T, Iguchi-Ariga SM, Takahashi K, Ariga H. DJ-1 has a role in antioxidative stress to prevent cell death. EMBO Rep 2004; 5: 213-8.

Takahashi-Niki K, Niki T, Taira T, Iguchi-Ariga SM, Ariga H. Reduced anti-oxidative stress activities of DJ-1 mutants found in Parkinson's disease patients. Biochem Biophys Res Commun 2004; 320: 389-97.

Takahashi K, Taira T, Niki T, Seino C, Iguchi-Ariga SM, Ariga H. DJ-1 positively regulates the androgen receptor by impairing the binding of PIASx alpha to the receptor. J Biol Chem 2001; 276: 37556-63.

Tang B, Xiong H, Sun P, Zhang Y, Wang D, Hu Z, et al. Association of PINK1 and DJ-1 confers digenic inheritance of early-onset Parkinson's disease. Hum Mol Genet 2006; 15: 1816-25.

Tanner CM, Langston JW. Do environmental toxins cause Parkinson's disease? A critical review. Neurology 1990; 40: suppl 17-30; discussion 30-1.

Tao X, Tong L. Crystal structure of human DJ-1, a protein associated with early onset Parkinson's disease. J Biol Chem 2003; 278: 31372-9.

Thomas B, Beal MF. Parkinson's disease. Hum Mol Genet 2007; 16 Spec No. 2: R183-94.

Tissingh G, Berendse HW, Bergmans P, DeWaard R, Drukarch B, Stoof JC, et al. Loss of olfaction in de novo and treated Parkinson's disease: possible implications for early diagnosis. Mov Disord 2001; 16: 41-6.

Toulouse A, Sullivan AM. Progress in Parkinson's disease-where do we stand? Prog Neurobiol 2008; 85: 376-92.

Trimmer PA, Bennett JP, Jr. The cybrid model of sporadic Parkinson's disease. Exp Neurol 2009.

Tsuji Y. JunD activates transcription of the human ferritin H gene through an antioxidant response element during oxidative stress. Oncogene 2005; 24: 7567-78.
Uchihara T, Ikeda K, Tsuchiya K. Pick body disease and Pick syndrome. Neuropathology 2003; 23: 318-26.
Ule J, Jensen KB, Ruggiu M, Mele A, Ule A, Darnell RB. CLIP identifies Nova-regulated RNA networks in the brain. Science 2003; 302: 1212-5.
Unoki M, Nakamura Y. Growth-suppressive effects of BPOZ and EGR2, two genes involved in the PTEN signaling pathway. Oncogene 2001; 20: 4457-65.
Valente EM, Abou-Sleiman PM, Caputo V, Muqit MM, Harvey K, Gispert S, et al. Hereditary early-onset Parkinson's disease caused by mutations in PINK1. Science 2004a; 304: 1158-60.
Valente EM, Salvi S, Ialongo T, Marongiu R, Elia AE, Caputo V, et al. PINK1 mutations are associated with sporadic early-onset parkinsonism. Ann Neurol 2004b; 56: 336-41.
Van Den Eeden SK, Tanner CM, Bernstein AL, Fross RD, Leimpeter A, Bloch DA, et al. Incidence of Parkinson's disease: variation by age, gender, and race/ethnicity. Am J Epidemiol 2003; 157: 1015-22.
van der Brug MP, Blackinton J, Chandran J, Hao LY, Lal A, Mazan-Mamczarz K, et al. RNA binding activity of the recessive parkinsonism protein DJ-1 supports involvement in multiple cellular pathways. Proc Natl Acad Sci U S A 2008; 105: 10244-9.
Vilarino-Guell C, Soto AI, Lincoln SJ, Ben Yahmed S, Kefi M, Heckman MG, et al. ATP13A2 variability in Parkinson disease. Hum Mutat 2009; 30: 406-10.
Waak J, Weber SS, Gorner K, Schall C, Ichijo H, Stehle T, et al. Oxidizable residues mediating protein stability and cytoprotective interaction of DJ-1 with apoptosis signal-regulating kinase 1. J Biol Chem 2009.
Wagenfeld A, Gromoll J, Cooper TG. Molecular cloning and expression of rat contraception associated protein 1 (CAP1), a protein putatively involved in fertilization. Biochem Biophys Res Commun 1998; 251: 545-9.
Wakabayashi K, Hayashi S, Yoshimoto M, Kudo H, Takahashi H. NACP/alpha-synuclein-positive filamentous inclusions in astrocytes and oligodendrocytes of Parkinson's disease brains. Acta Neuropathol 2000; 99: 14-20.
Wakabayashi K, Tanji K, Mori F, Takahashi H. The Lewy body in Parkinson's disease: molecules implicated in the formation and degradation of alpha-synuclein aggregates. Neuropathology 2007; 27: 494-506.
Wang Y, Chandran JS, Cai H, Mattson MP. DJ-1 is Essential for Long-Term Depression at Hippocampal CA1 Synapses. Neuromolecular Med 2008; 10: 40-5.
Ward CD, Duvoisin RC, Ince SE, Nutt JD, Eldridge R, Calne DB. Parkinson's disease in 65 pairs of twins and in a set of quadruplets. Neurology 1983; 33: 815-24.
Watts RL, Koller WC. Movement disorders : neurologic principles & practice. New York: McGraw-Hill Medical Publishing ; London : McGraw-Hill, 2004.
Weihofen A, Ostaszewski B, Minami Y, Selkoe DJ. Pink1 Parkinson mutations, the Cdc37/Hsp90 chaperones and Parkin all influence the maturation or subcellular distribution of Pink1. Hum Mol Genet 2008; 17: 602-16.
Weingarten MD, Lockwood AH, Hwo SY, Kirschner MW. A protein factor essential for microtubule assembly. Proc Natl Acad Sci U S A 1975; 72: 1858-62.
West AB, Maraganore D, Crook J, Lesnick T, Lockhart PJ, Wilkes KM, et al. Functional association of the parkin gene promoter with idiopathic Parkinson's disease. Hum Mol Genet 2002; 11: 2787-92.

West AB, Moore DJ, Biskup S, Bugayenko A, Smith WW, Ross CA, et al. Parkinson's disease-associated mutations in leucine-rich repeat kinase 2 augment kinase activity. Proc Natl Acad Sci U S A 2005; 102: 16842-7.

Westerlund M, Belin AC, Anvret A, Hakansson A, Nissbrandt H, Lind C, et al. Cerebellar alpha-synuclein levels are decreased in Parkinson's disease and do not correlate with SNCA polymorphisms associated with disease in a Swedish material. FASEB J 2008; 22: 3509-14.

Wilms H, Rosenstiel P, Sievers J, Deuschl G, Zecca L, Lucius R. Activation of microglia by human neuromelanin is NF-kappaB dependent and involves p38 mitogen-activated protein kinase: implications for Parkinson's disease. FASEB J 2003; 17: 500-2.

Wilson MA, Collins JL, Hod Y, Ringe D, Petsko GA. The 1.1-A resolution crystal structure of DJ-1, the protein mutated in autosomal recessive early onset Parkinson's disease. Proc Natl Acad Sci U S A 2003; 100: 9256-61.

Wilson MA, Ringe D, Petsko GA. The atomic resolution crystal structure of the YajL (ThiJ) protein from Escherichia coli: a close prokaryotic homologue of the Parkinsonism-associated protein DJ-1. J Mol Biol 2005; 353: 678-91.

Witt AC, Lakshminarasimhan M, Remington BC, Hasim S, Pozharski E, Wilson MA. Cysteine pKa depression by a protonated glutamic acid in human DJ-1. Biochemistry 2008; 47: 7430-40.

Xu J, Kao SY, Lee FJ, Song W, Jin LW, Yankner BA. Dopamine-dependent neurotoxicity of alpha-synuclein: a mechanism for selective neurodegeneration in Parkinson disease. Nat Med 2002; 8: 600-6.

Xu J, Zhong N, Wang H, Elias JE, Kim CY, Woldman I, et al. The Parkinson's disease-associated DJ-1 protein is a transcriptional co-activator that protects against neuronal apoptosis. Hum Mol Genet 2005; 14: 1231-41.

Yang Y, Gehrke S, Haque ME, Imai Y, Kosek J, Yang L, et al. Inactivation of Drosophila DJ-1 leads to impairments of oxidative stress response and phosphatidylinositol 3-kinase/Akt signaling. Proc Natl Acad Sci U S A 2005; 102: 13670-5.

Yang Y, Gehrke S, Imai Y, Huang Z, Ouyang Y, Wang JW, et al. Mitochondrial pathology and muscle and dopaminergic neuron degeneration caused by inactivation of Drosophila Pink1 is rescued by Parkin. Proc Natl Acad Sci U S A 2006; 103: 10793-8.

Yoshida K, Sato Y, Yoshiike M, Nozawa S, Ariga H, Iwamoto T. Immunocytochemical localization of DJ-1 in human male reproductive tissue. Mol Reprod Dev 2003; 66: 391-7.

Yu H, Sternad D, Corcos DM, Vaillancourt DE. Role of hyperactive cerebellum and motor cortex in Parkinson's disease. Neuroimage 2007; 35: 222-33.

Zarranz JJ, Alegre J, Gomez-Esteban JC, Lezcano E, Ros R, Ampuero I, et al. The new mutation, E46K, of alpha-synuclein causes Parkinson and Lewy body dementia. Ann Neurol 2004; 55: 164-73.

Zecca L, Casella L, Albertini A, Bellei C, Zucca FA, Engelen M, et al. Neuromelanin can protect against iron-mediated oxidative damage in system modeling iron overload of brain aging and Parkinson's disease. J Neurochem 2008a; 106: 1866-75.

Zecca L, Wilms H, Geick S, Claasen JH, Brandenburg LO, Holzknecht C, et al. Human neuromelanin induces neuroinflammation and neurodegeneration in the rat substantia nigra: implications for Parkinson's disease. Acta Neuropathol 2008b; 116: 47-55.

Zhang L, Shimoji M, Thomas B, Moore DJ, Yu SW, Marupudi NI, et al. Mitochondrial localization of the Parkinson's disease related protein DJ-1: implications for pathogenesis. Hum Mol Genet 2005a; 14: 2063-73.

Zhang W, Wang T, Pei Z, Miller DS, Wu X, Block ML, et al. Aggregated alpha-synuclein activates microglia: a process leading to disease progression in Parkinson's disease. FASEB J 2005b; 19: 533-42.

Zhang Y, Gao J, Chung KK, Huang H, Dawson VL, Dawson TM. Parkin functions as an E2-dependent ubiquitin- protein ligase and promotes the degradation of the synaptic vesicle-associated protein, CDCrel-1. Proc Natl Acad Sci U S A 2000; 97: 13354-9.

Zhong N, Kim CY, Rizzu P, Geula C, Porter DR, Pothos EN, et al. DJ-1 transcriptionally up-regulates the human tyrosine hydroxylase by inhibiting the sumoylation of pyrimidine tract-binding protein-associated splicing factor. J Biol Chem 2006; 281: 20940-8.

Zhou W, Freed CR. DJ-1 up-regulates glutathione synthesis during oxidative stress and inhibits A53T alpha-synuclein toxicity. J Biol Chem 2005; 280: 43150-8.

Zhou W, Zhu M, Wilson MA, Petsko GA, Fink AL. The oxidation state of DJ-1 regulates its chaperone activity toward alpha-synuclein. J Mol Biol 2006; 356: 1036-48.

Zhu X, Siedlak SL, Smith MA, Perry G, Chen SG. LRRK2 protein is a component of Lewy bodies. Ann Neurol 2006; 60: 617-8; author reply 618-9.

Zimprich A, Biskup S, Leitner P, Lichtner P, Farrer M, Lincoln S, et al. Mutations in LRRK2 cause autosomal-dominant parkinsonism with pleomorphic pathology. Neuron 2004; 44: 601-7.

# 8. Publications